METABOLISM OF HYDROXYALKYL DERIVATIVES OF 3-METHYLCHOLANTHRENE BY LIVER MICROSOMES

1991

SHOU

UNIFORMED SERVICES UNIVERSITY OF THE HEALTH SCIENCES
F. EDWARD HÉBERT SCHOOL OF MEDICINE
4301 JONES BRIDGE ROAD
BETHESDA, MARYLAND 20889-4799

PHARMACOLOGY

APPROVAL SHEET

TEACHING HOSPITALS
WALTER REED ARMY MEDICAL CENTER
NAVAL HOSPITAL, BETHESDA
MALCOLM GROW AIR FORCE MEDICAL CENTER
WILFORD HALL AIR FORCE MEDICAL CENTER

Title of Dissertation: "Metabolism of Hydroxyalkyl Derivatives of 3-Methylcholanthrene by Liver Microsomes"

Name of Candidate: Magang Shou
Doctor of Philosophy Degree
April 5, 1991

Dissertation and Abstract Approved:

Committee Chairperson — Date: May 10, 1991

Committee Member — Date: May 16, 1991

Committee Member — Date: May 24, 1991

Committee Member — Date: May 24, 1991

Committee Member — Date: May 24, 1991

The author hereby certifies that the use of any copyrighted material in the thesis manuscript entitled:

"Metabolism of Hydroxyalkyl Derivatives of 3-methylcholanthrene by Liver Microsomes"

beyond brief excerpts is with the permission of the copyright owner, and will save and hold harmless the Uniformed Services University of the Health Sciences from any damage which may arise from such copyright violations.

Magang Shou

Magang Shou
Department of Pharmacology
Uniformed Services University
of the Health Sciences

ABSTRACT

Title of Dissertation: Metabolism of Hydroxylalkyl Derivatives of 3-Methylcholanthrene by Liver Microsomes.

Magang Shou Doctor of Philosophy, 1991

Dissertation directed by: Shen K. Yang, Ph.D., Professor, Department of Pharmacology

3-Methylcholanthrene (3MC) is a potent carcinogen and requires metabolism by mammalian drug-metabolizing enzyme systems to exert its mutagenic and/or carcinogenic activities. 1-Hydroxy-3MC (1-OH-3MC), 2-hydroxy-3MC (2-OH-3MC), and 3-hydroxymethylcholanthrene (3-OHMC) are the major initial metabolites of 3MC. 1-OH-3MC and 2-OH-3MC are further metabolized to form 3MC-1-one, 3MC-2-one, 3MC *trans*-1,2-diol, and 3MC *cis*-1,2-diol. 2-OH-3MC and 3MC-2-one are potent carcinogens. Hence, the major ultimate carcinogens are believed to be derived from further metabolism of 2-OH-3MC, 3MC-2-one, and/or 3-OHMC. The objectives of this investigation are: (1) to characterize the products and to determine the relative amounts formed by metabolism of 1-OH-3MC, 2-OH-3MC, 3-OHMC, 3MC-1-one, 3MC-2-one, 3MC *trans*-1,2-diol, and 3MC *cis*-1,2-diol (3MC hydroxylalkyl derivatives), by liver microsomes from untreated and P-450 enzyme inducer-treated rats, and (2) to compare the metabolism of a racemic ^{3}H-labeled 1-OH-3MC by rat and human liver microsomes. The results will significantly contribute to the eventual understanding of the metabolic activation pathways of 3MC.

3MC hydroxylalkyl derivatives were synthesized for metabolism studies. Absolute configuration of enantiomeric 1-OH-3MC, 2-OH-3MC, 3MC *cis*- and 3MC *trans*-1,2-diols were established by the exciton chirality method. Relative amounts of 3MC alcohols formed in 3MC metabolism by liver microsomes from untreated, 3MC- and PB-treated rats were 2-OH-3MC > 3-OHMC > 1-OH-3MC. The 1(*S*)-OH-3MC (53-73%) and 2(*S*)-OH-3MC (86-98%) were found to be the major enantiomers. By using racemic 1-OH-3MC

and 2-OH-3MC, respectively, as substrates, liver microsomes from either PB- or 3MC-treated rats preferentially metabolized the 1*S*-enantiomer and the 2*R*-enantiomer. Metabolites formed in the metabolism of each 3MC hydroxylalkyl derivative were separated by a combination of reversed-phase and normal-phase high performance liquid chromatography (HPLC). They were identified by ultraviolet-visible absorption spectrophotometry, by mass spectral analysis and by comparison with authentic compounds. Enantiomeric composition and absolute configuration of major chiral metabolites were determined by chiral stationary phase HPLC and circular dichroism spectropolarimetry. Stereoselective formation of products and enantioselective disposition of substrates were highly dependent on the particular substrate used, the enzyme inducer utilized, and the microsomal enzyme concentration employed. The metabolic profiles obtained by incubation of [^{3}H]-1-OH-3MC with rat and human liver microsomes are qualitatively similar. 9,10-Dihydrodiols were the major metabolites formed by the metabolism of these 3MC hydroxylalkyl derivatives. These dihydrodiols could be precursors of 9,10-diol-7,8-epoxides and have the potential to be the ultimate carcinogens of 3MC.

METABOLISM OF HYDROXYALKYL DERIVATIVES OF 3-METHYLCHOLANTHRENE BY LIVER MICROSOMES

by

Magang Shou

Dissertation submitted to the Faculty of the Department of Pharmacology
Graduate Program of the Uniformed Services University of the
Health Sciences in partial fulfillment of the
requirements for the degree of
Doctor of Philosophy 1991

DEDICATION

To my parents, Drs. Shujie Ma and Huashan Shou, for their continuous love, belief, encouragement and support from my home town, Zhengzhou, The People's Republic of China.

To my wife, Ruiping Wang, for her love, patience, understanding and support at the times I needed her the most.

To my young brother, Dr. Matie Shou for his help and friendship.

Acknowledgments

I wish to express my sincere appreciation to my advisor, Dr. Shen K. Yang for his guidance, scientific intuition and invaluable ideas throughout the course of my dissertation research. I will always feel fortunate and honored that I was strictly and professionally trained in his laboratory.

I would also like to thank Henri B. Weems for his assistance in providing the mass spectral analysis, useful advice, and direction in laboratory techniques.

I thank my Dissertation Advisory committee, Drs. Lewis Aronow, Shen K. Yang, Alvito P. Alvares, Leon A. Moore and Doris H. Corcoran for their insightful comments and constructive criticisms which contributed greatly to the quality of the work contained herein.

I am grateful to Shen K. Yang, Henri B. Weems, Xiang-Lin Lu, Mohammad Mushtag, Ziping Bao, Kan Liu and Premakala Prasanna for their technical assistance and friendship.

Many thanks to Dr. Alvito P. Alvares and Dr. Doris H. Corcoran for many discussions about drug metabolism and enzymology.

Many thanks to Dr. Shen K. Yang, Dr. Leon A. Moore and Stephen R. Brown for helping with use of the computer.

Many thanks to Dr. Lewis Aronow, Chairman of Pharmacology Department and to departmental office personnel for their earnest help.

Many thanks to all the Department of Pharmacology faculty for their efforts in my education.

Many thanks to Drs. Brian M. Cox, former director and Jeffrey M. Harmon, director of graduate training in Pharmacology, and USUHS for Continuing and Graduate Education.

Many thanks to Dr. Shen K. Yang and Henri B. Weems for their assistance on my thesis writing.

I gratefully acknowledge the supports by NIH grant No. CA29133 and USUHS protocol No. RO7502 awarded to Dr. Shen K. Yang. I also thank the support of a USUHS graduate research fund TO75BT.

TABLE OF CONTENTS

List of Figures

List of Tables

Abbreviations and Definitions

PAHs, polycyclic aromatic hydrocarbons; BaP, Benzo[a]pyrene; DMBA, 7,12-dimethylbenz[a]anthracene; 3MC, 3-methylcholanthrene; 3MCE, 3-methylcholanthrylene; 1-OH-3MC, 1-hydroxy-3-methylcholanthrene; 2-OH-3MC, 2-hydroxy-3-methylcholanthrene; 3MC-1-one, 3-methylcholanthrene-1-one; 3MC-2-one, 3-methylcholanthrene-2-one; 3-OHMC, 3-hydroxymethylcholanthrene; 1-OH-3-OHMC, 1-hydroxy-3-hydroxymethylcholanthrene; 3MC *trans*-1,2-diol, *trans*-1,2-dihydroxy-3-methylcholanthrene; 3MC *cis*-1,2-diol, *cis*-1,2-dihydroxy-3-methylcholanthrene; 3MC-2-one 9,10-dihydrodiol, 9,10-dihydroxy-9,10-dihydro-3MC-2-one; 2-OH-3MC 9,10-dihydrodiol, 9,10-dihydroxy-9,10-dihydro-2-OH-3MC; 7-MBA 3,4-dihydrodiol, 3,4-dihydroxy-3,4-dihydro-7-methylbenz[*a*]anthracene; 6-MBP, 6-methylbenz[a]pyrene; 1-OH-BA, 1-hydroxy-benz[a]anthracene; PB, phenobarbital; PCB, polychlorinated biphenyls (Aroclor 1254); CSP, chiral stationary phase; *R*-DNBPG, (*R*)-*N*-(3,5-dinitrobenzoyl)phenylglycine; *S*-DNBL, (*S*)-*N*-(3,5-dinitrobenzoyl)leucine; G-6-P, glucose 6-phosphate; THF, tetrahydrofuran; DDQ, 2,3-dichloro-5,6-dicyanobenzoquinone; OsO_4, osmium tetroxide.

INTRODUCTION

PAHs are ubiquitous environmental pollutants released into the atmosphere, primarily due to their production from combustion processes. Among the environmental chemicals, polycyclic aromatic hydrocarbons (PAHs) comprise the largest group of carcinogens (Wynder *et al.*, 1972; Shubik, 1972). Some PAHs are believed to cause cancer induction in man.

Carcinogenicity of PAHs has mainly been observed for tri-, tetra-, penta-, and hexacyclic compounds. The carcinogenic activity of a particular compound is dependent on various structural features of the molecule. Shape, size, and steric factors all seem to be important. Isomeric parent PAHs may differ markedly in their activities. For example, benzo[a]pyrene (BaP) has significantly greater activity than benzo[e]pyrene (Hueper *et al.* 1972). Enantiomeric PAH metabolites may also differ in their mutagenic and carcinogenic activities (Cavalieri *et al.*, 1978; Levin *et al.*, 1979; Chouroulinkov *et al.*, 1979).

Alkyl groups on PAHs might retard or block the metabolic formation of arene oxides at the ring carbon atoms to which they are attached; may shift the point of metabolic attack to distal areas of the molecule, or may serve as sites of metabolic activation or detoxification. Hence the carcinogenicity of PAHs may be enhanced, diminished, or left unaffected by alkyl substitution (Schoental, 1964; Newman, *et al.*, 1976). Parent PAHs require metabolic activation by drug metabolizing enzyme systems. Some oxygenated metabolites formed in the metabolism of parent PAHs may react with biological macromolecules.

Cytochrome P-450 isozymes are responsible for catalyzing stereoselective hydroxylation and epoxidation reactions of xenobiotics such as the PAHs as well as certain endogenous metabolic intermediates (e.g., steroids). Epoxides are key intermediates in the formation of phenols and *trans*-dihydrodiols. Metabolism of PAHs can be schematically illustrated as shown in Fig. 1 (Yang, 1988). Because of the stereoselective characteristics

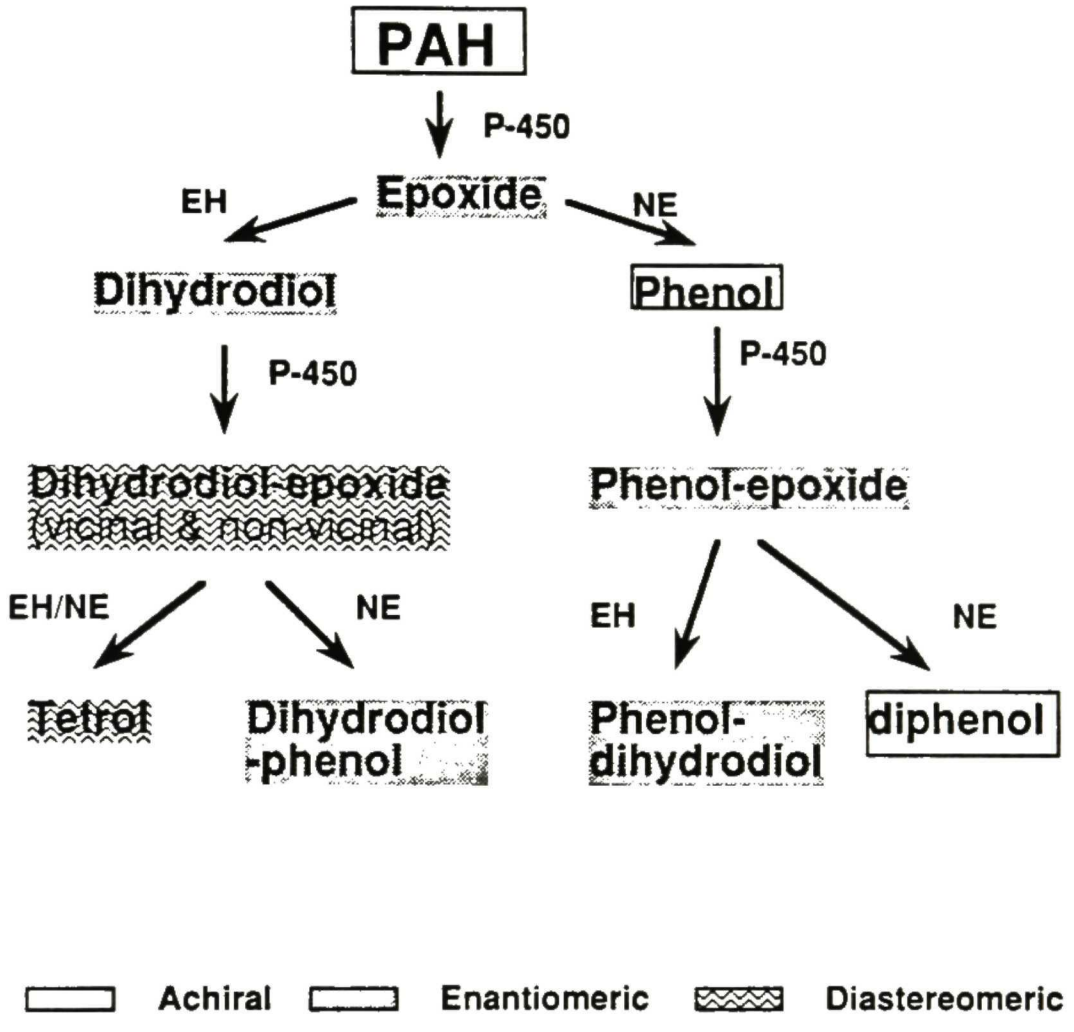

Figure 1. Oxidative pathways of metabolism of a fully unsaturated PAH leading to chiral (enantiomeric and diastereomeric) and a chiral products. P-450: cytochrome P-450; EH: epoxide hydrolase; NE: non-enzymatic rearrangement. Vicinal dihydrodiol-epoxide is a ultimate carcinogenic bay region diol epoxide.

of the enzymes, an epoxidation reaction at prochiral unsaturated double bonds of a PAH catalyzed by cytochrome P-450 isozymes may result in optically active epoxides. Hydration of epoxides catalyzed by epoxide hydrolase may further produce *trans*-dihydrodiols enriched in one enantiomer.

1. *Theoretical background*

1.1 *Bay region theory*

In 1976, Jerina *et al.* examined the structure-activity relationships of substituted PAHs and proposed the bay-region theory as a concept for understanding the carcinogenicity of PAHs (Jerina *et al.*, 1978; 1976; Chouroulinkov *et al.*, 1979). The bay region theory postulates that tetrahydroepoxides with the epoxide oxygen in the bay region of a PAH should be highly reactive (see Fig. 2). The bay-region diol epoxides are presumably the active intermediates, and the data indicated that the bay-region theory applies to substituted as well as unsubstituted PAHs.

The bay region theory of PAH carcinogenesis, which predicts an unusually high ease of formation of benzylic carbonium ions derived from bay region epoxides has received much attention. Perturbational molecular orbital calculations have indicated that an epoxide on a saturated, angular benzo ring that forms part of a bay region of the hydrocarbon should have high chemical reactivity and presumably high biological activity (Jerina *et al.*, 1978). The bay-region diol-epoxides of a PAH should be good candidates as ultimate carcinogenic metabolites. The reactive tetrahydro-epoxide can yield a reactive carbonium ion which exhibits electrophilic property and binds to biological macromolecules. Hence the bay-region theory became important to explain a correlation between the formation of bay-region diol-epoxides and biological activity of PAHs (Fig. 3).

3MC is a C_7-C_8 ethylene substituted benz[a]anthracene derivative. If bay-region theory is applied to 3MC, the 3MC 9,10-dihydrodiol-7,8-epoxide is predicted to have the

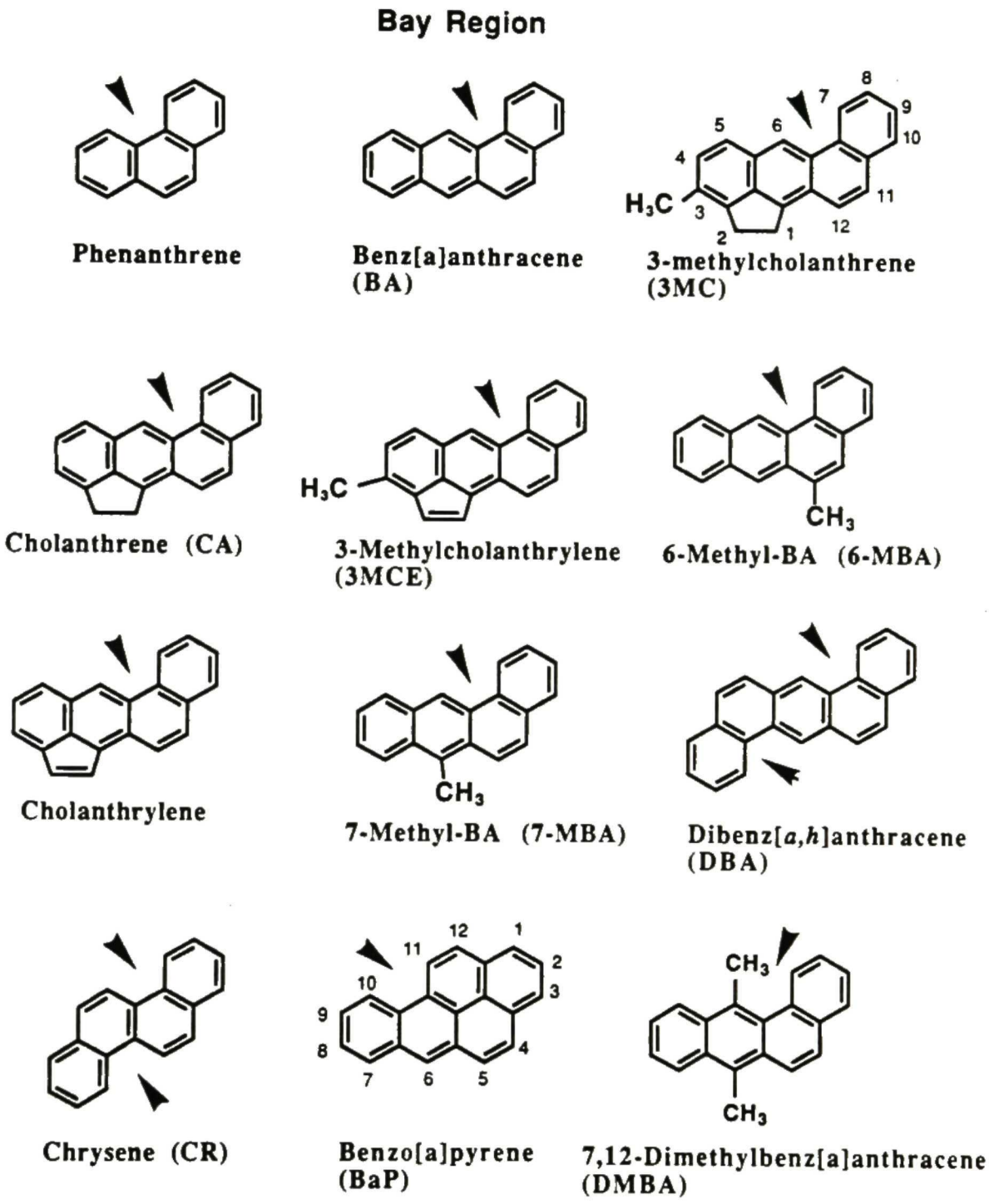

Figure 2. Structure and abbreviation of polycyclic aromatic hydrocarbons. Bay-region is the sterically hindered region of the molecule.

The Major Activation Pathway of Benzo[a]pyrene

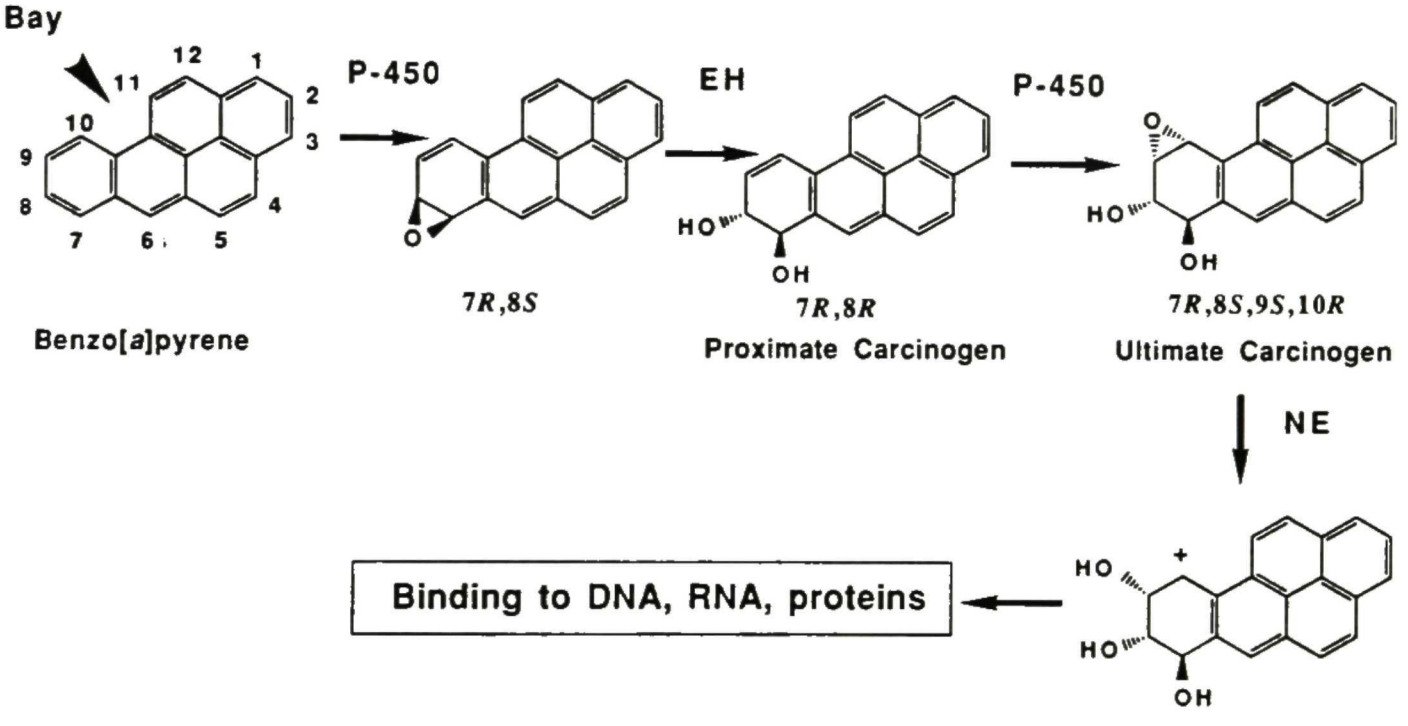

Figure 3. Pathways of stereoselective metabolism at the 7,8,9,10-positions of benzo[a]pyrene (BP). BP 7*R*,8*R*-dihydrodiol is metabolized predominantly to the 7*R*,8*S*-diol-*anti*-9*S*,10*R*-epoxide which is the most potent carcinogen.

highest chemical reactivity. Mutagenicity (Malaveille *et al.*, 1978; Wood *et al.*, 1978) and tumorigenicity (Levin *et al.*, 1979; Chouroulinkov *et al.*, 1979) studies indicated that the 9,10-dihydrodiols of both 3MC and 1-hydroxy-3MC (1-OH-3MC) were the most mutagenic dihydrodiols tested. For example, 9,10-dihydrodiol of 1-OH-3MC is metabolically activated to mutagens toward the *Salmonella typhimurium* test strain TA100 to a 10-fold or greater extent than is 3MC. In the case of 3MC, the critical binding activation would be mediated via a 9,10-diol-7,8-epoxide. This metabolite has been suggested to bind DNA from mouse embryo cells (King *et al.*, 1977) and fluorescence spectral evidence on DNA from mouse skin is consistent with the 3MC diol-epoxide. These data suggest that 9,10-dihydrodiols are the proximate carcinogens of 3MC and the bay-region diol-epoxides (9,10-diol-7,8-epoxides of both 3MC and 1-OH-3MC) could be the ultimate mutagens and carcinogens of 3MC. The 3MC *trans*-9,10-dihydrodiol-7,8-epoxides have been synthesized and implicated as the ultimate carcinogen metabolites of the potent carcinogen 3MC (Jacobs *et al.*, 1983).

The metabolic activation of PAH requires two enzyme systems, cytochrome P-450 and epoxide hydrolase. 3MC may be converted to 3MC 9,10-epoxide, which is enzymatically hydrated to the 9,10-dihydrodiol. 3MC 9,10-dihydrodiol is further metabolized to the bay region 9,10-dihydrodiol-7,8-epoxide (Thakker *et al.*, 1978) (Fig. 4).

1.2 *Theory of one electron oxidation to radical cation*

Bay region theory is not the only theory proposed to explain PAH carcinogenicity. Accumulated evidence suggests that one-electron oxidation of aromatic hydrocarbons to radical cations might be another critical mechanism of activation to initiate the multistep process which results in cancer (Cavalieri *et al.*, 1985). Nucleophilic trapping of the 3MC radical cation generated by iodine or Mn^{3+} oxidation occurs specifically at C_1, which is the alkyl substitution attached to the position of highest charge density. In these model reactions it was established that the rate determining step is fragmentation of the C_1-H bond

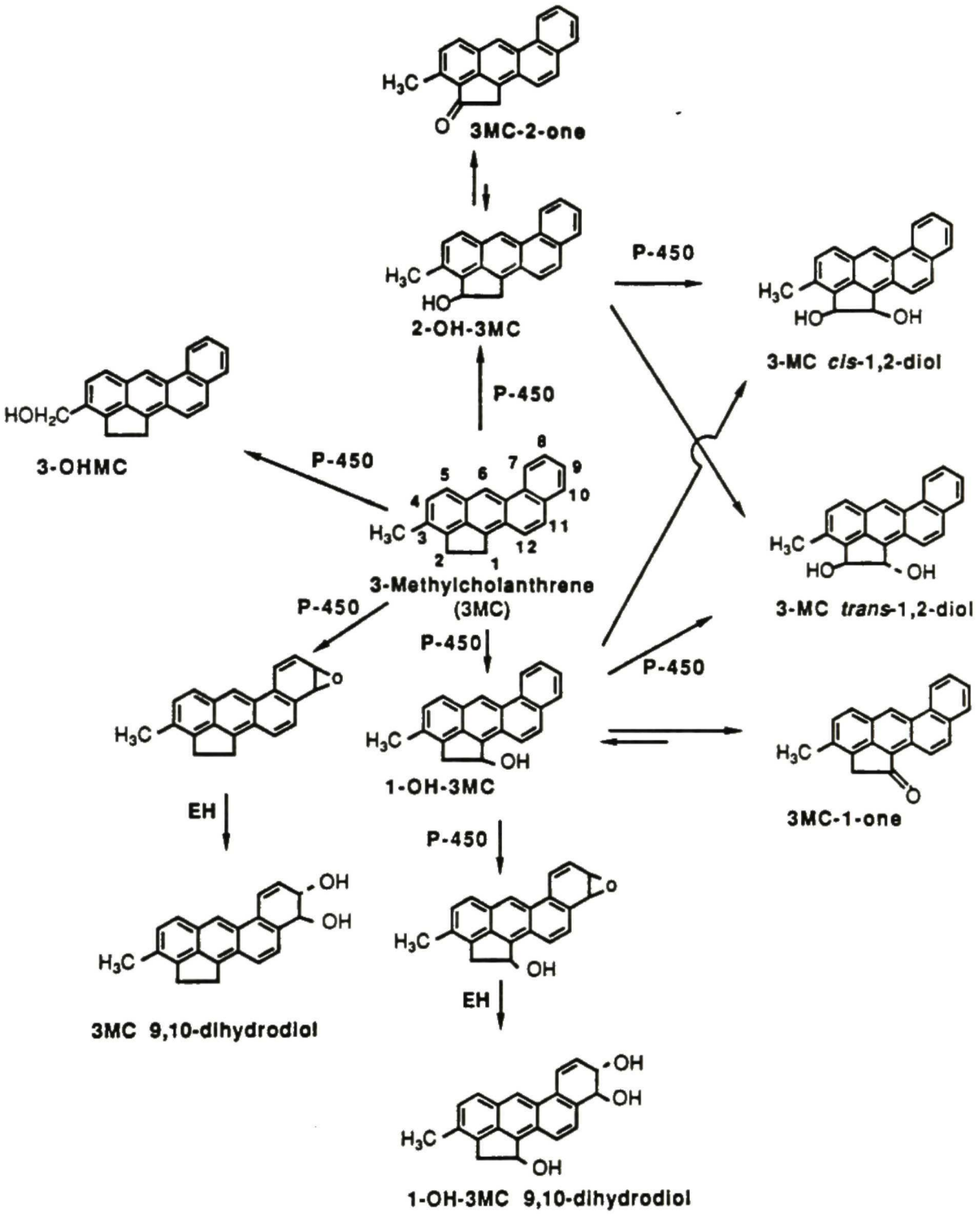

Figure 4. The known and proposed metabolic pathways of 3-methylcholanthrene (3MC). EH, epoxide hydrolase; P-450, cytochrome P-450.

(Cavalieri *et al.*, 1985). This is analogous to the alkyl trapping products obtained with 7-methylbenz[a]anthracene (7-MBA), 7,12-dimethylbenz[a]anthracene (DMBA) and 6-methylbenzo[a]pyrene (6-MBaP). Thus, the critical activation step in 3MC, 2-hydroxy-3MC (2-OH-3MC) and 3MC-2-one carcinogenesis, by analogy with 6-methylbenzo[a]pyrene, might be the formation of the corresponding radical cations by one-electron oxidation and subsequent reaction of the intermediates to cellular nucleophiles through the 1-carbon atom. This mechanism may form the basis of the activation of all carcinogenic aliphatic aromatic hydrocarbons.

In order to test the hypothesis that the critical mechanism of activation of 3MC is one-electron oxidation, the carcinogenicity of 3MC was compared to that of 1-OH-3MC, 3MC-1-one, 2-OH-3MC, 3MC-2-one and 3-methylcholanthrylene (3MCE) by repeated application on mouse skin. The relative carcinogenicity was found to be: 3MC and 2-OH-3MC (carcinogen) > 3MC-2-one and 3MCE > 1-OH-3MC > 3MC-1-one (noncarcinogen) (Cavalieri *et al.*, 1978, 1988).

1.3 *Other non bay-region theories of the proximate and ultimate carcinogen*

Other modes of activation of PAHs are also possible. Methylated PAHs can be activated by hydroxylation (proximate carcinogen) of the methyl group followed by esterification to yield a benzylic ester (the postulated ultimate carcinogen, bearing a good leaving group). If a good leaving group is present, a carbonium ion can be formed which could react with critical cellular nucleophiles. For example, mutagenic and carcinogenic activities of the hydroxymethyl derivatives of 6-methylbenzo[a]pyrene (6MBaP) (Flesher *et al.*, 1973; Sydnor *et al.*, 1980), DMBA and 7MBA (Watabe *et al.*, 1985; 1986;), and sulfate or acetate esters of the hydroxymethyl derivatives of BaP, 7MBaP, DMBA, 3MC (Rogan *et al.*, 1986), and 6MBaP (Cavalieri *et al.*, 1979).

2. *Chemistry of 3MC and derivatives*

The chemical oxidation of 3MC in an ascorbic acid-ferrous sulphate-EDTA reaction mixture gave all five possible dihydrodiols (Tierney *et al.*, 1978). The structures of the dihydrodiols were established by uv-visible absorption, mass spectral and NMR spectral studies to be *cis-2a-3*-dihydrodiol, *trans*-4,5-dihydrodiol, *trans*-7,8-dihydrodiol, *trans*-9,10-dihydrodiol, *cis*- and *trans*-11,12-dihydrodiol (Tierney *et al.*, 19781). Jacobs *et al.* (1983) synthesized 3MC *trans*-9,10-dihydrodiol and 3MC *trans*-9,10-dihydrodiol-7,8-epoxide, implicated as the proximate and ultimate carcinogenic metabolites, respectively, of the potent carcinogen 3MC. 3MC can also be oxidized to yield dihydroxy derivatives such as the *cis* isomer of the 1,2-dihydrodiol as well as the 1-OH-3MC, 3MC-1-one, 2-OH-3MC, 3MC-2-one and 3MCE by lead tetraacetate and osmium tetraoxide (Cavalieri *et al.*, 1978; Sims *et al.*, 1966; Fieser *et al.*, 1938).

3. *Metabolism of 3MC and its derivatives*

3.1 *Metabolic conversion*

In a previous study of the metabolism of 3-[^{14}C]-MC by liver microsomes prepared from immature, male Long-Evans rats (Thakker *et al.*, 1978), 1-OH-3MC, 2-OH-3MC, 3MC-1-one and 3MC-2-one were found to account for >80% of all the metabolites formed. In the experiments described, ~4% of 3MC was metabolized. Only trace amounts of metabolites (3%) could be identified as dihydroxylated species, mainly 3MC *trans*-11,12-dihydrodiol and 3MC *trans*-1,2-dihydrodiol.

3.2 *Metabolism of 3MC and effects of enzyme induction*

The early work on the metabolism of 3MC, mainly by hepatic preparations, has been reviewed (Cavalieri *et al.*, 1978; Sims, 1966; Tierney *et al.*, 1978 & 1979; Thakker *et al.*, 1978; Sims *et al.*, 1974; Gangarosa *et al.*, 1983; Stoming *et al.*, 1977) (Fig.4). 1-OH-3MC, 2-OH-3MC, and to a minor extent, their ketones, as well as 3MC *cis*- and *trans*-1, 2-diols, 3-hydroxylmethylcholanthrene (3-OHMC) were tentatively identified as major metabolites. There was also some evidence for the presence of small amounts of non-K-

region dihydrodiol as metabolites. Later investigation by Stoming *et al.* (1977) identified the K-region *cis*-11,12-dihydrodiol as a metabolite. An examination by HPLC of the dihydrodiols formed in the metabolism of 3MC by rat liver microsomal preparations showed the presence of *trans*-4,5-dihydrodiol, *trans*-7,8-dihydrodiol, *trans*-9,10-dihydrodiol and *trans*-11,12-dihydrodiol, identified by their spectral properties and chromatographic characteristics. Tentative identifications of *cis*- and *trans*-1,2-dihydrodiol, *cis*-2a,3-dihydrodiol as metabolites were made. A quantitative comparison of the dihydrodiols formed from ^{3}H-labelled 3MC by microsomal preparations from the livers of untreated and 3MC-treated rats was carried out (Sims *et al.*, 1974).

Pretreatment of rats with PB, PCN and 3MC results in a 2-, 3- and 5-fold increase in the total metabolism of 3MC. Thakker *et al.* (1978) investigated the metabolism of 3MC both by hepatic microsomal fractions from rats pretreated with either 3MC, PB or PCN and by a purified monooxygenase system, with or without the addition of purified epoxide hydrolase. The results indicated that most of the major metabolites arose through hydroxylation at C_1 and C_2. Thakker *et al.* (1978) further extended their earlier observations and, using large-scale hepatic microsomal fractions from 3MC-treated rats, was able to isolate two dihydrodiols formed in the metabolism of racemic 1-OH-3MC that were characterized by uv-visible spectral and NMR spectroscopy analyses and shown to be the diastereomeric forms of the 9,10-dihydrodiols of 1-OH-3MC (these two diastereomeric dihydrodiols were designated as 9,10-dihydrodiol-*a* and 9,10-dihydrodiol-*b*).

With the availability of reference dihydrodiols, comparisons between the amounts of metabolites formed by hepatic microsomal fractions from untreated or PB- and 3MC-pretreated rats indicated that the amounts of the 3MC *trans*-7,8-, 9,10- and 11,12-dihydrodiols were increased, that of the *cis*-2a, 3-diol was decreased (Tierney *et al.*, 1979). Many of the above diols and dihydrodiols, as well as the 1- and 2-hydroxy and keto derivatives were detected as products in the metabolism of 3MC by hepatic nuclei from untreated and 3MC-treated rats. The level of metabolism was greater in nuclei from

pretreated animals than in those from untreated animals (Tierney *et al.*, 1979). However, the absolute configurations and enantiomeric compositions of chiral metabolites formed in the metabolism of 3MC by liver microsomes of rats treated with various inducers were not reported.

3.3 *Metabolism of 3MC at C_1 and C_2 positions*

C_1 and C_2 positions of 3MC are major sites of oxidative metabolism, resulting in the formation of primarily 1-OH-3MC and 2-OH-3MC, and to a minor extent, 3MC-1-one and 3MC-2-one (Cavalieri *et al.*, 1978; Sims, 1966; Thakker *et al.*, 1978; Tierney *et al.*, 1979; Stoming *et al.*, 1977; Eastman *et al.*, 1979). When 3MC is present in saturating amount, as much as 45% to 75% of rat liver microsomal metabolism of 3MC occurs at C_1 and C_2 positions.

Conflicting results were reported on the relative amounts of 1-OH-3MC and 2-OH-3MC formed in the metabolism of 3MC by rat liver microsomes (Thakker *et al.*, 1978; Tierney *et al.*, 1979 Stoming *et al.*, 1977; Eastman *et al.*, 1979). A [1-OH-3MC]:[2-OH-3MC] ratio of 32:68 (Stoming *et al.*, 1977) and of 43:57 (Tierney *et al.*, 1979) were reported in the metabolism of 3MC by liver microsomes from 3MC-treated rats. Another study reported that 2-OH-3MC was formed predominantly in the metabolism of 3MC by liver microsomes from Aroclor 1254-treated rats (Eastman *et al.*, 1979). Liver nuclei from untreated and 3MC-treated rats metabolize 3MC to form 1-OH-3MC and 2-OH-3MC in ratios of 59:41 and 29:71, respectively (Tierney *et al.*, 1979). In contrast, Thakker *et al.* (1978) reported the ratios of [1-OH-3MC]:[2-OH-3MC], formed in the metabolism of 3MC by four rat liver microsomal preparations, were 78:22 (untreated control), 93:7 (PB-treated), 66:34 (3MC-treated), and 97:3 (PCN-treated), respectively. In our study (see later), the amount of 2-OH-3MC formed in the metabolism of 3MC was consistently found to be higher than that of 1-OH-3MC by liver microsomes from untreated, PB-treated, and 3MC-treated rats (Shou and Yang, 1990a). The discrepancy of results in our study versus those in earlier studies (Thakker *et al.*, 1978; Tierney *et al.*, 1979; Stoming *et al.*, 1977;

Eastman *et al.*, 1979) was apparently due to differences in analytical methods employed. In our study, 1-OH-3MC and 2-OH-3MC were first isolated by reversed-phase HPLC as a mixture, and their relative amounts were reliably determined by normal-phase HPLC, which allowed baseline separation of 1-OH-3MC and 2-OH-3MC. It is worthy noting that 2-OH-3MC is a considerably more potent carcinogen than 1-OH-3MC.

3.4 *Metabolism of 1-OH-3MC and 2-OH-3MC*

Previous studies indicated that 3MC 9,10-dihydrodiol is a minor metabolic product. However, one major metabolite, 1-OH-3MC, is further metabolized to form a pair of diastereomeric 9,10-dihydrodiols (9% of total metabolites) (Thakker *et al.*, 1978; Eastman *et al.*, 1979).

Since 1-OH-3MC and 2-OH-3MC are the two major primary oxidative metabolites of 3MC, it was of interest to see if either or both of these primary oxidative metabolites could be further converted to dihydrodiols or other oxygenated metabolites by the cytochrome P-450 system. To study the metabolism of 1-OH-3MC, tritium-labeled substrate was prepared by reduction of the 3MC-1-one with KB^3H_4 in a solution of ethanol /tetrahydrofuran (3:1). The metabolite profiles of [1-^{3}H]1-OH-3MC obtained with the purified monooxygenase system in the presence of epoxide hydrase indicate that at least four metabolite peaks are formed in the incubation medium. These four metabolites appear to be *trans* dihydrodiols. The two major fractions were characterized and assigned as diastereomerically related *trans* -9,10-dihydrodiols generated from racemic 1-OH-3MC (Gardiner *et al.*, 1984). The other two metabolites were identified as *trans*- and *cis*-1,2-diol-3MC. As is the case with 3MC as the substrate, very little 3MC *cis*-1,2-dihydrodiol is formed from either 1-OH-3MC or 2-OH-3MC. Several phenols were also produced in the incubation and were characterized.

Thakker *et al.* (1978) showed that the metabolism of racemic 1-OH-3MC gave rise to at least 13 products. It is interesting to note that when liver microsomes prepared from Aroclor-induced rats were used, total metabolism was only slightly increased above that

using untreated rats, whereas PB and 3MC induction resulted in approximately a 4-fold increase in total metabolism. In the study of 2-OH-3MC metabolism, at least 10 metabolites are formed. However, the majority of metabolites formed from either 1-OH-3MC or 2-OH-3MC were not characterized.

The results of earlier studies on the metabolism of 3MC, 1-OH-3MC and 2-OH-3MC can be summarized as follows: (a) 3MC is extensively metabolized to 1-OH-3MC and 2-OH-3MC as well as other dihydrodiols by rat liver monoxygenases, (b) only small amounts of dihydrodiols are formed from this hydrocarbon, (c) 1-OH-3MC and 2-OH-3MC can be further metabolized by the liver monooxygenase system, (d) 1-OH-3MC is metabolized by liver microsomes to at least four dihydrodiols and several phenols. The two major dihydrodiols of 1-OH-3MC appear to be diastereomerically related *trans*-9,10-dihydrodiols, and (e) metabolites formed in the metabolism of 2-OH-3MC, 3MC-2-one and 3MC-1-one have either not been characterized or poorly characterized.

3.5 *Stereoselectivity of enzymes*

PAHs are stereoselectively metabolized by mammalian drug-metabolizing enzyme systems to optically active intermediates, including epoxides, dihydrodiols and dihydrodiol-epoxides. Enantiomeric epoxides and dihydrodiols as well as diastereomeric dihydrodiol-epoxides of benz[a]anthracene (BA) and benzo[a]pyrene (BP) vary substantially in their mutagenic and carcinogenic activities (Conney *et al.*, 1982). The optical purity of dihydrodiol metabolites of some PAHs can be determined by resolution of diastereomers derivatized with (–)menthoxyacetyl chloride (Yang *et al.*, 1977). A chiral stationary phase (CSP) HPLC method was developed to resolve some epoxide, dihydrodiol, and tetrahydrodiol enantiomers formed in the metabolism of several PAHs by hepatic microsomal enzymes (Yang *et al.*, 1989, 1990). 3MC may undergo enzymatic hydroxylation at the methylene carbons to form enantiomeric 1-OH-3MC. The enantiomers of 1-OH-3MC can be separated by CSP-HPLC (Yang and Li, 1984). A 1-OH-3MC was obtained as a metabolite formed in the metabolism of 3MC by liver microsomes from PB

treated rats and was shown to have a an (R):(S) enantiomer ratio of 54:46 (enantiomeric purity of 8% enriched in the *R* enantiomer). The enantiomers of 2-OH-3MC were not resolved by the CSP-HPLC procedure. But a 2-OH-3MC formed in the metabolism of 3MC was found to be optically active by circular dichroism (CD) spectral analysis (Yang and Li, 1984).

4. *Tests of Biological Activity*

4.1 *Reactions with nucleic acids*

DNA binding studies *in vitro* and *in vivo* indicated that, in addition to being activated to a 3MC 9,10-diol-7,8-epoxide, 3MC was also activated to other products that bind covalently to DNA (King *et al.*, 1977; Eastman *et al.*, 1979; Vigny *et al.*, 1977; Cooper *et al.*, 1980; King *et al.*, 1978; Phillips *et al.*, 1978; Osborne *et al.*, 1986). These were believed to be the 9,10-diol-7,8-epoxides formed via hydroxylation at the C_1 or C_2 position and/or the 3-methyl group (Eastman *et al.*, 1979; Cooper *et al.*, 1980; Phillips *et al.*, 1978).

Examination by Vigny *et al.* (1977) and by Cooper *et al.* (1980) of the fluorescence spectra of DNA and of adducts present in DNA isolated from the skin of mice treated with 3MC showed that the emission spectra were anthrancene-like. The results indicated that the covalently bound adducts derived from 3MC involved saturation of the 7,8,9,10-ring of the hydrocarbon. Some laboratories (Cooper *et al.*, 1980; King *et al.*, 1977) employed HPLC in adduct analyses and detected five products in the mixtures of adducts derived from DNA of cultured mouse embryo cells pretreated with 3MC. The fluorescence spectra were similar to that of 7,8,9,10-tetrahydro-3MC, which has an anthracene nucleus. The adducts were suggested to be drived from binding of DNA with 1-OH-3MC 9,10-diol-7,8-epoxide and the 3MC 9,10-diol-7,8-epoxide, respectively. However, the identities of metabolites responsible for binding to DNA were not definitively established.

Osborne (1983) analyzed the DNA adducts formed by reaction of the *anti*-isomer of 3MC 9,10-diol 7,8-oxide and showed that reaction with DNA occurred mainly on the exocyclic amino group of deoxyguanosine.

The available evidence on the metabolic activation of 3MC implicates one or more bay region 9,10-diol-7,8-epoxides, presumably arising from further metabolism of more than one 9,10-dihydrodiol. Although 3MC 9,10-dihydrodiol is shown to possess high biological activity, it is a very minor metabolite of 3MC. The biological activity of 3MC may be primarily due to further metabolism of hydroxyalkyl derivatives such as 1-OH-3MC, 2-OH-3MC, and 3-OHMC.

4.2 *Sister Chromatid Exchanges (SCEs)*

The induction of sister chromatid exchanges (SCEs) in Chinese hamster ovary (CHO) cells by 3MC and some of the related dihydrodiols was investigated. Increased numbers of SCEs were seen in the chromosomes of cells exposed to non-K-region dihydrodiols. The most active compounds were the 7,8- and 9,10-dihydrodiols of 3MC. The parent hydrocarbons and their corresponding K-region dihydrodiols were relatively less active (Pal *et al.*, 1979).

4.3 *Mutagenicity in vitro*

When *salmonella typhimurium* strain TA98 was used to detect mutagens and when hepatic microsomes were the source of metabolizing enzyme, 1-OH-3MC was metabolically activated to a 10-fold greater extent than was 3MC and was the most active compound tested. 1-OH-3MC 9,10-dihydrodiol and 3MC-2-one, the second and third most active compounds, respectively, were also activated to a greater extent than was 3MC. 2-OH-3MC had similar mutagenicity as 3MC. 3MC-1-one and the K-region 3MC 11,12-dihydrodiol were less active and inactive, respectively (Wood *et al.*, 1978).

When *S. typhimurium* strain TA100 and Chinese hamster V79 cells were used to detect mutations and both hepatic microsomes and the highly purified and reconstituted monooxygenase system was the enzyme source, 1-OH-3MC 9,10-dihydrodiol was

activated to a greater extent than was 3MC or 4,5-, 7,8-, 11,12- and 2a,3-dihydrodiol and was the most active compound (Malaveille *et al.*, 1978). Metabolites formed from 1-OH-3MC 9,10-dihydrodiol were 15-100 times more mutagenic than were the metabolites formed from 3MC. 3MC-2-one and 1-OH-3MC were the second and third most active substrates (Wood *et al.*, 1978). Among two diastereomeric 1-OH-3MC 9,10-dihydrodiols, the one designated as 1-OH-3MC 9,10-dihydrodiol-*a* was more active both in *S. Typhimurium* strain TA100 and V79 cells than that designated as 1-OH-3MC 9,10-dihydrodiol-*b*. 1-OH-3MC, 2-OH-3MC, 3MC-1-one, and 3MC-2-one all showed varying degrees of mutagenicity, depending on the system used.

4.4 *Carcinogenicity test*

Carcinogenic activities of 3MC, 1-OH-3MC, 2-OH-3MC, 3MC-1-one and 3MC-2-one were tested by three weekly subcutaneous injections into mice; all four 3MC derivatives were active carcinogens, but less so than 3MC itself (Sims, 1967). In tests for the induction of pulmonary and hepatic tumors in newborn mice (Levin *et al.*, 1978), it was found that 3MC and 3MC-2-one were the most active in inducing pulmonary tumors, 2-OH-3MC was slightly less active, 1-OH-3MC showed marginal activity and 3MC-1-one was inactive. In the induction of hepatic tumors in newborn male mice, 3MC, 2-OH-3MC and, to a lesser extent, 3MC-2-one were active.

In the tumorgenicity study on mouse skin (Levin *et al.*, 1978; Chouroulinkov *et al.*, 1979; Cavalieri *et al.*, 1978), a single topical application of 3-30 nmol of compound was followed 7 days later by twice weekly applications of the tumors promotor 12-*O*-tetradecanoylphorbol-13-acetate for 30 weeks. The average number of tumors per mouse indicated that 3MC, 2-OH-3MC, 3MC-2-one and 1-OH-3MC 9,10-dihydrodiol diastereomers were approximately equipotent as tumor initiators. 1-OH-3MC had approximately one-fourth the tumor-initiating activity of the most active compounds and 3MC-1-one and *trans-11,12*-dihydrodiol-3MC had no significant tumorigenic activity at the doses tested (Sims, 1967).

The high tumorigenic activity of 1-OH-3MC 9,10-dihydrodiol on mouse skin and in newborn mice provided evidence for bay-region activation of 3MC to an ultimate carcinogen (Levin *et al.*, 1979). 1-OH-3MC 9,10-dihydrodiol at the 21 and 49 nmol doses also produced hepatic tumors in 50-81% of the male mice, respectively. 3MC and 2-OH-3MC had one-fourth to one-tenth the activity of 1-OH-3MC 9,10-dihydrodiol in the liver. The other 3MC metabolites were essentially inactive in producing hepatic tumors. But it is not clear at present time whether or not the presence of a hydroxy group on the methylene bridge is an essential feature in the metabolic activation of 3MC in a target tissue *in vivo*.

5. Significance and Specific Aims

Since the initial report (Vigny *et al.*, 1977) that 3MC is activated at the 7,8,9,10-benzo ring, additional evidence indicated that 9,10-diol-7,8-epoxides derived from 1-OH-3MC, 2-OH-3MC, and 3-OHMC may be more important activated metabolites than the 9,10-diol-7,8-epoxide of 3MC (King *et al.*, 1977; Osborne *et al.*, 1986). To date, there has not been definitive data establishing the activation pathways of 3MC. In fact, there may be more than one activated metabolite responsible for the carcinogenicity exhibited by 3MC. Inspite of intensive efforts in the past, metabolites of 3MC and its oxidative derivatives formed at C_1, C_2, and C_3-methyl groups had not been carefully studied. Hence, relative to the detailed understanding in many other PAHs, the metabolic activation pathway(s) is poorly understood. Very little has been reported on the stereochemical pathways in the metabolism of 3MC. The major difficulty has been the lack of a good analytical system in the separation of the complex mixture of metabolites formed in the metabolism of 3MC as well as methodology in the separation of enantiomeric pairs of 3MC derivatives.

The objectives of this study are to identify the metabolites formed in the metabolism of 3MC and its oxidative derivatives formed at C_1, C_2, and C_3-methyl groups such as 1-OH-3MC, 2-OH-3MC, 3-OHMC, 3MC *trans*-1,2-diol, and 3MC *cis*-1,2-diol by at liver

microsomes. The stereochemistry of major metabolites will also be examined. The results will significantly contribute to the understanding of the metabolic activation pathways of the potent carcinogen 3MC. The specific aims are:

(1). Chemical synthesis of 1-OH-3MC, 2-OH-3MC, 3MC-1-one, 3MC-2-one, 3MC *trans*- and *cis* -1,2-diols as source materials for the proposed metabolism studies.

(2). Separation and elucidation of the absolute configurations of enantiomeric 1-OH-3MC, 2-OH-3MC, 3MC *trans*-1,2-diol, and 3MC *cis*-1,2-diol.

(3). Stereoselective hydroxylation at C_1 and C_2 positions of 3MC.

(4). To examine if 3-OHMC is a metabolite of 3MC. If it is, to determine the amount of its formation under a variety of experimental conditions.

(5). To determine enantioselective disposition of racemic 1-OH-3MC and 2-OH-3MC by various rat liver microsomal preparations.

(6). Stereoselective metabolism studies of 1-OH-3MC, 2-OH-3MC, 3MC-2-one, 3-OHMC, 3MC *cis*-1,2-diol and 3MC *trnas*-1,2-diol, respectively, by rat liver microsomes and effects of enzyme induction. These studies include:

6a. Separation of metabolites by reversed-phase and normal-phase HPLC.

6b. Structural identification of metabolites.

6c. Determination of absolute configuration of major chiral metabolites.

6d. Determination of enantiomeric composition of major chiral metabolites.

6e. Effect of pretreatment of rats with phenobarbital, Aroclor 1254 (polychlorinated biphenyls), or 3MC on the metabolic activity of liver microsomal preparations.

6f. Quantitative comparison of product formation and substrate disposition.

6g. Comparative metabolism study of racemic [^{3}H]1-OH-3MC by rat and human liver microsomes.

MATERIALS AND METHODS

Materials

3MC, $NADP^+$, glucose 6-phosphate (G-6-P), and G-6-P dehydrogenase (G-6-PD) were purchased from Sigma Chemical Co. (St. Louis, MO). Small amounts of authentic 1-OH-3MC, 2-OH-3MC, 3MC-1-one, 3MC-2-one and 3MC *cis*-1,2-diol, 1-hydroxybenz[a]anthracene (1-OH-BA), 2-OH-BA, 3-OH-BA, 4-OH-BA, 5-OH-BA and 6-OH-BA were obtained from the Chemical Respository of the National Cancer Institute, Bethesda, MD. Phenobarbital (PB) and PCB (Aroclor 1254) were purchased from Merck & Co., Inc. (Rahway, NJ) and from Analabs, Inc. (North Haven, CT), respectively. The liquid scintillation cocktail used in the quantitative studies (Scinti Verse I) and sodium borohydride ($NaBH_4$) were purchased from Fisher Scientific Co. (Fair Lawn, NJ). Bromine, osmium tetroxide (OsO_4) and 2,3-dichloro-5,6-dicyano-1,4-benzoquinone (DDQ) from Aldrich Chemical Co. (Milwaukee, WI) were used for synthesis of 3MC derivatives. All other reagents, solvents, biochemicals, and materials were purchased form commercial sources. Spraque-Dawley male rats (80-100 g, Charles River Breeding Laboratories, Wilmington, MA) were used for preparation of liver microsomes.

Methods

1. *Synthesis of 3MC Derivatives and Tritium Labeled 1-OH-3MC*

1.1 *Synthesis of 3MC cis-1,2-diol, 3MC-2-one and 2-OH-3MC (Sims, 1966)*

3MC (1.4 g) in 280 ml dry CCl_4 was cooled to 0°C and 0.5 ml of bromine in CCl_4 (20 ml) was added during 15 min. Pyridine (15 ml) was added and after 1 hr, the mixture was filtered to remove pyridine hydrobromide. The solvent was removed under reduced pressure and the residue was extracted twice with ethyl acetate. The extract contained 3-methylcholanthrylene (3MCE, ~0.8 g). A solution of OsO_4 (1 g) in ether (8 ml) was added

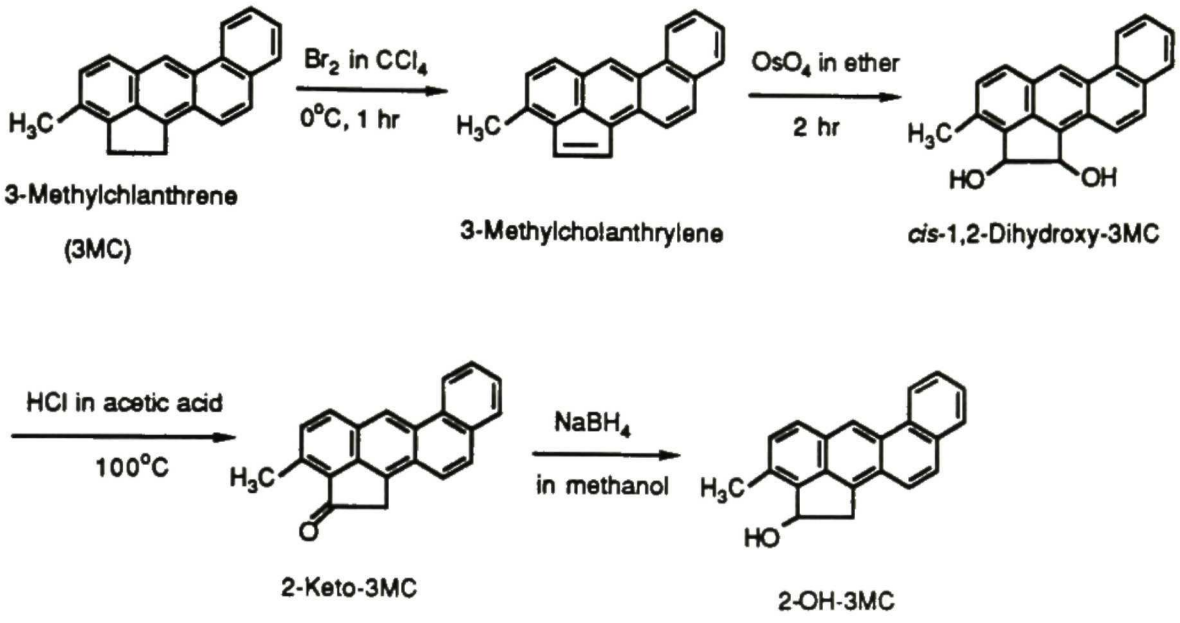

Figure 5. Synthesis of 3MC *cis*-1,2-diol, 3MC-2-one and 2-OH-3MC.

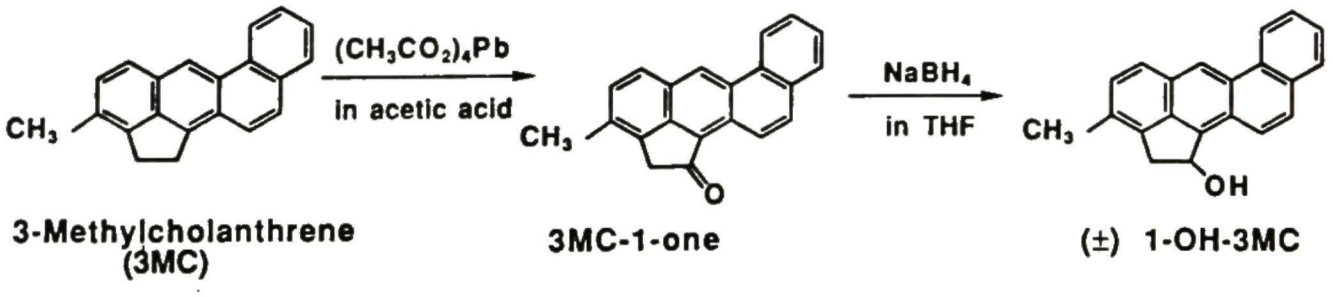

Figure 6. Synthesis of 3MC-1-one and 1-OH-3MC.

dropwise to a solution of 3MCE (~0.8 g) in benzene (60 ml) and ether (60 ml). After 1.5 hr, pyridine (4 ml) was added, and the reaction mixture was reduced on a rotatory evaporator. The concentrate was diluted with pyridine (25 ml), and a solution of sodium bisulfite (2 g) in 20 ml of water and 10 ml of pyridine were added separately followed by an excess of water to precipitate the 3MC *cis*-1,2-diol (~1.0 g). 3MC *cis*-1,2-diol (1.0 g) in 13 ml acetic acid containing a few drops of concentrated HCl was heated at 100°C for 5 min. Water was added until the solution became cloudy and it was allowed to cool, and then filtered and dried. The yield of 3MC-2-one was ~0.67 g. 2-OH-3MC (~0.5 g) was obtained by reduction of 3MC-2-one (0.67 g) with $NaBH_4$ in methanol at room temperature for 20 min (Fig. 5).

1.2 *Synthesis of 3MC-1-one and 1-OH-3MC (Sims, 1966)*

A suspension of lead tetraacetate (3.4 g) in 100 ml glacial acetic acid was added over 1 hr to a solution of 3MC (2 g) in 200 ml benzene with ice bath cooling. After 15 min of additional reaction time at room temperature, ethyl acetate was added and the mixture was washed to neutrality with water. The ethyl acetate phase was dried over anhydrous sodium sulfate (Na_2SO_4). The crude product (3MC-1-one) was obtained by evaporation of the solvent. The crude 3MC-1-one was dissolved in 25 ml dry tetrahydrofuran (THF) and added dropwise to a solution of 1 g $NaBH_4$ in 75 ml THF at room temperature. The reduction products (containing 1-OH-3MC) were chromatographed on alumina with hexane (Fig. 6). The elution order of chromatographed fractions was 3MC, 3MC-1-one, 2-OH-3MC and the major product 1-OH-3MC. A fraction containing 1-OH-3MC was isolated and purified from 3MC-1-one and 2-OH-3MC by normal-phase HPLC (on a silica gel column) with methylene chloride/hexane (3:1, v/v) as the elution solvent.

1.3 *Synthesis of 3MC trans-1,2-diol*

3MC *cis*-1,2-diol (8 mg) obtained as described above was further oxidized to 3MC-1,2-dione by reaction with 2,3-dichloro-5,6-dicyano-1,4-benzoquinone (DDQ, 34 mg) in 5 ml of benzene and by refluxing at 80°C for 6 hr. The resulting 3MC-1,2-dione was

converted to 3MC *trans*-1,2-diol (~5.6 mg) by reduction with $NaBH_4$ in methanol at room temperature for 30 min.

1.4 *Synthesis of tritium labeled 1-OH-3MC (Gardiner and Stoming, 1984)*

3MC-1-one (5.6 mg, 0.02 mmol) was dissolved in 2 ml of methanol/THF in a 10-ml screw-cap tube containing NaB^3H_4 (100 mCi/0.01 mmol). Approximately 5 mg of unlabeled $NaBH_4$ was added to the tube to complete the reduction reaction. After 30 min at room temperature, 5 ml ethyl acetate and 2 ml water were added and the organic phase was transferred to another test tube. The organic phase was evaporated to dryness at 50°C under a stream of nitrogen. The residue was dissolved in acetonitrile/THF and purified on a DuPont Zorbax ODS column eluted with a 20-min linear gradient from acetonitrile/water (2:3, v/v) to acetonitrile at 2 ml/min. The retention time of [^{3}H]-1-OH-3MC was 18 min and specific activity was 184 mCi/mmol.

2. *Preparation of Rat and Human Liver Microsomes*

Male Sprague-Dawley rats weighing 80-100 g were treated intraperitoneally with PB (sodium salt; 75 mg/kg body weight, injected in 0.5 ml of water) once daily on each of three consecutive days or with 3MC (25 mg/kg body weight, injected in 0.5 ml of corn oil) or PCB (50 mg/kg body weight, injected in 0.5 ml of corn oil) injected once daily for each of four consecutive days. The rats were sacrificed the next day after the last injection of the drug. Liver microsomes were prepared as described (Alvares *et al.*, 1970). Microsomal protein was determined by the method of Lowry *at al.* (1951) with bovine serum albumin as the protein standard. Human liver microsomes were generously provided by Dr. F. Peter Guengerich, Center in Molecular Toxicology, Department of Biochemistry, Vanderbilt University. Liver microsomes were prepared from two non-smoking subjects, one died in a motor vehicle accident with head injury and the other by a gun shot wound to head, respectively. Human liver microsomes were prepared similarly

as rat liver microsomes and the P-450 concentrations were 0.74 and 0.29 nmol/mg protein respectively. All liver microsomes were stored at –80°C until use.

3. *In Vitro Metabolism of 3MC Derivatives*

3.1 *A typical 100-ml metabolic incubation*

Typically, a 100-ml reaction mixture contained 100-mg protein equivalent of rat liver microsomes, 5 mmol of Tris-HCl (PH 7.5), 0.3 mmol of $MgCl_2$, 10 units of G-6-P dehydrogenase (type XII, Sigma Chemical Co.), 10 mg of $NADP^+$, and 48 mg of G-6-P. The reaction mixture is pre-incubated at 37°C for 2 min in a water shaker bath. 3MC (or one of its derivatives, 8 mmol in 4 ml of acetone) is then added and incubated for 30 min with liver microsomes derived from untreated, PB- or 3MC-treated rats. Remaining substrate and metabolites are extracted by sequential additions of 100 ml of acetone and 200 ml of ethyl acetate. The organic solvent extract is dehydrated with anhydrous $MgSO_4$, filtered, and evaporated at 50°C to dryness under reduced pressure. The residue is redissolved in THF or methanol for reversed-phase HPLC analysis. For quantification of various metabolites formed, the incubation time and volume, protein content, and substrate concentration were adjusted as required. An internal standard, whenever required for quantification, is added following the addition of acetone to the reaction mixture.

3.2 *Incubation of [^{3}H]-1-OH-3MC*

[^{3}H]-1-OH-3MC was incubated in a 1-ml reaction mixture containing microsomes prepared from livers of either untreated, PB-treated, or 3MC-treated rats or from human liver. Each ml of reaction mixture contained 0.5 (or 2) mg protein equivalent of liver microsomes, 0.05 mmol of Tris-HCl (pH 7.5), 3 μmol of $MgCl_2$, 0.1 unit of G-6-P dehydrogenase, 0.1 mg of $NADP^+$ and 0.48 mg of G-6-P. A 10-ml screw-cap test tube containing the reaction mixture was pre-incubated at 37°C for 2 to 5 min in a water shaker bath. [^{3}H]-1-OH-3MC (80 nmol in 50 μl of acetone/ml of incubation mixture, specific activity 184 mCi/mmol) was then added and the mixture was incubated for 30 min.

Unreacted substrate and its metabolites were extracted by sequential additions of 1 vol of acetone and 2 vol of ethyl acetate. The organic phase was removed and the aqueous phase was re-extracted with ethyl acetate (2 ml). Ethyl acetate extracts were combined and evaporated at 50°C to dryness under a stream of nitrogen. To each residue was added reference metabolites formed in the metabolism of unlabeled 1-OH-3MC by liver microsomes from PB-treated rats. The sample (50 µl) was injected onto a Nova-Pak C_{18} cartridge (8 mm i.d. x 10 cm; 4 µm particles). HPLC analysis was conducted according to the method described below and the solvent flow rate was 1 ml/min.

4. *High Performance Liquid Chromatography*

HPLC was performed on either one of the two following systems: a Waters Associates (Milford, MA) liquid chromatograph consisting of a model 6000A solvent delivery system, a model 660 solvent programmer, and a model 440 absorbance (254 or 280 nm) detector. Samples were injected via a Valco model N60 loop injector (Valco Instruments, Houston, TX). Retention times and ratios of chromatographic peaks were recorded with a Hewlett-Packard model 3390A integrator. Alternatively, a Hewlett-Packard Model HP1090A LC equipped with an HP 9153B personal computer, an HP Model 1040 diode-array detector, a ternary solvent delivery system, and an automatic sampler/injector was used.

4.1 *Normal-Phase HPLC*

Metabolites formed in the metabolism of a PAH were separated on a Golden Series Zorbax SIL column (Du Pont Co., Wilmington, DE) using a nonpolar solvent such as methylene chloride or hexane containing THF or ethyl acetate as the elution solvent.

4.2 *Reversed-Phase HPLC*

A PAH and its metabolites were separated with a Waters Associates RCM-100 radial compression module fitted with a Nova-Pak C_{18} cartridge (8 mm i.d. x 10 cm; 4 µm particles) eluted with a 50-min linear gradient from methanol/water (2:3, v/v) to methanol at

2 ml/min or on a Du Pont Golden Series Zorbax ODS (C_{18}) column (6.2 mm i.d. x 25 cm) eluted with a 30-min linear gradient from acetonitrile/water (2:3 v/v) to acetonitrile at 2 ml/min.

4.3 *Chiral Stationary Phase HPLC*

The enantiomeric pairs of some chiral derivatives of 3MC were separated on an analytical column (4.6 or 10 mm i.d. x 25 cm (Regis Chemical Co., Morton Grove, IL) packed with spherical particles of 5 μm diameter of γ-aminopropylsilanized silica to which either (*S*)-*N*-(3,5-dinitrobenzoyl)leucine (*S*-DNBL) or (*R*)-*N*-(3,5-dinitrobenzoyl) phenylglycine (*R*-DNBPG) are either convalently or ionically bonded. The elution solvent was <20 % (v/v) of solvent A (ethanol:acetonitrile, 2:1, v/v) in hexane. Enantiomeric pairs of 1-OH-3MC, 3MC *cis*-1,2-diol or 3MC *trans*-1,2-diol were resolved by CSP HPLC (Figs. 7 and 12).

5. *Determination of Absolute Configurations and Preparation of 1-OH-3MC , 2-OH-3MC, 3MC cis-1,2-diol and 3MC trans-1,2-diol Enantiomers*

5.1 *Enantiomeric separation of 1-OH-3MC, 3MC cis-1,2-diol and 3MC trans-1,2-diol*

Each enantiomeric pair of 1-OH-3MC, 3MC *cis*-1,2-diol and 3MC *trans*-1,2-diol were resolved using either covalently or ionically bonded *R*-DNBPG columns (Figs. 7 and 12).

5.2 *Preparation of optically pure enantiomers of 2-OH-3MC*

The racemic 2-OH-3MC was converted to a pair of diastereomeric esters by reaction with an excess amount of (–)-menthoxyacetyl chloride similarly as described (Cook *et al.*, 1950). The resulting diastereomeric (–)-menthoxyacetates were injected onto a DuPont Zorbax ODS column (6.2 mm i.d. x 25 cm) eluted with methanol/water (19:1) at flow rate of 2 ml/min. The peak with retention time of 29 min contained the 2-(–)-menthoxyacetate of 2-OH-3MC. Two diastereomeric (–)-menthoxyacetates of 2-OH-3MC were resolved by normal-phase HPLC. The retention times were 28 and 30 min, respectively (right

chromatogram, Fig. 7). Methanolysis of the resolved (–)-menthoxyacetates in methanol/THF/0.1 NaOH (1:1:1, v/v) at 50°C for 40 min gave optically pure 2-OH-3MC enantiomers. Optically pure 2*R*- and 2*S*-OH-3MC in methanol have Φ_{257}/A_{294} values of –5 and +5 millidegrees, respectively (Fig. 9).

5.3 *Determination of absolute configuration of enantiomeric 1-OH-3MC , 2-OH-3MC, 3MC trans-1,2-diol and 3MC cis-1,2-diol*

The absolute configurations of 1-OH-3MC, 2-OH-3MC and 3MC *trans*-1,2-diol enantiomers were determined by the exciton chirality CD method (Harada *et al.*, 1972). Enantiomeric 1-OH-3MC, 2-OH-3MC or 3MC *trans*-1,2-diol (0.3 mg) was dissolved with 2 ml of ethyl acetate which had been dried with sodium hydride. Additional sodium hydride (1 mg) was then added, followed by the addition of 5 mg of *p*-nitrobenzoyl chloride or *p-N,N*-dimethylaminobenzoyl chloride. The test tube was placed on ice for about 5 min. 2 Drops of *p-N,N*-dimethylaminopyridine (10 mg/ml in ethyl acetate) were added as a catalyst, and the solution was stirred overnight, allowing it to come to ambient temperature. Solid material was removed by centrifugation and the supernatant was evaporated to dryness. The residue was redissolved in THF/acetonitrile (1:1, v/v) for reversed-phase HPLC separation of 1-OH-3MC and 2-OH-3MC *p*-nitrobenzoate or 3MC *trans*-1,2-diol *p-N,N*-dimethylaminobenzoate. The absolute configurations of enantiomeric mono-ols and 3MC *trans*-1,2-diol was assigned on the basis of the CD spectrum of a benzoate derivative, according to the exciton chirality CD method as indicated in Figs. 8, 9 and 14. Absolute configuration of 3MC *cis*-1,2-diol enantiomers was deduced by the *cis*-1,2-diol formed in the metabolism of enantiomeric 1-OH-3MC.

6. *Spectral Analysis*

6.1 *Ultraviolet absorption spectroscopy*

Uv-visible absorption spectra of samples in solvent are determined using a 1-cm path length quartz cuvette with a Varian Model Cary 118C spectrophotometer or a DW2000

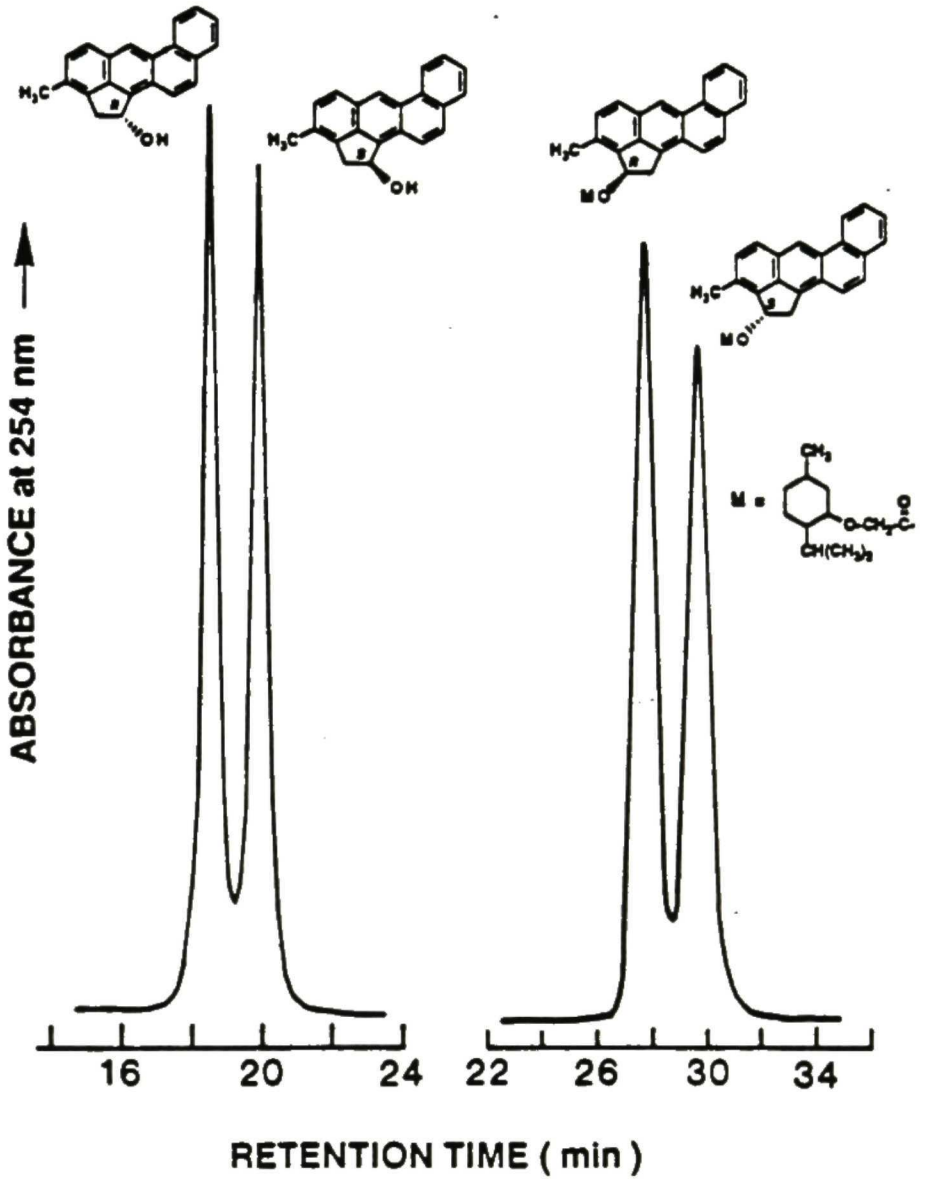

Figure 7.

Left chromatogram: Separation of enantiomeric 1-OH-3MC by CSP HPLC. A covalently bonded *R*-DNBPG column was used and the mobile phase was 5% (v/v) of ethanol/acetonitrile (2:1, v/v) in hexane at a flow rate of 2 ml/min.

Right chromatogram: Separation of diastereomeric (–)-menthoxyacetates of 2-OH-3MC by normal-phase HPLC. A DuPont Zorbax SIL column (6.2 mm i.d. x 250 mm) was used and the mobile phase was ethyl acetate/methylene chloride/hexane (0.8:10:89.2, vol ratio) at a flow rate of 2 ml/min.

Figure 8. CD spectrum of 1*R*-OH-3MC (· · · · , Φ_{258}/A_{294} = –2.7 millidegrees; enantiomerically pure; concn. 1.0 A_{294}/ml, methanol) and uv absorption (– – – –, methanol) and CD (——, concn. 1.0 A_{294}/ml, methanol) spectra of the *p*-nitrobenzoate of 1*R*-OH-3MC. 1*R*-OH-3MC was the less strongly retained enantiomer on a covalently bonded *R*-DNBPG column (see Fig. 7, left chromatogram). BA and Bz indicate the longitudinal transition dipole of the benz[*a*]anthracene chromophore (by looking from the side of the aromatic plane) and that of the *p*-nitrobenzoate, respectively. H_1 and H_2 indicate hydrogen atoms at C_1 and C_2, respectively.

Figure 9. CD spectrum of 2*R*-OH-3MC (· · · · , Φ_{258}/A_{294} = –5.0 millidegrees; enantiomerically pure; concn. 1.0 A_{294}/ml, methanol) and uv absorption (– – –, methanol) and CD (——, concn. 1.0 A_{294}/ml, methanol) spectra of the *p*-nitrobenzoate of 2*R*-OH-3MC. 2*R*-OH-3MC was derived by methanolysis of the diastereomeric (–)-menthoxyacetate of 2-OH-3MC less strongly retained on normal-phase HPLC (see Fig. 7, right chromatogram). BA and Bz indicate the longitudinal transition dipole of the benz[*a*]anthracene chromophore (by looking from the side of the aromatic plane) and that of the *p*-nitrobenzoate, respectively. H_1 and H_2 indicate hydrogen atoms at C_1 and C_2, respectively.

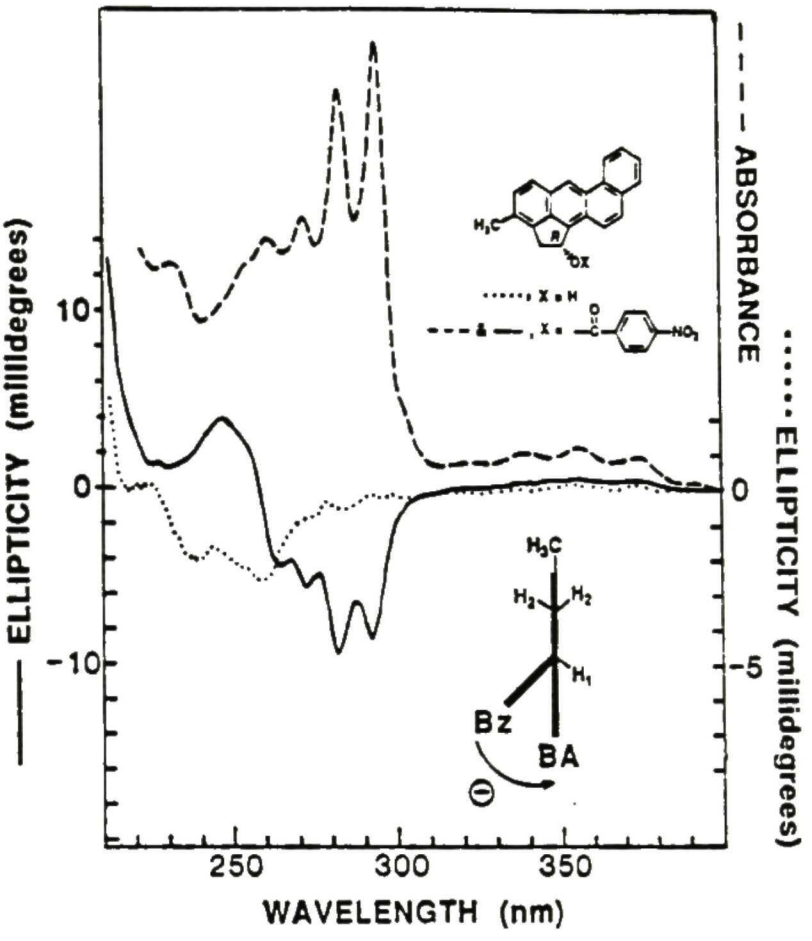
ELLIPTICITY (millidegrees)
ABSORBANCE
ELLIPTICITY (millidegrees)
10
0
-10
0
-5
250
300
350
WAVELENGTH (nm)
Bz
BA

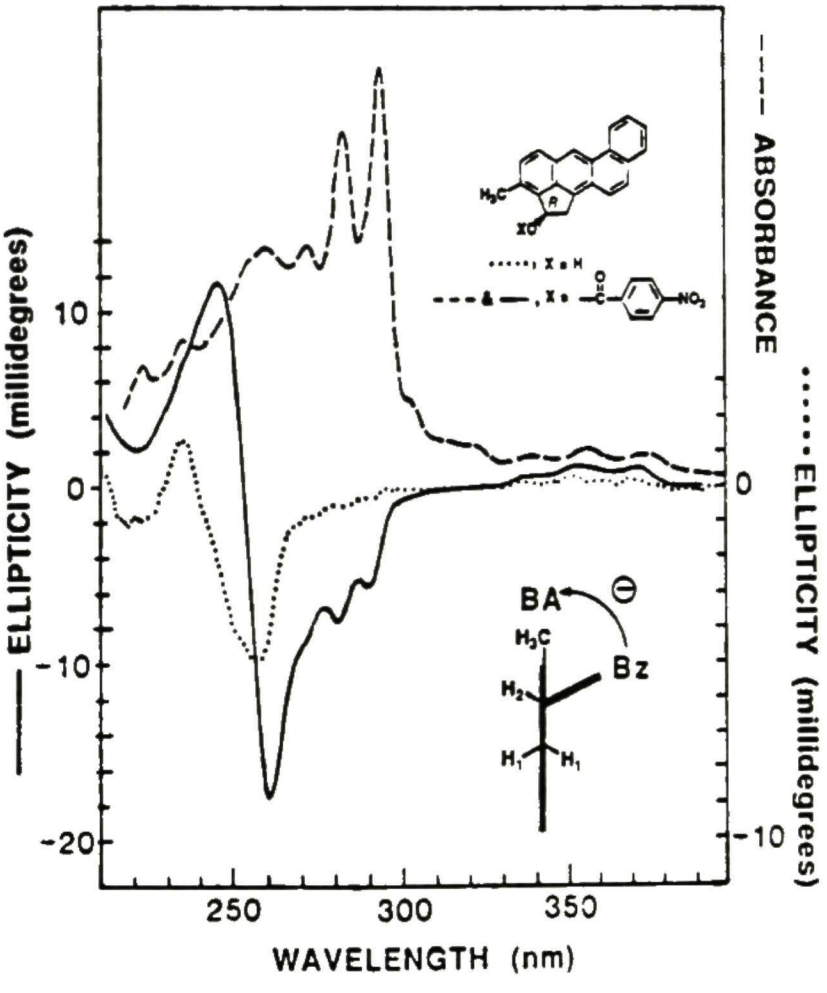
ELLIPTICITY (millidegrees)
ABSORBANCE
ELLIPTICITY (millidegrees)
10
0
-10
-20
0
-10
250
300
350
WAVELENGTH (nm)
BA
Bz

UV/VIS scanning spectrophotometer (slit 2 nm and scan rate 2 nm/sec; SLM Instruments, Inc., Urbana, IL).

6.2 *Mass spectrometry*

Mass spectral analysis was performed on a Finnigan Model 4000 gas chromatograph-mass spectrometer-data system by either electron impact or chemical ionization (methane) with a solid probe at 70 eV and 250°C ionizer temperature.

6.3 *Circular dichroism spectroscopy*

CD spectra of samples in a quartz cell of 1 cm path length at room temperature (23°C) were measured using a Jasco Model 500A spectropolarimeter equipped with a Model DP500 data processor. The concentration of the sample is indicated by $A_{\lambda 2}$/ml (absorbance units at wavelength $\lambda 2$ per ml of solvent). CD spectra are expressed by ellipticity ($\Phi_{\lambda 1}/A_{\lambda 2}$, in millidegrees) for solutions that have an absorbance of $A_{\lambda 2}$ unit per ml of solvent at wavelength $\lambda 2$ (usually the wavelength of maximal absorption). Under conditions of measurements indicated above, the molar ellipticity ($[\theta]_{\lambda 1}$, in deg cm^2 $dmole^{-1}$) and ellipticity ($\Phi_{\lambda 1}/A_{\lambda 2}$, in millidegrees) are related to the molar extinction coefficient ($\varepsilon_{\lambda 2}$, in cm^{-1} M^{-1}) as follows:

$$[\theta]_{\lambda 1} = 0.1\ \varepsilon_{\lambda 2}\ (\Phi_{\lambda 1}/A_{\lambda 2})$$

6.4 *Liquid scintillation spectrometry*

Liquid scintillation counting of radioactive ^3H vials, obtained from the HPLC fraction collector, was performed on a Beckman model LS3801 in the single channel mode. The conversion of radioactivity (DPM) to concentration (pmols) was calculated based on the specific activity of compounds.

RESULTS

1. *Stereoselective Formation and Disposition of 1-OH-3MC and 2-OH-3MC in the Metabolism of 3MC* (Shou and Yang, 1990a)

1.1 *Separation of enantiomeric pairs of 1-OH-3MC and 2-OH-3MC*

In an earlier report (Yang *et al.*, 1984), enantiomers of 1-OH-3MC were resolved on an ionically bonded *R*-DNBPG column, while enantiomers of 2-OH-3MC were not resolved. In this study, we found that the covalently bonded *R*-DNBPG column afforded improved resolution of enantiomeric 1-OH-3MC (left chromatogram, Fig. 7), while enantiomers of 2-OH-3MC were still not separable.

Racemic 2-OH-3MC was derivatized with (–)-menthoxyacetyl chloride and the resulting diastereomers were resolved by normal-phase HPLC (right chromatogram, Fig. 7). Repetitive chromatography afforded optically pure diastereomeric (–)-menthoxyacetates. Optically pure 2-OH-3MC enantiomers were each obtained by methanolysis of the respective diastereomeric (–)-menthoxyacetate. CD spectra of 2-OH-3MC enantiomers are mirror images of each other and have CD Cotton effects characteristically different from those of 1-OH-3MC enantiomers (Fig. 9 vs. Fig. 8). Enantiomers of 1-OH-3MC can also be resolved, with lower efficiency than those of 2-OH-3MC, as diastereomers of (–)-menthoxyacetates. However, the resolved diastereomers were unstable and could not be used to prepare sufficient quantity of optically pure 1-OH-3MC enantiomers for further metabolic studies.

Optically pure enantiomers have the following CD Cotton effects (in millidegrees): 1*R*-OH-3MC, $\Phi_{258}/A_{294} = -2.7$; 1*S*-OH-3MC, $\Phi_{258}/A_{294} = +2.7$; 2*R*-OH-3MC, $\Phi_{258}/A_{294} = -5.0$; 2*S*-OH-3MC, $\Phi_{258}/A_{294} = +5.0$ (see the section below for assignment of absolute configuration of enantiomers). Availability of CD spectral data of optically pure enantiomers of 1-OH-3MC and 2-OH-3MC allowed the determination of enantiomeric

compositions of 1-OH-3MC and 2-OH-3MC formed in the metabolism of 3MC (see below).

1.2 *Absolute configurations of enantiomeric 1-OH-3MC and 2-OH-3MC*

A 2-OH-3MC enantiomer, derived from the methanolysis of the less strongly retained 2-OH-3MC (–)-menthoxyacetate on normal-phase HPLC (Fig. 7, right chromatogram), was converted to a *p*-nitrobenzoate by reaction with *p*-nitrobenzoyl chloride. Since the extinction coefficient of *p*-nitrobenzoyl group (ε_{260} = 15100, Harada *et al.*, 1983) is considerably lower than that of benz[*a*]anthracene (ε_{260} ≈ 47000), uv absorption spectrum of the *p*-nitrobenzoate is essentially the same as that of benz[*a*]anthracene (Fig. 9). Mass spectral analysis of the *p*-nitrobenzoate indicated molecular ions at *m/z* 433 with characteristic fragment ions at *m/z* 266 (loss of *p*-nitrobenzoic acid). CD spectrum of the *p*-nitrobenzoate exhibited a strongly split Cotton effect due to chiral exciton coupling between the electric transition dipole moments of *p*-nitrobenzoate and benz[*a*]anthracene chromophores; positive at ~245 nm, negative at ~261 nm, and passing through zero at 254 nm (Fig. 9). The negative chirality exhibited in the CD spectrum of the *p*-nitrobenzoate (Fig. 9) indicated that the 2-OH-3MC, derived by methanolysis of the less strongly retained diastereomeric (–)-menthoxyacetate on normal-phase HPLC (Fig. 7, right chromatogram), has a 2*R* absolute stereochemistry (Harada *et al.*, 1983).

The 1-OH-3MC enantiomer less strongly retained on a covalently bonded *R*-DNBPG column was also converted to a *p*-nitrobenzoate by reaction with *p*-nitrobenzoyl chloride. Mass spectral analysis of the *p*-nitrobenzoate indicated molecular ions at *m/z* 433 with a characteristic fragment ion at *m/z* 266 (loss of *p*-nitrobenzoic acid). CD spectrum of this *p*-nitrobenzoate exhibited a split Cotton effect due to chiral exciton coupling between the electric transition dipole moments of *p*-nitrobenzoate and benz[*a*]anthracene chromophores; positive at ~246 nm, negative at ~262 nm, and passing through zero at 258

nm (Fig. 8). The negative chirality exhibited in the CD spectrum of the *p*-nitrobenzoate indicated that the less strongly retained enantiomer on the covalently bonded *R*-DNBPG column has a 1*R* absolute stereochemistry (Harada *et al.*, 1983). This confirms the assignments of absolute configurations of 1-OH-3MC enantiomers reported earlier (Yang *et al.*, 1984), which was based on the HPLC elution order on an ionically bonded *R*-DNBPG column.

The absolute configuration of an enantiomeric 1-OH-3MC has recently been determined by another method (Shou and Yang, 1990c). In that study, enantiomers of 3MC *trans*-1,2-diol were resolved on a covalently bonded *R*-DNBPG column and their absolute configurations were determined by the exciton chirality CD method (Harada *et al.*, 1983) after conversion to a *bis-p-N,N*-dimethylaminobenzoate derivative. Subsequently, a 1-OH-3MC enantiomer, which is more strongly retained on the *R*-DNBPG column (Fig. 7, left chromatogram), was incubated with rat liver microsomes and a 3MC *trans*-1,2-diol was isolated from a mixture of metabolites by reversed-phase HPLC. This metabolically formed 3MC *trans*-1,2-diol was found to be a 3MC *trans*-1*R*,2*R*-diol. Hence, the 1-OH-3MC enantiomer, from which the 3MC *trans*-1*R*,2*R*-diol was derived from, was deduced to be the 1*S*-enantiomer. The result of that study (see later) was consistent with the conclusion reached in the present report regarding the absolute configuration-CD spectra-CSP HPLC elution order relationship of 1-OH-3MC enantiomers. By an approach similar as described (Shou and Yang, 1990c), we have also established the absolute configurations of enantiomeric 2-OH-3MC (Shou and Yang, 1990d). These results provided additional evidence consistent with the conclusion reached in the present report regarding the absolute configurations of enantiomeric 1-OH-3MC and 2-OH-3MC.

1.3 *Regioselective metabolism at the C_1 and C_2 positions of 3MC*

1-OH-3MC and 2-OH-3MC were previously reported to be closely eluted on reversed-phase HPLC (Thakker *et al.*, 1978; Stoming *et al.*, 1977; Tierney *et al.*, 1979; Eastman *et al.*, 1979). In this study, 1-OH-3MC and 2-OH-3MC formed in the

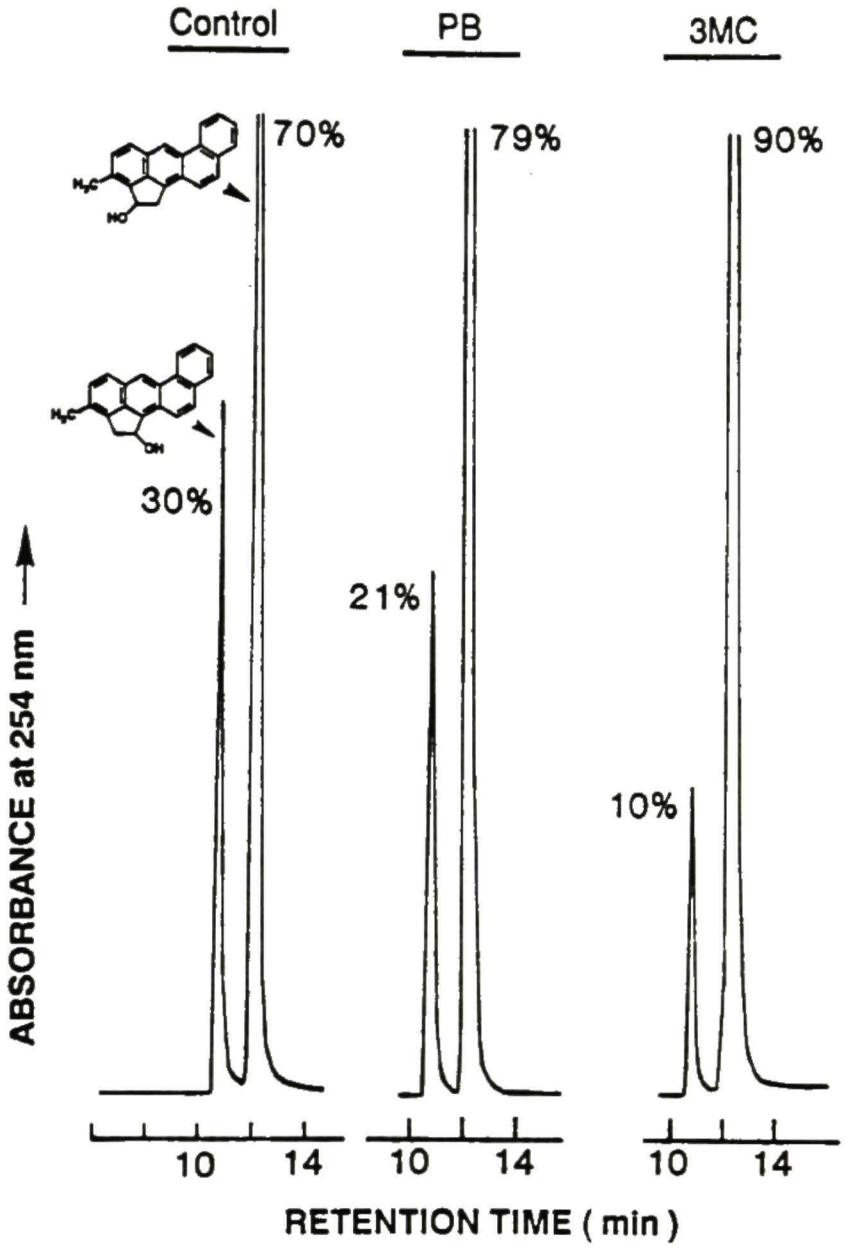

Figure 10. Normal-phase HPLC separation of 1-OH-3MC and 2-OH-3MC formed in the metabolism of 3MC by liver microsomes from untreated (control), PB-treated, and 3MC-treated rats, respectively. Relative amounts of 1-OH-3MC and 2-OH-3MC were determined by areas under the curves at 254 nm.

metabolism of 3MC by rat liver microsomes were collected as a mixture on reversed-phase HPLC by using a C_{18} radial compression column. Consistent with several reports (Thakker *et al.*, 1978; Stoming *et al.*, 1977; Tierney *et al.*, 1979; Eastman *et al.*, 1979) but contrary to one report (King *et al.*, 1977), 2-OH-3MC was eluted slightly ahead of 1-OH-3MC under our chromatographic conditions.

1-OH-3MC and 2-OH-3MC, collected on reversed-phase HPLC, were separated on normal-phase HPLC (Fig. 10). The metabolically formed 1-OH-3MC and 2-OH-3MC were identical to the authentic compounds with respect to uv-vis absorption spectra, mass spectra, and retention times on both reversed-phase and normal-phase HPLC. Incubations of 3MC (Table 2) were performed with reaction mixtures (shown in Materials and Methods) containing 0.5 mg of protein equivalent of rat liver microsomes per ml of reaction mixture at 37°C for 10 or 60 min. For a 10 min incubation, percentages of 3MC metabolized, determined with the aid of an internal standard (anthanthrene), were ~6 (control), ~17 (PB-treated), and ~15% (3MC-treated), respectively. For a 60 min incubation, percentages of 3MC metabolized were ~24 (control), ~39 (PB-treated), and ~35% (3MC-treated), respectively. The concentration ratios of [1-OH-3MC]:[2-OH-3MC], formed in the metabolism of 3MC by rat liver microsomes, were determined by normal-phase HPLC (Fig. 10); 30:70 (control), 21:79 (PB-treated), and 10:90 (3MC-treated), respectively, for a 10 min incubation, and 34:66 (control), 15:85 (PB-treated), and 2:98 (3MC-treated), respectively, for a 60 min incubation (Table 1). The results indicated that cytochrome P-450 isozymes in all three rat liver microsomal preparations were more regioselective in catalyzing the hydroxylation reaction at the C_2 position than at the C_1 position of 3MC. Cytochrome P-450 isozymes in liver microsomes from 3MC-treated rats have the highest regioselectivity toward the C_2 position.

1.4 *Stereoselective hydroxylation at the C_1 and C_2 positions of 3MC*

1-OH-3MC and 2-OH-3MC, formed in the metabolism of 3MC by each of the three rat liver microsomal preparations, were isolated by reversed-phase (see chromatographic

Table 1. Regioselective and stereoselective metabolism at C_1 and C_2 positions of 3MC by rat liver microsomes.

Microsomes[a]	% of 3MC Metabolized[b]	% Formed[c]		Enantiomer Ratio (*R*/*S*)[d]	
		1-OH-3MC	2-OH-3MC	1-OH-3MC	2-OH-3MC
Experiment 1					
Untreated (Control)	~6	30	70	35:65	14:86
PB-treated	~17	21	79	39:61	6:94
3MC-treated	~15	10	90	46:54	6:94
Experiment 2					
Untreated (Control)	~24	34	66	27:73	7:93
PB-treated	~39	15	85	47:53	8:92
3MC-treated	~35	2	98	42:58	2:98

[a] Liver microsomes (0.5 mg protein per ml of incubation mixture) from untreated (control), PB-treated, and MC-treated rats. Each ml of reaction mixture contains 80 nmol of 3MC and was incubated at 37°C for 10 min (experiment 1) or 60 min (experiment 2). Incubation conditions of experiment 1 were similar to those described by Thakker *et al.* (1978).

[b] Percent of 3MC metabolized was estimated with the aid of an internal standard (anthanthrene) for chromatography.

[c] Percentage of the sum of 1-OH-3MC and 2-OH-3MC, determined by normal-phase HPLC (Fig. 10). Average values of duplicate samples which agree within 10% of the values shown.

[d] Enantiomeric ratio of 1-OH-3MC was determined by CSP HPLC on a covalently bonded *R*-DNBPG column (Fig. 7, left chromatogram). Enantiomeric ratio of 2-OH-3MC was determined by the magnitude of CD Cotton effect at 258 nm.

Table 2. Enantioselective metabolism of racemic 1-OH-3MC and 2-OH-3MC by rat liver microsomes.

Microsomes[a]	Substrate unmetabolized (nm/ml)	Incubation Time (min)	Substrate Metabolized (%)[b]	*R/S* Ratio of Substrate[c]
Untreated (Control)	1-OH-3MC (8)	10	53.9	58:42
	(8)	20	60.3	62:38
	(8)	30	65.4	65:35
	(8)	40	66.7	67:33
PB-treated	1-OH-3MC (30)	10	23.4	61:39
	(30)	20	35.0	62:38
	(30)	40	65.8	79:21
3MC-treated	1-OH-3MC (40)	10	63.4	61:39
	(40)	20	81.2	73:37
	(40)	30	83.5	70:30
	(40)	40	89.1	72:28
Untreated (Control)	2-OH-3MC (20)	10	58.2	43:57
	(20)	20	76.7	43:57
	(20)	30	79.0	41:59
PB-treated	2-OH-3MC (40)	10	68.7	42:58
	(40)	20	77.1	41:59
	(40)	30	82.2	36:64
3MC-treated	2-OH-3MC (40)	10	27.6	36:64
	(40)	20	38.8	33:67
	(40)	30	46.7	25:75

a Liver microsomes (1 mg protein per ml of incubation mixture) from untreated (control), PB-treated, and 3MC-treated rats. Each ml of reaction mixture contained the amount of 1-OH-3MC (or 2-OH-3MC) indicated in the parenthesis and was incubated at 37°C for the length of time indicated.

b Average values of duplicate samples which agree within 10% of the values shown. Percent of substrate metabolized was estimated with the aid of an internal standard (7-methylbenzo[*a*]pyrene) for chromatography.

c Enantiomeric ratios of 1-OH-3MC and 2-OH-3MC were determined as described in the footnote of Table 1.

conditions in Materials and Methods) and normal-phase (Fig. 10) HPLC. Enantiomeric compositions of 1-OH-3MC were determined by CSP HPLC using the covalently bonded *R*-DNBPG column (Fig. 7, left chromatogram). The 1*R*/1*S* enantiomeric ratios of 1-OH-3MC formed in the metabolism of 3MC by liver microsomes from untreated, PB-treated, and 3MC-treated rats were found to be 35:65, 39:61, and 46:54, respectively for a 10 min incubation (Fig. 11) and 27:73, 47:53, and 42:58, respectively for a 60 min incubation (Table 1). The 1-OH-3MC formed in the metabolism of 3MC by rat liver microsomes was consistently observed to be slightly enriched in the 1*S*-enantiomer by CD spectral analysis; Φ_{258} values were positive in all CD spectral measurements.

Enantiomeric compositions of 2-OH-3MC were determined by their magnitudes of CD Cotton effects at 258 nm, using Φ_{258}/A_{294} values of –5.0 and + 5.0 millidegrees for enantiomerically pure 2*R* and 2*S* enantiomers, respectively. The 2*R*/2*S* enantiomeric ratios of 2-OH-3MC formed in the metabolism of 3MC by liver microsomes from untreated, PB-treated, and 3MC-treated rats were found to be 14:86, 6:94, and 6:94, respectively for a 10 min incubation (Fig. 11) and 7:93, 8:92, and 2:98, respectively for a 60 min incubation (Table 1). It is interesting to note that, although the extent of further metabolism of 1-OH-3MC and 2-OH-3MC in the 60 min incubation was considerably higher than that in the 10 min incubation, enantiomeric ratios of 1-OH-3MC and 2-OH-3MC were not drastically different (Table 1). These results indicated that further metabolism of the metabolically formed 1-OH-3MC (or 2-OH-3MC) did not drastically change the enantiomeric ratios of the two alcoholic products.

1.5 *Enantioselective disposition of racemic 1-OH-3MC and 2-OH-3MC*

Racemic 1-OH-3MC (or 2-OH-3MC) was incubated for 10-40 min at 37°C with liver microsomes prepared from untreated, PB-treated, and 3MC-treated rats, respectively. In order to observe differences in the rates of metabolism of enantiomeric 1-OH-3MC (or 2-OH-3MC), relatively high protein concentrations of rat liver microsomes (1 mg protein/ml of incubation mixture) were used. Unmetabolized 1-OH-3MC (or 2-OH-3MC)

Regioselective and Stereoselective Hydroxylation at 1 and 2 Positions of 3-Methylcholanthrene

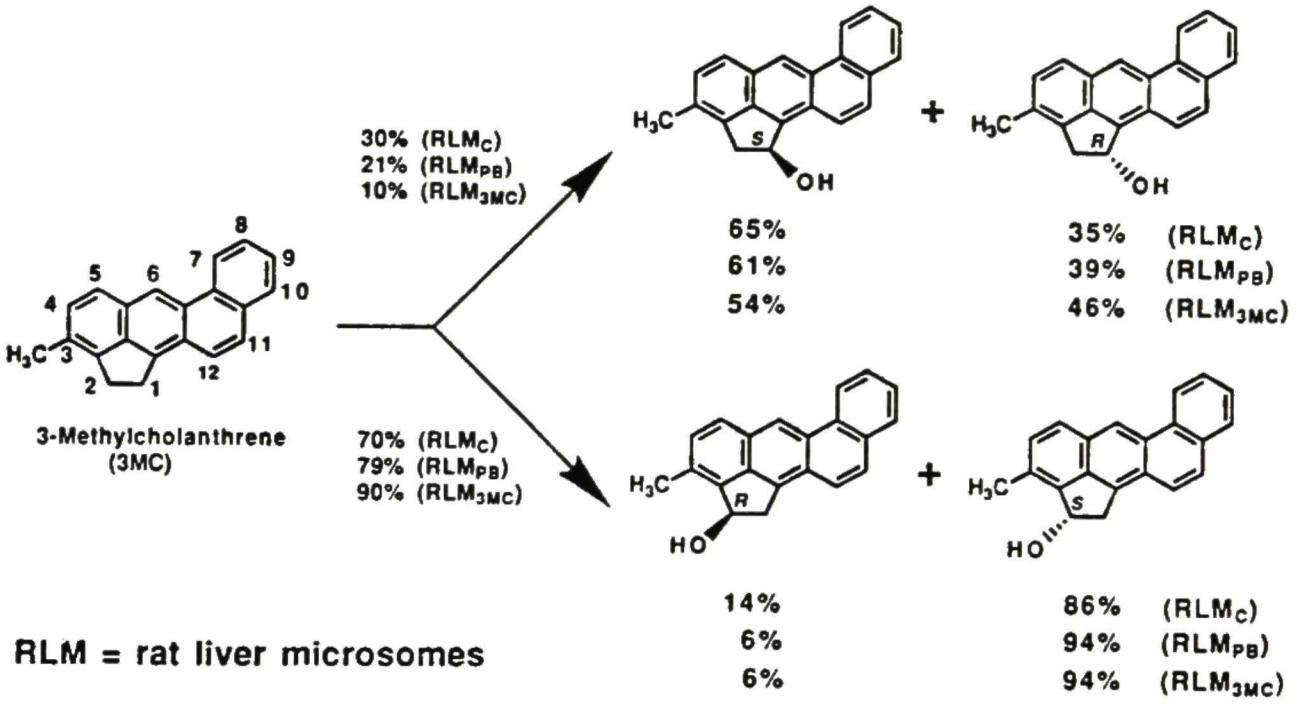

Figure 11. Regioselective and stereoselective hydroxylation reactions at C_1 and C_2 positions of 3MC by rat liver microsomes. RLM_C, RLM_{PB}, and RLM_{3MC} are liver microsomes from untreated control, PB-treated, and 3MC-treated rats, respectively. The percentage numbers were obtained from an experiment using 0.5 mg protein equivalent of rat liver microsomes and an incubation time of 10 min. The exact numbers are dependent on the concentration of microsomal enzymes and incubation time (see text for discussion).

was isolated by reversed-phase HPLC and its enantiomeric composition was determined either by CSP HPLC in the case of 1-OH-3MC (Fig. 7, left chromatogram) or by CD spectral data in the case of 2-OH-3MC (Fig. 9). In the metabolism of racemic 1-OH-3MC, all three rat liver microsomal preparations preferentially metabolize the 1*S*-enantiomer; increasing proportion of the 1*S*-enantiomer is metabolized when the time of incubation is increased (Table 2). Liver microsomes from 3MC-treated rats have slightly higher enantioselectivity toward the 1*S*-enantiomer than those from untreated and PB-treated rats (Table 2).

Unmetabolized 2-OH-3MC contains mainly the 2*S*-enantiomer. Thus all three rat liver microsomal preparations preferentially metabolize the 2*R*-enantiomer; increasingly more of the 2*R*-enantiomer is metabolized when the time of incubation is increased (Table 2). In contrast to the metabolism of racemic 1-OH-3MC, liver microsomes from 3MC-treated rats are more enantioselective toward the *R*-enantiomer of 2-OH-3MC than those from untreated and PB-treated rats (Table 2).

2. *Enantioselective Aliphatic Hydroxylations of Racemic 1-OH-3MC (Shou and Yang, 1990c)*

2.1 *CSP HPLC separation and CD spectra of enantiomeric 3MC 1,2-Diols*

Enantiomeric pairs of synthetic 3MC *trans*- and *cis*-1,2-diols were separated by HPLC on a covalently bonded *R*-DNBPG column (Fig. 12). The mobile phases, at a flow rate of 2 ml/min, were 10% and 7% of solvent A in hexane, respectively. Resolved enantiomers are indicated in Fig. 13 as t1 and t2 for the *trans* isomers and c1 and c2 for the *cis* isomers, respectively. Uv-vis absorption and CD spectra of resolved enantiomers are shown in Fig. 13. Absolute configurations of resolved enantiomers have been established in this study (see below).

2.2 *Absolute configuration of an enantiomeric 3MC trans-1,2-diol*

The uv-vis absorption and CD spectra of the *bis-p-N,N*-dimethylaminobenzoate derived by reaction of the more strongly retained enantiomer of 3MC *trans*-1,2-diol on the covalently bonded *R*-DNBPG column (peak t2, Fig. 13A) are shown in Fig. 14. The uv-vis absorption spectrum indicated characteristic absorption bands due to both benz[a]anthracene (λ_{max} 294 nm) and two *p-N-N*-dimethylaminobenzoate (λ_{max} 319 nm) chromophores. A strongly negative CD band at 321 nm in the CD chirality spectrum of the *bis-p-N,N*-dimethylaminobenzoate was due to electronic transition dipole-dipole interactions between the two benzoate groups. This characteristic negative CD band at 321 nm indicated that the enantiomeric 3MC *trans*-1,2-diol enantiomer under study has a 1*R*,2*R* absolute stereochemistry (Harada *et al.*, 1983).

2.3 *Reversed-phase HPLC separation of metabolites of 1-OH-3MC*

Metabolites formed in the incubation of racemic 1-OH-3MC were separated by reversed-phase HPLC (Fig. 15). 3MC *cis*-1,2-diol and 1-OH-3-OHMC were among the most abundant metabolites formed. The AUC of 3MC *trans*-1,2-diol was about one-third of that of 3MC *cis*-1,2-diol (Fig. 15). The metabolically formed 3MC *trans*- and *cis*-1,2-

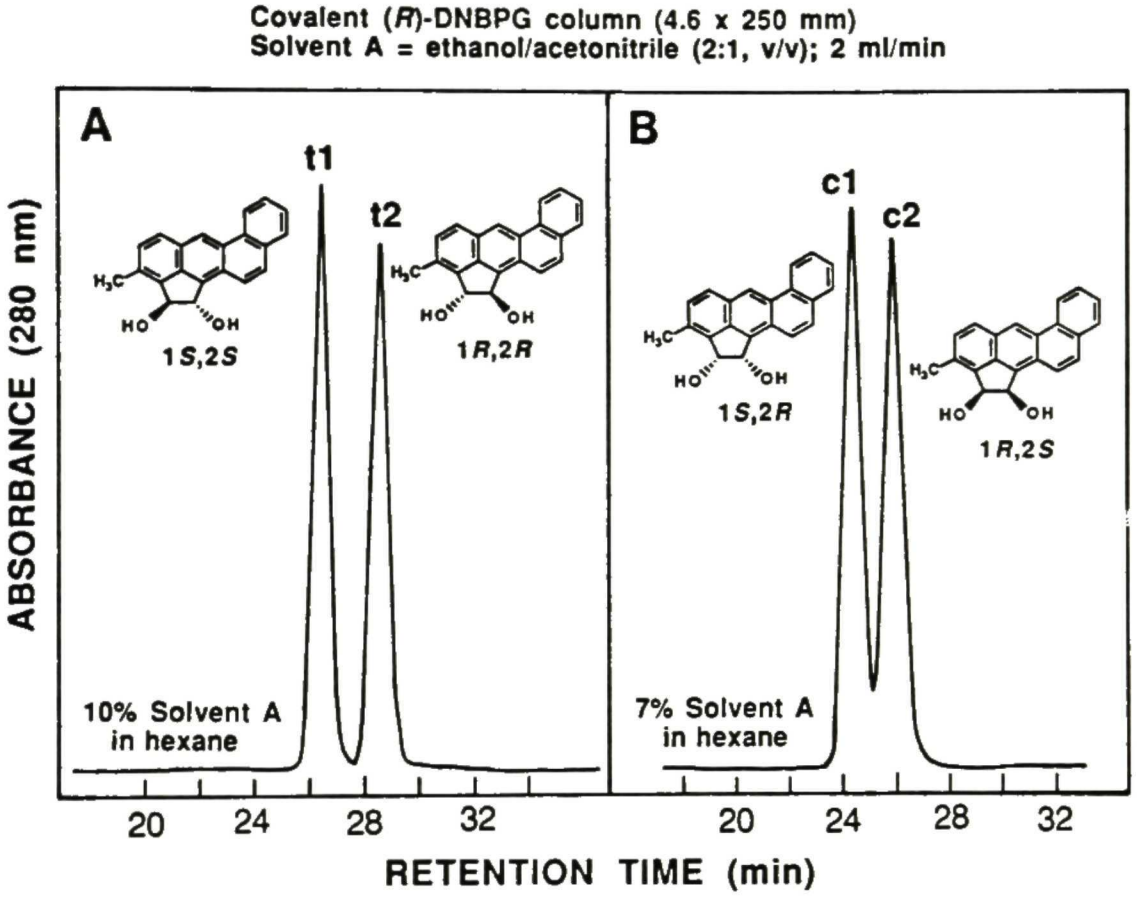

Figure 12. CSP HPLC separation of enantiomeric 3MC *trans*-1,2-diols (A) and 3MC *cis*-1,2-diols (B). A covalently bonded (*R*)-DNBPG column was used and the mobile phase was 10% and 7% (v/v) of solvent A in hexane, respectively, at a flow rate of 2 ml/min. See text on the assignment of absolute configuration of resolved enantiomers.

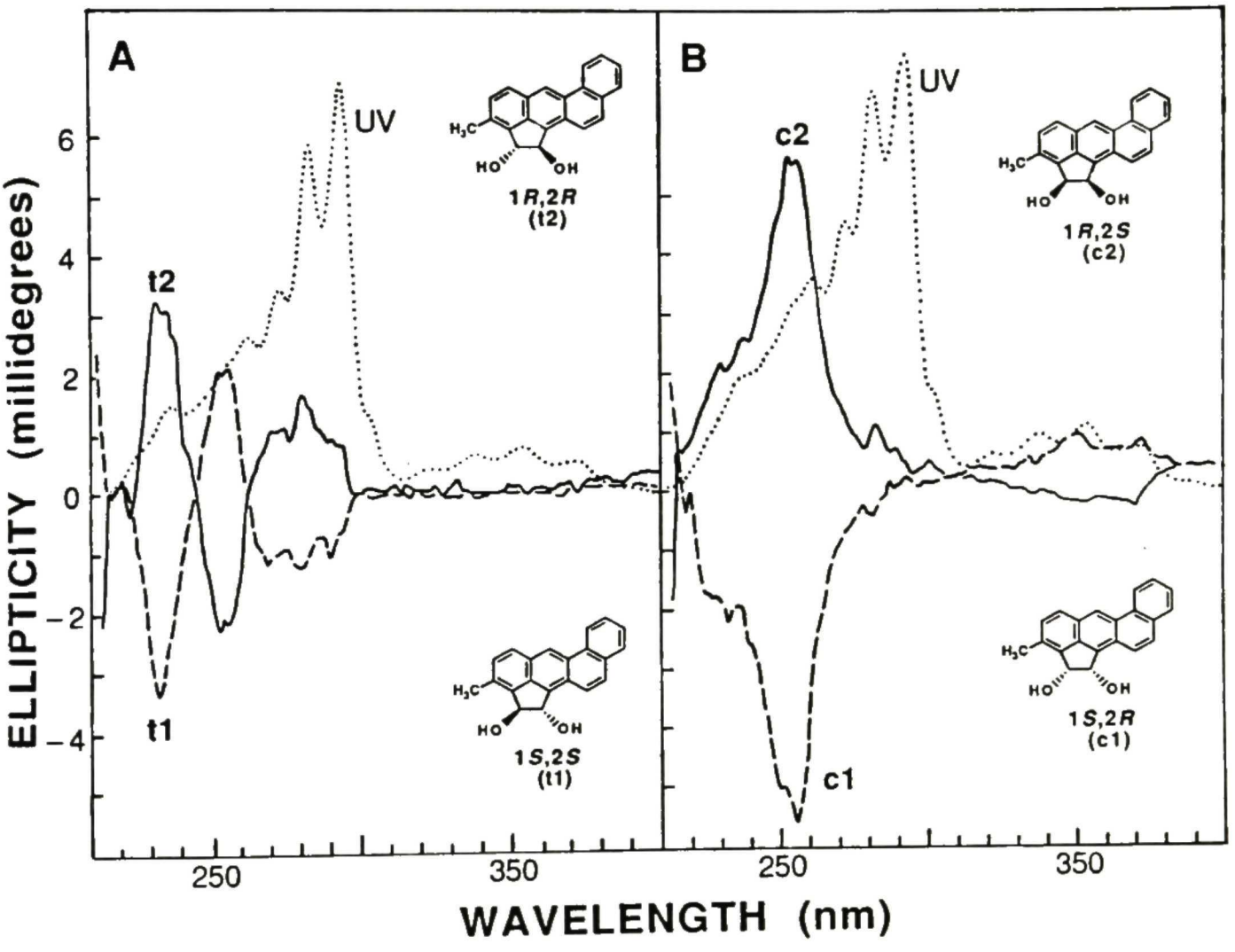

Figure 13. Uv-vis absorption and CD spectra of enantiomeric 3MC *trans*-1,2-diols (A) and 3MC *cis*-1,2-diols (B). Enantiomers were resolved as described in Fig. 12. See text on the assignment of absolute configurations.

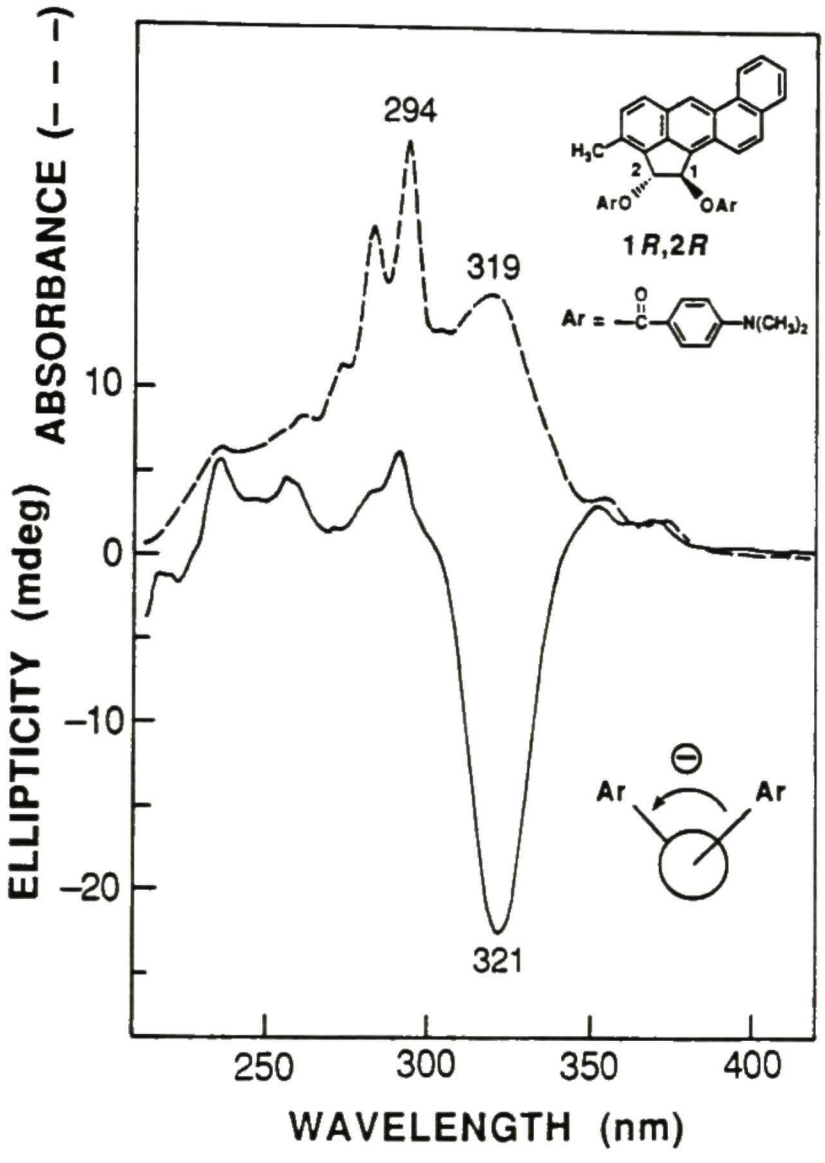

Figure 14. Uv absorption (– – –) and CD (———, 1.0 A_{294}/ml, methanol) spectra of a *bis-p-N,N*-dimethylaminobenzoate derived from an enantiomeric 3MC *trans*-1,2-diol (enantiomeric excess 96%). Uv-vis absorption spectra of two monoesters of 3MC *trans*-1,2-diol had a lower value of absorbance at 315 nm relative to that at 294 nm.

diols were identical to the corresponding synthetic compounds with respect to uv-vis absorption (Fig. 13) and mass spectra [M^+ at *m/z* 300 and a characteristic fragment ion at *m/z* 282 (loss of H_2O)], and retention times on reversed-phase HPLC (Fig. 15). The identification of 1-OH-3-OHMC was based on its uv-vis absorption spectrum (Fig. 16), which indicated an intact benz[a]anthracene nucleus, and by mass spectral analysis [M^+ at *m/z* 300 and characteristic fragment ions at *m/z* 282 (loss of H_2O), 265 (loss of H_2O and OH), and 253 (loss of H_2O and CHO)]. The 1-OH-3-OHMC, one of the major metabolites of 1-OH-3MC identified in this study, was not found to be a metabolite of either 1-OH-3MC or 3MC in earlier studies (Sims *et al.*, 1966; 1981; Stoming *et al.*, 1977; Tierney *et al.*, 1979; Thakker *et al.*, 1978; 1978; Eastman *et al.*, 1979 Gardiner *et al.*, 1984; Shou and Yang, 1990a; Cavalieri *et al.* 1978).

Peaks a and b in Fig. 15, with an AUC ratio of ~63/37, were diastereomeric *trans*-9,10-dihydrodiols derived from racemic 1-OH-3MC. These two diastereomeric 9,10-dihydrodiols were identical to 1-OH-3MC 9,10-dihydrodiol-*a* and 1-OH-3MC 9,10-dihydrodiol-*b* previously described by Thakker *et al* (Thakker *et al.*, 1978). Peak c was identified as 3MC-1-one, which was identical to the authentic compound with respect to uv-vis absorption and mass spectra (M^+ at *m/z* 282) as well as retention time on reversed-phase HPLC. In an earlier report (Sims *et al.*, 1966), 3MC-1-one was found by thin layer chromatography to be a metabolite of 1-OH-3MC. In two other studies (Thakker *et al.*, 1978; Gardiner *et al.*, 1984), however, 3MC-1-one was not recognized as a product formed in rat liver microsomal metabolism of 1-OH-3MC. Because of the large number (>14) of other metabolites formed, the stereochemistry of peaks a and b as well as the identities of unmarked chromatographic peaks in Fig. 15 will be fully described in a later report.

The relative amount of three aliphatic hydroxylation products was 1-OH-3-OHMC > 3MC *cis*-1,2-diol > 3MC *trans*-1,2-diol with an AUC ratio of 70/48/15. These results are in contrast to earlier reports (Thakker *et al.*, 1978; Gardiner *et al.*, 1984), indicating

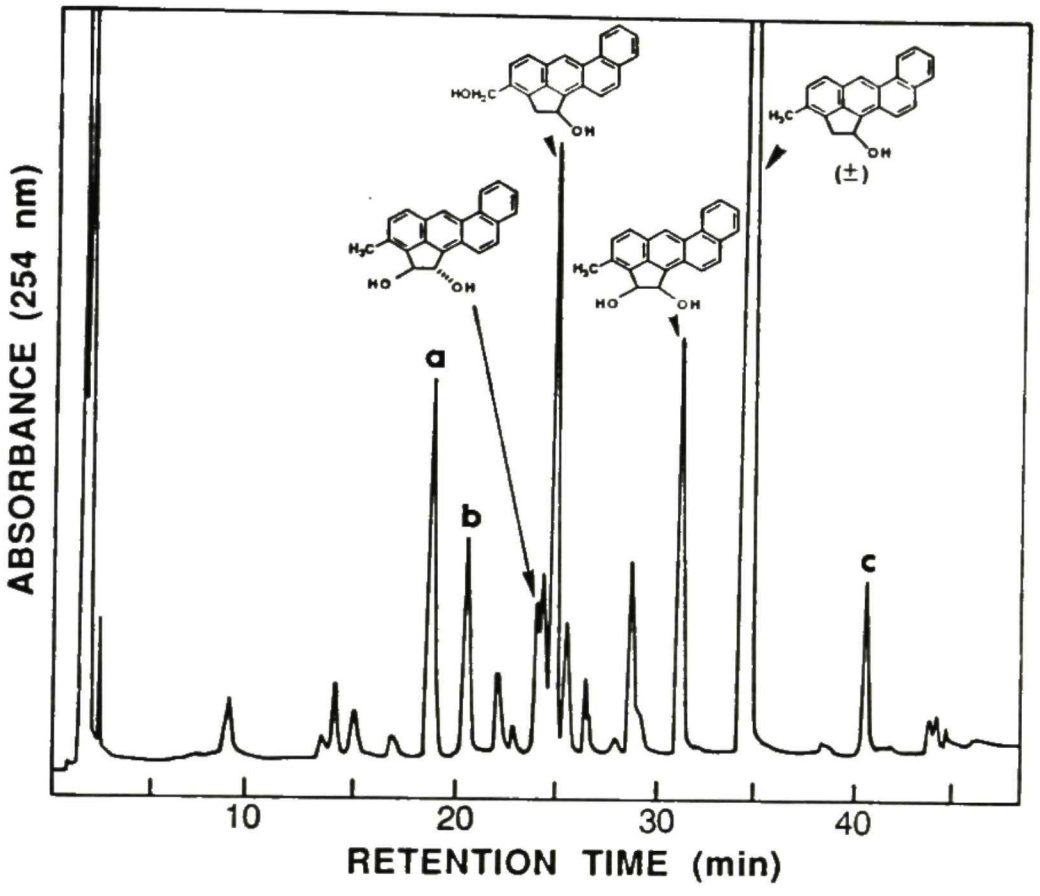

Figure 15. Reversed-phase HPLC separation of products formed in the metabolism of racemic 1-OH-3MC by liver microsomes from PB-treated rats. Peaks a and b correspond to the diastereomeric 1-OH-3MC 9,10-dihydrodiol-*a* and 1-OH-3MC 9,10-dihydrodiol-*b*, respectively, reported by Thakker et al. (Thakker *et al.*, 1978). Peak c contains the 3MC-1-one.

that very little of the 3MC *cis*-1,2-diol was formed in the metabolism of 1-OH-3MC by rat liver microsomes. 3MC *trans*-1,2-diol and *cis*-1,2-diol were formed with an AUC ratio of 24/76 in the metabolism of (±) 1-OH-3MC (Fig. 15). Upon further purification by normal-phase HPLC by using 15% of solvent A in hexane as the eluent, the metabolically formed 3MC *trans*-1,2-diol was subsequently analyzed by CSP HPLC according to the conditions described in Fig. 12 and was found to have an enantiomeric ratio [(peak t1):(peak t2)] of 63/37. Similarly, the metabolically formed 3MC *cis*-1,2-diol was found to have an enantiomeric ratio [(peak c1):(peak c2)] of 12/88. In principle, 1-OH-3-OHMC may be further hydroxylated at C_2 to form both *trans*- and *cis*-1,2-diols. These metabolites, if formed, should be minor chromatographic peaks in Fig. 15 and are yet to be found.

2.4 *Enantioselective hydroxylation at C_3-methyl group of racemic 1-OH-3MC*

The metabolically formed 1-OH-3-OHMC, isolated as described in Fig. 15, was further purified by normal-phase HPLC using 15% of solvent A in hexane as the eluent. Enantiomers of 1-OH-3-OHMC were separated by CSP HPLC on a covalently bonded *R*-DNBPG column (Fig. 17). The enantiomeric ratio was found to be 58/42 in favor of the less strongly retained enantiomer (Fig. 17). An optically pure and less strongly retained enantiomer was obtained by repetitive chromatography and it had a CD spectrum (Fig. 16) with Cotton effects closely similar to those of an optically pure 1*R*-OH-3MC. The absolute stereochemistry of enantiomeric 1-OH-3MC has been established by two different methods; one method is described in this study (see below) and the other method is described earlier (Shou *et al.*, *Carcinogenesis*, 11:933-940; 1990). The 1-OH-3-OHMC, formed during the rat liver microsomal metabolism of optically pure 1*R*-OH-3MC, had a CD spectrum similar to (Fig. 16) and a retention time identical to (Fig. 17) the less strongly retained enantiomer of 1-OH-3-OHMC on CSP HPLC.

2.4 *Absolute configuration of enantiomeric 1-OH-3MC and 3MC cis-1,2-Diol*

3MC *trans*- and *cis*-1,2-diols were two of the major rat liver microsomal metabolites of 1-OH-3MC (Fig. 15). We took advantage of these rat liver microsome-

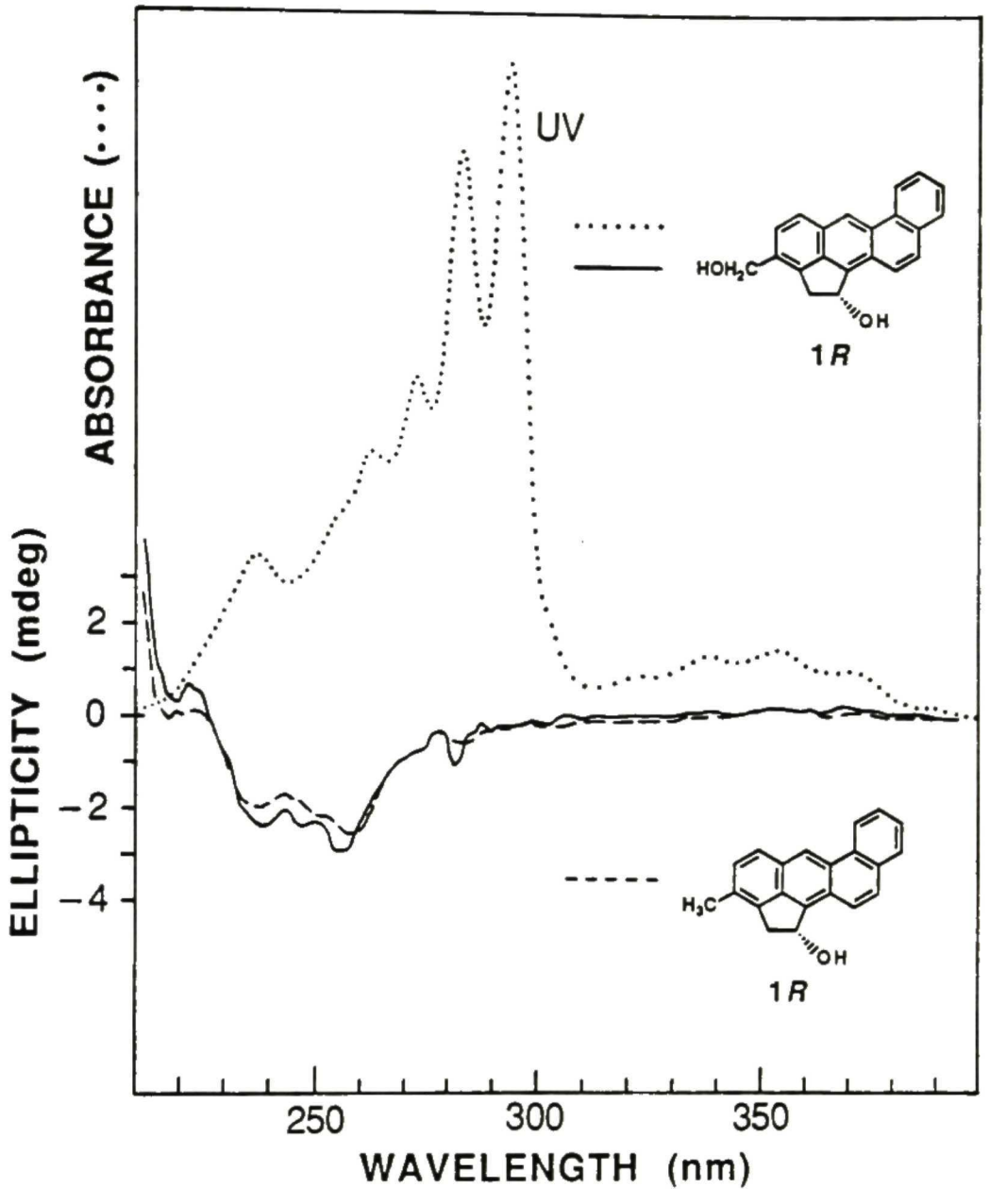

Figure 16. Uv-vis absorption and CD spectra of 1*R*-OH-3-OHMC, which was less strongly retained on the covalently bonded *R*-DNBPG column (see Fig. 17), and the CD spectrum of 1*R*-OH-3MC whose absolute configuration has been established by two independent methods in this and an earlier study.

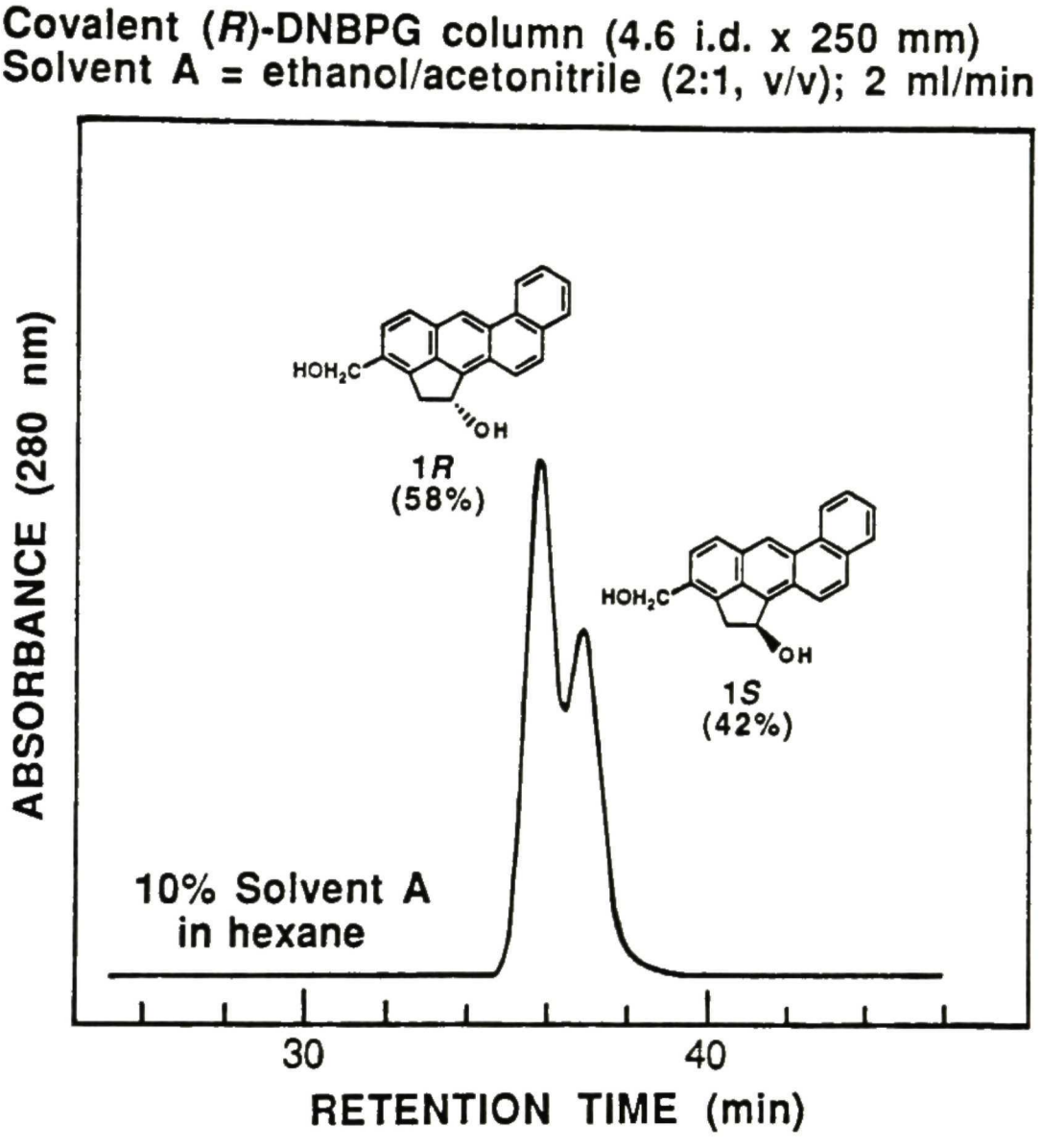

Figure 17. CSP HPLC separation of enantiomeric 1-OH-3-OHMC. A covalently bonded *R*-DNBPG column was used and the mobile phase was 10% (v/v) of solvent A in hexane at a flow rate of 2 ml/min. See text on the assignment of absolute configuration of resolved enantiomers.

catalyzed hydroxylation reactions to elucidate the absolute configurations of enantiomeric 1-OH-3MC and 3MC *cis*-1,2-diol. The enantiomer 1-OH-3MC, which was less strongly retained on the covalently bonded *R*-DNBPG column, was used as the substrate in the *in vitro* incubation. The 3MC *trans*- and *cis*-1,2-diols formed in the metabolism of the 1-OH-3MC enantiomer were isolated as described in Fig. 15. CSP HPLC analysis indicated that they coeluted with peaks t1 and c1 of Fig.12, respectively. Since peak t2 in Fig. 12A has been established to be the 1*R*,2*R*-enantiomer, the 1-OH-3MC from which the 1*S*,2*S*-diol was derived from was easily established to the 1*R*-enantiomer (see structures in Fig. 18). Consequently the *cis*-1,2-diol, which was derived from the 1*R*-OH-3MC, was deduced to be the 1*S*,2*R* enantiomer (see structures in Fig. 18). It should be pointed out that, due to the addition of a chiral center at C_2, the hydroxyl group with 1*R* designation in 1-OH-3MC is changed to 1*S* (and vice versa) in the enantiomeric 3MC *trans*- and *cis*-1,2-diols (Fig. 18). These results were consistent with the earlier finding that the more strongly retained enantiomer of 1-OH-3MC on the covalently bonded *R*-DNBPG column was the 1S enantiomer (Fig. 7, left chromatogram). The absolute configuration of 1*S* enantiomer was determined by analysis of the CD spectrum of its *p*-nitrobenzoate derivative (Fig. 8).

As can be seen in Fig. 15, the AUC ratio of (*trans*-1,2-diol)/(*cis*-1,2-diol) formed in the metabolism of racemic 1-OH-3MC was ~1/3. However, when 1*R*-OH-3MC was used as the substrate in the rat liver microsomal incubation, the AUC ratio of (*trans*-1,2-diol)/(*cis*-1,2-diol) was 71/29 (chromatogram not shown). This result suggested that, in the metabolism of racemic 1-OH-3MC, the *trans*-1,2-diol was mainly derived from the 1*R*-OH-3MC, whereas the *cis*-1,2-diol was mainly derived from the 1*S*-OH-3MC. Further analysis of the data obtained by using racemic 1-OH-3MC as the substrate in the *in vitro* incubation with rat liver microsomes (see below) confirmed the enantioselective/stereoselective hydroxylation reactions.

2.5 *Enantioselective C_2-hydroxylation of racemic 1-OH-3MC*

The relative amounts and enantiomeric ratios of *trans*-1,2-diol and *cis*-1,2-diol,

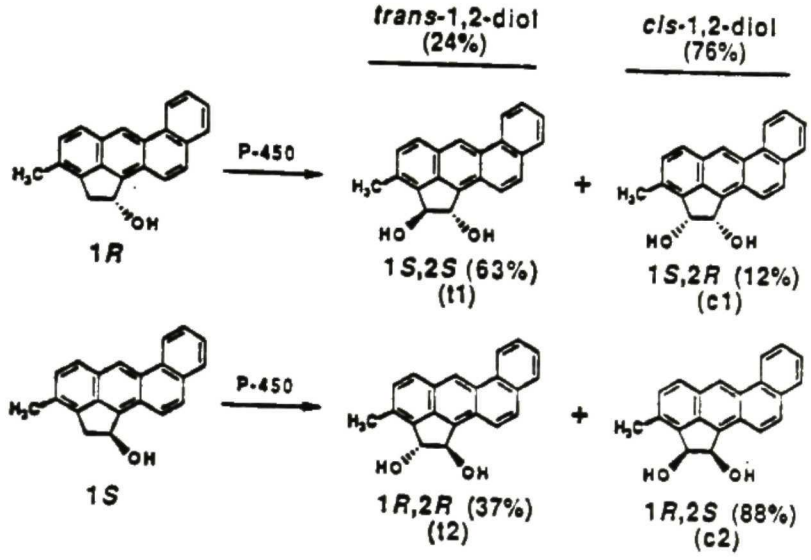

Figure 18. Absolute configurations of *trans*- and *cis*-1,2-diols derived from C_2-hydroxylation of 1*R*-OH-3MC and 1*S*-OH-3MC. Note the change of stereochemical designation (1*S* → 1*R* and 1*S* → 1*R*, respectively) of the hydroxyl group at C_1 upon C_2-hydroxylation. The corresponding chromatographic peak in Fig. 12 and CD spectrum (Fig. 13) are indicated under each structure. The enantiomeric compositions (determined as described in Fig. 12) of *trans*-1,2-diol (24% of all the 1,2-diols formed) and *cis*-1,2-diol (76% of all the 1,2-diols formed), formed in rat liver microsomal metabolism of racemic 1-OH-3MC and isolated as described in Fig. 15, are indicated in the parenthesis.

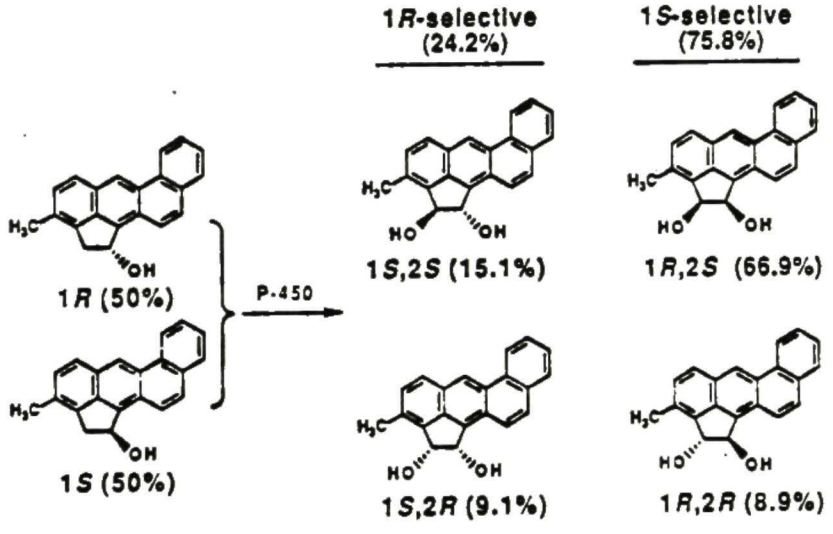

Figure 19. Summary of the analysis in the degree of substrate enantioselectivity and product stereoselectivity in rat liver microsomal metabolism of racemic 1-OH-3MC.

formed in the metabolism of racemic 1-OH-3MC by liver microsomes from PB-treated rats, were determined by AUC in the reversed-phase HPLC analysis (Fig. 15) and CSP HPLC analysis (Fig. 12) respectively and the results are summarized in Fig. 19. The percentage of 1*S* enantioselective C_2-hydroxylation of racemic 1-OH-3MC can be calculated by: (the percentage of 1*R*,2*R*-diol in the metabolically formed *trans*-1,2-diol) x (the percentage of *trans*-1,2-diol in the sum of *trans*- and *cis*-1,2-diols) + (the percentage of 1*R*,2*S*-diol in the metabolically formed *cis*-1,2-diol) x (percentage of *cis*-1,2-diol in the sum of *trans*- and *cis*-1,2-diols). The percentage of 1*R*-OH-3MC enantioselective C_2-hydroxylation can be similarly calculated. The results of these calculations are summarized in Fig. 19, which indicated that the C_2-hydroxylation of racemic 1-OH-3MC was enantioselective toward the 1*S*-enantiomer over the 1*R*-enantiomer in a ratio of ~3/1.

It can be seen in Fig. 19, that, in the C_2-hydroxylation of 1*R*-OH-3MC, the *trans*-hydroxylation (i.e., the formation of *trans*-1,2-diol) was more prevalent than the *cis*-hydroxylation (i.e., the formation of *cis*-1,2-diol) by a ratio of ~15/9. In contrast, in the C_2-hydroxylation of 1*S*-OH-3MC the *cis*-hydroxylation was more prevalent than the *trans*-hydroxylation by a ratio of ~67/9. Thus the metabolism of racemic 1-OH-3MC was not only substrate enantioselective, but also stereoselective in the C_2-hydroxylation of an enantiomeric 1-OH-3MC. The 1*R*-OH-3MC underwent (*trans*)-C_2-hydroxylation more favorably than the (*cis*)-C_2-hydroxylation, whereas the 1*S*-OH-3MC underwent (*cis*)-C_2-hydroxylation more favorably than the (*trans*)-C_2-hydroxylation.

In a recent report (Shou and Yang, 1990a), the enantiomeric composition of the remaining 1-OH-3MC (recovered by reversed-phase HPLC) following incubation of racemic 1-OH-3MC with rat liver microsomes was also found to be enriched in the 1*R*-enantiomer. Thus the overall metabolism of racemic 1-OH-3MC was enantioselective toward the 1*S*-enantiomer. The same 1*S*-enantioselective metabolism was found regardless of whether liver microsomes from untreated, PB-treated, or 3MC-treated rats were used. Pretreatment of rats with PB and 3MC induces different forms of cytochrome P-450 (Lu *et*

al., 1971 and 1972). In this study, two aliphatic hydroxylation reactions by rat liver microsomes had been analyzed. Hydroxylation at the C_3-methyl group of racemic 1-OH-3MC was found to be enantioselective toward the 1*R*-enantiomer. In contrast, hydroxylation at C_2-carbon of racemic 1-OH-3MC was enantioselective toward the 1*S*-enantiomer. Preliminary results indicated that peak a in Fig. 15 was derived predominantly from the 1*S*-enantiomer, whereas peak b was derived mainly from the 1*R*-enantiomer. Since peaks a and b in Fig. 15 as well as 1-OH-3-OHMC, 3MC *trans*-1,2-diol and 3MC *cis*-1,2-diol accounted for the majority of the metabolites formed, the results of this study are consistent with the earlier findings on the substrate enantioselectivity in rat liver microsomal metabolism of racemic 1-OH-3MC.

3. *Metabolism of 2S-OH-3MC* (Shou and Yang, 1990d)

The substrate (2*S*-OH-3MC) used in this study was isolated from a mixture of metabolites formed by incubation of 3MC with liver microsomes from 3MC-treated rats. Consistent with the results of an earlier report (Shou *et al.*, *Carcinogenesis*, 11:933-940; 1990), the 2-OH-3MC formed in the metabolism of 3MC by liver microsomes from 3MC-treated rats was highly enriched in the 2*S*-enantiomer (enantiomeric excess ~98%). The absolute configuration of the major 2-OH-3MC enantiomer formed in the metabolism of 3MC has been established in this study by a method independent of that reported earlier. The results of this and the earlier study provided an identical conclusion regarding the absolute configuration of the enantiomeric 2-OH-3MC. Because 2-OH-3MC is itself a potent carcinogen (Sims, 1967; Levin *et al.*, 1978, 1979; Chouroulinkov *et al.*, 1979; Cavalieri *et al.*, 1978, 1988) and 2*S*-OH-3MC is the most abundant metabolite of 3MC, the metabolic activation pathway(s) of 2*S*-OH-3MC may play an important role in the metabolic activation of 3MC.

3.1 *Reversed-phase HPLC separation of metabolites*

Metabolites formed by incubation of 2-OH-3MC [(2*S*)/(2*R*): ~99/1] by liver microsomes from PB-treated rats were separated by reversed-phase HPLC (Fig. 20). The retention time of 3MC is indicated in Fig. 20. In this particular sample, ~45% of the substrate was metabolized. Chromatographic peaks are numbered as indicated in Fig. 20 and the metabolite(s) contained in each chromatographic peak was characterized as described below. Peak 17 contained the unreacted substrate 2*S*-OH-3MC (see mass spectrum of Fig. 33). Characterization of metabolites is presented below primarily according to the region of 2*S*-OH-3MC at which the metabolite is formed. The CD spectrum of a 2-OH-3MC highly enriched in the 2*S*-enantiomer is shown in Fig. 21B. Retention times on reversed-phase and normal-phase HPLC as well as molecular weight from mass spectra of various 2*S*-OH-3MC metabolites are summarized in Table 3.

3.2 *Oxidation at bay-region 7,8-double bond*

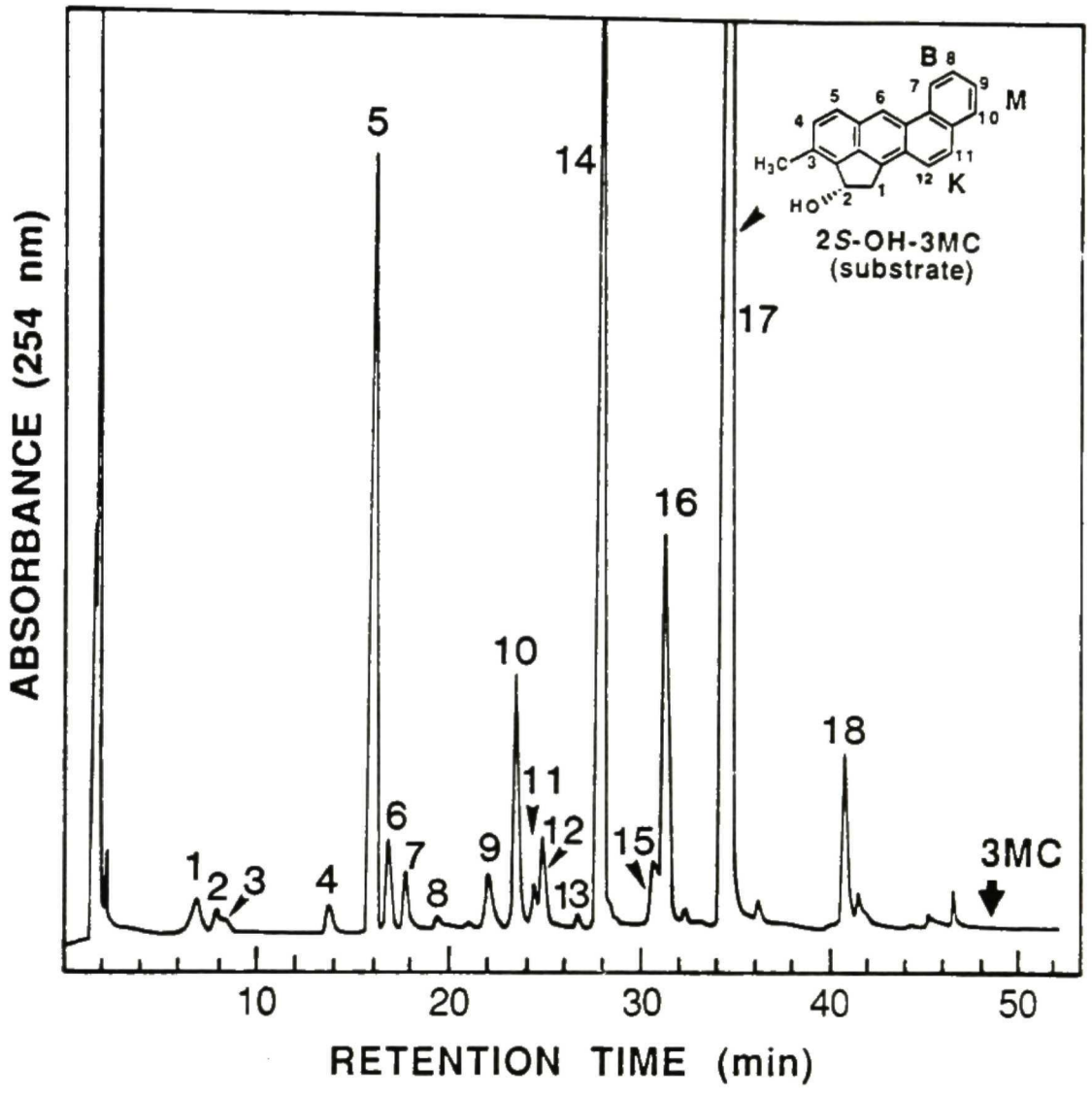

Figure 20. Reversed-phase HPLC separation of 2*S*-OH-3MC and its metabolites. Identities of metabolites contained in various chromatographic peaks are described in the text and summarized in Table 3. Retention time of 3MC is indicated by an arrow. B (bay), M (site of formation of procarcinogenic dihydrodiol), and K (the most electron-rich double bond) regions are indicated in the structure of 2*S*-OH-3MC shown.

Table 3. Characterization of products formed in the metabolism of 2*S*-OH-3MC by rat liver microsomes.

Peak no. in RP HPLC (r_t, min)[a]	Elution solvent used in NP HPLC (r_t, min)[b]	M^+ (*m/z*)[c]	Identity of Metabolite
1 (6.9)	EA20 (16.3)	334	2*S*-OH-3-OHMC 9,10-dihydrodiol[e]
2 (7.8)	EA20 (14.9)	ND (334)[d]	2*S*-OH-3-OHMC 11,12-dihydrodiol[e]
3 (8.4)	EA20 (15.5)	ND (334)[d]	2*S*-OH-3-OHMC 9,10-dihydrodiol[e]
4 (13.7)		ND (334)[d]	3MC *cis*-1*S*,2*R*-diol:*trans*-9,10-dihydrodiol[e]
5 (15.9)	EA15 (5a, 15.3)	318	2*S*-OH-3MC 9*R*,10*R*-dihydrodiol
	EA15 (5b, 16.8)	318	2*S*-OH-3MC 11*R*,12*R*-dihydrodiol
6 (16.8)	EA10 (22.8)	318	2*S*-OH-3MC 11*S*,12*S*-dihydrodiol
7 (17.7)	EA15 (16.0)	318	2*S*-OH-3MC 9*S*,10*S*-dihydrodiol
8 (19.4)		ND (316)[d]	3-OHMC (*trans*)-1*R*,2*R*-diol[e]
9 (22.0)	EA15 (11.0)	316	3MC-2-one 9,10-dihydrodiol[f]
10 (23.4)	EA10 (15.6)	300	8-hydroxy-2*S*-OH-3MC
11 (24.4)		300	3MC (*trans*)-1*R*,2*R*-diol
12 (24.8)		ND (300)[g]	unknown[g]
13 (26.7)		300	10-hydroxy-2*S*-OH-3MC
14 (27.8)	EA15 (9.1)	300	2*S*-OH-3-OHMC
15 (30.6)		ND	unknown
16 (31.3)		300	3MC (*cis*)-1*S*,2*R*-diol
17 (34.3)		284	2*S*-OH-3MC (substrate)
18 (40.7)		282	3MC-2-one

[a] Metabolites are separated by reversed-phase HPLC and numbered as described in Fig. 20. Retention times (r_t) are indicated in parenthesis.

[b] Elution solvents are defined in abbreviations and normal-phase HPLC conditions are described in Materials and Methods. Retention times are indicated in parenthesis.

[c] Molecular ion from mass spectral analysis. ND = not determined.

[d] Expected molecular weight.

[e] Tentative identification (see text for discussion). Metabolites contained in peaks 1 and 3 are probably a pair of diastereomers.

[f] (9*R*,10*R*)/(9*S*,10*S*) = ~ 62/38.

[g] coeluted with 9-hydroxy-2-OH-3MC, which is derived by acid-catalyzed dehydration of a 2*S*-OH-3MC 9,10-dihydrodiol.

The angular area including C_6 and C_7 positions is defined as the bay region (Conney *et al.*, 1982). Hence the 7,8-double bond is a bay region double bond. The metabolite contained in peak 10 of Fig. 20 had uv-visible absorption characteristics similar to those of 2-OH-BA (Fig. 21A). Relative to those of 2-OH-BA, red-shifts of some absorption bands were observed in the absorption spectrum of metabolite peak 10 due to additional substituents (Fig. 21A). Mass spectral analysis indicated a M^+ at *m/z* 300 and a characteristic fragment ion at *m/z* 282 (loss of H_2O). The uv-visible absorption spectra of other monohydroxylated (phenolic) derivatives of BA are all different from that of 2-OH-BA. In the CD spectrum of metabolite peak 10 (Fig. 21B), the major Cotton effects between 230-270 nm were similar to those of 2*S*-OH-3MC. Taken together, these results indicated that metabolite peak 10 of Fig. 20 is 8-OH-2*S*-OH-3MC.

The non-benzylic phenolic product 8-OH-2*S*-OH-3MC is the expected major product derived by non-enzymatic rearrangement of the metabolically formed bay region 2*S*-OH-3MC 7,8-epoxide intermediate (Fu *et al.*, 1978). This is similar to the finding that the nonbenzylic phenolic product 9-OH-BaP is the major nonenzymatic rearrangement product of the bay region 9,10-epoxide intermediate of BaP (Yang *et al.*, 1977). It is interesting to note, however, that the potentially microsomal epoxide hydrolase-catalyzed hydration product, 2*S*-OH-3MC 7,8-dihydrodiol, was not a detectable metabolite of 2*S*-OH-3MC. This finding suggests that 2*S*-OH-3MC 7,8-epoxide was a poor substrate for the microsomal epoxide hydrolase and was readily rearranged to form 8-OH-2*S*-OH-3MC. Similar to those of BaP *trans*-9,10-dihydrodiol, the hydroxyl groups of the bay region 2*S*-OH-3MC *trans*-7,8-dihydrodiol adopt a quasidiaxial conformation (Yang *et al.*, 1980). If the 2*S*-OH-3MC *trans*-7,8-dihydrodiol was a metabolite, it should be more polar than 2*S*-OH-3MC 9,10-dihydrodiol and would be expected to elute between 6 and 10 min in reversed-phase HLPC (Fig. 20).

3.3 *Hydroxylation at C_1 and absolute configuration of the substrate.*

The absolute configuration of the enantiomeric 2-OH-3MC, following conversion

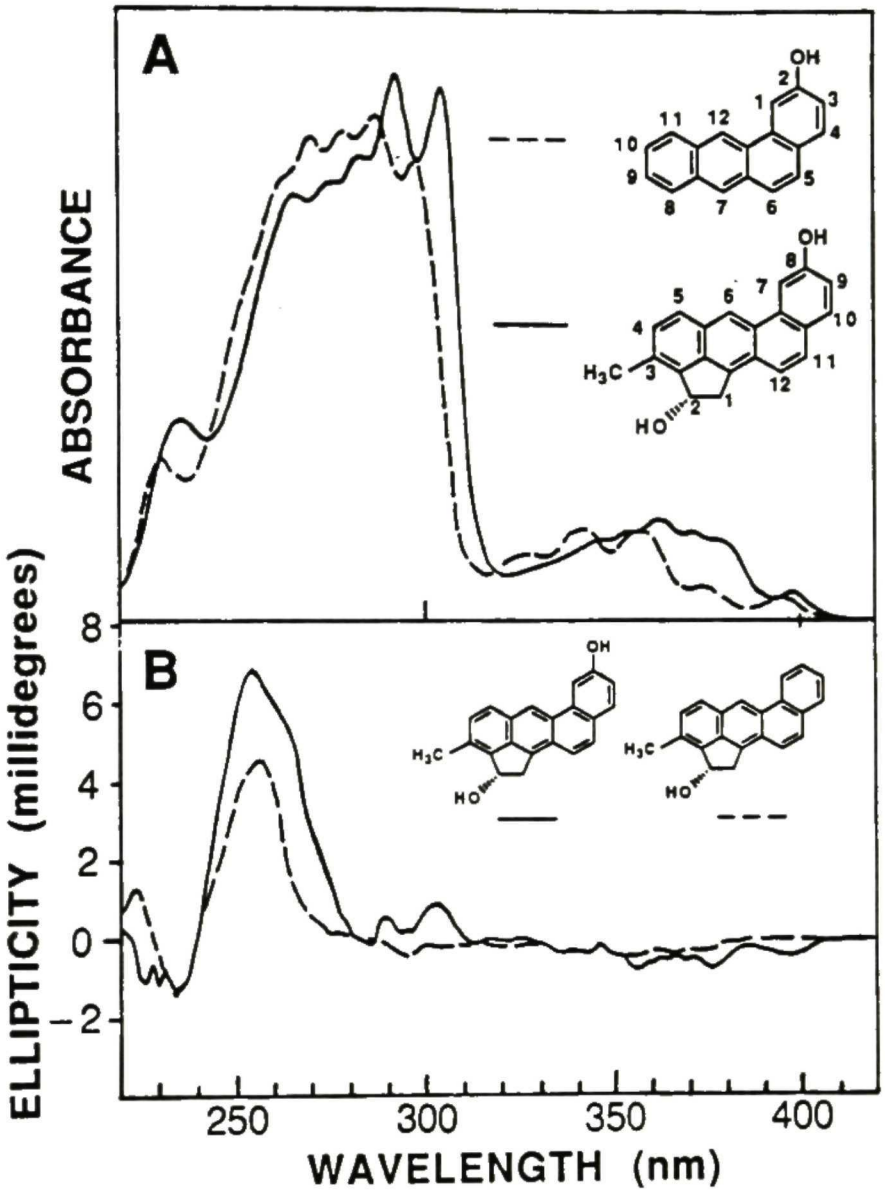

Figure 21. (A). Uv-vis absorption spectra of 2-OH-BA (authentic compound, in methanol) and a metabolite (peak 10 of Fig. 20) identified as 8-OH-2*S*-OH-3MC (in methanol). (B). CD spectra of 2*S*-OH-3MC (——; concn. 1.0 A_{294}/ml, methanol; Φ_{257}/A_{294} = 4.6 millidegrees, (2*S*)/(2*R*): 96/4) and the metabolite identified as 8-OH-2*S*-OH-3MC (– – – –; concn. 1.0 A_{292}/ml, methanol; Φ_{256}/A_{292} = 7.0 millidegrees).

to a *p*-nitrobenzoate, has been established by the exciton chirality CD method as described earlier. Because the transition dipole in the longitudinal axis of the *p*-nitrobenzoate chromophore intersects at near the midpoint of that of the BA chromophore, we were concerned that the exciton splitting resulting from the interaction between the two transition dipoles may not be interpreted in a simple manner to provide a definitive answer on the absolute configuration of the enantiomeric 2-OH-3MC. The absolute configuration of the enantiomeric 2-OH-3MC has been elucidated by a method independent of that previously described and this is described below.

Enantiomeric pairs of 3MC *trans*-1,2-diol and 3MC *cis*-1,2-diol can be separated by HPLC using a *R*-DNBPG-C column (Fig. 12). UV-visible absorption and CD spectra of resolved enantiomers are shown in Fig. 13. The absolute configuration of a 3MC *trans*-1,2-diol enantiomer, following conversion to a *bis-p-N,N*-dimethylaminobenzoate, has been established by the exciton chirality CD method (Fig. 14). The metabolites contained in peaks 11 and 16 (AUC ratio 11:89) of Fig. 20 had uv-visible absorption and mass spectra and retention times identical to those of the authentic 3MC *trans*-1,2-diol and 3MC *cis*-1,2-diol, respectively. The metabolically formed *trans*-1,2-diol and *cis*-1,2-diol co-eluted with the more strongly retained 3MC 1*R*,2*R*-diol and the less strongly retained 3MC 1*S*,2*R*-diol, respectively, on a *R*-DNBPG-C column (Fig. 22). It should be pointed out that, due to the addition of a chiral center at C_1, the hydroxyl group with 2*S* designation in an enantiomeric 2-OH-3MC is changed to 2*R* (and vice versa) in the enantiomeric 3MC *trans*- and *cis*-1,2-diols (see illustration at the top of Fig. 22). Since the absolute configurations of the metabolically formed 1,2-diols have been established, the 2-OH-3MC enantiomer from which the 1,2-diols are derived from is deduced to be the 2*S*-enantiomer (Fig. 22). These results are consistent with those described in an earlier report, indicating that the 2-OH-3MC enantiomer which has a positive CD Cotton band centered around ~258 nm (Fig. 21B) is the 2*S*-enantiomer. In the earlier study, the absolute configuration of the 2-OH-3MC enantiomer was determined by analysis of the CD spectrum of a *p*-nitrobenzoate.

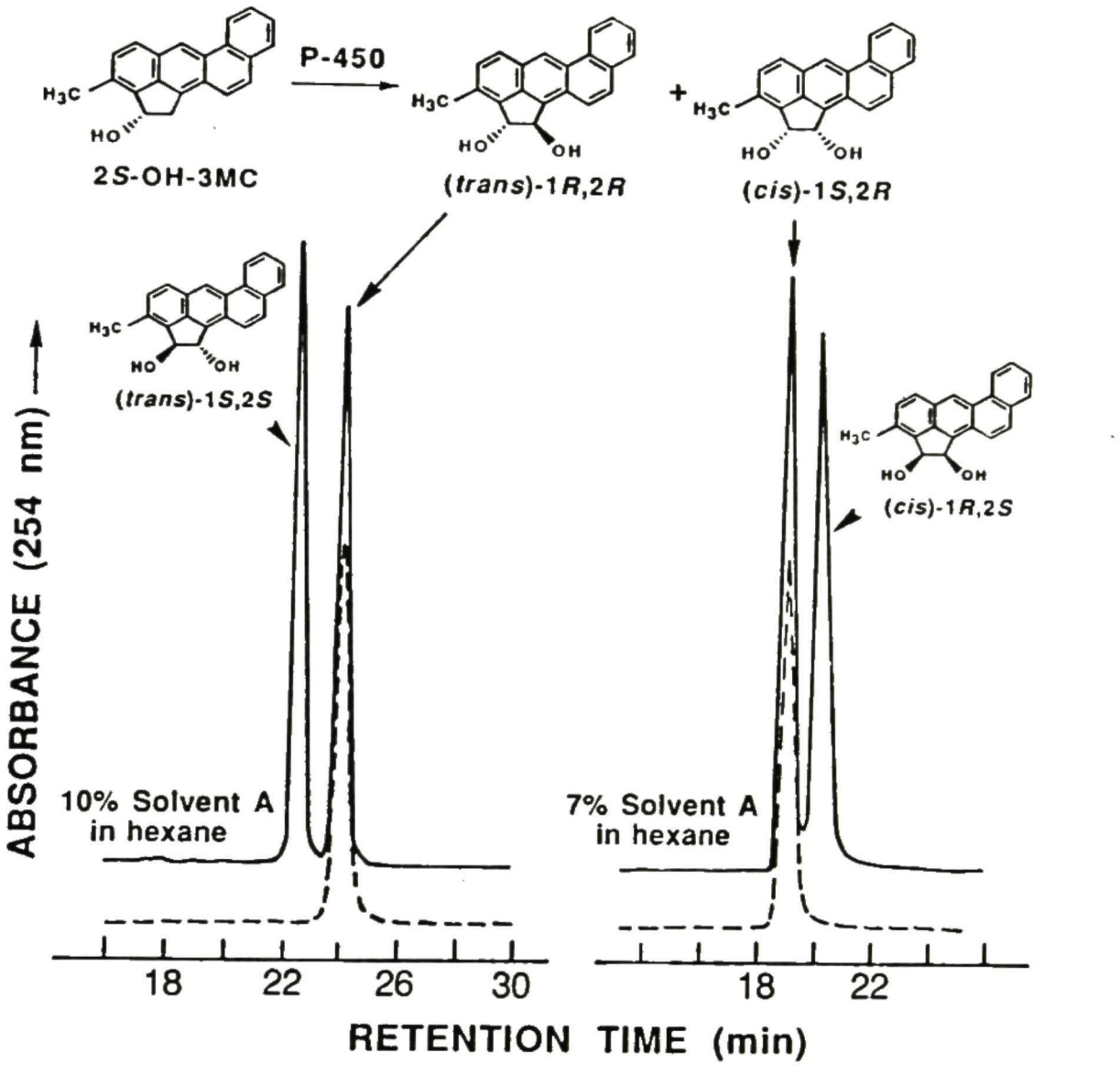

Figure 22. CSP HPLC separation of enantiomeric 3MC *trans*-1,2-diols (left chromatogram) and 3MC *cis*-1,2-diols (right chromatogram). Retention times of 3MC *trans*-1,2-diol (– – – –, left chromatogram) and 3MC *cis*-1,2-diol (– – – –, right chromatogram), formed in the metabolism of 2*S*-OH-3MC, are indicated. A *R*-DNBPG-C column was used and the mobile phase was 10% and 7% (v/v) of solvent A (ethanol/acetonitrile, 2/1, v/v) in hexane, respectively, at a flow rate of 2 ml/min. Absolute configurations of enantiomeric 3MC *trans*-1,2-diol and 3MC *cis*-1,2-diol have been established in an earlier study (King *et al.*, 1978). Structure and stereochemistry of products formed by C_1-hydroxylation of 2*S*-OH-3MC are shown at the top of the figure.

3.4 *Oxidation of C_3-methyl group*

The metabolite contained in peak 14 of Fig. 20 was the most abundant metabolite of 2*S*-OH-3MC and was identified as 2*S*-OH-3-OHMC. It had a uv-vis absorption spectrum (Fig. 23) essentially the same as that of 2-OH-3MC and a M^+ at *m/z* 300 and characteristic fragment ions at *m/z* 282 (loss of H_2O) and 265 (loss of H_2O and OH) (Fig. 25). 3MC, 3-OHMC, 1-OH-3MC, 2-OH-3MC, 1-OH-3-OHMC, 2-OH-3-OHMC, and the *trans*-1,2-diol and the *cis*-1,2-diol derived from both 3-MC and 3-OHMC all have the same absorption characteristics because of their common BA chromophore. The second hydroxyl group of metabolite peak 14 was not located at the C_1 position, because the retention time of metabolite peak 14 on reversed-phase HPLC (Fig. 20) was different from those of 3MC *trans*-1,2-diol (peak 11) and 3MC *cis*-1,2-diol (peak 16). Furthermore, if the second hydroxyl group were located at an aromatic ring position (*i.e.*, the hydroxyl group is phenolic), the uv-visible absorption spectrum would have been different from that of 2-OH-3MC (or 3MC). The CD spectrum of this metabolite (Φ_{256}/A_{294} = 5.7 millidegrees, Fig. 23) had Cotton effects similar to those of 2*S*-OH-3MC (Fig. 21B). Thus the metabolite contained in peak 14 was established to be 2*S*-OH-3-OHMC.

The minor metabolite contained in peak 8 was tentatively identified as 3-OHMC *trans*-1,2-diol. It had a uv-visible absorption spectrum (not shown) similar to that of 2-OH-3-OHMC (Fig. 23). When 3MC *trans*-1,2-diol was incubated with rat liver microsomes and cofactors, a metabolite (identified as 3-OHMC *trans*-1,2-diol, see later) with a retention time identical to that of peak 8 was detected. Metabolite peak 8 was unlikely to be derived from the minor metabolite 3MC *trans*-1,2-diol (peak 11), but rather from microsome-catalyzed *trans*-hydroxylation at C_1 of 2*S*-OH-3-OHMC.

3.5 *Oxidation of C_2-hydroxyl group*

The metabolite contained in peak 18 (Fig. 20) was identified as 3MC-2-one (see mass spectrum of Fig. 34). It had uv-vis absorption and mass spectra and a retention time on reversed-phase HPLC identical to those of the authentic 3MC-2-one (Yang *et al.*, 1990).

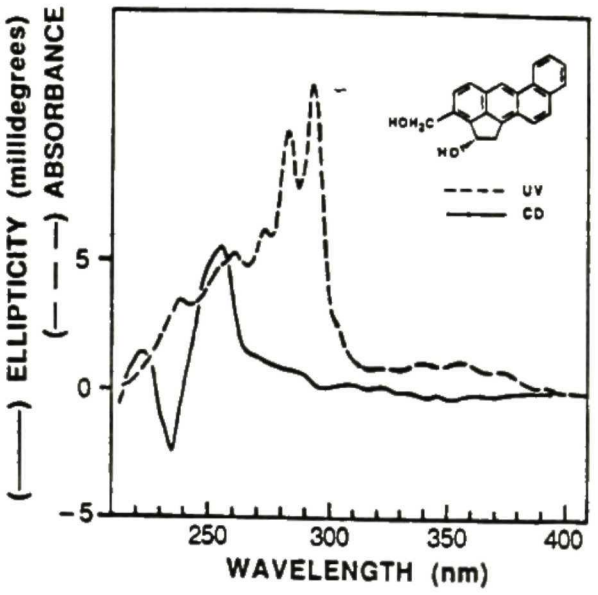

Figure 23. Uv-vis absorption (– – – –, methanol) and CD (——, concn. 1.0 A_{294}/ml, methanol; Φ_{256}/A_{294} = 5.7 millidegrees) spectra of the metabolite (2*S*-OH-3-OHMC) contained in peak 14 of Fig. 20.

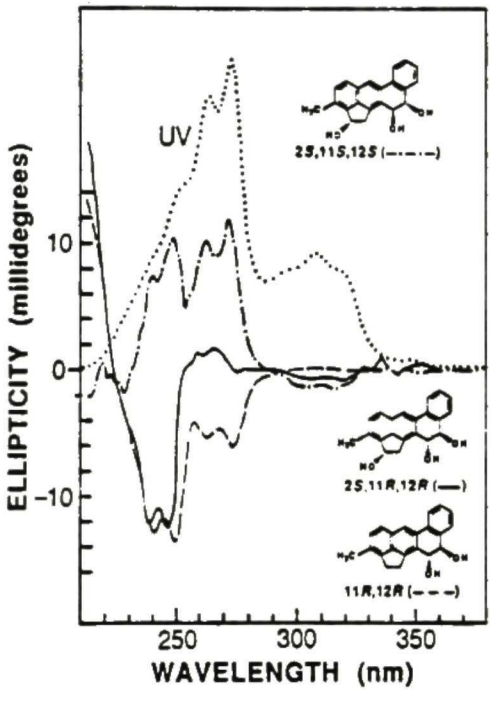

Figure 24. Uv-vis absorption spectrum of the metabolite contained in peak 5a of Fig. 30 (· · · ·) and CD spectra of 3MC 11*R*,12*R*-dihydrodiol (– – – –, methanol; Φ_{250}/A_{274} = – 13.7 millidegrees, (11*R*,12*R*)/(11*S*,12*S*) = 98/2; data taken from Lu *et al.*, 1980), 2*S*-OH-3-MC 11*R*,12*R*-dihydrodiol (metabolite contained in peak 5a of Fig. 30; ——, concn. 1.0 A_{273}/ml, methanol; Φ_{247}/A_{273} = – 12.7 millidegrees), and 2*S*-OH-3MC 11*S*, 12*S*-dihydrodiol (metabolite contained in peak 6 of Fig. 20; – · – · –, concn. 1.0 A_{273}/ml, methanol; Φ_{248}/A_{273} = 10.4 and Φ_{272}/A_{273} = 11.9 millidegrees). Uv-visible absorption spectra of metabolite contained in peaks 2 and 6 are closely similar to that of peak 5a of Fig. 30.

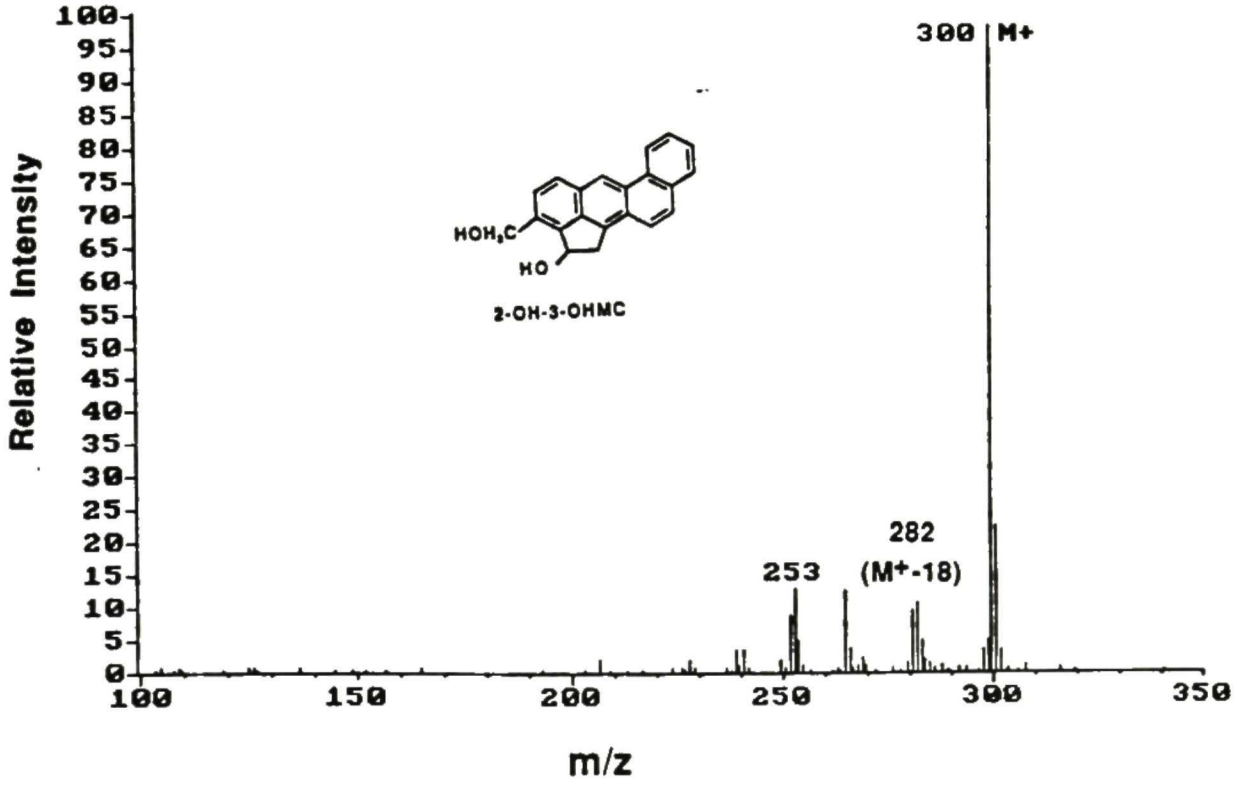

Figure 25. Mass spectrum of 2-OH-3-OHMC.

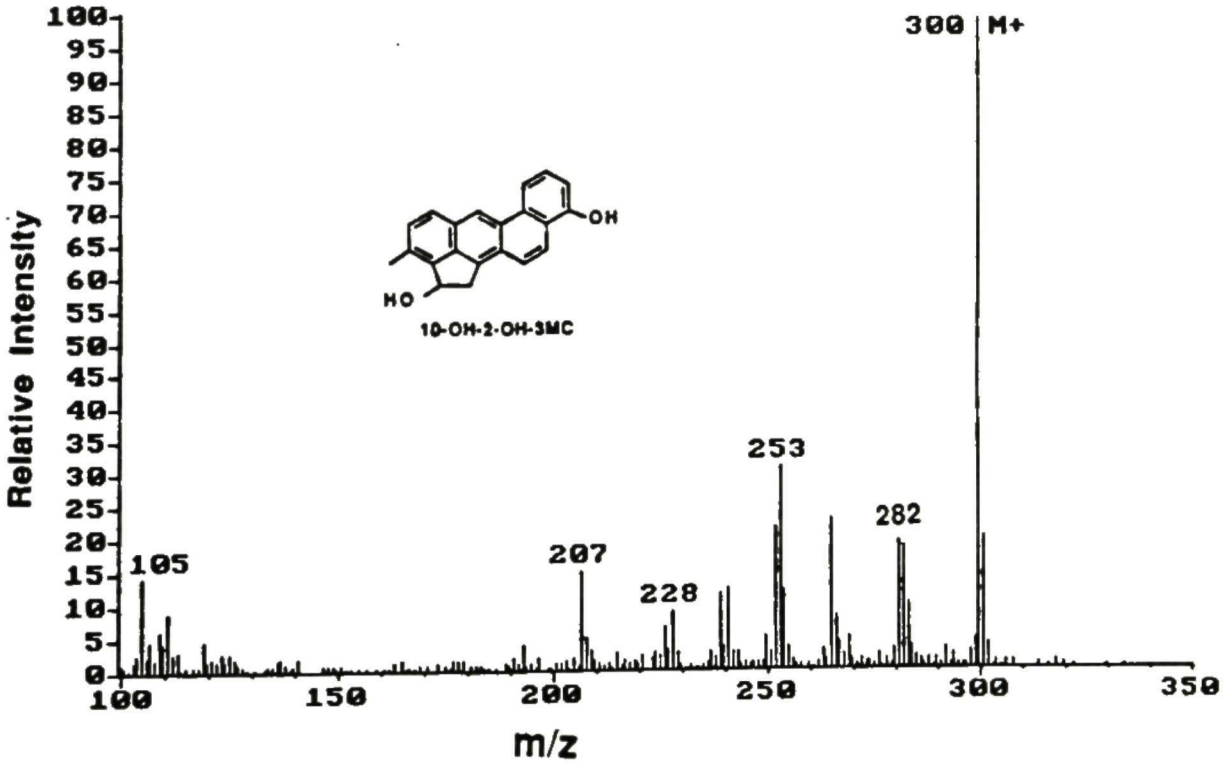

Figure 26. Mass spectrum of 10-OH-2-OH-3MC.

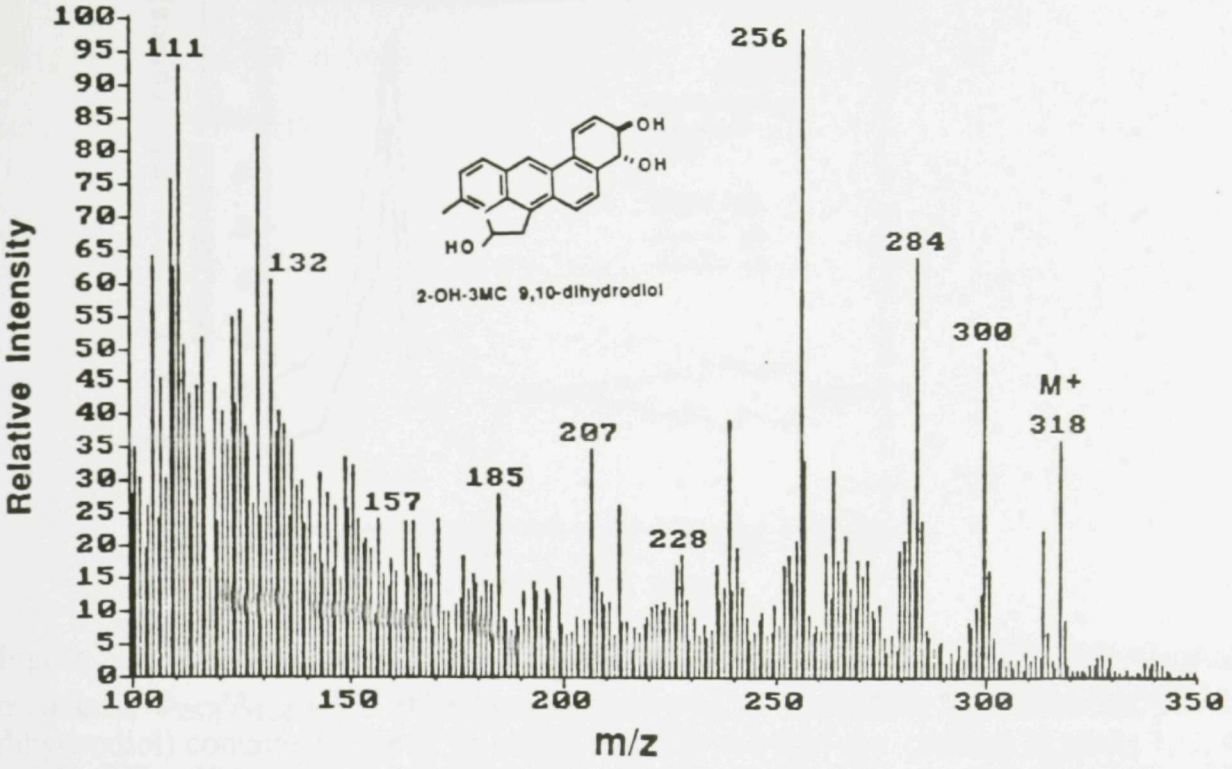

Figure 27. Mass spectrum of 2-OH-3MC *trans*-9,10-dihydrodiol.

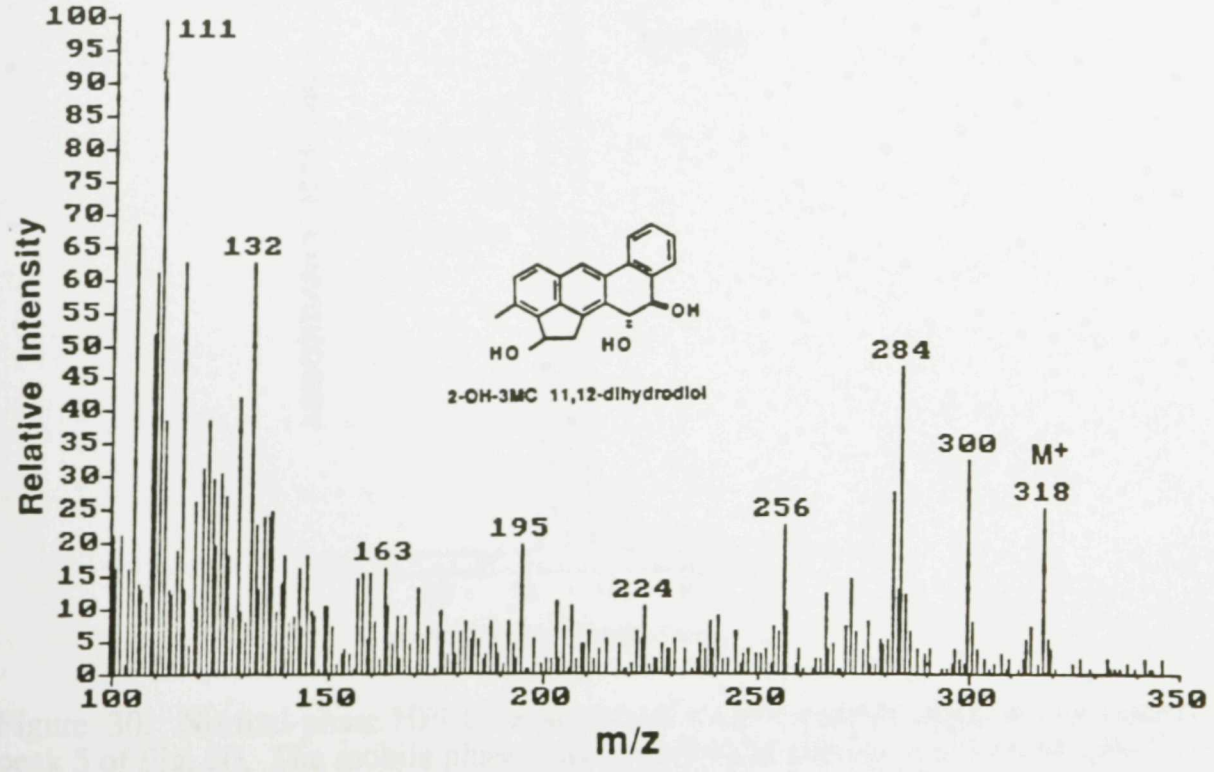

Figure 28. Mass spectrum of 2-OH-3MC *trans*-11,12-dihydrodiol.

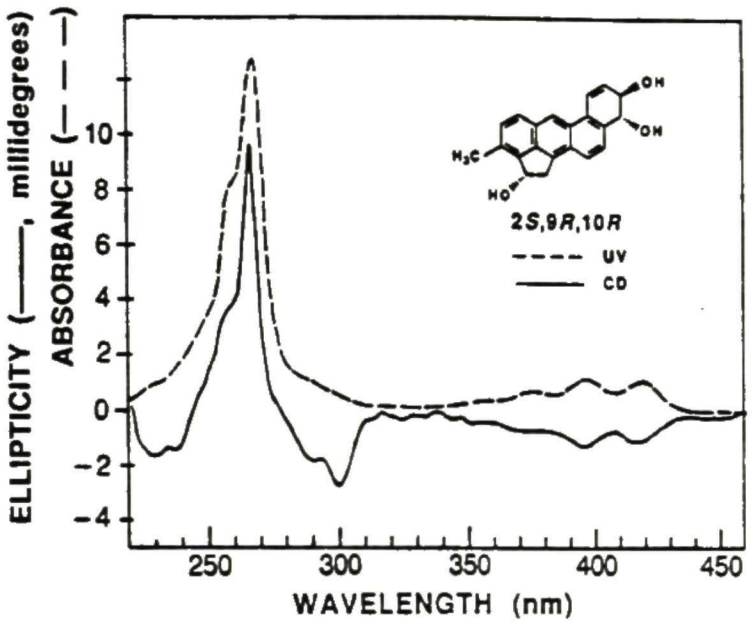

Figure 29. Uv-vis absorption (– – – –, methanol) and CD (——, concn. 1.0 A_{268}/ml, methanol; Φ_{267}/A_{268} = 9.7 millidegrees) spectra of the metabolite (2*S*-OH-3-MC 9*R*,10*R*-dihydrodiol) contained in peak 5b of Fig. 30. The metabolite contained in peaks 1, 3, 4, and 7 of Fig. 20 had uv-visible absorption spectra closely similar to that of peak 5b of Fig. 30.

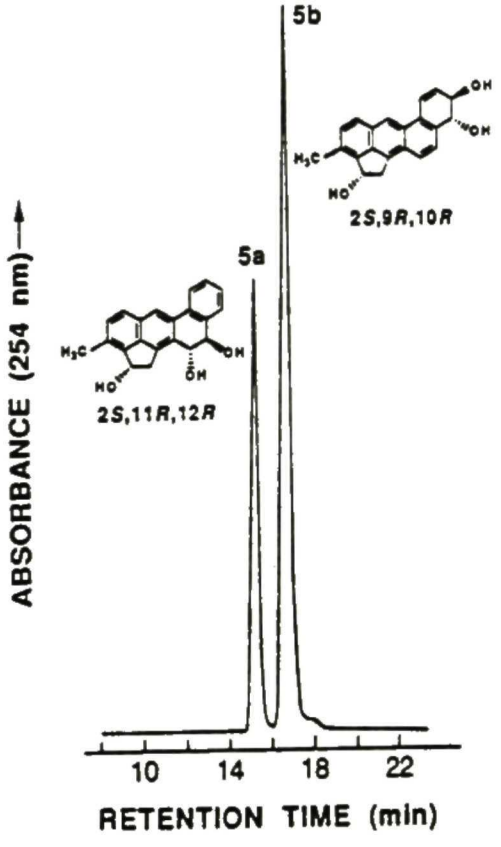

Figure 30. Normal-phase HPLC separation of the two major components contained in peak 5 of Fig. 20. The mobile phase was 15% (v/v) of solvent A in hexane, at a flow rate of 2 ml/min. Identities of metabolites contained in the chromatographic peaks are shown. Evidence for the identification of these two metabolites is described in the text.

This confirms the earlier finding by Sims (1966) who reported that 3MC-2-one is a metabolite of 2-OH-3MC.

In principle, 3-OHMC-2-one may be formed by oxidation of the C_2-hydroxyl group of 2-OH-3-OHMC and/or hydroxylation of C_3-methyl group of 3MC-2-one. 3-OHMC-2-one should have a uv-visible absorption spectrum similar to that of 3MC-2-one and is expected to be eluted between 30 and 33 min in Fig. 20. However, normal-phase HPLC and uv-visible absorption spectral analyses of metabolites eluted between 30 and 33 min of Fig. 20 did not reveal the presence of 3-OHMC-2-one.

3.6 *Oxidation at M-region 9,10-double bond*

M-region is defined, in the context of the bay-region theory of polyaromatic hydrocarbon carcinogenesis (Conney., 1982), as the double bond (such as the 9,10-double bond of 2-OH-3MC or 3MC) at which the procarcinogenic dihydrodiol is formed (Yang *et al.*, 1980). There were six 9,10-dihydrodiols detected as metabolites of 2*S*-OH-3MC. These were: 3MC-2-one 9,10-dihydrodiol (peak 9), 2*S*-OH-3MC 9*S*,10*S*-dihydrodiol (peak 7), 2*S*-OH-3MC 9*R*,10*R*-dihydrodiol (the major component in peak 5, which also contained a K-region 11,12-dihydrodiol, see below), two 9,10-dihydrodiols probably derived from 2*S*-OH-3-OHMC (metabolites contained in peaks 1 and 3), and a 9,10-dihydrodiol (peak 4 of Fig. 20) probably derived from 3MC *cis*-1*S*,2*R*-diol. Peak 5 contained two metabolites, which were separated by normal-phase HPLC (peaks 5a and 5b in Fig. 30). Peak 5b had uv-visible absorption and CD spectra (Fig. 29) identical to that of 2*S*-OH-3MC 9*R*,10*R*-dihydrodiol reported below (Fig. 43). The uv-visible absorption spectrum of peak 5b was also similar to that of 3MC 9,10-dihydrodiol (Tierney *et al.*, 1978; Jacobs *et al.*, 1983). The major metabolite contained in peak 5 and the predominant component contained in peak 7 had retention times on reversed-phase HPLC (Fig. 20) and uv-visible absorption spectra (Fig. 29) identical to those of the two diastereomeric 2-OH-3MC 9,10-dihydrodiols derived by $NaBH_4$ reduction of the 3MC-2-one 9,10-dihydrodiol

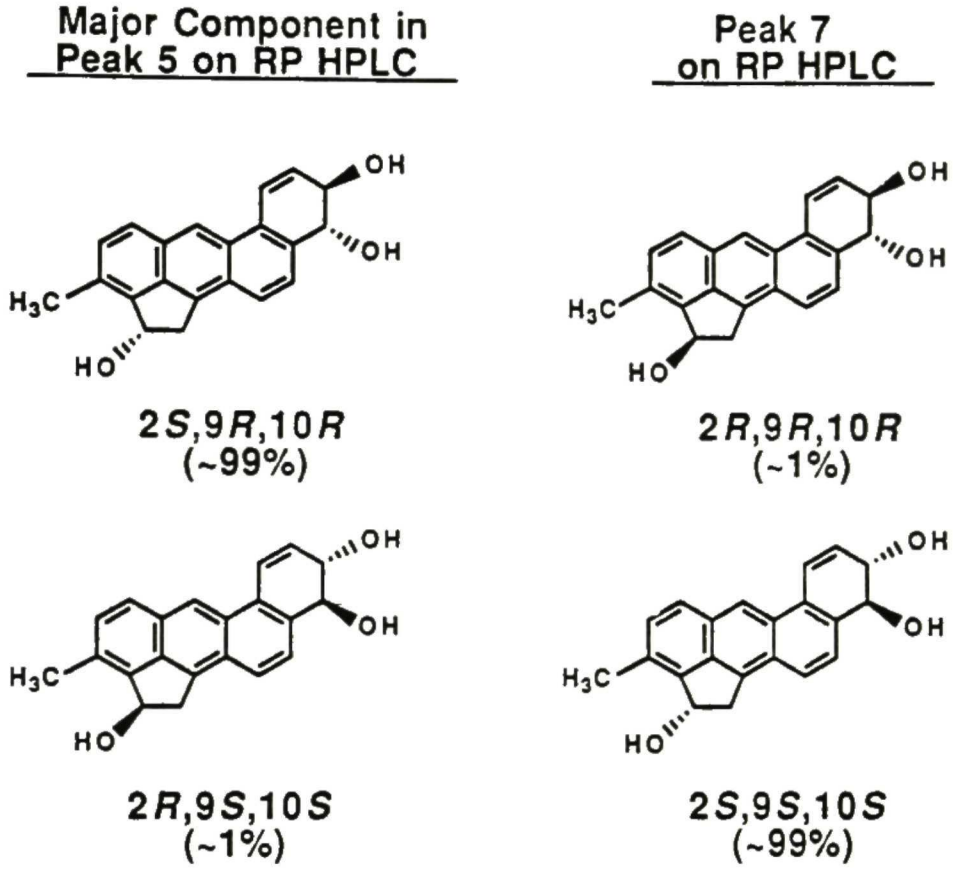

Figure 31. Structure and absolute configuration of two pairs of enantiomeric 2-OH-3MC 9,10-dihydrodiols contained in peak 5b of Fig. 30 (the major component in peak 5 of Fig. 20) and peak 7 of Fig. 20. These four 9,10-dihydrodiols are derived from metabolism of a 2-OH-3MC with a (2*S*)/(2*R*) enantiomer ratio of ~99:1.

(see below; Shou and Yang, 1990b), respectively. 3MC-2-one 9,10-dihydrodiol is the principal metabolite formed in rat liver microsomal metabolism of 3MC-2-one.

The metabolite contained in peak 7 of Fig. 20 was further purified by normal-phase HPLC and it had a uv-visible absorption spectrum identical to that of the 9,10-dihydrodiol contained in peak 5b of Fig. 30. Its retention time on reversed-phase HPLC (Fig. 20) was identical to that of 2*S*-OH-3MC 9*S*,10*S*-dihydrodiol reported later (Fig. 43). Only two diastereomeric 9,10-dihydrodiols, highly enriched either in the 9*R*,10*R*-enantiomer or the 9*S*,10*S*-enantiomer, can be derived from 2-OH-3MC containing a (2*S*)/(2*R*) enantiomer ratio of ~99/1 (Fig. 31). Hence the structures of the major component in peak 5 and the predominant component in peak 7 of Fig. 20 were established to be 2*S*-OH-3MC 9*R*,10*R*-dihydrodiol and 2*S*-OH-3MC 9*S*,10*S*-dihydrodiol, respectively. Based on the AUC of peaks 5 and 7 (~93/7) in Fig. 20 and those of the two major components separated on normal-phase HPLC (~34/66; Fig. 30), the relative amount of 2*S*-OH-3MC 9*R*,10*R*-dihydrodiol and 2*S*-OH-3MC 9*S*,10*S*-dihydrodiol was found to be ~9/1.

The metabolite contained in peak 9 of Fig. 20 had a retention time and uv-visible absorption and mass spectra identical to those of the most abundant metabolite (3MC-2-one 9,10-dihydrodiol) formed in rat liver microsomal metabolism of 3MC-2-one (see metabolism of 3MC-2-one). Since 3MC-2-one was one of the major metabolites (peak 18 in Fig. 20), the formation of 3MC-2-one 9,10-dihydrodiol was to be expected.

The predominant components contained in the minor metabolite peaks 1 and 3 of Fig. 20, following purification by normal-phase HPLC, had uv-visible absorption characteristics (not shown) identical to those of 2*S*-OH-3MC 9*R*,10*R*-dihydrodiol (Fig. 29). The metabolite contained in peak 1 had a M^+ at *m/z* 334 by mass spectra. On the basis of their short retention times, these polar metabolites were tentatively identified as 9,10-dihydrodiols derived from the most abundant metabolite 2*S*-OH-3-OHMC (peak 14).

The minor metabolite contained in peak 4 of Fig. 20 had uv-visible absorption characteristics (not shown) identical to those of 2*S*-OH-3MC 9*R*,10*R*-dihydrodiol (Fig.

29). It had a retention time identical to the 9,10-dihydrodiol derived by incubation of 3MC *cis*-1*S*,2*R*-diol (see later). Hence the metabolite contained in peak 4 of Fig. 20 was tentatively identified as a 3MC *cis*-1,2-diol:*trans*-9,10-dihydrodiol derived either from further metabolism of 3MC *cis*-1*S*,2*R*-diol (peak 16) or from (*cis*)-C_1-hydroxylation of either 2*S*-OH-3MC 9*R*,10*R*-dihydrodiol (peak 5b) or 2*S*-OH-3MC 9*S*,10*S*-dihydrodiol (peak 7).

Since 2*S*-OH-3MC 9*R*,10*R*-dihydrodiol (major component in peak 5 of Fig. 20) was a major metabolite, its metabolic precursor 2*S*-OH-3MC 9,10-epoxide is expected to be formed in the metabolism of 2*S*-OH-3MC. In addition to being hydrated to form diastereomeric 9,10-dihydrodiols, 2*S*-OH-3MC 9,10-epoxide is expected to partially isomerize to form 9-hydroxy-2*S*-OH-3MC and 10-hydroxy-2*S*-OH-3MC (see uv-visible absorption and mass spectra in Fig. 32B and 26). 10-hydroxy-2*S*-OH-3MC is expected to be the major isomerization product of 2*S*-OH-3MC 9,10-epoxide (Fu *et al.*, 1978). The metabolite contained in peak 13 had a uv-visible absorption spectrum similar to that of 4-OH-BA (Fig. 32A). Acid-catalyzed dehydration of 2*S*-OH-3MC 9*R*,10*R*-dihydrodiol (major component in peak 5 of Fig. 32B) formed both 9-OH-2*S*-OH-3MC (uv-visible absorption spectrum in Fig. 20) and 10-OH-2*S*-OH-3MC (uv-visible absorption spectrum in Fig. 20), which had retention times identical to those of peaks 12 and 13 of Fig. 20, respectively. However, the uv-visible absorption spectrum of metabolite peak 12 was not that of 9-OH-2*S*-OH-3MC and its identity was not established. Since 10-OH-2*S*-OH-3MC (peak 13 of Fig. 20) was a minor metabolite, 9-OH-2*S*-OH-3MC was probably present in peak 12, but the amount might have been too small to be detected.

3.7 *Oxidation at K-region 11,12-double bond*

The 11,12-double bond of 2*S*-OH-3MC (or 3MC) is the most electron-rich K-region of the molecule. There were three K-region 11,12-dihydrodiols detected as metabolites of 2*S*-OH-3MC. These were: 2*S*-OH-3MC 11*S*,12*S*-dihydrodiol (peak 6 of Fig. 20), 2*S*-OH-3MC 11*R*,12*R*-dihydrodiol (peak 5a of Fig. 30), and a minor metabolite

(peak 2 of Fig. 20) tentatively identified as a 11,12-dihydrodiol derived from 2*S*-OH-3-OHMC.

Peak 2 was further purified by normal-phase HPLC (Table 3). This and peaks 5a (Fig. 30) and 6 (Fig. 20) had uv-visible absorption spectra (Fig. 24) similar to that of an authentic 3MC *trans*-11,12-dihydrodiol. Both peaks 5a and 6 had M^+ at *m/z* of 318 and characteristic fragment ions at m/z 300 (loss of H_2O) and 282 (loss of two H_2O) (Fig. 28).

There are two sets of CD Cotton bands in the CD spectrum of 3MC 11*R*,12*R*-dihydrodiol (Fig. 24), the absolute configuration of which has been established earlier (Yang *et al.*, 1986). Except red-shifts by ~3 nm, the major CD Cotton effects of peak 5a of Fig. 30 in the wavelength region between ~230-255 nm were the same as those of 3MC 11*R*,12*R*-dihydrodiol (Fig. 24). It should be noted that 2*S*-OH-3MC has positive CD Cotton bands centered around 256 nm (Fig. 21B). In the CD spectrum of metabolite peak 5a, the positive CD Cotton bands between ~255-275 nm owing to the additional *S*-chiral center at C_2 appeared to have cancelled the negative CD Cotton bands between ~255-285 nm owing to the C_{11} and C_{12} chiral centers, resulting in small but positive CD Cotton bands (Fig. 24).

The CD Cotton effects of metabolite peak 6 in the wavelength region between ~230-252 nm were opposite in signs to those of the metabolite peak 5a (Fig. 24). However, due to positive CD bands contributed by the *S*-chiral center at C_2, the CD Cotton effects in the wavelength region between ~255-275 nm became considerably larger in magnitude (Fig. 24); *i.e.*, the positive CD bands between ~255-275 nm owing to the additional *S*-chiral center at C_2 were additive to the positive CD bands between ~255-285 nm owing to the C_{11} and C_{12} chiral centers.

Taken together, the above results indicated that the major component contained in peak 5 (which is peak 5a of Fig. 30) and the predominant component contained in peak 6 of Fig. 20 were 2*S*-OH-3MC 11*R*,12*R*-dihydrodiol and 2*S*-OH-3MC 11*S*,12*S*-dihydrodiol, respectively. Based on the AUC of peaks 5 and 6 (~90:10) in Fig. 20 and

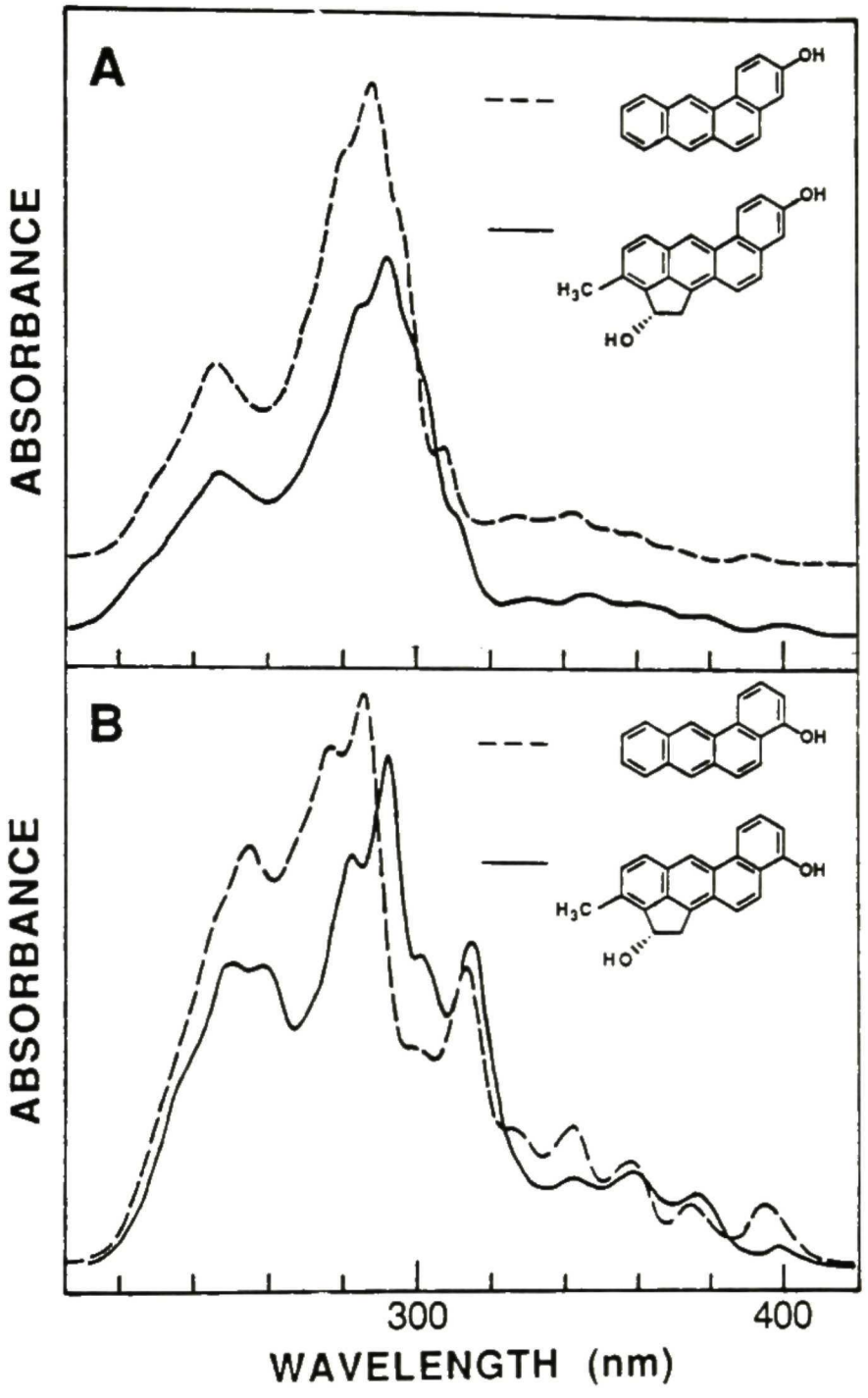

Figure 32. (A). Uv-vis absorption spectra of 3-OH-BA (– – – –, in methanol; an authentic compound) and 9-OH-2*S*-OH-3MC (——, in methanol; a product derived from acid-catalyzed dehydration of a 2-OH-3MC 9,10-dihydrodiol). (B). Uv-vis absorption spectra of 4-OH-BA (– – – –, in methanol; an authentic compound) and 10-OH-2*S*-OH-3MC (———, in methanol; a product derived from acid-catalyzed dehydration of a 2*S*-OH-3MC 9,10-dihydrodiol. The latter is identical to that of the metabolite contained in peak 13 of Fig. 20.

those of the two components in peak 5 separated by normal-phase HPLC (5a/5b: ~34/66; Fig. 30), the relative amount of 2*S*-OH-3MC 11*R*,12*R*-dihydrodiol and 2*S*-OH-3MC 11*S*,12*S*-dihydrodiol was found to be ~77/23.

Peak 17 of Fig. 20 was an unreacted substrate (2*S*-OH-3MC, mass spectrum as shown in Fig. 33). The product contained in peak 18 of Fig. 20 was identified as 3MC-2-one, by the comparison of its retention time on HPLC, uv-visible absorption and mass spectra with those of authentic compound (Fig. 34).

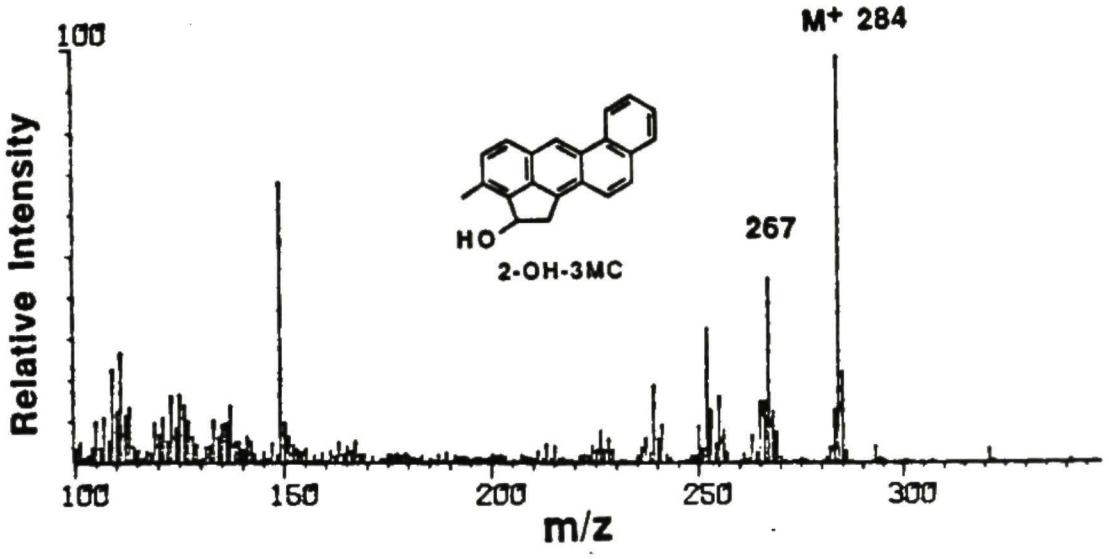

Figure 33. Mass spectrum of 2-OH-3MC.

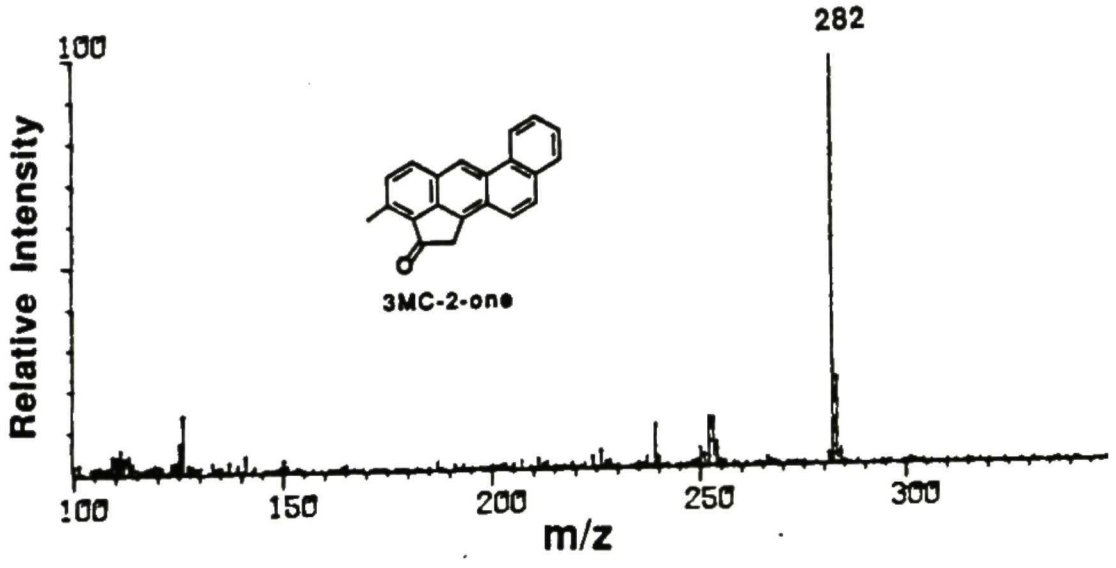

Figure 34. Mass spectrum of 3MC-2-one.

4. *Stereoselective Metabolism of Racemic 2-OH-3MC*

4.1 *HPLC separation and identification of the metabolites*

Metabolites formed in the incubation of (±)2-OH-3MC by liver microsomes from PB-treated rats were separated by reversed-phase HPLC (Fig. 35). The retention time of 3MC was indicated in Fig. 35 as an internal standard. In this study, ~53% of the substrate was metabolized. Peak 16 contained the unreacted substrate 2-OH-3MC. The structures of metabolites contained in most of the chromatographic peaks in Fig. 35 have been characterized as described in the metabolism of 2*S*-OH-3MC. Some metabolites which were not found in the metabolism of 2*S*-OH-3MC were identified as described below.

Because the substrate was a racemic compound, the number of metabolites formed in the metabolism of (±) 2-OH-3MC were more than those from 2*S*-OH-3MC. Absolute configurations and enantiomeric compositions of major chiral products formed in the metabolism of (±)2-OH-3MC were determined by CD spectral data.

Peak 1 in reversed-phase HPLC in Fig. 35 contained two components and were further separated by normal-phase HPLC (Fig. 36A). Peak 1a of Fig. 36A had uv-visible absorption spectrum similar to that of BA 1,2-dihydrodiol (Yang *et al.*, 1983) (Fig. 37) and was tentatively identified as 2-OH-3MC 7,8-dihydrodiol, which was not formed in the metabolism of 2*S*-OH-3MC. Relative to those of BA 1,2-dihydrodiol, red-shifts of some absorption bands of this metabolite were observed due to additional substituents (Fig. 37). Because the hydroxyl groups at C_7 and C_8 adopt preferentially a quasidiaxial conformation, the more polar and quasidiaxial 2-OH-3MC 7,8-dihydrodiol was eluted with a shorter retention time than the other quasiequatorial dihydrodiols on reversed-phase HPLC. CD spectrum of peak 1a of Fig. 36A exhibited Cotton effects similar to those of 7-MBA 1*R*,2*R*-dihydrodiol (Yang and Fu, 1984) and thus this metabolite is enriched in the 7*R*, 8*R*-enantiomer (Fig. 37).

Peak 6 of Fig. 35 contained two components and were separated by normal-phase HPLC. One of the two components in peak 6 was not found in the metabolism of 2*S*-OH-

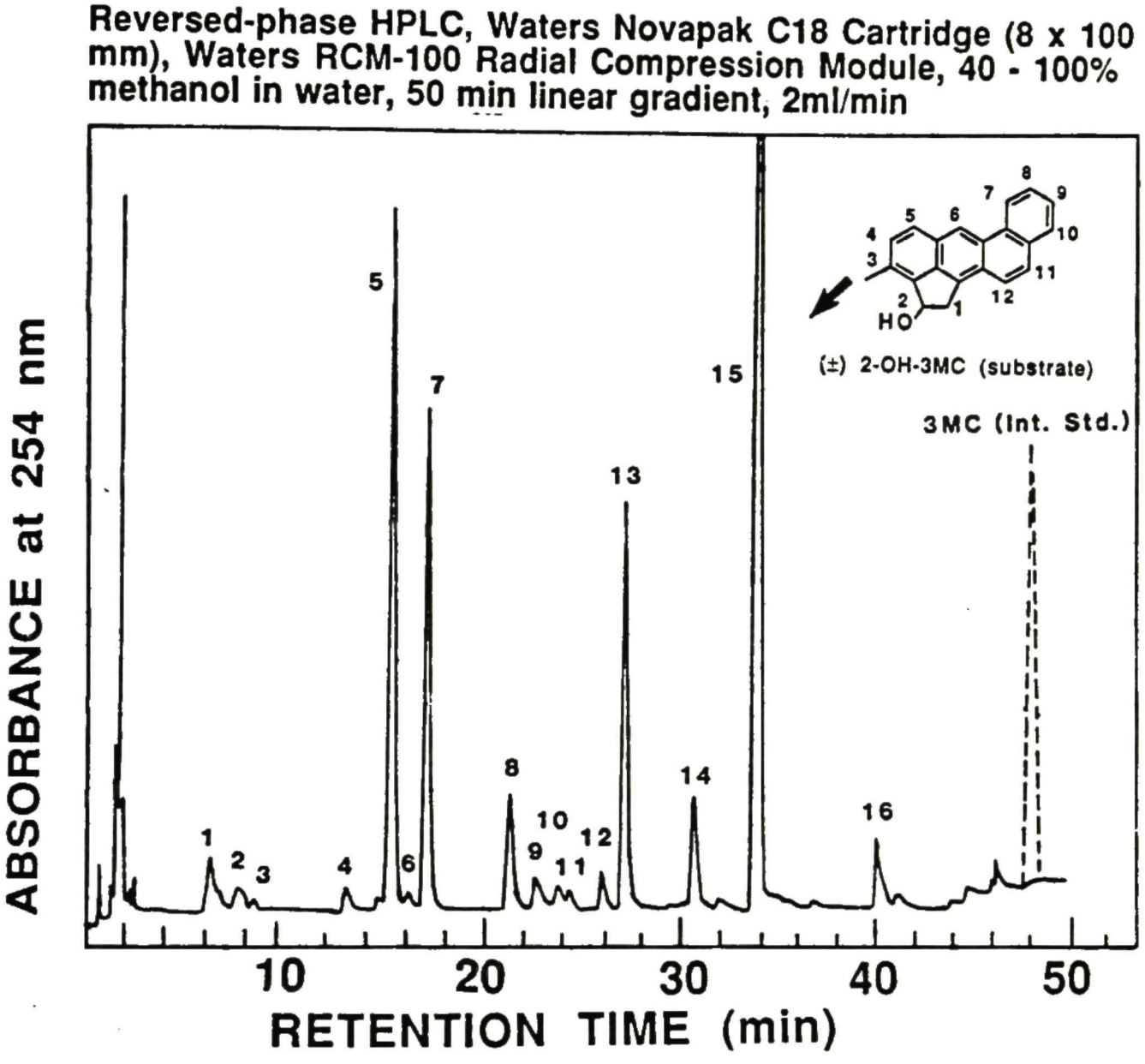

Figure 35. Reversed-phase HPLC separation of racemic 2-OH-3MC and its metabolites. Identities of metabolites contained in various chromatographic peaks are: peak 1, a mixture of 2-OH-3MC 7,8-dihydrodiol and a diastereomeric 2-OH-3-OHMC 9,10-dihydrodiol; peak 2, a mixture of 2-OH-3-OHMC 11,12-dihydrodiol and a diastereomeric 2-OH-3-OHMC 9,10-dihydrodiol; peak 3, unknown; peak 4, 3MC *cis*-1,2-diol:9,10-dihydrodiol; peak 5, a mixture of a diastereomeric 2-OH-3MC 11,12-dihydrodiol and 2*S*-OH-3MC 9,10-dihydrodiol (major); peak 6, a mixture of a diastereomeric 2-OH-3MC 11,12-dihydrodiol and 8-OH-2-OH-3-OHMC; peak 7, 2*R*-OH-3MC 9,10-dihydrodiol; peak 8, 3MC-2-one 9,10-dihydrodiol; peak 9, 8-OH-2-OH-3MC; peak 10, 3MC *trans*-1,2-diol peak 11, 9-OH-2-OH-3MC; peak 12, 10-OH-2-OH-3MC; peak 13, 2-OH-3-OHMC; peak 14, 3MC *cis*-1,2-diol; peak 15, 2-OH-3MC (remaining substrate) and peak 16, 3MC-2-one.

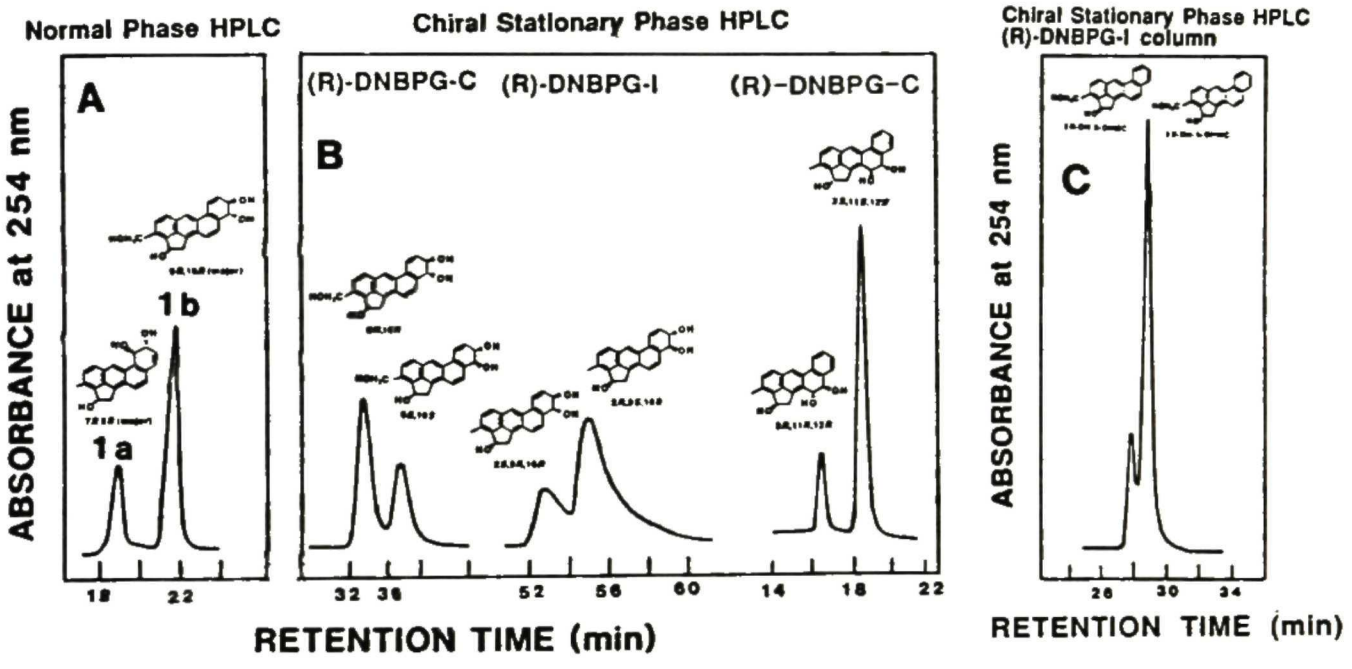

Figure 36. (A) Normal-phase HPLC separation of the two major components contained in peak 1 of Fig. 35. The mobile phase was 20% (v/v) of solvent A in hexane, at a flow rate of 2 ml/min. Identities of metabolites contained in the chromatographic peaks are shown. Evidence for the identification of these two metabolites is described in the text. (B) Chiral stationary phase HPLC separation and absolute configurations of metabolite enantiomers are indicated in this figure. (C) Chiral stationary phase HPLC separation of 2-OH-3-OHMC in peak 13 of Fig. 35 in the metabolism of (±) 2-OH-3MC by liver microsomes of rats treated with PB.

3MC and had uv-visible absorption spectrum identical to that of 8-OH-2*S*-OH-3MC, the latter is a metabolite of 2*S*-OH-3MC (see Fig. 21A). Due to a shorter retention time (hence more polar) on reversed-phase HPLC than that of 8-OH-2-OH-3MC contained in peak 9 of Fig. 35, the metabolite contained in peak 6 was tentatively identified as 8-OH-2-OH-3-OHMC.

There were six 9,10-dihydrodiols detected as metabolites of (±)2-OH-3MC. These were: 3MC-2-one 9,10-dihydrodiol (peak 8), two diastereomeric 2-OH-3MC 9, 10-dihydrodiols contained in peaks 5 and 7, two diastereomeric 9,10-dihydrodiols (peaks 1b and 2) probably derived from 2-OH-3-OHMC and one 9,10-dihydrodiol probably derived from 3MC *cis*-1,2-diol (peak 4 of Fig. 35).

Peak 5 contained two components, 2-OH-3MC 11,12-dihydrodiol (peak 5a of Fig. 30) and 2-OH-3MC 9,10-dihydrodiol (peak 5b of Fig. 30), which were separated as described in Fig. 30. Peaks 5b and 7 in Fig. 35 were two diastereomeric 2-OH-3MC 9,10-dihydrodiols. CD Cotton effects of 2-OH-3MC 9,10-dihydrodiol contained in peak 5 of Fig. 35 were opposite to those of 2*S*-OH-3MC 9*R*,10*R*-dihydrodiol (Fig. 29). Thus this metabolite (peak 5b) is highly enriched in 2*R*,9*S*,10*S* enantiomer. In contrast, CD spectrum of peak 7 of Fig. 35 indicated the presence of mainly 2*R*-OH-3MC 9*R*,10*R*-dihydrodiol. Based on the AUC ratio of peak 5 and peak 7 in Fig. 35 (59/41) and those of the two major components in peak 5 separated on normal-phase HPLC (~18/82; not shown), the ratio of two diastereomeric 2-OH-3MC 9,10-dihydrodiols in peak 5 and 7 was estimated to be ~54/46.

The 2-OH-3MC 9,10-dihydrodiols contained in peaks 5 and 7 were products of 2-OH-3MC 9,10-epoxides which are hydrated by epoxide hydrolase to form diastereomeric 9,10-dihydrodiols. 2-OH-3MC 9,10-epoxides are also partially isomerized to form 9-OH-2-OH-3MC and 10-OH-2-OH-3MC (peaks 11 and 12 of Fig. 35). 10-OH-2-OH-3MC was a major isomerization product of 2-OH-3MC 9,10-epoxides in the metabolism of (±) 2-OH-3MC.

Peak 2 of Fig. 35 contained two components and were separated by normal-phase HPLC (not shown). One of the two components in peak 2 and peak 1b of Fig. 36A had uv-vis absorption spectra identical to that of 2-OH-3-OHMC 9,10-dihydrodiol which had been identified as a metabolite in 2*S*-OH-3-MC metabolism. Metabolites contained in peak 1b of Fig. 36A and peak 2 of Fig. 35 were probably two diastereomeric 2-OH-3-OHMC 9,10-dihydrodiols.

The component contained in peak 8 of Fig. 35 was identified as 3MC-2-one 9,10-dihydrodiol as described in the metabolism of 2*S*-OH-3MC. CD spectrum of this metabolite compared with the 3MC-2-one 9*R*,10*R*-dihydrodiol formed in the metabolism of 3MC-2-one (Fig. 40) indicated that the metabolite was enriched in the 9*R*,10*R*-enantiomer.

The minor metabolite contained in peak 4 of Fig. 35 was 3MC *cis*-1,2-diol:9,10-dihydrodiol. It had a retention time identical to that of a 9,10-dihydrodiol derived by incubation of 3MC *cis*-1*S*,2*R*-diol (see below).

Two diastereomeric 2-OH-3MC 11,12-dihydrodiols (peak 5a of Fig. 30 and peak 6 of Fig. 35) which were identified in the metabolism of 2*S*-OH-3MC. One minor 11,12-dihydrodiol probably derived from 2-OH-3-OHMC was contained in peak 2 of Fig. 35; it was not found in the metabolism of 2*S*-OH-3MC. Peak 2 of Fig. 35 had a shorter retention time than those 11,12-dihydrodiols contained in peaks 5 and 6 of Fig. 35. The metabolite in peak 2 of Fig. 35 was therefore tentatively identified as a 2-OH-3-OHMC 11,12-dihydrodiol.

3MC *trans*-1,2-diol in peak 10 and 3MC *cis*-1,2-diol in peak 14 of Fig. 35 had an AUC ratio of 20/80. Their enantiomeric compositions were analyzed on a *R*-DNBPG-C column as described below. The metabolite contained in peak 13 of Fig. 35 was 2-OH-3-OHMC, which had been established in the metabolism of 2*S*-OH-3MC.

4.2 *Absolute configuration and enantiomeric composition of chiral metabolites*

The CD spectrum of the metabolically formed 2-OH-3MC *trans*-7,8-dihydrodiol from peak 1a of Fig. 36A is shown in Fig. 37 and exhibited Cotton effects similar to those

of 7-MBA *trans*-1*R*,2*R*-dihydrodiol (Yang and Fu, 1984). We concluded that the major enantiomer of 2-OH-3MC *trans*-7,8-dihydrodiol has the 7*R*,8R absolute configuration. The optical purity of this metabolite was not determined.

The metabolically formed 2-OH-3-OHMC 9,10-dihydrodiol contained in peak 1 of Fig. 35 had CD Cotton effects similar to those of 2*S*-OH-3MC 9*R*,10*R*-dihydrodiol (Fig. 29), indicating that the major enantiomer of this metabolite was 2-OH-3-OHMC 9*R*, 10*R*-dihydrodiol. The absolute configuration of the C_2-hydroxyl group is unknown. Enantiomeric composition of 2-OH-3-OHMC 9,10-dihydrodiol was determined by CSP HPLC. The (9*R*,10*R*):(9*S*,10*S*) ratio was found to be 62:38 (Fig. 36B). CD Cotton effects of each enantiomer collected from *R*-DNBPG-C column were opposite in signs and mirror images of each other. The two diastereomeric 2-OH-3MC 9,10-dihydrodiols obtained from peaks 5 and 7 of Fig. 35 had a ratio of 54:46. Each diastereomer has a pair of enantiomers. The diastereomeric 2-OH-3MC 9,10-dihydrodiol contained in peak 5 of Fig. 35 had a CD spectrum with negative Cotton effects between 245 and 275 nm, resulting from major 2*R*-OH-3MC 9*S*,10*S*-dihydrodiol. Enantiomers of 2-OH-3MC 9,10-dihydrodiol contained in peak 5 of Fig. 35 were separated on *R*-DNBPG-I column (Fig. 36B) and had a ratio of (2*S*, 9*R*,10*R*):(2*R*,9*S*,10*S*) of 24:76. Positive CD Cotton effects of the 2-OH-3MC 9,10-dihydrodiol contained in peak 7 of Fig. 35 (not shown) indicated that this product was enriched in 2*R*,9*R*,10*R* enantiomer. Since the Φ_{267}/A_{268} value of the enantiomerically pure 2*R*-OH-3MC 9*R*,10*R*-dihydrodiol was 8.8 millidegrees (see metabolism of 3MC-2-one), the enantiomeric composition of the 2-OH-3MC 9,10-dihydrodiol in peak 7 of Fig. 35 was readily determined by its CD spectral data and the ratio of (2*R*,9*R*,10*R*):(2*S*,9*S*,10*S*) was 81:19. The percentages of enantiomer in two diastereomeric 2-OH-3MC 9,10-dihydrodiols, formed in the metabolism of (±) 2-OH-3MC by liver microsomes of rats treated with PB, were found to be 14.6 (2*S*,9*R*,10*R*), 39.4 (2*R*,9*S*,10*S*), 37.3 (2*R*,9*R*,10*R*) and 8.7 (2*S*,9*S*,10*S*).

Two diastereomers of 2-OH-3MC 11,12-dihydrodiols were also obtained in peak

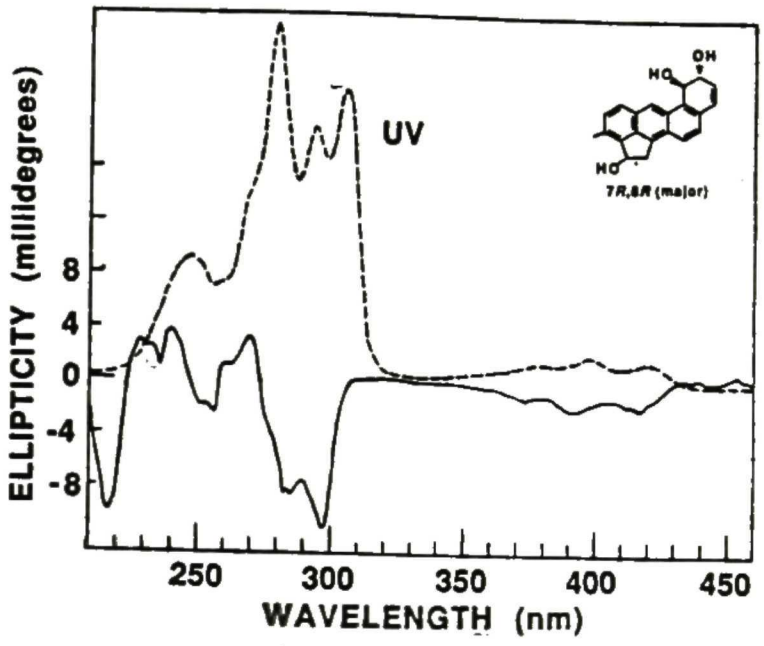

Figure 37. Uv-vis absorption (– – – –, methanol) and CD (——, concn. 1.0 A_{272}/ml, methanol; Φ_{296}/A_{272} = -11.2 millidegrees) spectra of the metabolite 2-OH-3-MC 7*R*,8*R*-dihydrodiol (major) contained in peak 1 of Fig. 35.

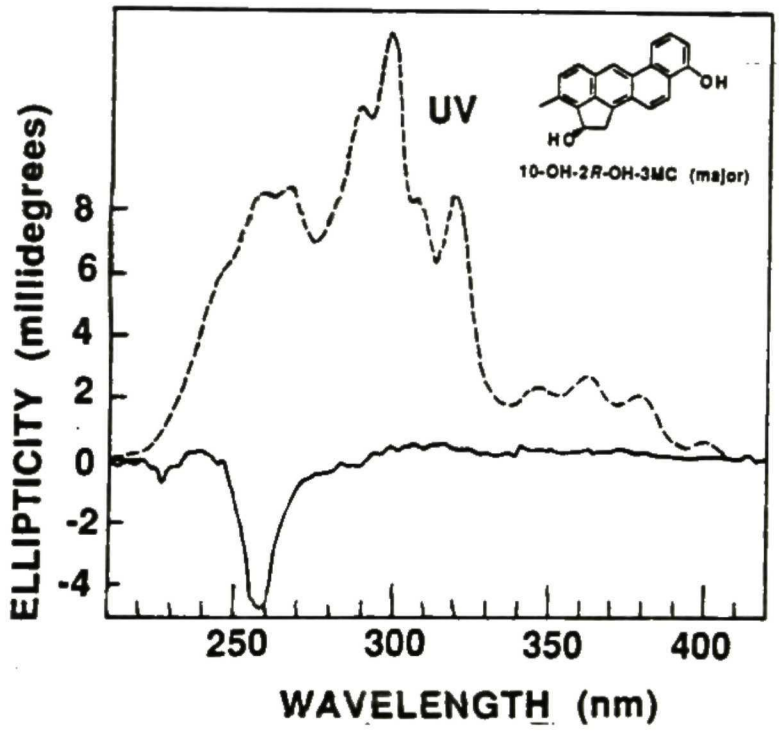

Figure 38. Uv-vis absorption (– – – –, methanol) and CD (——, concn. 1.0 A_{292}/ml, methanol; Φ_{258}/A_{292} = -4.8 millidegrees) spectra of the metabolite 10-OH-2*R*-OH-3MC (major) contained in peak 12 of Fig. 35.

5a of Fig. 30 and peak 6 of Fig. 35 and absolute configurations of major enantiomers in each diastereomer were determined by CD spectra (not shown) by comparing with that of 2*S*-OH-3MC 11*R*(*S*),12*R*(*S*)-dihydrodiol (Fig. 24). The metabolite in peak 5a of Fig. 30 contained an almost optically pure enantiomer with 2*S*,11*R*,12*R* stereochemistry based on CD data of enantiomeric 2*S*-OH-3MC 11*R*,12*R*-dihydrodiol formed in the metabolism of 2*S*-OH-3MC. The metabolite in peak 6 had a CD spectrum identical to that of 2*S*-OH-3MC 11*S*, 12*S*-dihydrodiol and had a relative amount of 19 (2*R*,11*R*,12*R*) to 81 (2*S*,11*S*,12*S*) which was resolved by *R*-DNBPG-C column (Fig. 36B).

The relative amount of 3MC *trans*-1,2-diol contained in peak 10 and 3MC *cis*-1,2-diol in peak 14 of Fig. 35 was found to be 20:80. Absolute configurations and enantiomeric compositions of *trans*- and *cis*-1,2-diol of 3MC have been established (Fig. 13). Enantiomeric ratios of the metabolically formed *trans*- and *cis*-1,2-diols derived from the metabolism of (±) 2-OH-3MC by liver microsomes prepared from rats treated with PB were 68 (1*S*,2*S*):32 (1*R*,2*R*) and 18 (1*S*,2*R*):82 (1*R*,2*S*) respectively (Table 4). Taken together, the relative amounts of these four stereoisomers in 3MC *trans*- and 3MC *cis*-1,2-diols formed were 65.6 (1*R*,2*S*) > 14.4 (1*S*,2*R*) > 13.8 (1*S*,2*S*) > 6.2 (1*R*,2*R*). The results indicated that regioselective C_1-hydroxylation of (±)2-OH-3MC by liver microsomes prepared from PB-pretreated rats was enantioselective toward 2*R*-enantiomer over the 2*S*-enantiomer, resulting in primarily *trans*-1*S*,2*S*-diol (68%) and *cis*-1*R*,2*S*-diol enantiomer (82%).

The 2-OH-3-OHMC, one of the most abundant metabolites contained in peak 13 of Fig. 35 had CD Cotton effects identical to those of 2*S*-OH-3-OHMC (Fig. 23). The enantiomers of 2-OH-3-OHMC formed were separated using the *R*-DNBPG-I column and had a (2*R*):(2*S*) ratio of 19:81 (Fig. 36C and Table 4). The hydroxylation of C_3-methyl sidechain of (±) 2-OH-3MC was enantioselective toward the 2*S*-OH-3MC, forming a major 2*S*-OH-3-OHMC metabolite.

Table 4. Enantiomeric composition of metabolites formed in the metabolism of racemic 2-OH-3MC by rat liver microsomes.

Metabolite[a] (peak no. on RP)	EA(%)[b]	Enantiomer Ratio (%)[c] A	B
2-OH-3-OHMC 9,10-DHD (1)	20	61.7 (9*R*,10*R*)	38.3 (9*S*,10*S*)
2-OH-3MC 9,10-DHD (5b)	15	24.0 (2*S*,9*R*,10*R*)	76.0 (2*R*,9*S*,10*S*)
2-OH-3MC 11,12-DHD (5a)	15	18.8 (2*R*,11*R*,12*R*)	82.2 (2*S*,11*S*,12*S*)
3MC *trans*-1,2-diol (10)	10	67.7 (1*S*,2*S*)	32.3 (1*R*, 2*R*)
2-OH-3-OHMC (13)	10	19.0 (2*R*)	81.0 (2*S*)
3MC *cis*-1,2-diol (14)	7	18.5 (1*S*,2*R*)	81.5 (1*R*,2*S*)

a. Racemic 2-OH-3MC (40 nmol per ml of incubation mixture) was incubated with liver microsomes (1.0 mg of protein per ml of incubation mixture) from PB-treated rats at 37°C for 30 min.

b. The columns were ionically or covalently bonded *R*-DNBPG and the percentage of eluent EA (ethanol-acetonitrile, 2:1, v/v) in hexane was shown in this table. The flow rate was 2 ml/min.

c. Enantiomers are designated as A and B according to their elution order on CSP HPLC.

The CD spectrum of the metabolite contained in peak 8 of Fig. 35 was optically active and had a major enantiomer of 3MC-2-one 9*R*,10*R*-dihydrodiol (not shown). CD data (Φ_{280}/A_{260} = 3.6 millidegrees) of 3MC-2-one 9,10-dihydrodiol indicated a (9*R*,10*R*):(9*S*,10*S*) enantiomeric ratio of 84:16 (see also the data in the metabolism of 3MC-2-one). The enantiomeric composition of 3-MC-2-one 9,10-dihydrodiol formed in the metabolism of (±) 2-OH-3MC by liver microsomes of rats treated with PB was estimated to have a (9*R*,10*R*):(9*S*,10*S*) ratio of 71:29. The metabolically formed 3MC-2-one 9,10-dihydrodiol could be derived from dehydrogenation of C_2-hydroxyl group of 2-OH-3MC 9,10-dihydrodiol (major metabolite) and epoxidation at 9,10-double bond of 3MC-2-one.

The CD spectrum of 8-OH-2-OH-3MC contained in peak 9 of Fig. 35 exhibited positive Cotton effects (Φ_{256}/A_{292} = 4.0 millidegrees) between 240 and 280 nm, similar to those of 8-OH-2*S*-OH-3MC established (Fig. 21B). Hence this metabolite was highly enriched in 8-OH-2*S*-OH-3MC. Since the value (Φ_{256}/A_{292}=7.0 millidegrees) of optically pure 8-OH-2*S*-OH-3MC formed in the metabolism of 2*S*-OH-3MC was obtained, the enantiomeric composition of the 8-OH-2-OH-3MC formed in the metabolism of (±) 2-OH-3MC was estimated to have a (2*R*):(2*S*) ratio of 21:79.

The CD spectrum of 10-OH-2-OH-3MC contained in peak 12 of Fig. 35 exhibited a strong negative Cotton effects between 245 and 290 nm (Φ_{258}/A_{292} = –4.8 millidegrees) (Fig. 38) and indicated that the major enantiomer of 10-OH-2-OH-3MC was derived from 2*R*-OH-3MC. Optical purity of this metabolite was not determined.

5. *Stereoselecitve Metabolism of 3MC-2-one* (Shou and Yang, 1990b)

5.1 *Effects of enzyme induction on metabolite formation*

The products formed in the metabolism of 3MC-2-one by liver microsomes from PB-treated rats were separated by reversed-phase HPLC (Fig. 39). Metabolites were obtained by a 10-min incubation of 3MC-2-one with 0.25 mg protein equivalent of rat liver microsomes and cofactors. Chromatographic peaks marked with 1 and 2 were identified as 3MC-2-one 9,10-dihydrodiol and 2-OH-3MC, respectively (see below). The metabolically formed 2-OH-3MC had an identical retention time and uv absorption spectrum to that of the authentic compound. Unmarked chromatographic peaks in Fig. 39 have not been characterized. For the purpose of estimating the relative amounts of 3MC-2-one 9,10-dihydrodiol and 2-OH-3MC formed by different rat liver microsomal preparations, an identical amount of an internal standard (3MC, retention time 48.3 min, Fig. 39) for chromatography was added to the incubation mixture after the metabolic reaction had been stopped by the addition of acetone. With the aid of the internal standard, the amounts of 3MC-2-one 9,10-dihydrodiol formed by liver microsomes from PB-treated and 3MC-treated rats were determined to be ~6.5-fold and ~3.3-fold of that formed by liver microsomes from untreated rats, respectively. The amounts of 2-OH-3MC formed by liver microsomes from PB-treated and 3MC-treated rats were ~1.47-fold and ~0.95-fold of that formed by liver microsomes from untreated rats, respectively. Thus pretreatment of rats with PB or 3MC, which induced the synthesis of cytochrome P450b and P450c respectively (Thomas *et al.*, 1981), substantially increased the formation of 3MC-2-one 9,10-dihydrodiol by liver microsomes. However, pretreatment of rats with 3MC had little or no effect on the metabolic conversion of 3MC-2-one to 2-OH-3MC, whereas pretreatment of rats with PB increased the reduction of 3MC-2-one by ~47%.

In order to increase the yield of metabolites for the purpose of identification, 3MC-2-one was incubated for 30 min with 1 mg protein equivalent of rat liver microsomes and cofactors. Metabolites were separated by reversed-phase HPLC as described in Fig. 39.

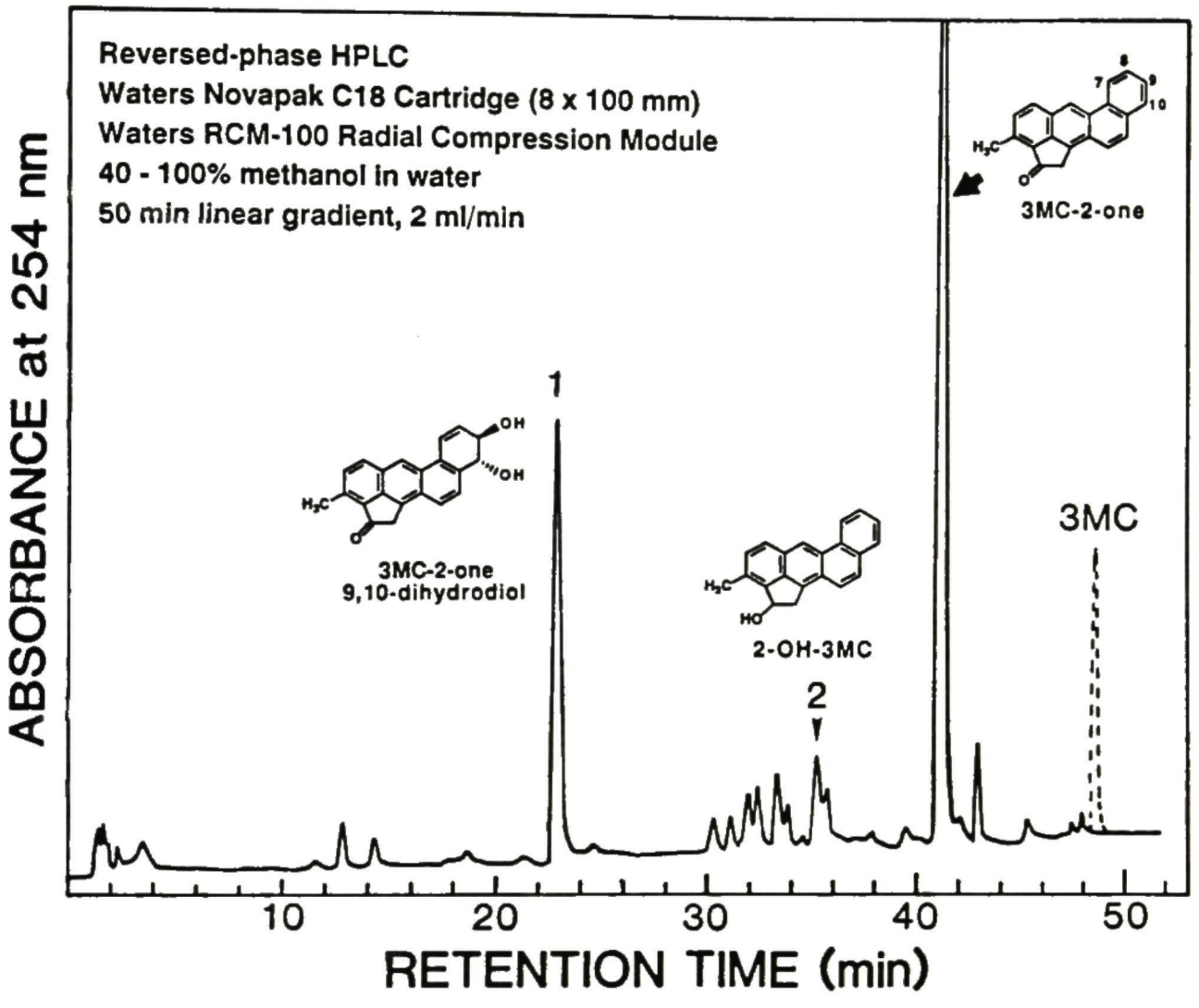

Figure 39. Reversed-phase HPLC separation of 3MC-2-one and its metabolites. The sample was prepared by incubation of 3MC-2-one for 10 min with liver microsomes (0.25 mg protein per ml of incubation mixture) from 3MC-treated rats. Identities of peaks 1 and 2 are shown and are described in the text. Retention time of 3MC, which was added for quantitative comparison of metabolites formed with different rat liver microsomal preparations, is indicated in the figure.

Additional chromatographic peaks were detected (chromatograms not shown), but they were relatively minor compared to the major metabolite (peak 1 in Fig. 39).

5.2 *Identification of the predominant metabolite.*

The metabolite contained in peak 1 of Fig. 39 has been identified as a 3MC-2-one 9,10-dihydrodiol. Uv-vis absorption spectrum (Fig. 40) of this major metabolite exhibited two major absorption bands centered at 260 and 277 nm, with several minor absorption bands at higher wavelength region. It was found to be optically active by CD spectral analysis (Fig. 40). The magnitudes of CD Cotton effects of the metabolite formed in the metabolism of 3MC-2-one by liver microsomes from untreated, PB-treated, and 3MC-treated rats were very similar, indicating similar optical purity and mechanism of formation. Mass spectral analysis indicated molecular ions at *m/z* 316 with characteristic fragment ions at *m/z* 298 and 280 (loss of water molecules), suggesting that the metabolite was a dihydrodiol.

The locations of the hydroxyl groups in the dihydrodiol metabolite were determined by the following experiments. 3MC-2-one is known to be easily converted to 2-OH-3MC by reduction of the 2-keto group with $NaBH_4$. Thus, by assuming that the dihydrodiol metabolite retained the 2-keto group of the parent hydrocarbon, reduction of 2-keto group of the metabolite should produce two diastereomeric products with an aromatic nucleus similar to that of a dihydrodiol of 3MC (or 7-methylbenz[*a*]anthracene). The $NaBH_4$-reduced products, after cleanup by ethyl acetate/water partition, were isolated as a single chromatographic peak on normal-phase HPLC (retention time 19.4 min). Its uv-vis absorption spectrum (Fig. 43) had similar absorption characteristics to those of 3MC *trans*-9,10-dihydrodiol (Jacobs *et al.*, 1983; Tierney *et al.*, 1978) and 7-MBA *trans*-3,4-dihydrodiol (Tierney *et al.*, 1978), indicating that the 9,10 positions of the diastereomer were saturated. Mass spectral analysis of this diastereomeric mixture showed molecular ions at *m/z* 318 with characteristic fragment ions at *m/z* 300 and 282 (loss of water molecules), indicating that the diastereomers were triols with a hydroxyl group at C_2

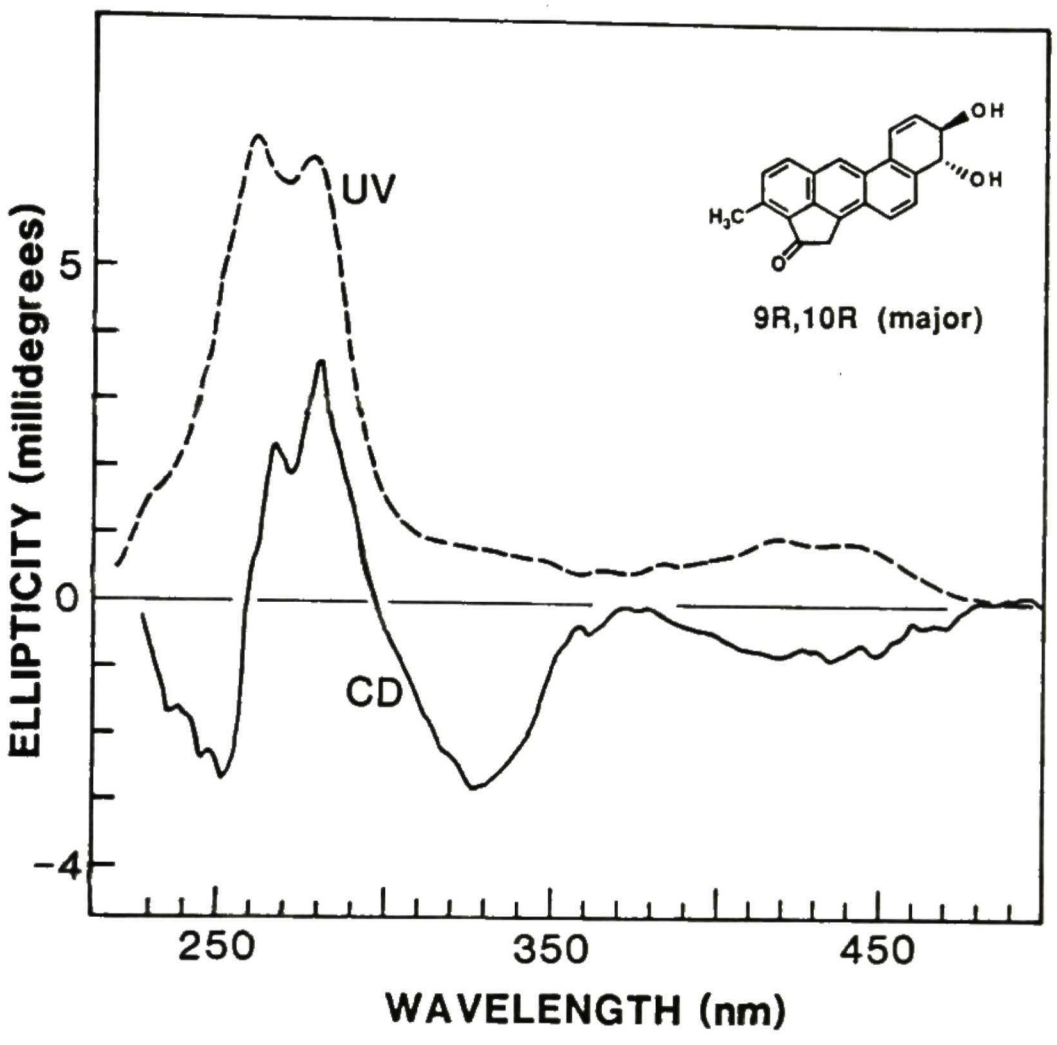

Figure 40. Uv-vis absorption (– – – –, methanol; λ_{max} 260 nm) and CD spectra of the 9,10-dihydrodiol (——; concn. 1.0 A_{260}/ml, methanol; Φ_{280}/A_{260} = 3.6 millidegrees) formed in the metabolism.of 3MC-2-one by liver microsomes from 3MC-treated rats.

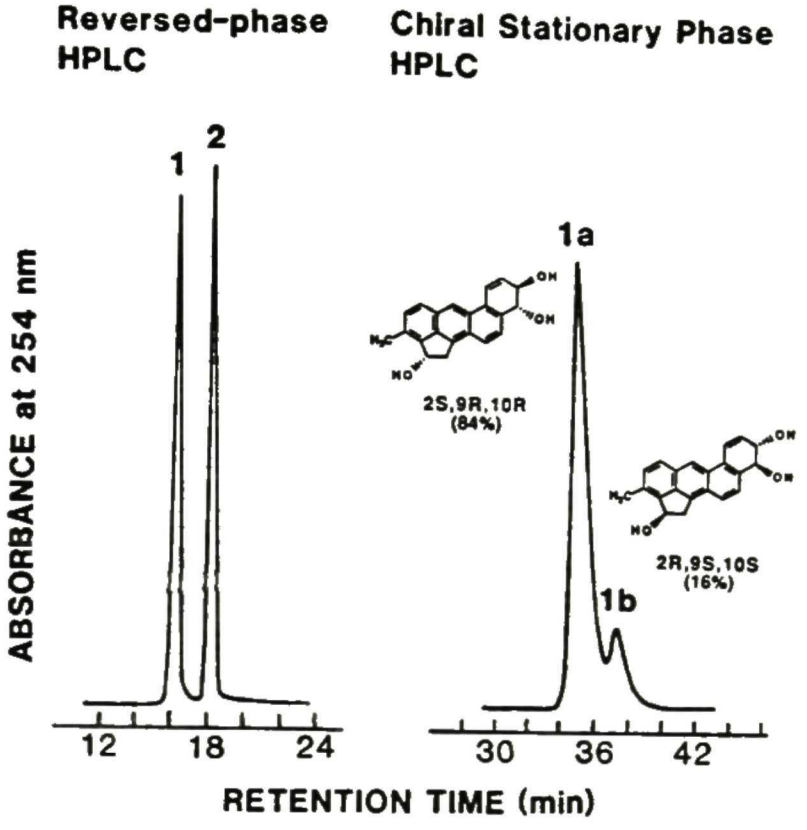

Figure 41. Left chromatogram: Reversed-phase HPLC separation of the diastereomeric 2-OH-3MC 9,10-dihydrodiols obtained by reduction with $NaBH_4$ of the metabolically formed 3MC-2-one 9,10-dihydrodiol. Right chromatogram: CSP HPLC separation of the enantiomers contained in peak 1 of the chromatogram on the left. The column was an ionically bonded *R*-DNBPG and the elution solvent was 18% of ethanol:acetonitrile (2:1, v/v) in hexane at 2 ml/min.

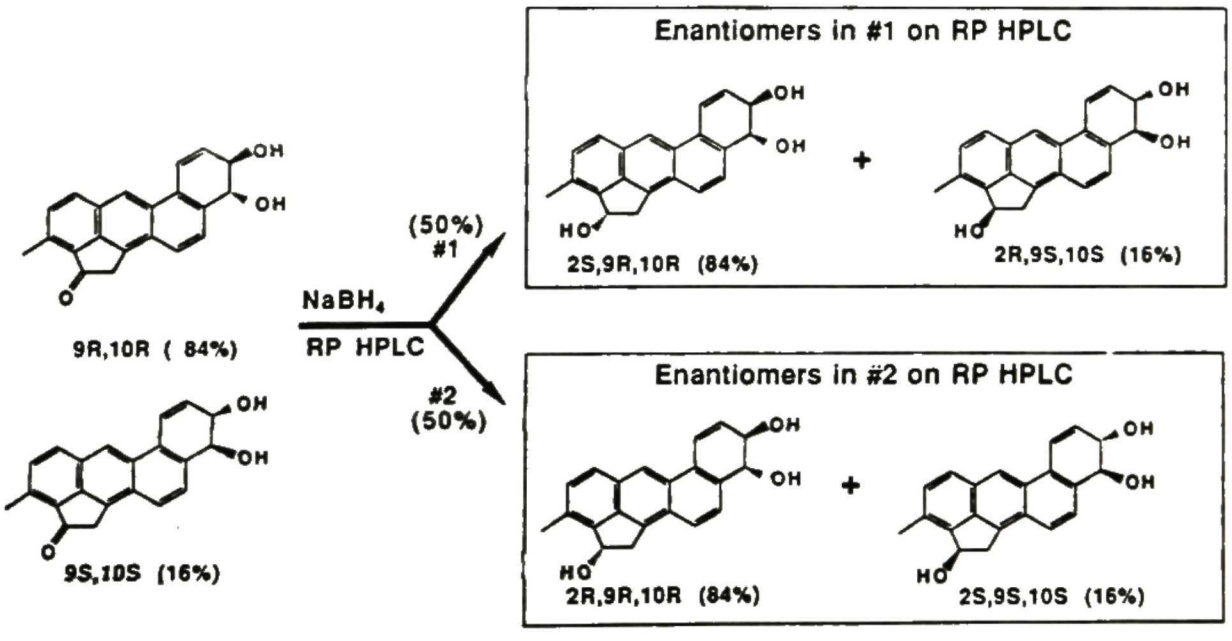

Figure 42. Structures of the metabolically formed 3MC-2-one *trans*-9,10-dihydrodiol and its $NaBH_4$-reduction products. Reversed-phase HPLC separation of two pairs of enantiomers is shown in Fig. 41. The major enantiomer in each enantiomeric pair was determined by CD spectral analysis (see text for discussion).

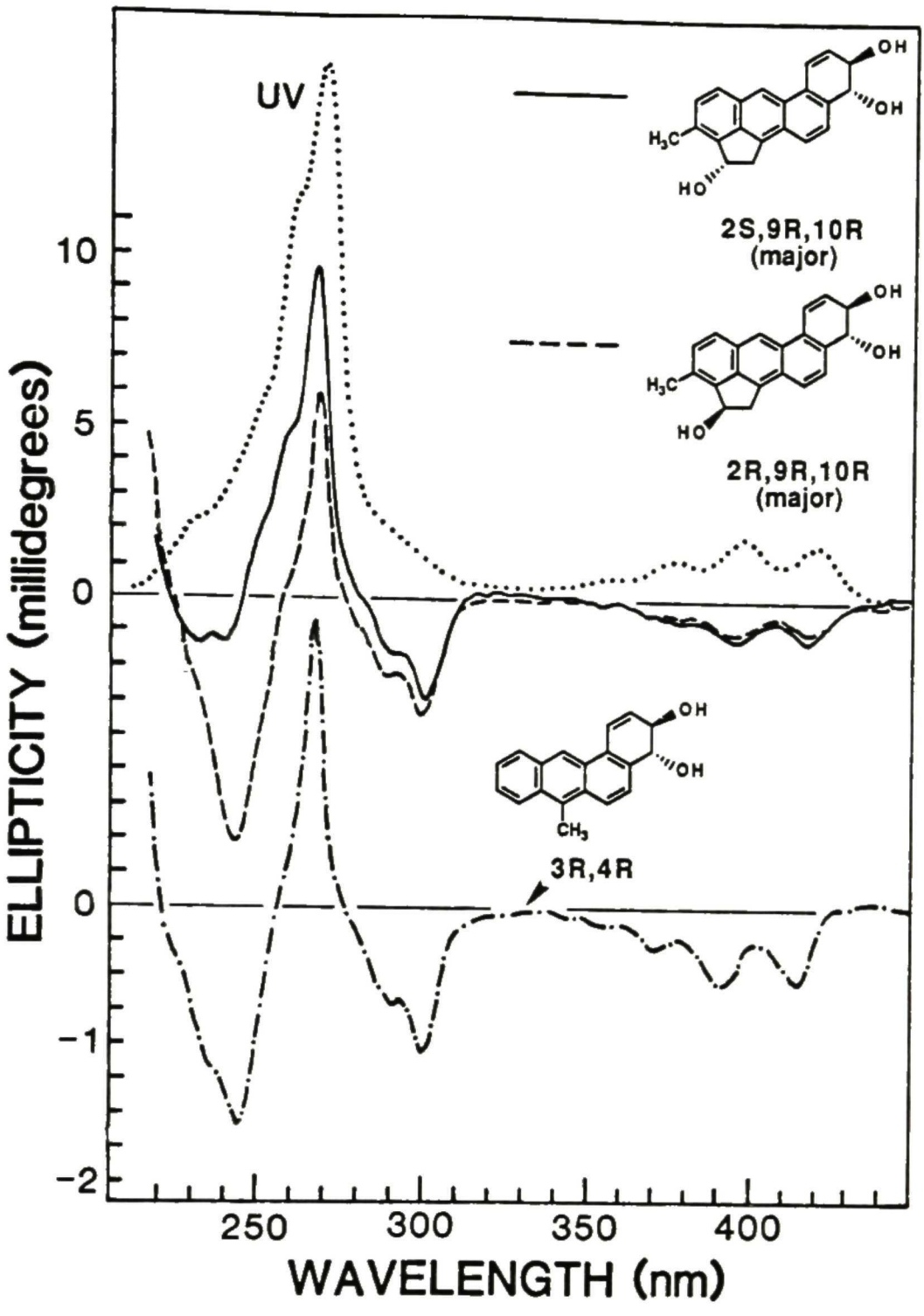

Figure 43. Uv-vis absorption (· · · ·, methanol; λ_{max} 268 nm) and CD spectra of the diastereomeric 2-OH-3MC 9,10-dihydrodiols derived by reduction of the metabolically formed 3MC-2-one 9,10-dihydrodiol with $NaBH_4$; peak 1 of Fig. 41 [——, Φ_{267}/A_{268} = 9.7 millidegrees, concn. 1.0 A_{268}/ml, methanol; (2*S*,9*R*,10*R*):(2*R*,9*S*,10*S*) enantiomer ratio = 84:16] and peak 2 of Fig. 41 [– – – –, Φ_{268}/A_{268} = 6.0 millidegrees, concn. 1.0 A_{268}/ml, methanol; (2*R*,9*R*,10*R*):(2*S*,9*S*,10*S*) enantiomer ratio = 84:16]. CD spectrum of 7-methylbenz[*a*]anthracene 3*R*,4*R*-dihydrodiol (– · – · –) was taken from Yang *et al.*, 1984 for ready comparison.

position. Two diastereomeric triols were separated by reversed-phase HPLC with identical areas under the curves (left chromatogram, Fig. 41). Their uv-vis absorption spectra had similar absorption characteristics to those of 3MC *trans*-9,10-dihydrodiol (Jacobs *et al.*, 1983; Tierney *et al.*, 1978) and 7-MBA *trans*-3,4-dihydrodiol (Tierney *et al.*, 1978), again indicating that the 9,10 positions of both diastereomers were saturated. Taken together, the results indicated that the $NaBH_4$-reduced products were diastereomeric 2-OH-3MC 9,10-dihydrodiols and the metabolite from which they were derived from was 3MC-2-one 9,10-dihydrodiol. It is known that the great majority of dihydrodiols formed in the metabolism of polycyclic aromatic hydrocarbons, including the 3MC *trans*-9,10-dihydrodiol and the diastereomeric 1-OH-3MC *trans*-9,10-dihydrodiols formed in rat liver microsomal metabolism of 3MC (Jacobs *et al.*, 1983) and racemic 1-OH-3MC (Thakker *et al.*, 1978; Vigny *et al.*, 1977) respectively, by mammalian drug-metabolizing enzymes are *trans* isomers (Yang *et al.*, 1980; Sims *et al.*, 1981). The 3MC-2-one 9,10-dihydrodiol formed in the metabolism of 3MC-2-one is presumably also a *trans* isomer with the hydroxyl groups preferentially adopting a quasidiequatorial conformation (Yang *et al.*, 1980) and this is supported by the CD Cotton effects of its reduction products 2-OH-3MC 9,10-dihydrodiol (see below).

5.3 *Absolute configuration.*

The absolute configuration of the major enantiomer in the metabolically formed 3MC-2-one 9,10-dihydrodiol could not be readily determined on the basis of its CD spectrum (Fig. 40). The keto group of the metabolically formed 3MC-2-one 9,10-dihydrodiol was converted to a hydroxyl group by reduction with $NaBH_4$ as described above and the resulting diastereomers were separated by reversed-phase HPLC (left chromatogram, Fig. 41). CD spectrum-absolute configuration relationship of enantiomeric 7-MBA *trans*-3,4-dihydrodiols had previously been established (Yang *et al.*, 1984). Thus by comparing the CD spectra of the diastereomeric 2-OH-3MC *trans*-9,10-dihydrodiols (see structures of two enantiomeric pairs in Fig. 42) derived from the metabolically formed

3MC-2-one *trans*-9,10-dihydrodiol, it should be possible to determine the absolute stereochemistry of the major enantiomer contained in each of the two diastereomeric 2-OH-3MC *trans*-9,10-dihydrodiols (peaks 1 and 2 in Fig. 41). Consequently the absolute configuration of the metabolically formed 3MC-2-one *trans*-9,10-dihydrodiol could be determined.

The characteristics of CD Cotton effects of both diastereomeric 2-OH-3MC *trans*-9,10-dihydrodiols contained in peaks 1 and 2 of Fig. 41 are nearly identical to those of 7-MBA 3*R*,4*R*-dihydrodiol between 250-450 nm, with an exception in the intensity of Cotton effects in the wavelength region 225-257 nm for peak 1 (Fig. 43). These results indicated that the major enantiomer contain in both peaks 1 and 2 are the 9*R*,10*R*-enantiomer.

The exact absolute stereochemistry of the 2-hydroxyl group in each of the major enantiomers contain in peaks 1 and 2 of Fig. 41 has been established in the following experiment. A 2*S*-OH-3MC, prepared as previously described (see metabolism of 2*S*-OH-3MC), was incubated with liver microsomes from PB-treated rats. Metabolites were separated by reversed-phase HPLC under conditions described in Fig. 39. Among the metabolites separated (chromatogram not shown), two 2-OH-3MC *trans*-9,10-dihydrodiols, in a ratio of approximately 6:1 favoring the early eluted peak, were detected with retention times identical to those of the two diastereomeric 2-OH-3MC *trans*-9,10-dihydrodiols shown in Fig. 41. The major 9,10-dihydrodiol had a CD spectrum (not shown) with Cotton effects identical to those of peak 1 in Fig. 41. Hence the major enantiomer contained in peak 1 of Fig. 41 was deduced to have a 2*S*,9*R*,10*R* absolute configuration. Consequently the major enantiomer contained in peak 2 of Fig. 41 was deduced to have a 2*R*,9*R*,10*R* absolute stereochemistry.

If the 2-OH-3MC 9,10-dihydrodiols derived from the metabolically formed 3MC-2-one 9,10-dihydrodiol were *cis* isomers, the CD Cotton effects of the major enantiomers contained in the two diastereomeric 2-OH-3MC 9,10-dihydrodiols (peaks 1 and 2 in Fig.

41) would have had very different characteristics from those of 7-methylbenz[*a*]anthracene (*trans*)-3*R*,4*R*-dihydrodiol (Yang *et al.*, 1984). The hydroxy groups of 2-OH-3MC *cis*-9,10-dihydrodiol should adopt both 9e10a (a = quasiaxial and e = quasiequatorial) and 9a10e conformations, whereas those of 2-OH-3MC *trans*-9,10-dihydrodiol should adopt only a 9e10e conformation (Yang *et al.*, 1980). For example, benzo[*a*]pyrene (*trans*)-7*R*,8*R*-dihydrodiol with a 7e8e conformation (Chiu *et al.*, 1986) and benzo[*a*]pyrene (*cis*)-7*R*,8*S*-dihydrodiol with both 7e8a and 7a8e conformations (Chiu *et al.*, 1985) have characteristically different CD Cotton effects between 310-380 nm. Since the CD Cotton effects of the major enantiomers contained in two diastereomeric 2-OH-3MC 9,10-dihydrodiols were nearly identical to those of 7-methylbenz[*a*]anthracene (*trans*)-3*R*,4*R*-dihydrodiol (Fig. 43), the CD spectral data provided confirmatory evidence that the metabolically formed 3MC-2-one 9,10-dihydrodiol was a *trans* isomer with a 9e10e conformation.

5.4 *Enantiomeric composition.*

The results presented above established the absolute stereochemistry of the major/sole enantiomer contained in each of the two enantiomeric pairs of diastereomers in Fig. 41. However, CD spectral data do not readily provide information regarding the enantiomeric composition in each pair of enantiomers. Additional steps were taken to determine the enantiomeric composition of each enantiomeric pair.

Enantiomers of the metabolically formed 3MC-2-one *trans*-9,10-dihydrodiol were not separated with various mobile phases on all four CSP columns employed in this study. However, one of the reduction product (peak 1 in Fig. 41) was separated on an ionically bonded *R*-DNBPG column into a pair of enantiomers with a (2*S*,9*R*,10*R*):(2*R*,9*S*,10*S*) enantiomer ratio of 84:16 (peak 1a and 1b in Fig. 41). A sufficient quantity (~3 A_{268} units) of peak 1b in Fig. 41 was isolated by repetitive chromatography. Its CD spectrum (not shown) was found to be a mirror image of that of peak 1a, confirming that peaks 1a and 1b are a pair of enantiomers.

Using identical CSP column and elution solvent, the enantiomers contained in peak 2 of Fig. 41 were not resolved. The use of other CSP columns also did not separate the enantiomers. However, its enantiomeric ratio [(2*R*,9*R*,10*R*):(2*S*,9*S*,10*S*)] should be identical to that of peak 1, since both peaks 1 and 2 are derived from the same precursor, the metabolically formed 3MC-2-one *trans*-9,10-dihydrodiol. Based on the enantiomeric ratio of peak 1a in Fig. 41, the metabolically formed 3MC-2-one *trans*-9,10-dihydrodiol is deduced to have a (9*R*,10*R*):(9*S*,10*S*) enantiomeric ratio of 84:16.

During the course of this study the enantiomeric ratio of 3MC-2-one *trans*-9,10-dihydrodiol (determined by peaks 1a and 1b as described in Fig. 41 following reduction by $NaBH_4$), formed by incubation of 3MC-2-one with liver microsomes from PB-treated rats, was found to vary between 69:31 and 85:15, in favor of the 2*S*,9*R*,10*R*-enantiomer. It was found that the higher the percentage of substrate (3MC-2-one) metabolized and the amount of 3MC-2-one *trans*-9,10-dihydrodiol formed, the lower the percentage of 9*R*,10*R*-enantiomer in the metabolically formed 3MC-2-one *trans*-9,10-dihydrodiol. The results thus suggest that the 9*R*,10*R*-enantiomer of 3MC-2-one *trans*-9,10-dihydrodiol is further metabolized at a faster rate than the 9*S*,10*S*-enantiomer.

6. *Stereoselecitve Metabolism of Racemic 1-OH-3MC*

6.1 *Reversed-phase HPLC separation of metabolites*

The absolute configurations and enantiomeric compositions of aliphatic hydroxylation products such as 1-OH-3-OHMC, 3MC *trans*-1,2-diol, and 3MC *cis*-1,2-diol formed in the metabolism of racemic 1-OH-3MC by liver microsomes from PB-treated rats have been described in an earlier section. In addition to these aliphatic hydroxylation products, other metabolites are also formed. More than 20 chromatographic peaks were separated by reversed-phase HPLC using a Nova-pack C_{18} column (Fig. 44). Under the incubation conditions, ~51% of the substrate was metabolized and this was determined by using 3MC as an internal standard. Chromatographic peaks are numbered as shown in Fig. 44 and the metabolite(s) contained in each chromatographic peak was characterized as described below. Peak 19 is the remaining substrate 1-OH-3MC. Extensive secondary and tertiary metabolism occurred because the high rate of metabolism. The structures of metabolites contained in most of the chromatographic peaks in Fig. 44 have been established (Table 5). More insight can be gained on the pathways of metabolism when secondary and tertiary metabolites are formed.

6.2 *Identification of metabolites*

Two metabolites were contained in peak 1 (Fig. 44) and were separated by normal-phase HPLC into two components (peak 1a and 1b in Fig. 45). These two metabolites were identified as 1-OH-3MC 7,8-dihydrodiol (peak 1a) and 1-OH-3-OHMC 9,10-dihydrodiol (peak 1b) on the basis of their uv-vis absorption and CD spectral data (see below). Peak 1a (Fig. 45) had a M^+ at *m/z* 318 and a characteristic fragment ion at *m/z* 300 (loss of H_2O) by mass spectral analysis (Fig. 46) and a uv-vis absorption spectrum similar to that of BA 1,2-dihydrodiol. Thus the metabolite contained in peak 1a (Fig. 45) was identified as 1-OH-3MC 7,8-dihydrodiol. Because of an additional chiral center, 1-OH-3MC *trans*-7,8-dihydrodiol should have two diastereomers. These two diastereomers

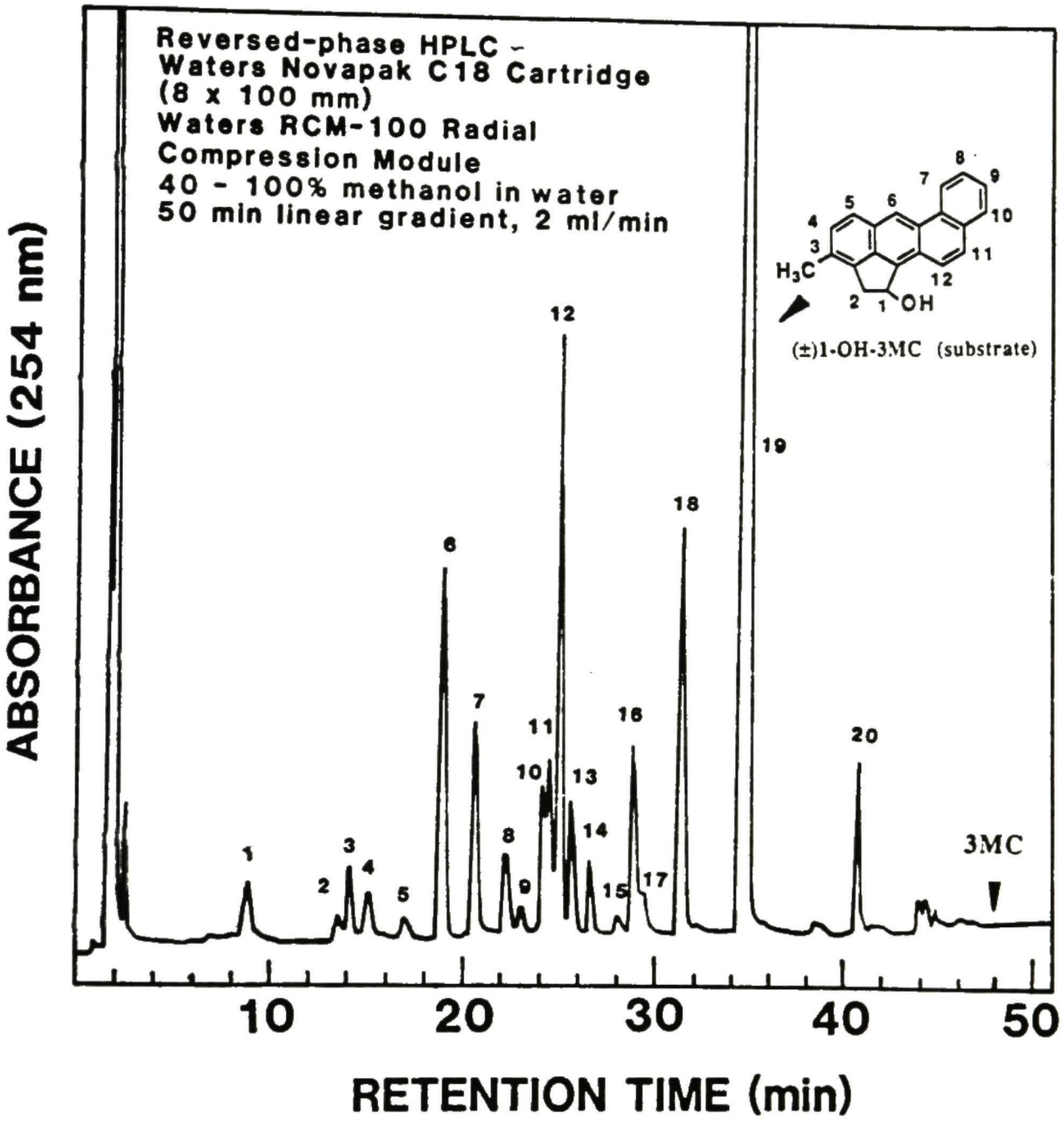

Figure 44. Reversed-phase HPLC separation of racemic 1-OH-3MC and its metabolites. Identities of metabolites contained in various chromatographic peaks are described in the text and summarized in Table 5. Retention time of 3MC as a internal standard is indicated by an arrow.

Table 5. Characterization of products formed in the metabolism of racemic 1-OH-3MC by rat liver microsomes

Peak No. in RP HPLC (Rt, min)[a]	Elution Solvent in NP HPLC (Rt, min)[b]	M^+ (m/z)[c]	Identity of Metabolite
1 (8.90)	EA20 (14.63)	318	1-OH-3MC 7,8-dihydrodiol
	EA20 (17.57)	334	1-OH-3MC 9,10-dihydrodiol
2 (13.5)			unknown
3 (14.0)	EA20 (13.40)	334	3MC *cis*-1,2-diol:9,10-diol
4 (15.2)	EA20 (15.52)	ND (316)[d]	8-OH-1-OH-3-OHMC
	EA20 (16.20)	316	9-OH-1-OH-3-OHMC
5 (16.9)	EA20 (16.90)	ND (316)	10-OH-1-OH-3-OHMC
6 (18.5)	EA15 (16.63)	318	1*S*-OH-3MC 9*R*,10*R*-dihydrodiol (major)
7 (20.2)	EA15 (15.43)	318	1*R*-OH-3MC 9*R*,10*R*-dihydrodiol (major)
8 (21.8)	EA15 (11.50)	316	3MC-1-one 9,10-dihydrodiol
9 (22.5)	EA15 (13.23)	316	3-OHMC *cis*-1,2-diol
10 (23.6)	EA15 (9.98)	300	3MC *trans*-1,2-diol
11 (24.2)	EA15 (11.82)	300	8-OH-1-OH-3MC
12 (24.5)	EA15 (13.55)	300	1-OH-3-OHMC
13 (25.4)	EA15 (14.10)	300	7-OH-1-OH-3MC
14 (26.3)	EA15 (14.00)	300	9-OH-1-OH-3MC
15 (27.6)			unknown
16 (28.4)	EA15 (12.46)	300	10-OH-1-OH-3MC
17 (28.9)	EA10 (14.80)	298	3-OHMC-1-one
18 (30.7)	EA10 (9.57)	300	3MC *cis*-1,2-diol
19 (34.0)		284	1-OH-3MC
20 (40.4)		282	3MC-1-one

a. Metabolites were separated by reversed-phase HPLC and numbered as indicated in HPLC chromatograph. Retention times (Rt) are shown in parenthesis.
b. Elution solvents were defined in percentage of eluent A (ethanol-acetonitrile, 2:1, v/v) in hexane. Retention times are indicated in parenthesis.
c. Molecular ion from mass spectral analysis. ND = not determined.
d. Expected molecular weight.

could not be separated by either reversed-phase or normal-phase HPLC. However, peak 1a (Fig. 45) was separated into two chromatographic peaks (peaks 1a1 and 1a2 of Fig. 45) on an *R*-DNBPG-C column with an AUC ratio of 54:46. Peaks 1a1 and 1a2 had identical uv-vis absorption spectra (Fig. 49). CD Cotton effects of these two metabolites were not exact mirror images of each other (Fig. 49). Hence peaks 1a1 and 1a2 were not a pair of enantiomers and they should be a pair of diastereomers; each of which has a pair of enantiomers. On the basis of their CD spectra data, peak 1a1 was judged to be enriched in the 7*R*,8*R*-enantiomer, whereas peak 1a2 was enriched in the 7*S*,8*S*-enantiomer.

The metabolites contained in peaks 11 and 13 (Fig. 44) were repurified by normal-phase HPLC (Table 5) and were identified as 8-OH-1-OH-3MC and 7-OH-1-OH-3MC, respectively. The 8-OH-1-OH-3MC in peak 11 had a uv-vis absorption spectrum similar to those of an authentic 2-OH-BA (Fig. 21) and 8-OH-2-OH-3MC (Fig. 21) and an M^+ at *m/z* 300 and a fragment ion at *m/z* 282 by mass spectral analysis. The 7-OH-1-OH-3MC in peak 13 had a uv-vis absorption spectrum similar to that of an authentic 1-OH-BA (Fig. 50) and a M^+ at *m/z* 300 and a fragment ion at *m/z* 282 by mass spectral analysis. Uv-vis absorption spectra of 7-OH-1-OH-3MC (Fig. 50) and 10-OH-1-OH-3MC (Fig. 61) are similar. Thus 7-OH-1-OH-3MC and 10-OH-1-OH-3MC cannot be distinguished by their uv absorption properties. In order to confirm that the metabolite contained in peak 13 was 7-OH-1-OH-3MC, the major component in peak 6 (1-OH-3MC 9,10-dihydrodiol) was converted to 9-OH-1-OH-3MC and 10-OH-1-OH-3MC (see uv-vis absorption spectra in Figs. 60 and 61). These two phenolic products had uv-vis absorption spectra and retention times on reversed-phase HPLC (Fig. 44) identical to those of peaks 14 and 15, respectively. Hence the metabolite contained in peak 13 was concluded to be 7-OH-1-OH-3MC.

Peak 4 in Fig. 44 was further separated by normal-phase HPLC into two components (Table 5). The component eluted earlier on normal-phase HPLC had a uv-vis absorption spectrum (not shown) similar to that of an authentic 2-OH-BA and a shorter

retention time than that of 8-OH-1-OH-3MC (peak 11 in Fig. 44). This metabolite was tentatively identified as 8-OH-2-OH-3-OHMC. Another component in peak 4 was identified as 9-OH-1-OH-3-OHMC (see below).

Five 9,10-dihydrodiols were formed and these were: 1-OH-3-OHMC 9,10-dihydrodiol (peak 1b in Fig. 45), 3MC *cis*-1,2-diol:9,10-dihydrodiol (peak 3 in Fig. 44), two diastereomeric 1-OH-3MC 9,10-dihydrodiols (peaks 6 and 7 in Fig. 44), and 3MC-1-one 9,10-dihydrodiol (peak 8 in Fig 44).

Two major metabolites contained in peaks 6 and 7 with an AUC ratio of 63:37 had uv-vis absorption spectra identical to that of 2-OH-3MC 9,10-dihydrodiol (see the section on the metabolism of 2*S*-OH-3MC) and an M^+ at *m/z* 318 with a characteristic fragment ion at *m/z* 300 by mass spectral analysis (Fig. 56). CD spectra of the metabolites contained in peaks 6 and 7 were similar to that of 2*S*-OH-3MC 9*R*,10*R*-dihydrodiol (Fig. 29), indicating they were enriched in the 9*R*,10*R*-enantiomer. Therefore, the predominant metabolites in peaks 6 and 7 were identified to be two diastereomeric 1-OH-3MC 9,10-dihydrodiols enriched in the 9*R*,10*R*-enantiomer (Fig. 58). The 1-OH-3MC 9,10-dihydrodiols formed in the metabolism of 1-OH-3MC were derived from epoxide hydrolase-catalyzed hydration of their 1-OH-3MC 9,10-epoxide precursors. 1-OH-3MC 9,10-dihydrodiols may be further oxidized to form the potentially reactive bay region 1-OH-3MC 9,10-diol-7,8-epoxides.

The uv-vis absorption and mass spectral data (Figs. 60 and 62) of the component in peak 14 were found to be identical to those of 9-OH-2-OH-3MC. Similarly, the metabolite in peak 16 of Fig. 44 had uv-vis absorption and mass spectral data (Figs. 61 and 63) identical to those of 10-OH-2-OH-3MC described earlier. In order to confirm the structures of metabolite contained in peaks 14 and 16, 1-OH-3MC 9,10-dihydrodiol (peak 7 in Fig. 44) was converted to 9-OH-1-OH-3MC and 10-OH-1-OH-3MC by acid-catalyzed dehydration. The two isomeric phenolic products were eluted on reversed-phase HPLC with retention times and uv-vis absorption spectra identical to those of metabolites

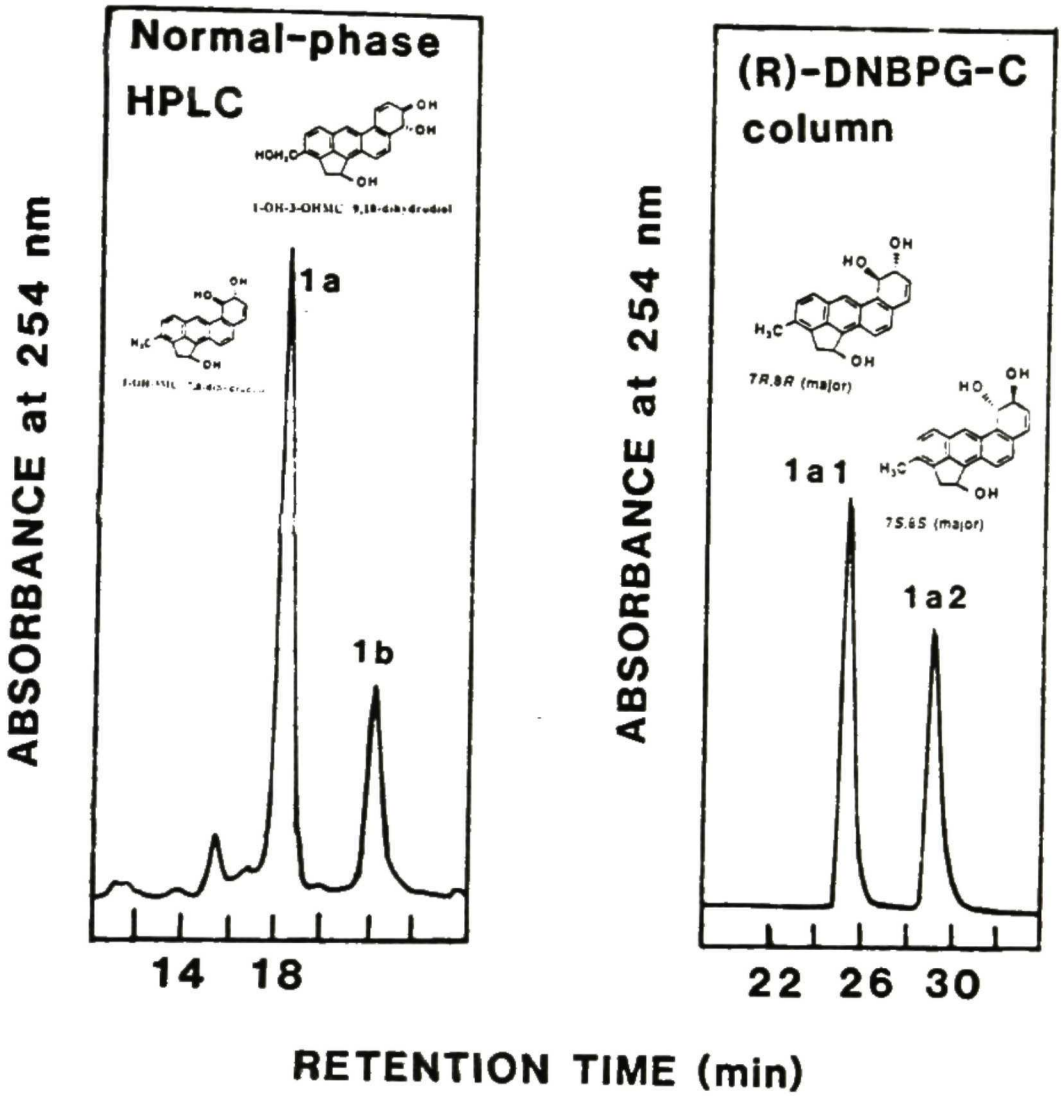

Figure 45. (A) Normal-phase HPLC separation of the two major components contained in peak 1 of Fig. 44. The mobile phase was 20% (v/v) of solvent A in hexane, at a flow rate of 2 ml/min. Identities of metabolites contained in the chromatographic peaks are shown. Evidence for the identification of these two metabolites is described in the text. (B) Chiral stationary phase HPLC separation and absolute configurations of metabolite 1-OH-3MC 7,8-dihydrodiol enantiomers are indicated in this figure.

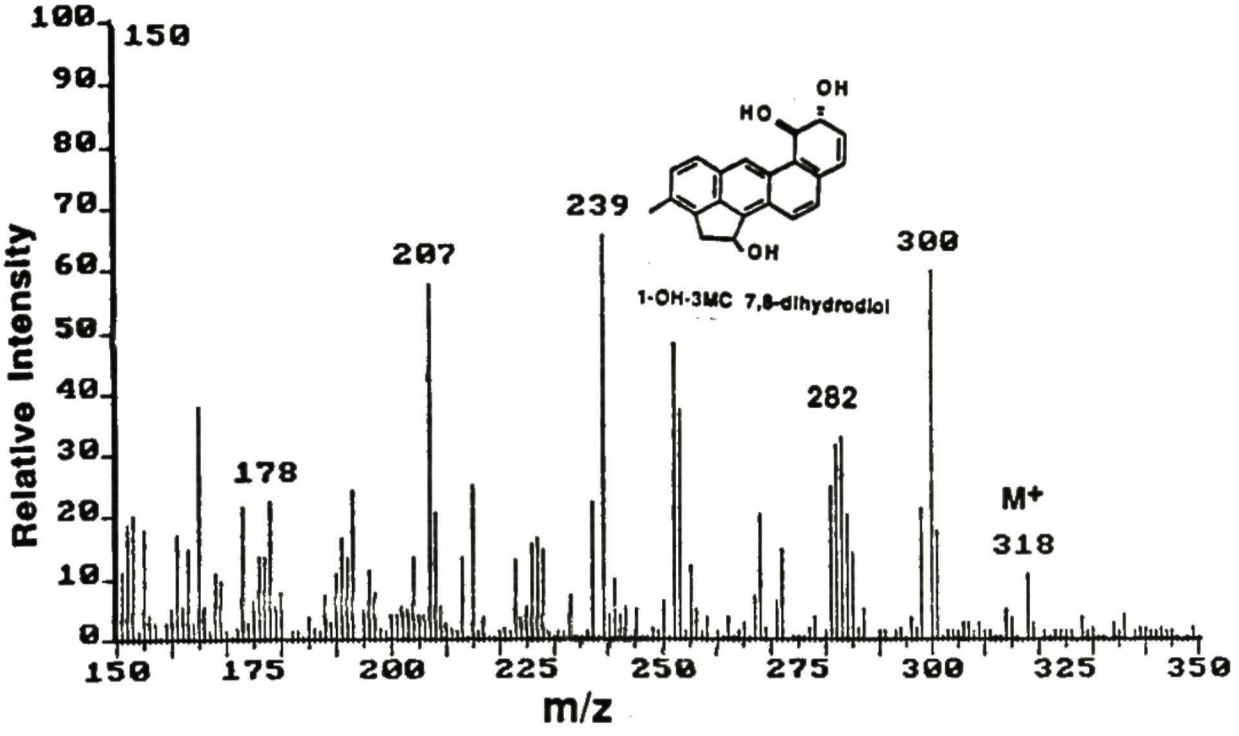

Figure 46. Mass spectrum of 1-OH-3MC *trans*-7,8-dihydrodiol.

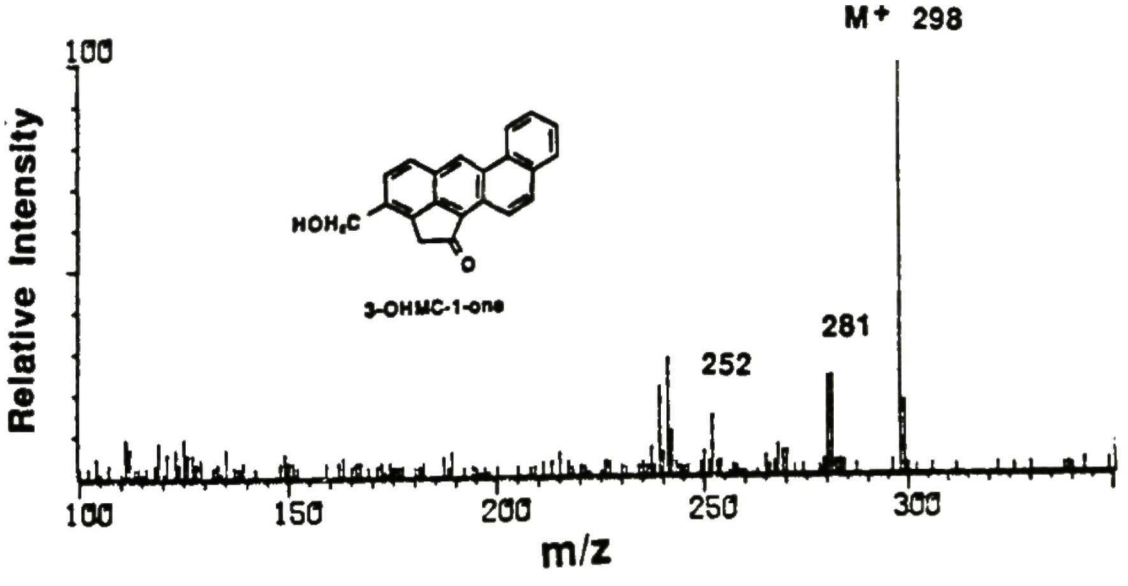

Figure 47. Mass spectrum of 3-OHMC-1-one.

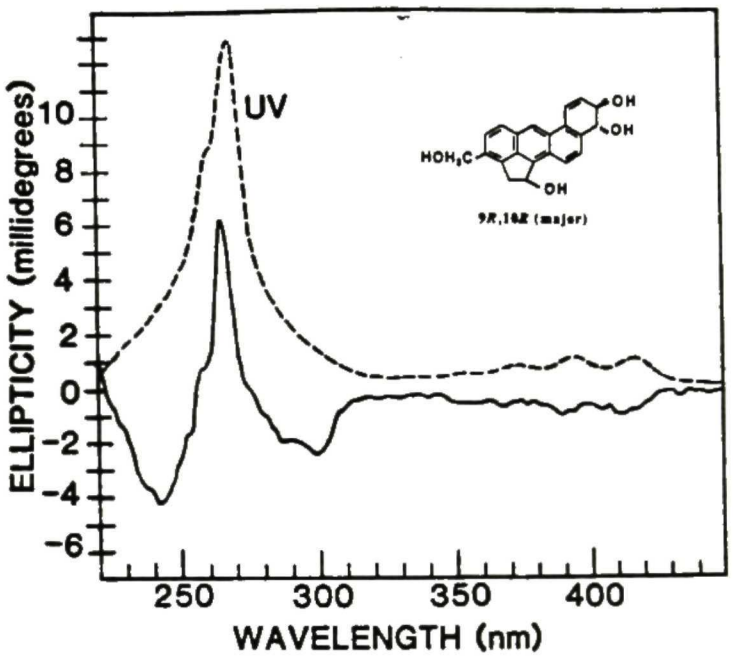

Figure 48. Uv-vis absorption (– – – –, methanol) and CD (———, concn. 1.0 A_{268}/ml, methanol; Φ_{267}/A_{268} = 6.2 millidegrees) spectra of the metabolite 1-OH-3-OHMC 9*R*,10*R*-dihydrodiol (major) contained in peak 1b of Fig. 45.

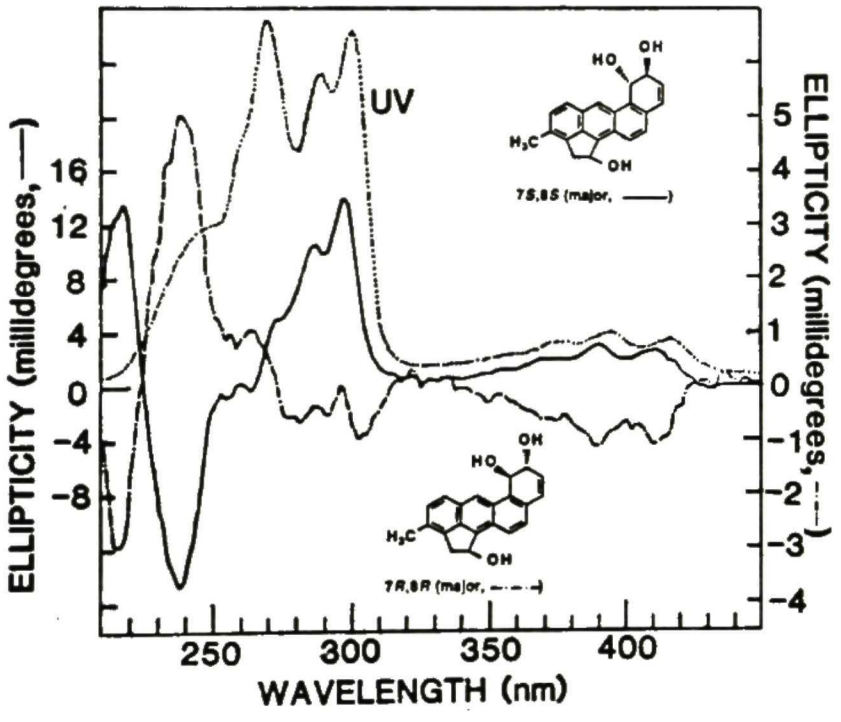

Figure 49. Uv-vis absorption spectrum of two diastereomeric 2-OH-3MC 7,8-dihydrodiol contained in peak 1a of Fig. 45 (• • • •) and CD spectra of major 2-OH-3MC 7*R*,8*R*-dihydrodiol (– • – • –, concn. 1.0 A 269/ml, methanol; Φ_{239}/A_{269} = 5.1 millidegrees) and major 2-OH-3MC 7*S*,8*S*-dihydrodiol (———, concn. 1.0 A_{273}/ml, methanol; Φ_{239}/A_{269} = – 14.8 millidegrees).

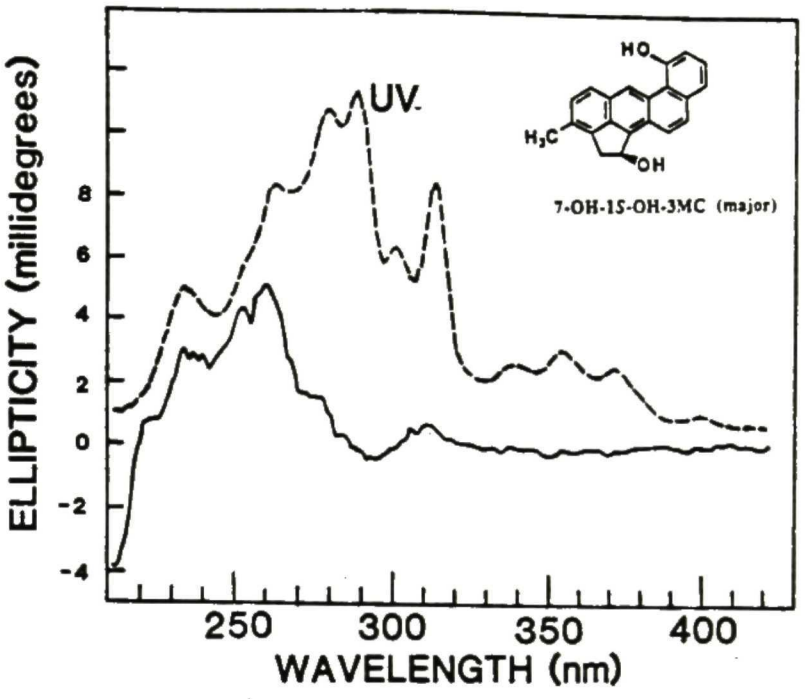

Figure 50. Uv-vis absorption (– – – –, methanol) and CD (——, concn. 1.0 A_{287}/ml, methanol; Φ_{269}/A_{287} = 5.1 millidegrees) spectra of the metabolite 7-OH-1*S*-OH-3MC (major) contained in peak 13 of Fig. 44.

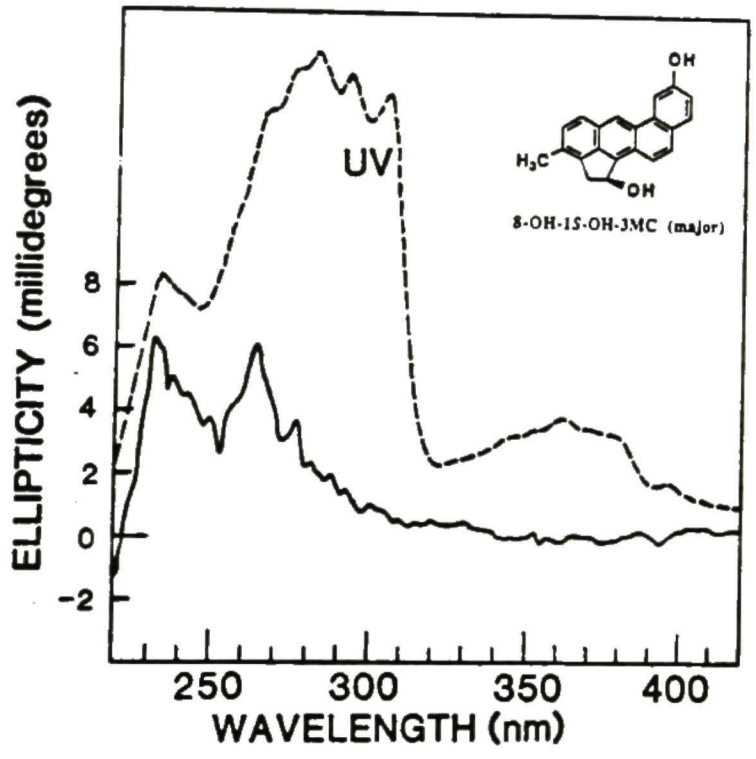

Figure 51. Uv-vis absorption (– – – –, methanol) and CD (——, concn. 1.0 A_{283}/ml, methanol; Φ_{265}/A_{265} = 6.1 millidegrees) spectra of the metabolite 8-OH-1*S*-OH-3MC (major) contained in peak 11 of Fig. 44.

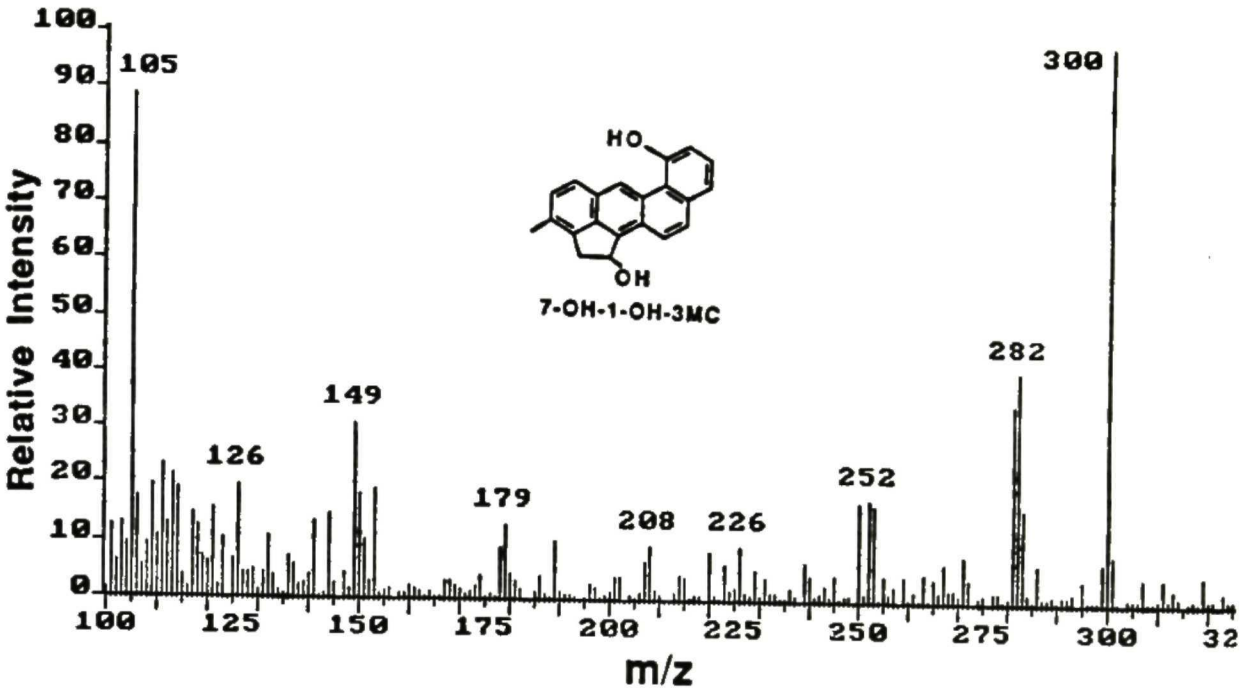

Figure 52. Mass spectrum of 7-OH-1-OH-3MC.

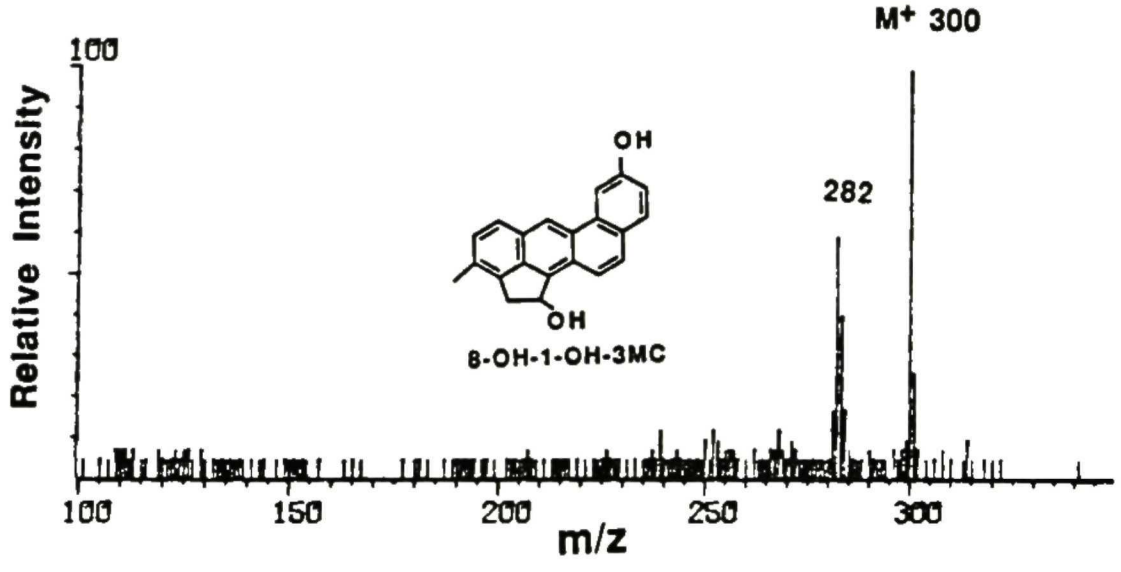

Figure 53. Mass spectrum of 8-OH-1-OH-3MC.

contained in peaks 14 and 16, respectively. Hence the metabolites contained in peaks 14 and 16 were confirmed as 9-OH-1-OH-3MC and 10-OH-1-OH-3MC, respectively.

Uv-vis absorption spectrum of the metabolite contained in peak 8 (Fig. 44) resembled that of 3MC-2-one 9,10-dihydrodiol (Fig. 40). Mass spectral analysis indicated a M^+ at *m/z* 316 and a fragment ion at *m/z* 298 (Fig. 57). These data suggested that the metabolite was a 9,10-dihydrodiol of 3MC-1-one. Furthermore, CD spectral analysis (Fig. 59) indicated this metabolite was optically active. In order to firmly establish the structure, this metabolite was converted by reduction with $NaBH_4$ to a pair of diastereomers, which had identical retention time, uv-vis absorption and CD spectra to those of 1-OH-3MC 9*R*,10*R*-dihydrodiols contained in peaks 6 and 7 of Fig. 44. These results confirmed that the metabolite contained in peak 8 of Fig. 44 was a 3MC-1-one 9,10-dihydrodiol.

As described earlier, peak 1 of Fig. 44 contained two components which were separated by normal-phase HPLC (peaks 1a and 1b in Fig. 45). Peak 1a was identified as 1-OH-3-MC 7,8-dihydrodiol. Peak 1b had a uv-vis absorption spectrum (Fig. 45) similar to those of 1-OH-3MC 9,10-dihydrodiols contained in peaks 6 and 7 of Fig. 58 and 2-OH-3MC 9,10-dihydrodiol (Fig. 29). Mass spectral analysis of the metabolite in peak 1b indicated a M^+ at *m/z* 334 and characteristic fragment ions at *m/z* 316 (loss of H_2O) and 298 (loss of two H_2O) (Fig. 54). CD spectrum of peak 1b was similar to that of 2*S*-OH-3MC 9*R*,10*R*-dihydrodiol (Fig. 29) formed in the metabolism of 2*S*-OH-3MC. The retention time of peak 1 in Fig. 44 was much shorter than those of the two diastereomeric 1-OH-3MC 9,10-dihydrodiols contained in peaks 6 and 7. On the basis of the above data, the metabolite in peak 1b of Fig. 45 was established to be 1-OH-3-OHMC 9,10-dihydrodiol enriched in the 9*R*,10*R*-enantiomer. In principle, 1-OH-3-OHMC 9,10-dihydrodiol should have two diastereomers. Only one 1-OH-3-OHMC 9,10-dihydrodiol was detected. The other diastereomeric 1-OH-3-OHMC 9,10-dihydrodiol was either not separable from peak 1b or was not detectable.

Peak 4 of Fig. 44 contained two components (Table 5). The minor component was tentatively identified as 8-OH-1-OH-3-OHMC which had a uv-vis absorption spectrum similar to those of 8-OH-1-OH-3MC (peak 11 in Fig. 44) and 8-OH-2-OH-3MC (Fig. 21A). The major component had a uv-vis absorption spectrum (Fig. 60) similar to those of 9-OH-1-OH-3MC (peak 14 in Fig. 44) and 9-OH-2-OH-3MC (Fig. 32A). Mass spectral analysis of the major component indicated a M^+ at *m/z* 316 (Fig. 55). The results indicated that the major component in peak 4 of Fig. 44 was 9-OH-1-OH-3-OHMC.

The 9,10-dihydrodiol contained in peak 3 was identified as 3MC *cis* 1,2-diol:9,10-dihydrodiol on the basis of its uv-vis absorption spectrum and retention time, which were identical to that of 3MC *cis* 1,2-diol:9,10-dihydrodiol formed in the metabolism of 3MC *cis*-1,2-diol (see section on the metabolism of 3MC *cis*-1,2-diol). Mass spectral analysis showed that molecular weight of this metabolite in peak 3 was 334. CD spectrum of this metabolite indicated that it was highly enriched in the 9*R*,10*R*-enantiomer. Since 3MC *cis*-1,2-diol (peak 18 in Fig. 44) was one of the major metabolites, the metabolically formed 3MC *cis*-1,2-diol was expected to be further metabolized and apparently the 9,10-double bond of 3MC *cis*-1,2-dihydrodiol was a major site of metabolism.

Metabolites contained in peaks 10 and 18 were readily identified as isomeric 3MC *trans*-1,2-diol and *cis*-1,2-diol on the basis of their identical retention times, uv-vis absorption and mass spectra (Figs. 64 and 65) to those of authentic 3MC *trans*-1,2-diol and 3MC *cis*-1,2-diol, respectively. Based on the areas under chromatographic peaks, the *cis*-1,2-diol was formed ~3-times that of the *trans* isomer (see Fig. 44).

Peak 12 contained the most abundant metabolite which had identical retention time, uv-vis absorption and mass spectra to those of 1-OH-3-OHMC. The latter had been described in an earlier section (Figs. 16 and 67). The metabolically formed 1-OH-3-OHMC was optically active and had a *R/S* enantiomer ratio of 58:42 (Fig. 17).

Peak 9 as a minor metabolite (mass spectrum in Fig. 66) was shwn to have an identical retention time as that of 3-OHMC *cis*-1,2-diol which has been found as a

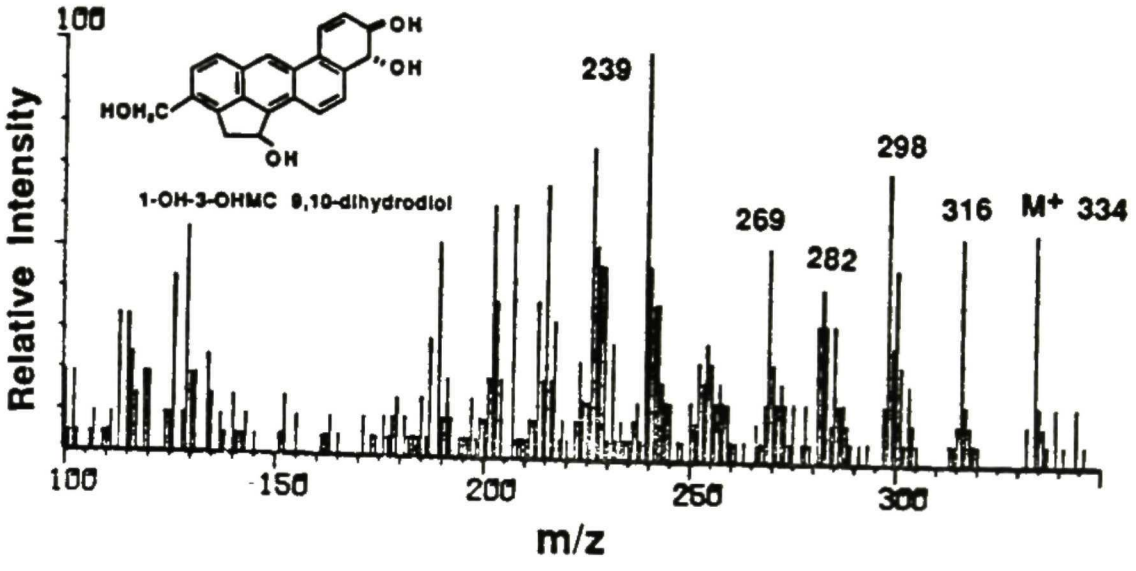

Figure 54. Mass spectrum of 1-OH-3-OHMC *trans*-9,10-dihydrodiol.

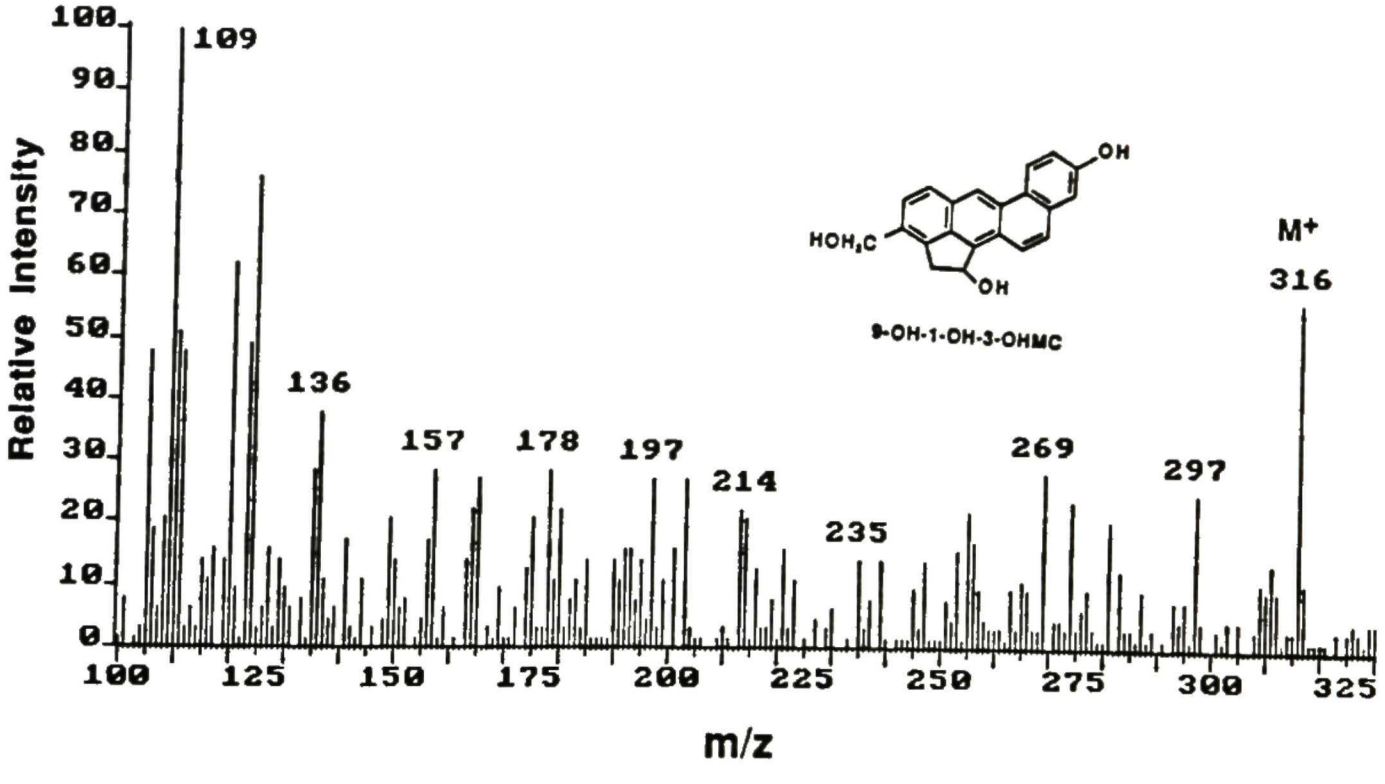

Figure 55. Mass spectrum of 9-OH-1-OH-3-OHMC.

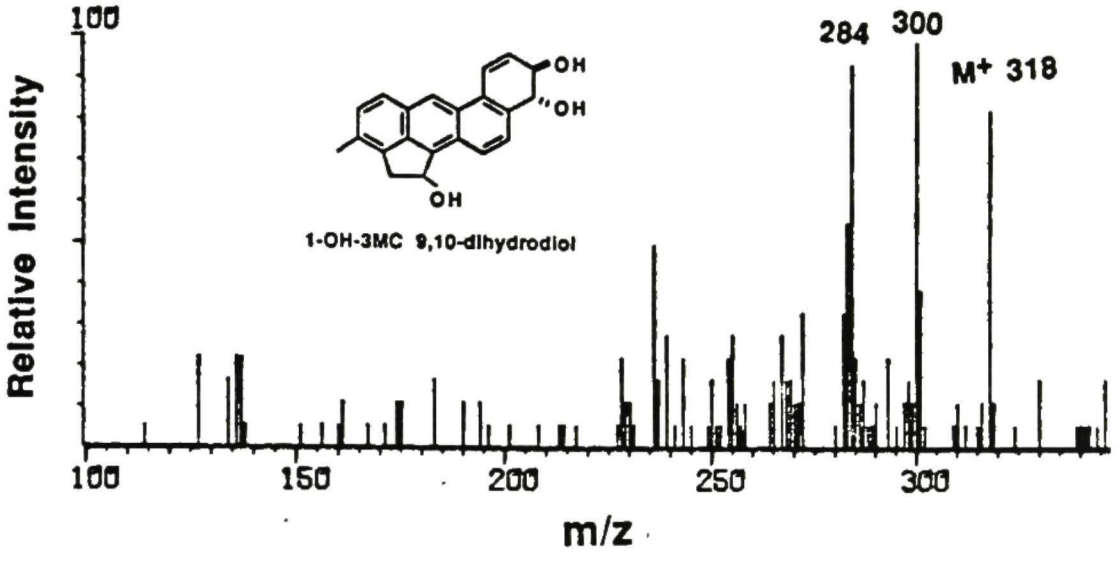

Figure 56. Mass spectrum of 1-OH-3MC *trans*-9,10-dihydrodiol.

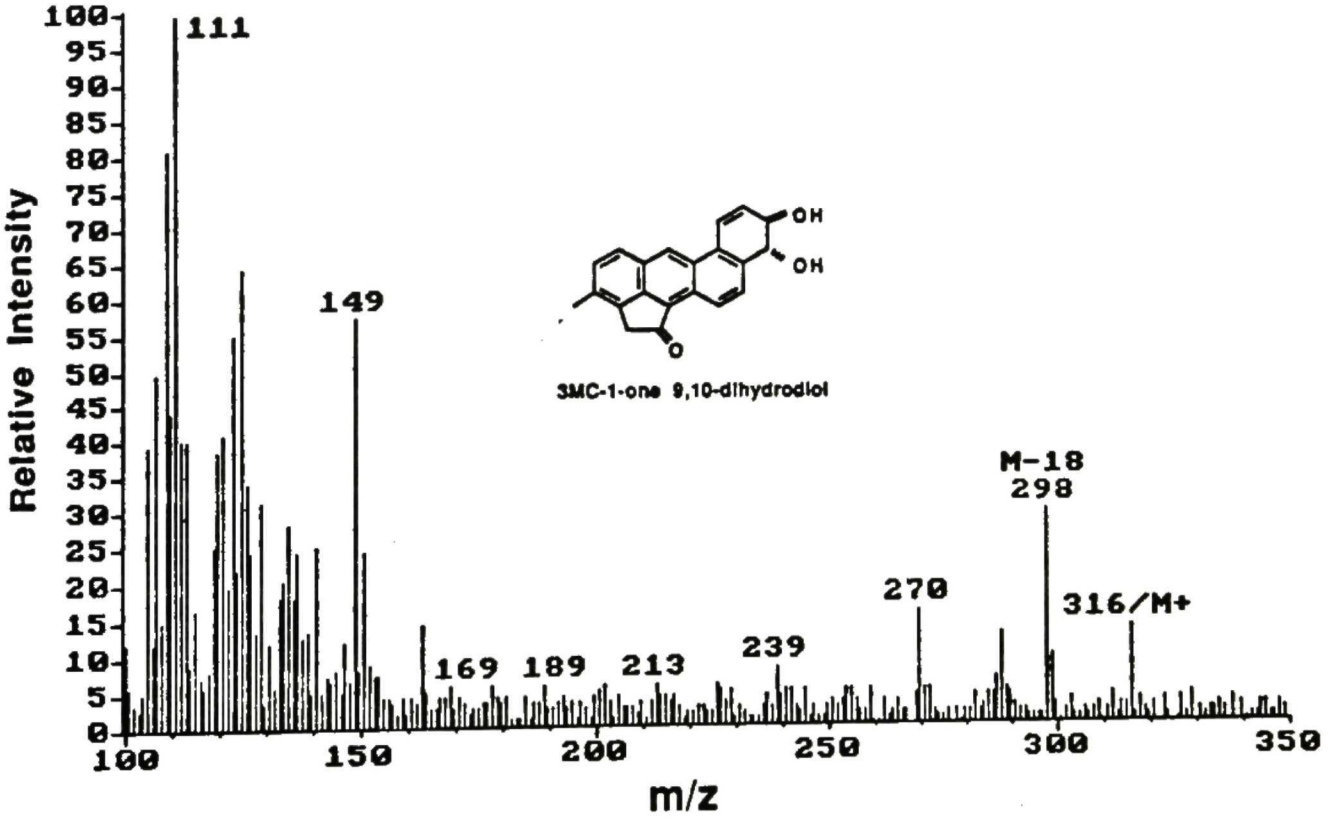

Figure 57. Mass spectrum of the 3MC-1-one *trans*-9,10-dihydrodiol.

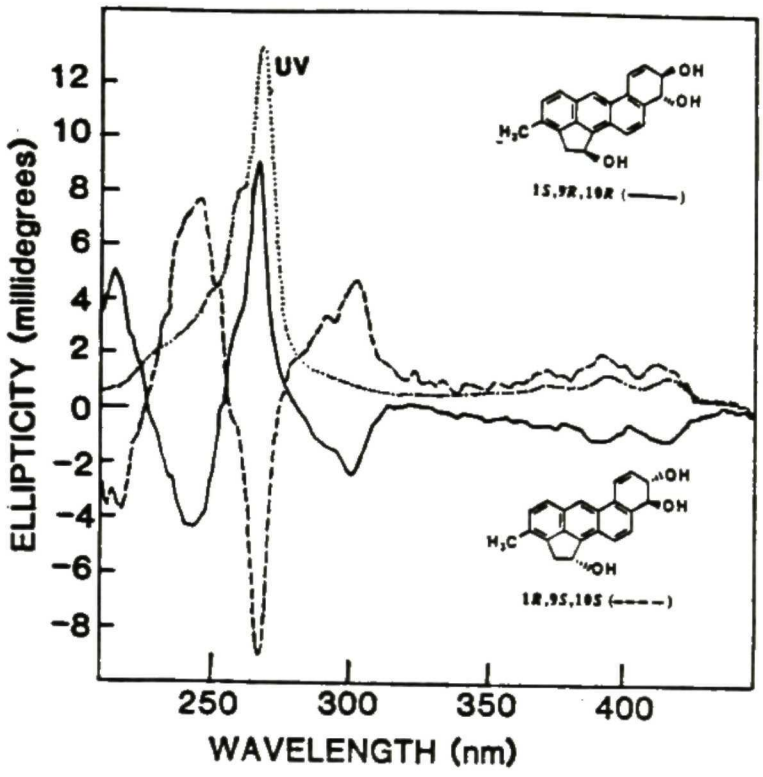

Figure 58. Uv-vis absorption spectrum of 1-OH-3MC 9,10-dihydrodiol contained in peak 6 of Fig. 44 (· · · ·) and CD spectra of optically pure 1*S*-OH-3MC 9*R*,10*R*-dihydrodiol (_____, concn. 1.0 A $_{268}$/ml, methanol; Φ_{267}/A_{268} = 9.6 millidegrees) and 1*R*-OH-3MC 9*S*,10*S*-dihydrodiol (--------, concn. 1.0 A_{268}/ml, methanol; Φ_{267}/A_{268} = -9.6 millidegrees).

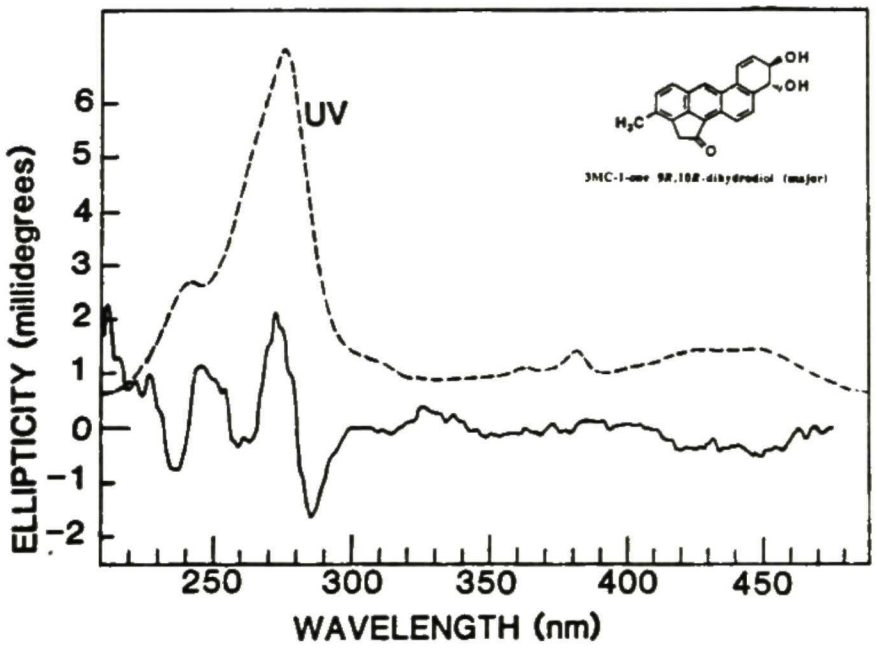

Figure 59. Uv-vis absorption (– – – –, methanol) and CD (——, concn. 1.0 A_{276}/ml, methanol; Φ_{271}/A_{276} = 2.15 millidegrees) spectra of the metabolite 3MC-1-one 9*R*,10*R*-dihydrodiol (major) contained in peak 8 of Fig. 44.

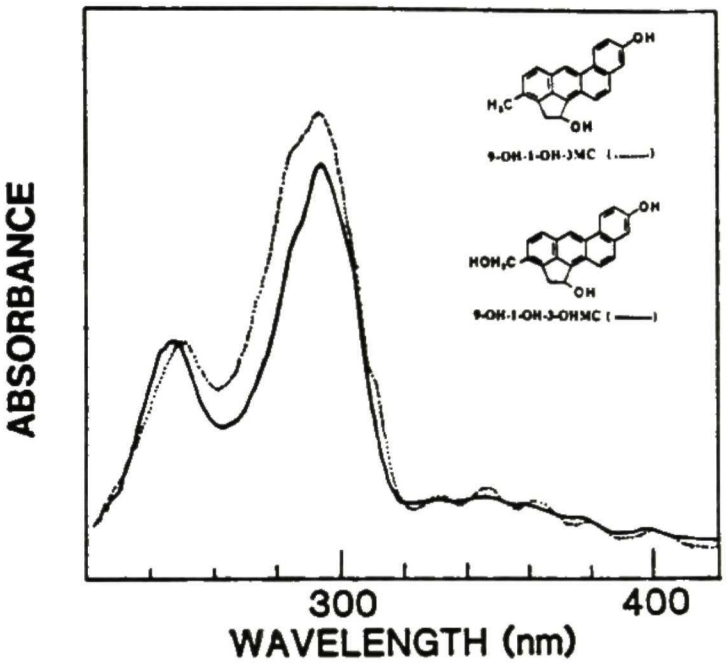

Figure 60. Uv-vis absorption spectra of 9-OH-1-OH-3-OHMC in peak 4 (_____, methanol) and 9-OH-1-OH-3MC in peak 14 of Fig. 44 (....., methanol).

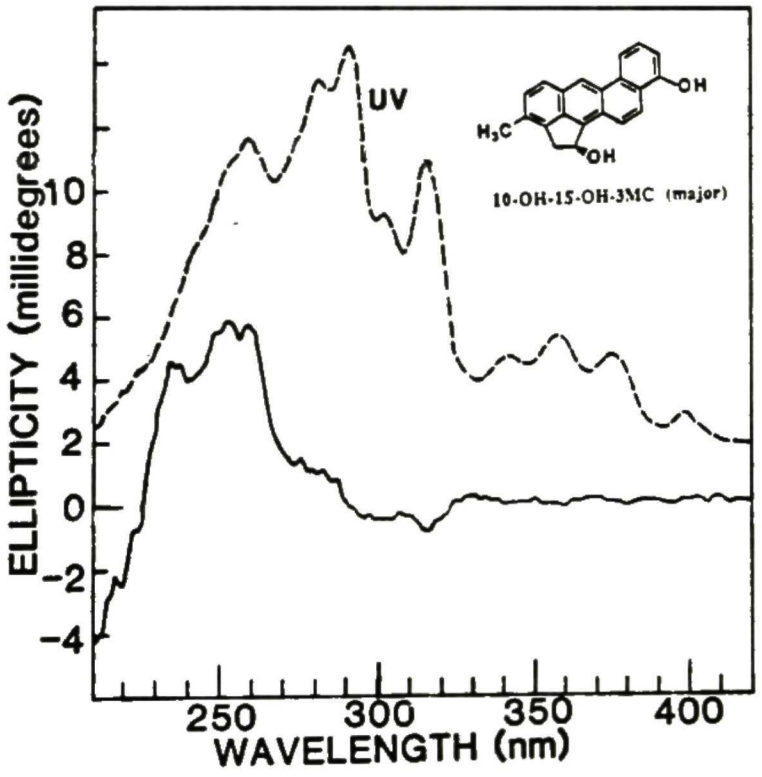

Figure 61. Uv-vis absorption (– – – –, methanol) and CD (——, concn. 1.0 A_{291}/ml, methanol; Φ_{253}/A_{291} = 5.9 millidegrees) spectra of the metabolite 10-OH-1*S*-OH-3MC (major) contained in peak 16 of Fig. 44.

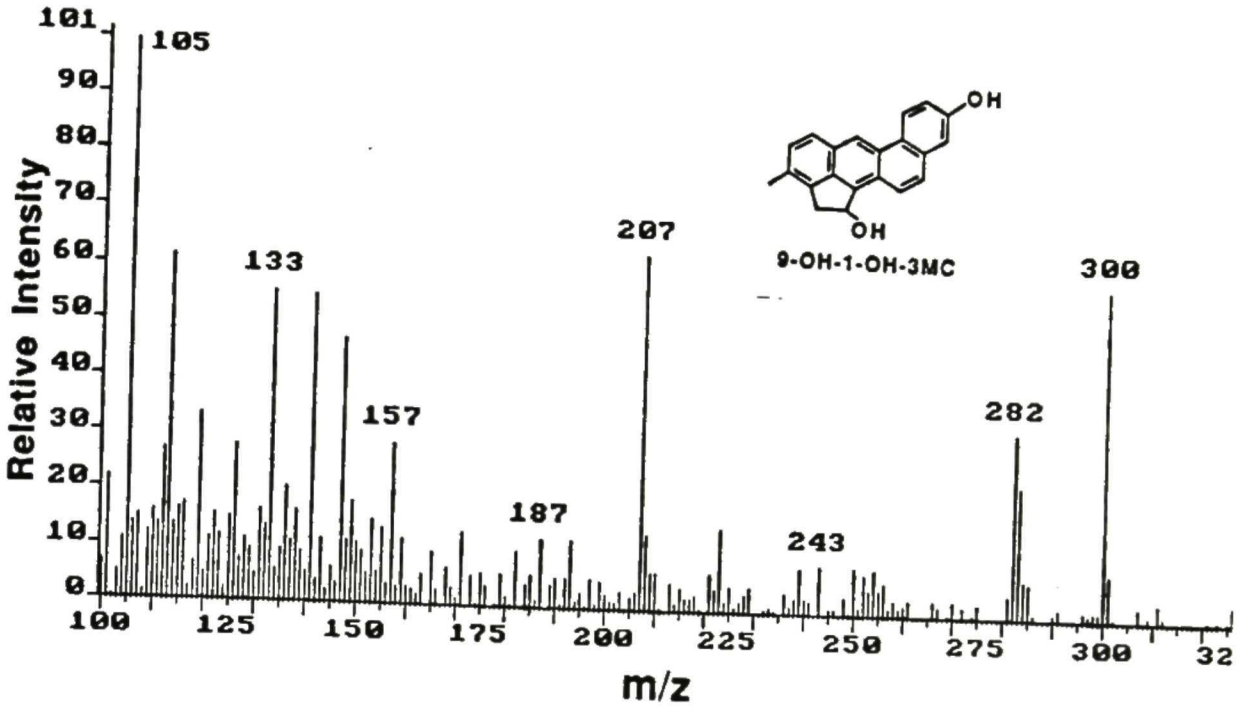

Figure 62. Mass spectrum of 9-OH-1-OH-3MC.

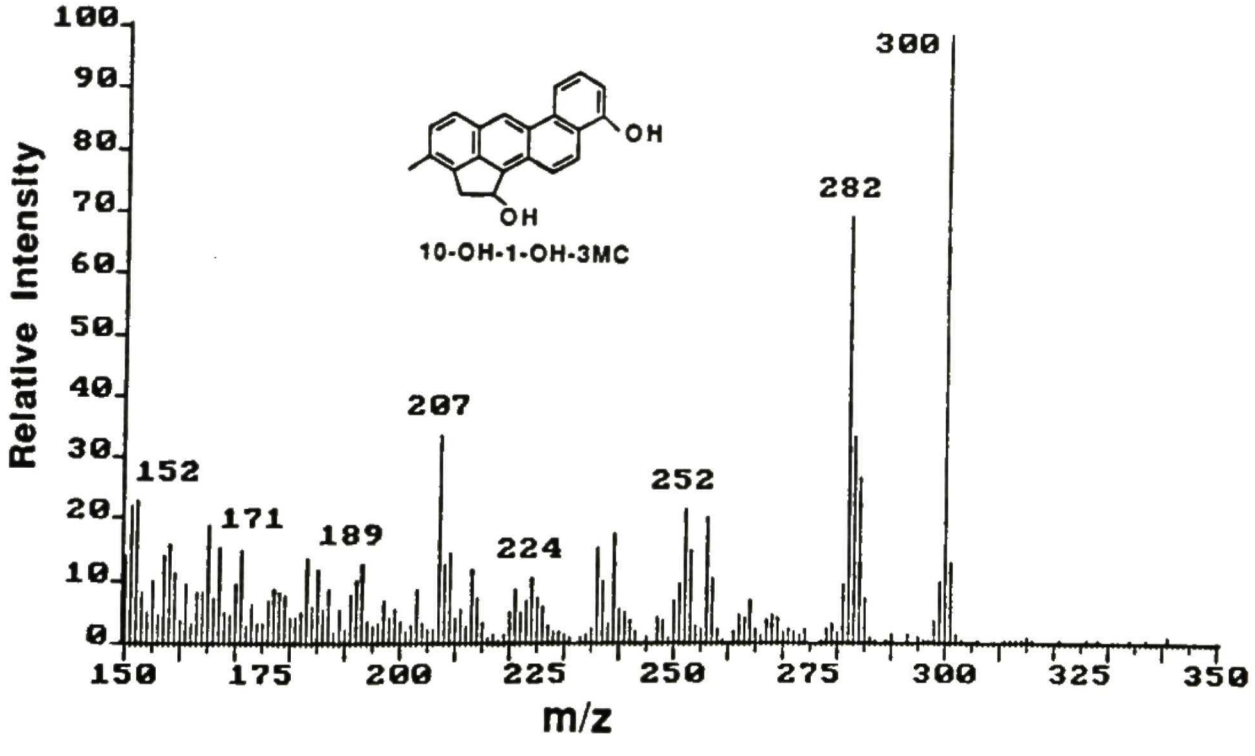

Figure 63. Mass spectrum of 10-OH-1-OH-3MC.

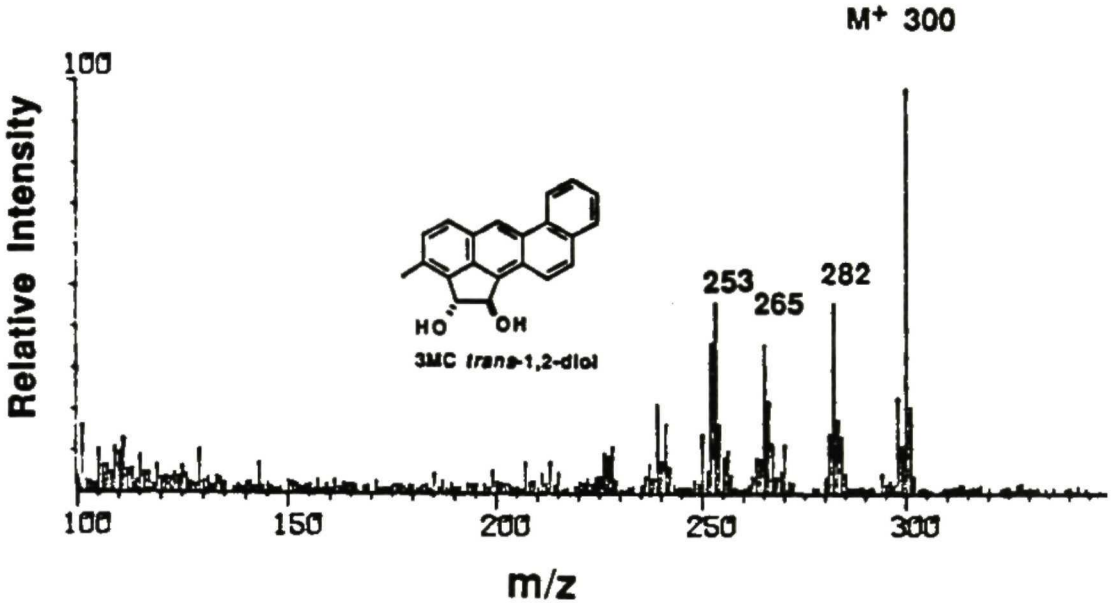

Figure 64. Mass spectrum of 3MC *trans*-1,2-diol.

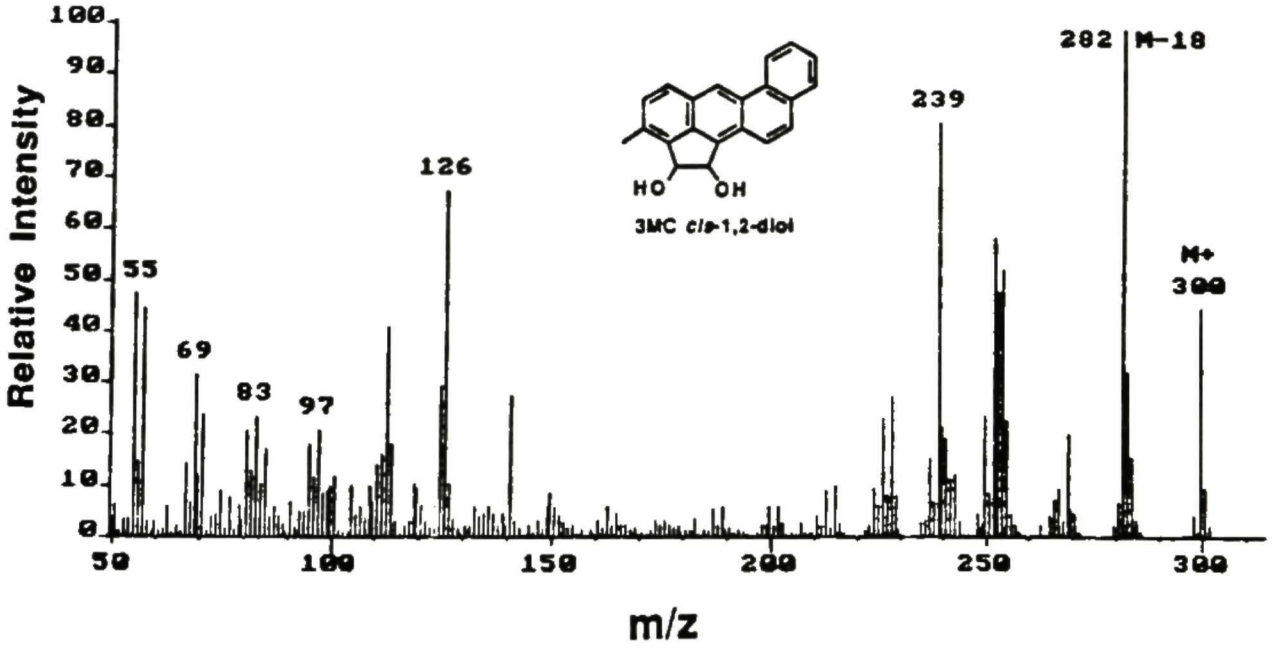

Figure 65. Mass spectrum of 3MC *cis*-1,2-diol.

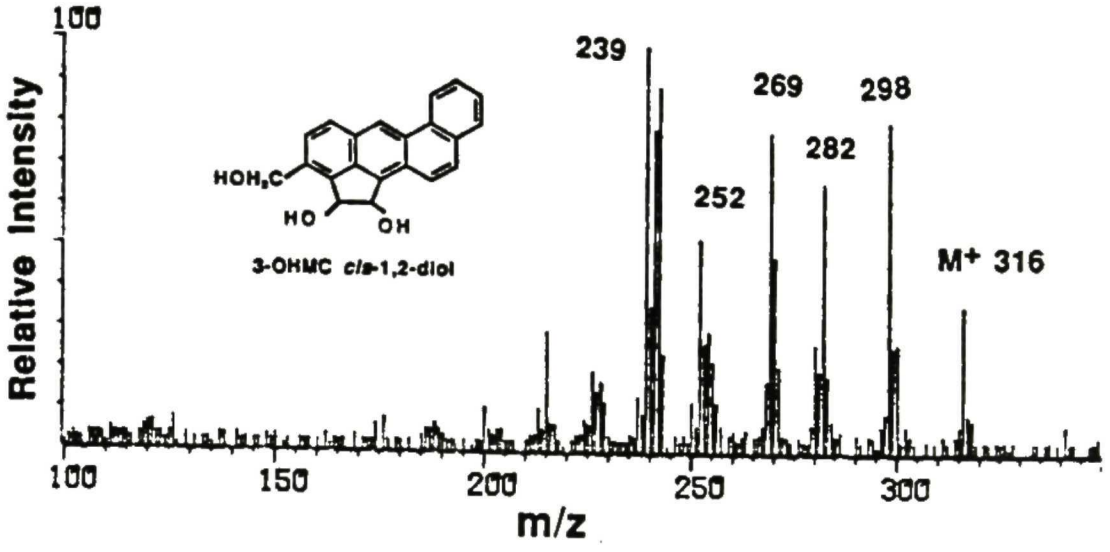

Figure 66. Mass spectrum of 3-OHMC *cis*-1,2-diol.

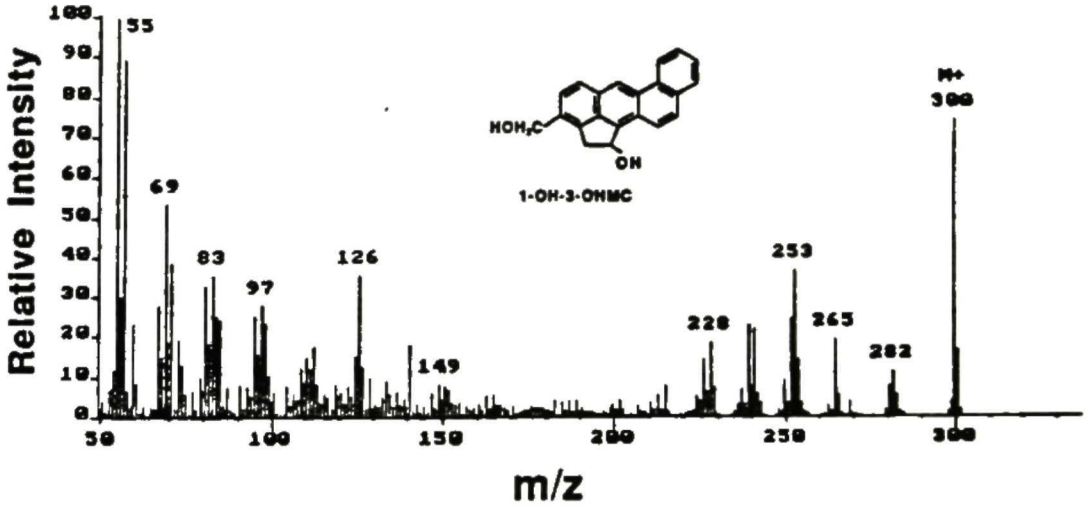

Figure 67. Mass spectrum of 1-OH-3-OHMC.

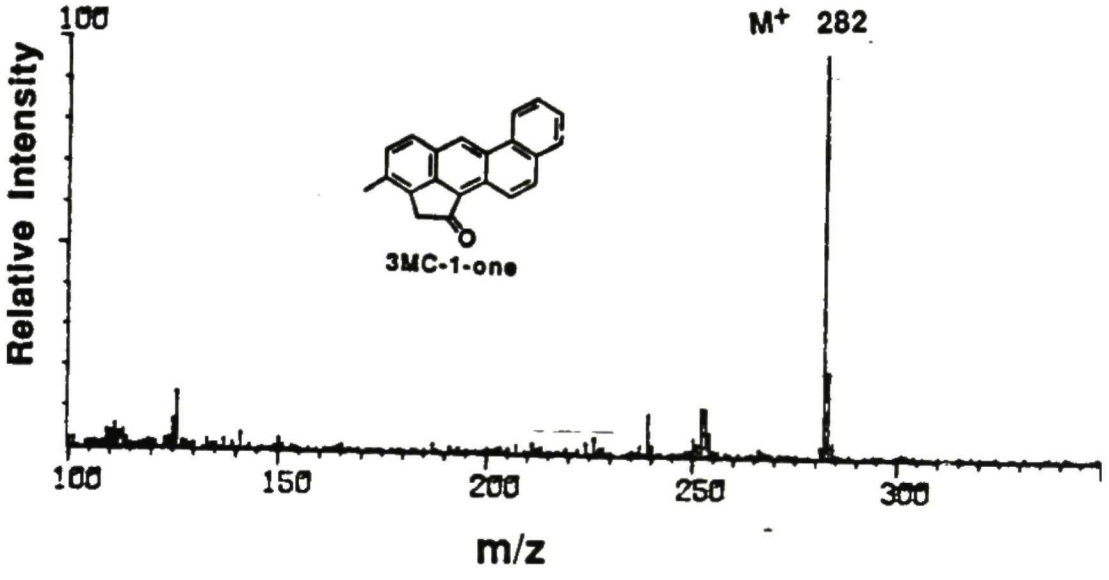

Figure 68. Mass spectrum of 3MC-1-one.

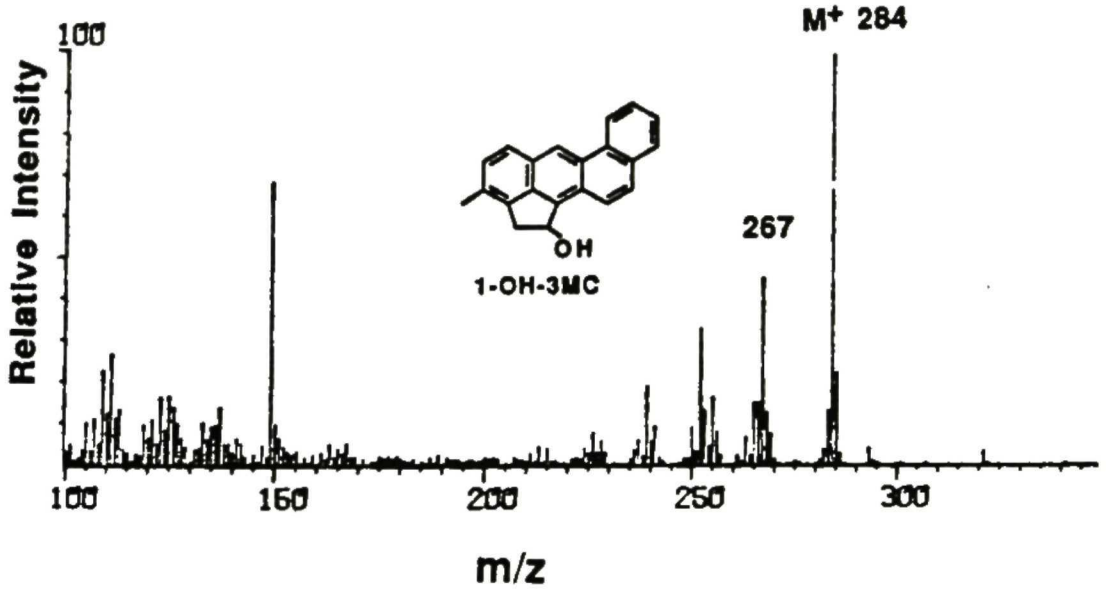

Figure 69. Mass spectrum of 1-OH-3MC.

metabolite of 3MC *cis*-1,2-diol (see section on the metabolism of 3MC *cis*-1,2-diol). The CD spectrum of peak 9 indicated that it was enriched in the 1*R*,2*S*-enantiomer (Fig. 16).

The metabolite contained in peak 20 of Fig. 44 was identified as 3MC-1-one because it had identical properties as that of an authentic 3MC-1-one (Fig. 68). The minor metabolite contained in peak 17 showed similar uv-vis absorption spectrum (not shown) but a different retention time and mass spectrum (Table 5) from 3MC-1-one. Mass spectrum of the product in peak 17 had a M^+ at *m/z* 298 and a characteristic fragment ion at *m/z* 280 (loss of H_2O) (Fig. 47) which indicated that this metabolite was probably 3-OHMC-1-one.

6.3 *Absolute configuration of enantiomeric metabolites*

The major component in peak 1 of Fig. 44 was established to be 1-OH-3MC 7,8-dihydrodiol and contained two diastereomers which have been separated by *R*-DNBPG-C column (peaks 1a1 and 1a2 of Fig. 45). Except for bathchromic shifts and higher magnitude in ellipticity, CD spectrum (Fig. 49) of peak 1a2 (Fig. 45) was similar to that of BA 1*S*,2*S*-dihydrodiol (Yang *et al.*, 1983). The major enantiomer of peak 1a2 was 1-OH-3MC 7*S*,8*S*-dihydrodiol; the absolute configuration of C_1-hydroxyl group. However, CD spectrum (Fig. 49) of peak 1a1 (Fig. 45) had slightly different Cotton effects between 250 and 300 nm from those of 7-MBA 1*R*,2*R*-dihydrodiol established by Yang *et al.* (1984). The cause is probably due to an additional *S* -chiral center at C_1 which displayed a positive CD Cotton bands centered around 258 nm (Fig. 8). Hence the 1*S* -chiral center may alter the negative CD Cotton effect between 250 and 300 nm caused by C_7 and C_8 chiral centers. The result suggested that the peak 1a1 of Fig. 45 contained major enantiomer of 1*S*-OH-3MC-7*R*,8*R*-dihydrodiol. The optical purities of 1-OH-3MC 7,8-dihydrodiols contained in either peak 1a1 or 1a2 cannot be determined. The absolute configuration of the metabolite in peak 1a1 of Fig. 45 can be established by comparing CD spectrum with a biosynthetic 1*S*-OH-3MC 7*R*,8*R*-dihydrodiol derived from the metabolism of 1*S*-OH-3MC (not shown).

The metabolites in peaks 6 and 7 of Fig. 44 were two diastereomeric 1-OH-3MC 9,10-dihydrodiols. The determination of absolute configuration of enantiomers was carried out by the following experiments (see below). The metabolism of 1*S*-OH-3MC produced only two diastereomeric products 1*S*-OH-3MC 9*R*,10*R*-dihydrodiol and 1*S*-OH-3MC 9*S*,10*S*-dihydrodiol. The metabolism of 1*R*-OH-3MC produced only two diastereomeric 1*R*-OH-3MC 9*R*, 10*R*-dihydrodiol and 1*R*-OH-3MC 9*S*,10*S*-dihydrodiol. Both 1*S*-OH-3MC 9*R*,10*R*-dihydrodiol derived from 1*S*-OH-3MC and 1*R*-OH-3MC 9*S*,10*S*-dihydrodiol derived from 1*R*-OH-3MC were a pair of enantiomers with opposite CD Cotton effects and were eluted on reversed phase HPLC to have retention time identical to that of 1-OH-3MC 9,10-dihydrodiol contained in peak 6 of Fig. 44 in metabolism of (±) 1-OH-3MC. *Vice versa* , the 1*S*-OH-3MC 9*S*,10*S*-dihydrodiol derived from 1*S*-OH-3MC and 1*R*-OH-3MC 9*R*,10*R*-dihydrodiol derived from 1*R*-OH-3MC were a pair of enantiomers with opposite CD Cotton effects and were eluted on reversed phase HPLC to have retention time identical to that of 1-OH-3MC 9,10-dihydrodiol contained in peak 7 of Fig. 44. The Positive CD Cotton effects of peak 6 of Fig. 44 showed that this 1-OH-3MC 9,10-dihydrodiol had a major enantiomeric 1*S*-OH-3MC 9*R*,10*R*-dihydrodiol. Enantiomeric composition of the metabolite in peak 6 of Fig. 44 was resolved by *R*-DNBPG-I column to be 79 (1*S*,9*R*,10*R*) : 21 (1*R*,9*S*,2*S*) (Fig. 70). The CD spectra of both enantiomers exhibited the entirely opposite Cotton effects (Fig. 58). The 1-OH-3MC 9,10-dihydrodiol in peak 7 of Fig. 44 had also a positive Cotton effects, showing that major enantiomer of peak 7 was highly enriched in 1*R*,9*R*,10R stereochemistry (not shown). Unfortunately, two enantiomers in peak 7 can not be separated by chiral columns employed. These results exhibited that PB-treated rat liver microsomal enzymes catalyzed preferentially stereoselective formation of 9*R*,10*R*-dihydrodiol derived from (±)1-OH-3MC regardless of the absolute configuration of the C_1-hydroxyl group.

The 1-OH-3-OHMC 9,10-dihydrodiol in peak 1, 3MC *cis*-1,2-diol:9,10-dihydrodiol in peak 3 of Fig. 44 and $NaBH_4$-reduced products of 3MC-1-one 9,10-

dihydrodiol in peak 8 of Fig. 44 resulted in similarly positive CD Cotton effect characteristics to those of 1-OH-3MC 9*R*,10*R*-dihydrodiol, which demonstrated the major enantiomers in those peaks above were enriched in 9*R*,10*R*-dihydrodiols. 3MC *cis*-1,2-diol:9,10-dihydrodiol of peak 3 of Fig. 44 had retention time identical to that of one diastereomeric 3MC *cis*-1,2-diol:9,10-dihydrodiol in peak 2 of Fig. 87 containing a pair of enantiomers (1*R*,2*S*,9*R*,10*R* and 1*S*,2*R*,9*S*,10*S*) formed in the metabolism of (±)3MC *cis*-1,2-dihydrodiol (see the metabolism of 3MC *cis*-1,2-diol). Hence CD spectrum of 3MC *cis*-1,2-diol:9,10-dihydrodiol in peak 3 of Fig. 44 indicated the major enantiomer was highly enriched in 1*R*,2*S*,9*R*,10R stereochemistry. The stereoselective formations of procarcinogenic 9*R*,10*R*-dihydrodiols derived from primarily parent 1-OH-3MC and from secondary oxidative metabolites at C_1, C_2 and 3-methyl sidechain of 3MC may play a significant role in the metabolic activation pathway of 1-OH-3MC and 3MC.

The major phenolic products 8-OH-1-OH-3MC (peak 11), 7-OH-1-OH-3MC (peak 13), 9-OH-1-OH-3MC (peak 14), and 10-OH-1-OH-3MC (peak 16) formed by enantioselective metabolism of racemic 1-OH-3MC by liver microsomes prepared from PB-pretreated rats have only one chiral center at C_1 and should have CD Cotton effects similar to those of either 1*S*-OH-3MC or 1*R*-OH-3MC. Except for the 9-OH-1-OH-3MC (peak 14), CD data (Figs. 50, 51 and 61) indicated that all the phenols formed displayed positive Cotton effects similar to those of 1*S*-OH-3MC. The magnitude of CD Cotton effects was dependent on the location of phenolic hydroxyl group on the benz[a]anthracene nucleus. However, the hydroxyl substituent should not alter the major Cotton effects induced by 1*S*-chiral center. Therefore, the phenolic products at C_7, C_8, and C_{10} positions of 1-OH-3MC were all enriched in the 1*S* -enantiomer.

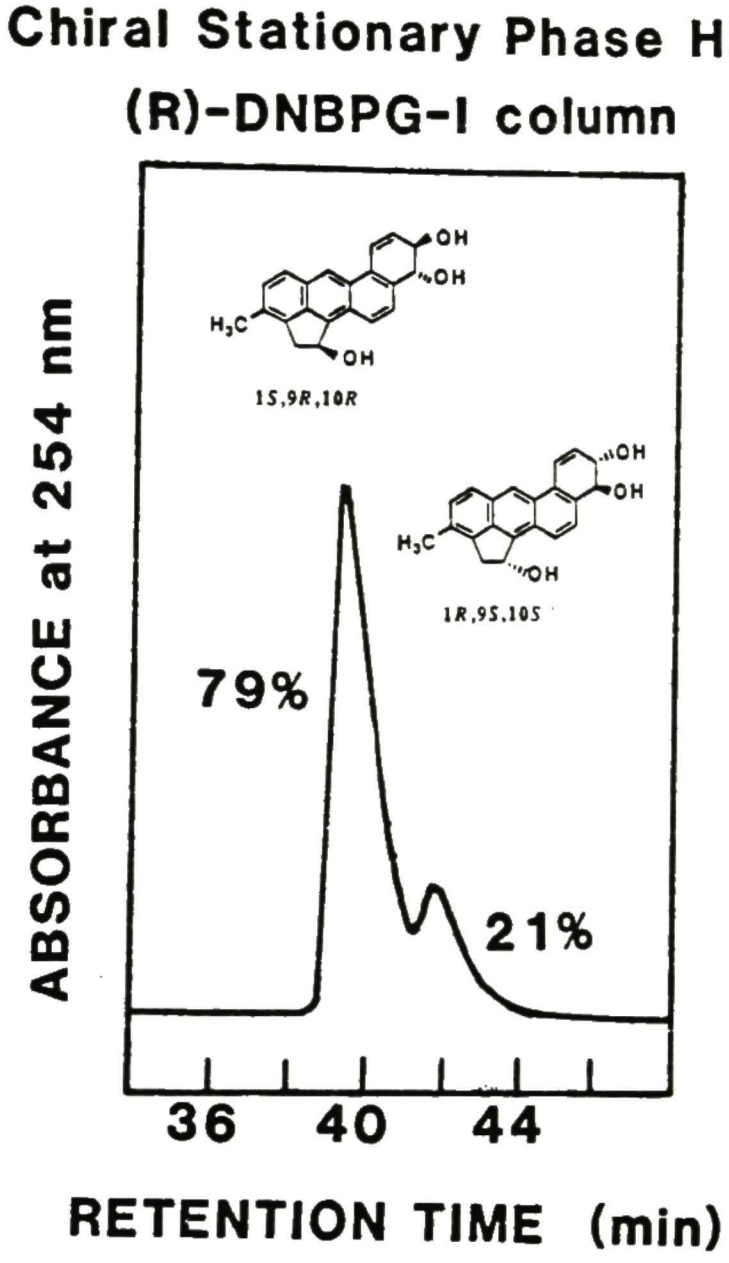

Figure 70. Chiral stationary phase HPLC separation and absolute configurations of 1-OH-3MC 9,10-dihydrodiol enantiomers contained in peak 6 of Fig. 44 are indicated in this figure.

7. *Comparative Metabolism of Racemic [^{3}H]1-OH-3MC by Rat and Human Liver Microsomes*

Metabolites formed in the metabolism of ^{3}H-labeled racemic 1-OH-3MC were analyzed with a Waters Associates RCM-100 radial compression module fitted with a Nova-Pak C_{18} cartridge (8 mm i.d. x 10 cm; 4 μm particles). The cartridge was eluted with a 50-min linear gradient from methanol/water (2:3, v/v) to methanol at a flow rate of 1 ml/min. An unlabeled metabolite mixture, prepared from an *in vitro* incubation of (±)1-OH-3MC with liver microsomes prepared from PB-treated rats, was added to each sample as uv markers. The eluents were monitored at 254 nm and 25 drops of eluent were collected in each fraction and the radioactivity of fractions was determined by liquid scintillation counting. Liquid scintillation counting data (dpm) were converted to concentration unit (pmol) based on the specific activity of labeled substrate. Total radioactivity under a chromatographic peak was determined as the amount of a particular metabolite formed. Their radioactivity elution profiles are shown in Fig. 71. Identities and quantitation of metabolites formed by incubation of [^{3}H]1-OH-3MC with liver microsomes prepared from rats and human are summarized in Table 6.

Distribution of metabolites formed in [^{3}H]1-OH-3MC (specific activity 184 mCi/mmol) metabolism by rat and human liver microsomal incubations were qualitatively similar (Fig. 71); 3MC *cis*-1,2-diol was the major metabolite formed in all samples. Liver microsomes prepared from human had lower metabolic activity than those prepared from rat livers (Table 6). It is interesting to note that *trans*- and *cis*-1,2-diols were the most abundant metabolites and 9,10-dihydrodiols were relatively minor metabolites (Table 6). Liver microsomes prepared from 3MC treated rats had the highest activity in the metabolism of 1-OH-3MC among three rat liver microsomal preparations. Metabolite pattern derived from human liver microsomes was qualitatively more similar to those from liver microsomes prepared from untreated and PB-treated rats.

Figure 71. Reversed-phase HPLC separation of metabolites formed in the metabolism of [^{3}H] 1-OH-3MC by liver microsomes from untreated (control), 3MC-treated and PB-treated rats and human. Identity of each metabolite in chromatographic peak was shown in this Fig. 71A. Radioactive metabolites formed from different microsomal preparations were identified based on known unlabeled metabolites prepared from a larger-scale *in vitro* incubation of 1-OH-3MC with PB-treated rat liver microsomes as a source of UV marker of HPLC profile. The conversion of liquid scintillation counting data (dpm) to concentration (pmol) was obtained on specific activity of [^{3}H] 1-OH-3MC.

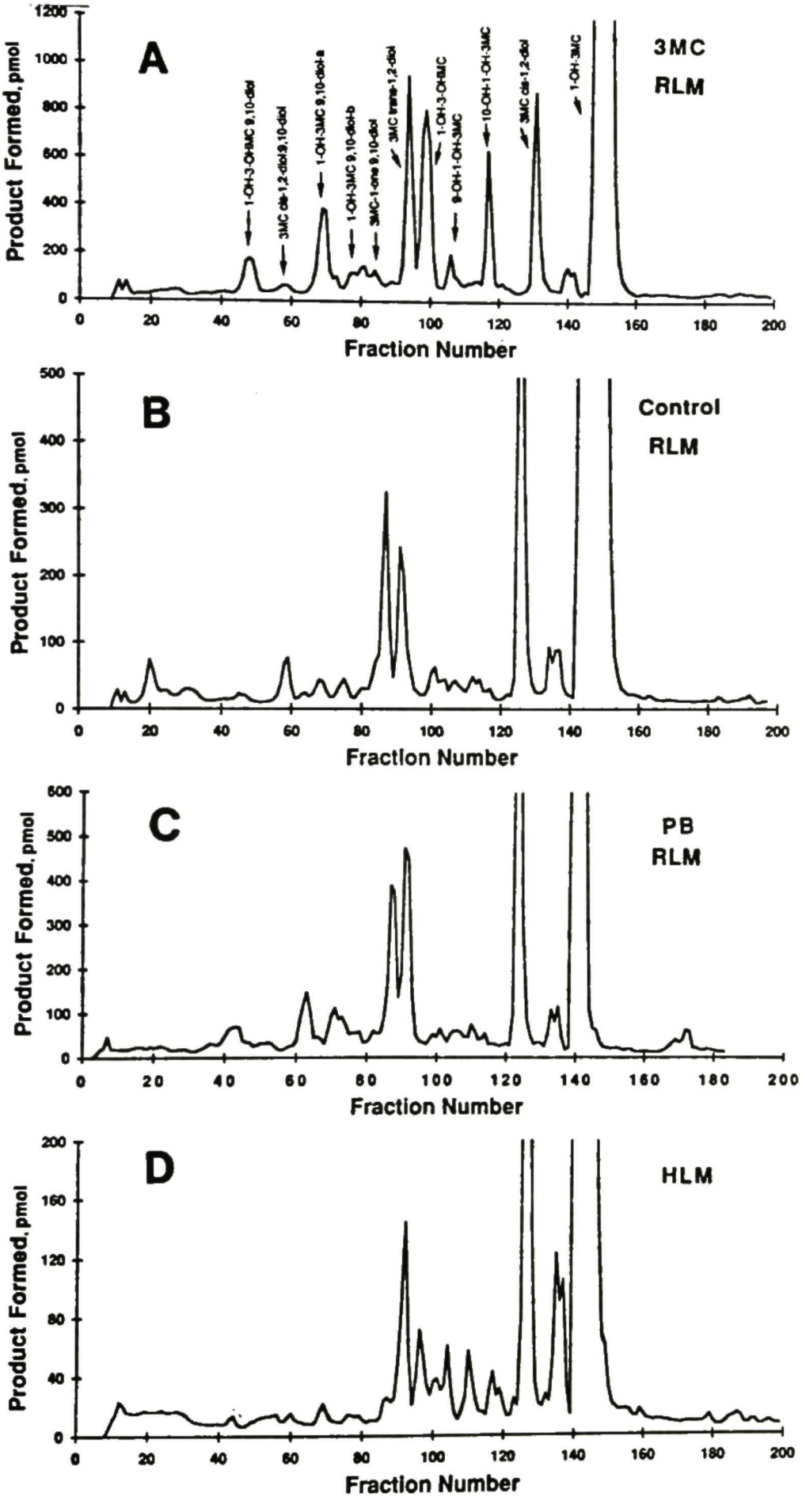
A
3MC
RLM
Product Formed, pmol
Fraction Number
1-OH-3-OH-3MC 9,10-diol
3MC cis-1,2-diol-9,10-diol
1-OH-3MC 9,10-diol-a
1-OH-3MC 9,10-diol-b
3MC-1-one 9,10-diol
3MC trans-1,2-diol
1-OH-3-OH-3MC
9-OH-1-OH-3MC
10-OH-1-OH-3MC
3MC cis-1,2-diol
1-OH-3MC
B
Control
RLM
Product Formed, pmol
Fraction Number
C
PB
RLM
Product Formed, pmol
Fraction Number
D
HLM
Product Formed, pmol
Fraction Number

Table 6. Comparative studies of racemic [^{3}H] 1-OH-3MC metabolism by liver microsomes from rats and human

Identity[a]	Product (pmoles)[b]					
	Rats					Human
	Control[c]		PB		3MC	
	0.5	2.0	0.5	1.0	0.5	2.0
1-OH-3-OHMC 9,10-dihydrodiol	211	330	400	784	1457	125
3MC *cis*-1,2-diol:9,10-dihydrodiol	88	155	211	340	595	98
1-OH-3MC 9,10-dihydrodiol-*a*	178	439	416	989	2663	132
1-OH-3MC 9,10-dihydrodiol-*b*	129	312	429	650	1357	107
3MC *trans*-1,2-diol	1346	1687	1567	2224	3876	740
1-OH-3-OHMC	738	1281	1483	2455	4729	359
9-OH-1-OH-3MC	324	325	380	293	1030	273
10-OH-1-OH-3MC	251	308	310	486	2312	345
3MC *cis*-1,2-diol	3176	3638	4302	4966	3467	3140
% substrate metabolized	14.2	17.9	19.6	25.1	40.1	11.9

a. Identity of metabolites was shown in Fig. 71A.

b. Concentration (pmol) of metabolite formed was converted from metabolite radioactivity (dpm) under chromatographic peak. Numbers shown are average values of duplicate samples.

c. Liver microsomes (mg of microsomal protein/ml incubation mixture) of untreated (control), 3MC-treated and PB-treated rats, and human were used.

8. *Stereoselective Metabolism of 3-OHMC*

8.1 *Identification of 3-OHMC and metabolic formations of 3-OHMC, 1-OH-3MC and 2-OH-3MC in metabolism of 3MC*

A 3-MeOMC has been chemically synthesized; however, all attempts to convert 3-MeOMC to 3-OHMC were unsuccessful (Lee *et al.*, 1988). In a metabolism study of 3MCE, a 3-OHMCE was found to be a major metabolite of 3MCE. The double bond of 3-OHMCE between C_1 and C_2 can be easily hydrogenated and saturated to 3-OHMC by catalytic hydrogenation (Yang *et al.*, 1990). Hence the 3-OHMC indirectly derived from 3MCE metabolism can be used to serve as an authentic standard in a 3MC metabolism study.

A mixture of 3-OHMC, 1-OH-3MC, and 2-OH-3MC was used to develop chromatographic systems that separate all three components. A reversed-phase HPLC system using a Zorbax ODS column has been found to provide satisfactory separation of the three 3MC alcohols (Fig. 72). Under the earlier reported reversed-phase HPLC conditions using a Waters Associates Nova-Pak C_{18} cartridge (Shou and Yang, 1990a; Yang *et al.*, 1990), 3-OHMC cochromatographed with 2-OH-3MC. The 1-OH-3MC was eluted as a shoulder immediately after 2-OH-3MC.

Metabolites formed by incubation of 3MC with liver microsomes from PB-treated rats were analyzed by reversed-phase HPLC (Fig. 72). Peaks 1, 2 and 3 in Fig. 72 had retention times identical to the authentic compounds 3-OHMC, 2-OH-3MC, and 1-OH-3MC, respectively. The identities and enantiomeric compositions of metabolically formed 1-OH-3MC and 2-OH-3MC have recently been reported (Shou and Yang, 1990a). In order to confirm the identity of the metabolite contained in peak 1, repetitive chromatography was carried out to collect sufficient quantity of peak 1 for uv-vis absorption and mass spectral analyses. The uv-vis absorption spectrum of the metabolite contained in peak 1 was identical to that of 3-OHMC derived by catalytic hydrogenation of

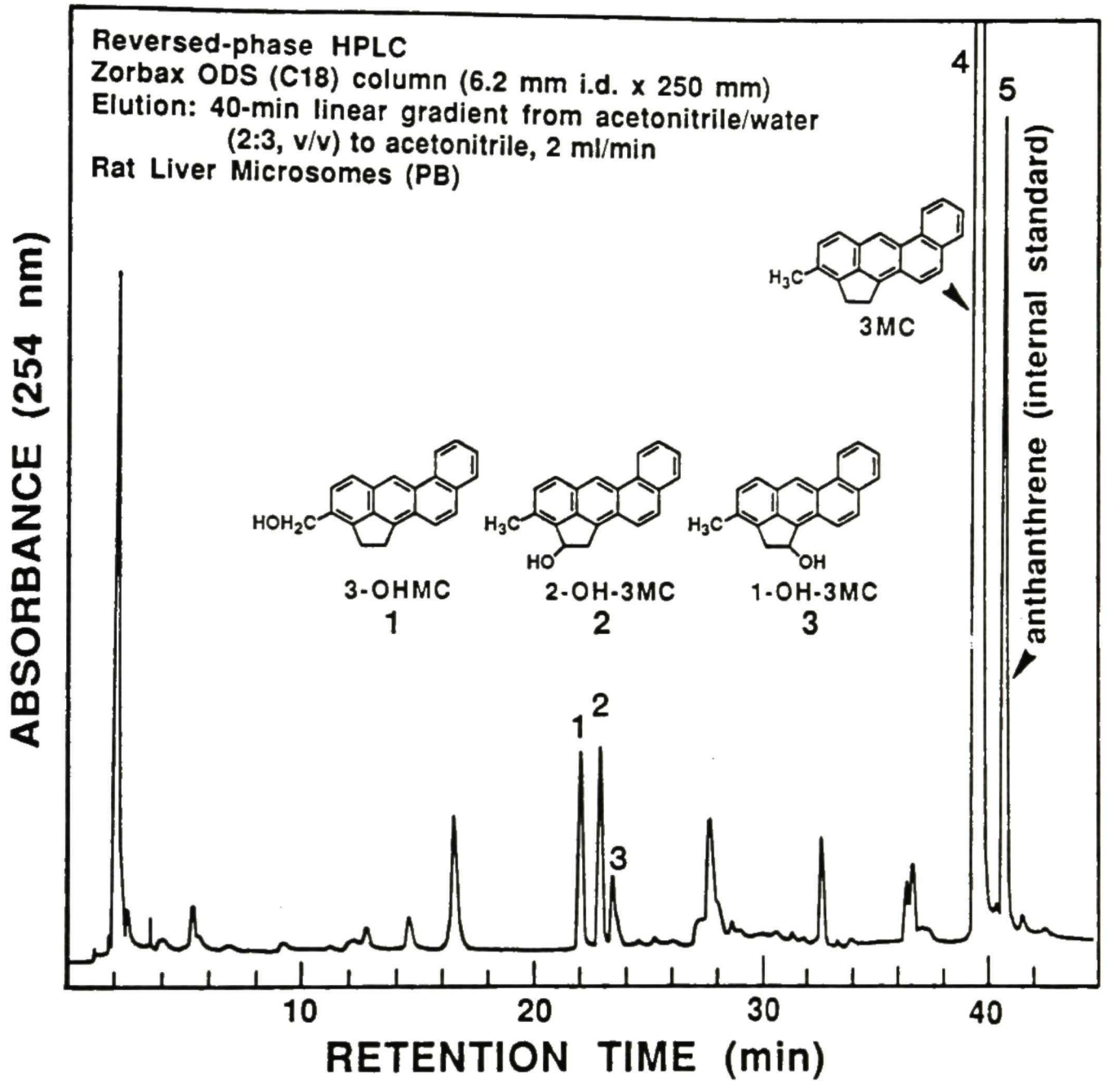

Figure 72. Reversed-phase HPLC separation of 3MC and its metabolites. Identities of chromatographic peaks 1, 2, and 3 are shown. peak 5 contains anthanthrene, a internal standard for chromatography. Unmarked metabolite peaks were not characterized. The sample was obtained by incubation of 3MC for 10 min with liver microsomes (1 mg protein/ml of incubation mixture) from PB-treated rats and other cofactors as described in text.

3-OHMCE (Yang *et al.*, 1990). Electron impact mass spectral analysis indicated a M^+ at *m/z* 284 and characteristic fragment ions at *m/z* 267 (loss of OH), 266 (loss of H_2O), 265, 253, and 252 (not shown). Hence the metabolite contained in peak 1 of Fig. 72 was definitively identified as 3-OHMC.

Relative amounts of 3MC alcohols formed by incubation of 3MC with liver microsomes from untreated, PB-treated, 3MC-treated, and PCB-treated rats are shown in Table 7. Each ml of incubation mixture which contained, among other ingredients, 1 mg protein equivalent of rat liver microsomes, was incubated for 10 min at 37°C. The incubation condition was chosen so that sufficient amounts of 3MC alcohols would be formed for detection at 254 or 280 nm and the possibility of secondary metabolism of the metabolically formed 3MC alcohols would be minimized.

Normalized AUC's were calculated from the results obtained by reversed-phase HPLC analyses (Fig. 72) by dividing the AUC of the individual alcohol by the AUC of the internal standard, and multipling by 100. Three 3MC alcohols formed by incubations of 3MC with liver microsomes from untreated, PB-treated, 3MC-treated, and PCB-treated rats, respectively, are expressed by normalized AUC's in Table 7. Since an identical amount of internal standard was used in each incubation mixture and since the three 3MC alcohols have identical uv-vis absorption properties (all three alcohols have an identical benz[*a*]anthrancene nucleus and similar aliphatic side chains), the normalized AUC's thus reflect the relative amount of 3MC alcohols formed.

The relative yield of three 3MC alcohols (the sum of three AUC's) formed in the metabolism of 3MC by four rat liver microsomal preparations was: 3MC > PCB > PB > control (Table 7). However, liver microsomes from PB-treated rats has the highest activity in the metabolism of 3MC, which is substantially higher than those from 3MC- and PCB-treated rats (Table 7). The relative amount of three 3MC alcohols formed was 2-OH-3MC > 3-OHMC > 1-OH-3MC. The results in Table 7 indicate that 3-OHMC is one of the major metabolites and constitutes 15 to 41% of all the 3MC alcohols combined. Enzyme

Table 7. Distribution of hydroxylation products formed at the aliphatic carbons of 3MC by rat liver microsomes.

Rat Liver Microsomes[a]	3MC Metabolized (%)	Metabolite Distribution (%)[b]						Yield[c]
		3-OHMC		2-OH-3MC		1-OH-3MC		
Control	15.2	11.5	(34.6) (27.4)	12.7	(38.1) (42.2)	9.1	(27.3) (30.4)	33.3
PB	33.5	25.7	(41.1) (38.2)	25.7	(41.1) (42.7)	11.2	(17.8) (19.1)	62.6
3MC	25.0	19.1	(15.5) (14.5)	95.9	(78.0) (78.5)	8.0	(6.5) (7.0)	123.0
PCB	27.1	18.8	(28.4) (23.3)	40.7	(60.9) (64.4)	7.2	(10.7) (12.3)	66.7

a Liver microsomes prepared from male Sprague-Dawley rats (in groups of 5 or 15) which were either untreated (control), PB-treated, 3MC-treated, or PCB-treated. Each ml of incubation mixture was incubated for 10 min at 37°C and contained 1 mg microsomal protein among other components as described in Materials and Methods.

b Numbers in the first row were normalized AUC's obtained from reversed-phase HPLC analysis (Fig. 72). Numbers in parentheses are percentages of the AUC sum of three alcohols. Normalized AUC's were calculated by dividing AUC of the individual alcohol by the AUC of the internal standard and multiplied by 100. Numbers in the second row were obtained from normal-phase HPLC analysis (Fig. 73). Numbers are averages from analyses with duplicate samples and agree within 10% of the values shown.

c Sum of normalized AUC's of 3-OHMC, 1-OH-3MC, and 2-OH-3MC.

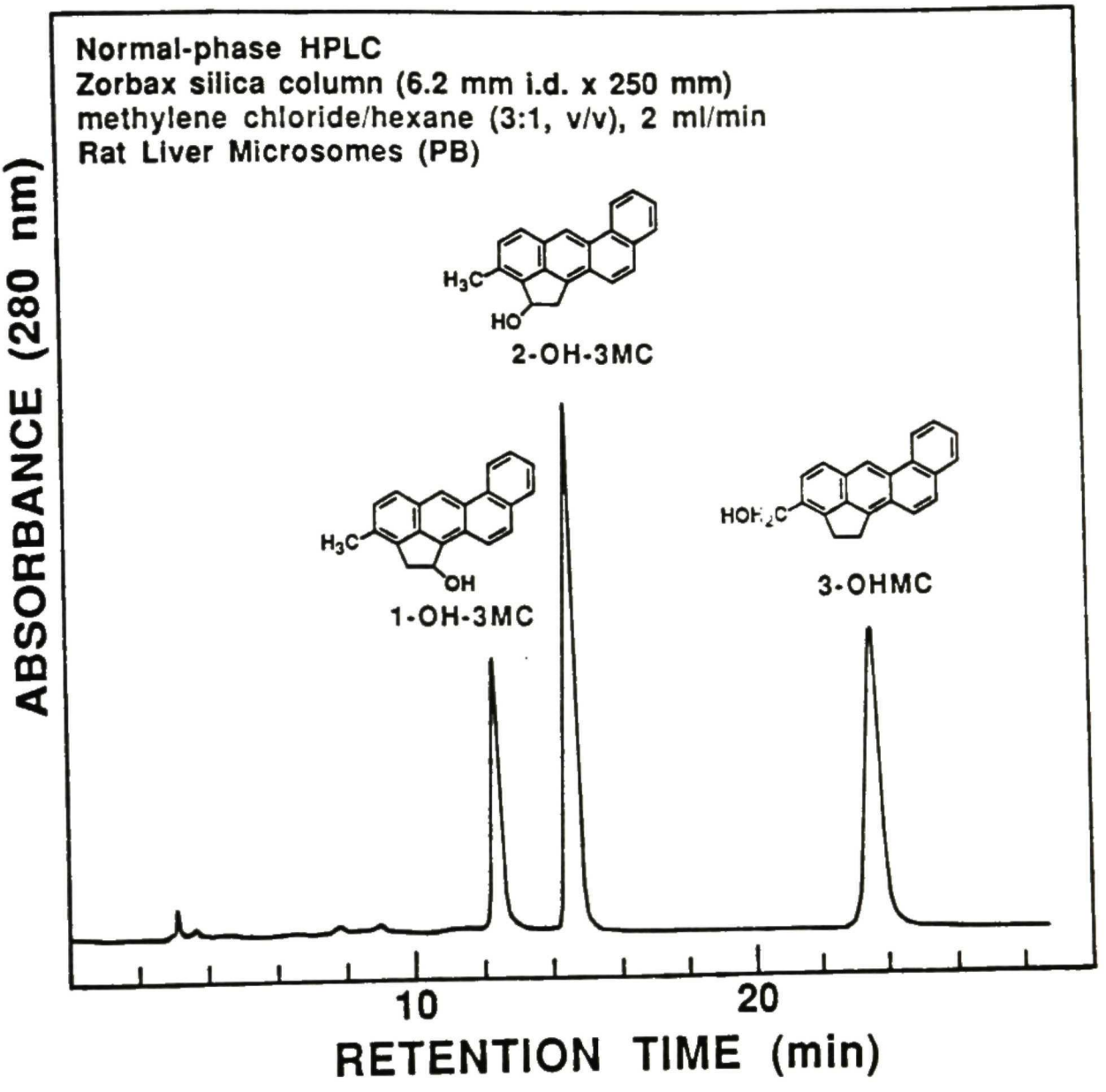

Figure 73. Normal-phase HPLC separation of 1-OH-3MC, 2-OH-3MC and 3-OHMC. The sample was a mixture of peaks 1, 2 and 3 collected in reversed-phase HPLC mode (Fig. 72).

induction does not significantly alter the amount of 1-OH-3MC formed. However, the formations of 3-OHMC and 2-OH-3MC by rat liver microsomes are significantly increased when rats were pretreated with either PB, 3MC, or PCB (Table 7). The increase in the formation of 2-OH-3MC was the most pronounced when rats were pretreated with 3MC.

We were concerned with the possibility that there may be impurities and/or other metabolites which coeluted with chromatographic peaks 1, 2, and 3 in the reversed-phase HPLC mode (Fig. 72). This would significantly alter the values of the relative distribution of the three 3MC alcohols. Hence chromatographic peaks 1, 2, and 3 Fig. 73 were collected as one fraction and , after removal of solvent, were further analyzed by normal-phase HPLC (Fig. 72). In the chromatogram shown in Fig. 73, each of the three alcohols were completely separated and cochromatographed with the corresponding authentic compound. The relative amount of three 3MC alcohols determined by normal-phase HPLC was generally consistent with those determined by reversed-phase HPLC (Table 7). The results suggest that, other than the 3MC alcohols, peaks 1, 2, and 3 in Fig. 72 do not contain a significant amount of other 3MC metabolites.

In conclusion, 3-OHMC is one of the major rat liver microsomal metabolites of 3MC. Pretreatment of rats with PB, 3MC, or PCB significantly increases the metabolite formation of 3-OHMC. To date 3-OHMC has not been chemically synthesized. In the absence of a synthetic compound, 3-OHMC may be prepared biosynthetically. Hence it is now possible to further examine the metabolic pathways, DNA-binding activity, mutagenicity, and tumorigenicity of 3-OHMC. These additional studies should give insights to the role of 3-OHMC in 3MC-induced carcinogenesis.

8.2 *Identification and separation of metabolites formed in 3-OHMC metabolism*

A relatively large quantity of 3-OHMC was isolated from the mixture of metabolites formed in the metabolism of 3MC by liver microsomes from PB-treated rats. Metabolites formed by incubation of 3-OHMC by liver microsomes from PB-treated rats were separated by reversed-phase HPLC (Fig. 74).

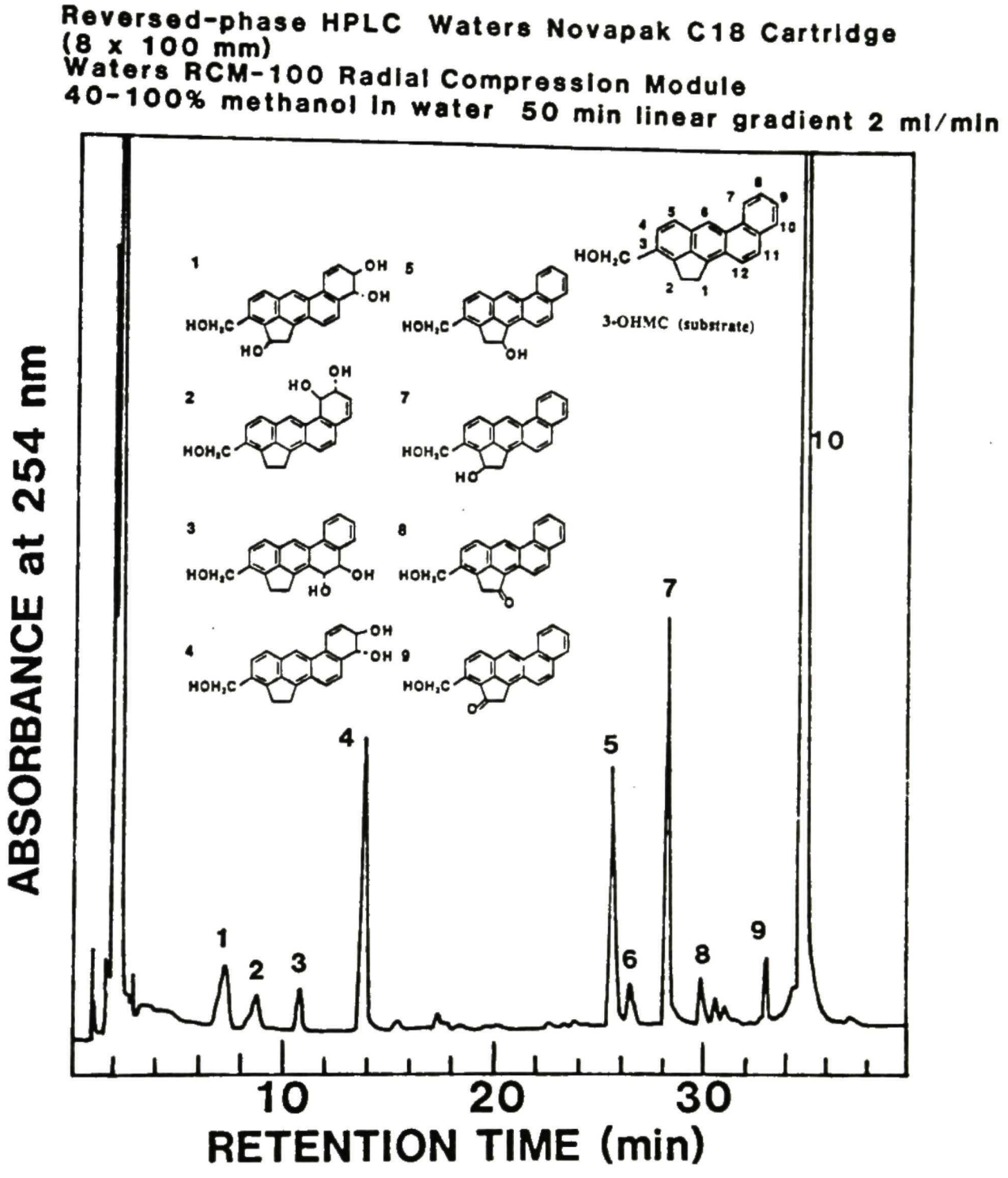

Figure 74. Reversed-phase HPLC separation of 3-OHMC and its metabolites. Identities of chromatographic peaks are shown. Unmarked metabolite peaks were not characterized. The sample was obtained by incubation of 3-OHMC for 30 min with liver microsomes (1 mg protein/ml of incubation mixture) from PB-treated rats and other cofactors as described in text.

Table 8. The Relative amount of metabolites formed in 3-OHMC metabolism by rat liver microsomes

Metabolites[a]	Relative Amount (Metab./Int.Std.)[b] Control	PB	3MC	PCB
2-OH-3-OHMC 9,10-dihydrodiol	0.08±0.02	0.71±0.15	0.73±0.10	0.71±0.08
3-OHMC 7,8-dihydrodiol	0.34±0.02	0.70±0.17	0.84±0.02	0.68±0.05
3-OHMC 11,12-dihydrodiol	0.90±0.03	1.19±0.10	0.89±0.03	1.33±0.02
3-OHMC 9,10-dihydrodiol	0.84±0.09	2.28±0.22	1.77±0.04	2.13±0.22
1-OH-3-OHMC + 8-OH-3-OHMC	2.76±0.42	1.28±0.16	1.59±0.07	1.80±0.58
2-OH-3-OHMC	0.79±0.02	0.94±0.08	0.25±0.01	0.55±0.01
3-OHMC-1-one	0.58±0.02	0.20±0.08	0.46±0.02	0.34±0.02
3-OHMC-2-one	0.44±0.03	0.36±0.01	0.15±0.03	0.38±0.04
% substrate metabolized	13.67	64.56	54.30	65.74

a. 3-OHMC (40 nmol per ml of incubation mixture) was incubated with liver microsomes of rats untreated and treated with PB, 3MC and PCB (1.0 mg of protein per ml of incubation mixture) at 37°C for 15 min.

b. Relative amount was determined by the ratio under chromatographic area of each metabolite formed to internal standard (3MC). HPLC separation of metabolites formed in metabolism of 3-OHMC was analyzed by using the column (Nova Pak C_{18}, 4 μ, 8 mm x 10 cm) eluted with a gradient from 40% methanol in water to methanol in 50 min at flow rate of 2 ml/min.

Table 9. Enantiomeric compositions of 3-OHMC 9,10-dihydrodiol, 2-OH-3-OHMC and 1-OH-3-OHMC formed in 3-OHMC metabolism by rat liver microsomes

Metabolites[a]	Enantiomeric Ratio %[b]			
	Control	PB	3MC	PCB
3-OHMC 9,10-dihydrodiol	82: 18	88 : 12	93 : 7	89 : 11 (*RR : SS*)
2-OH-3-OHMC	32 : 69	35 : 65	4 : 96	10 : 90 (*R : S*)
1-OH-3-OHMC	26 : 74	25 : 75	44 : 56	32 : 68 (*R : S*)

a. 3-OHMC (40 nmol per ml of incubation mixture) was incubated with liver microsomes of rats untreated and treated with PB, 3MC and PCB (1.0 mg of protein per ml of incubation mixture) at 37°C for 15 min.

b. Enantiomeric ratios were resolved by using either ionically or covalently bounded *R*-DNBPG column. Eluent A (ethanol-acetonitrile, 2:1, v/v) in hexane was used and the flow rate was 2 ml/min.

Chromatographic peaks were numbered as indicated in Fig. 74 and the metabolites contained in each chromatographic peak were characterized as described below. Peak 10 is the unmetabolized substrate 3-OHMC. Characterization of metabolites is described in below.

Two 9,10-dihydrodiols were formed in the metabolism of 3-OHMC. The product contained in peak 4 of Fig. 74 was identified as 3-OHMC 9,10-dihydrodiol. This metabolite had uv-vis absorption and CD spectra (Fig. 76) similar to those of 2*S*-OH-3MC 9*R*,10*R*-dihydrodiol (Fig. 29) and the molecular ion (M^+) at *m/z* was 318 (not shown). The component in peak 1 had a uv-absorption spectrum similar to that of peak 4, indicating that it was also a 9,10-dihydrodiol. This metabolite may be derived from either 2-OH-3-OHMC (peak 7) or 3-OHMC 9,10-dihydrodiol (peak 4), both of which were the major metabolites formed in the metabolism of 3-OHMC.

The metabolite contained in peak 7 was identified as 2-OH-3-OHMC. It had retention time, uv-vis absorption and mass spectra identical to those of 2-OH-3-OHMC (Figs. 23 and 25).

The major component contained in peak 5 was separated by normal phase HPLC (not shown). It had an uv-vis absorption spectrum and a retention time on reversed-phase HPLC identical to those of 1-OH-3-OHMC (see metabolism of 1-OH-3MC). Hence the major metabolite contained in peak 5 was identified as 1-OH-3-OHMC.

Peak 2 had uv-vis absorption and CD spectra (Fig. 75) similar to those of 7-MBA 1*R*,2*R*-dihydrodiol (Yang and Fu, 1984). Hence the metabolite in peak 2 was tentatively identified as 3-OHMC 7,8-dihydrodiol.

Peak 3 of Fig. 74 had a uv-vis absorption spectrum similar to that of 2-OH-3MC 11,12-dihydrodiol (Fig. 24) and had CD Cotton effects (Fig. 77) similar to those of 7-MBA 5*R*,6*R*-dihydrodiol (Yang and Fu, 1984). This metabolite in peak 3 was tentatively established as a K-region 3-OHMC 11,12-dihydrodiol.

Figure 75. Uv-vis absorption (– – – –, methanol) and CD (——, concn. 1.0 A_{270}/ml, methanol; Φ_{298}/A_{269} = -2.6 millidegrees) spectra of the metabolite 3-OHMC 7*R*,8*R*-dihydrodiol (major) contained in peak 2 of Fig. 74.

Figure 76. Uv-vis absorption (– – – –, methanol) and CD (——, concn. 1.0 A_{270}/ml, methanol; Φ_{268}/A_{270} = 3.8 millidegrees) spectra of the metabolite 3-OHMC 9*R*,10*R*-dihydrodiol (major) contained in peak 4 of Fig. 74.

Figure 77. Uv-vis absorption (– – – –, methanol) and CD (——, concn. 1.0 A_{274}/ml, methanol; Φ_{249}/A_{274} = - 8.0 millidegrees) spectra of the metabolite 3-OHMC 11*R*,12*R*-dihydrodiol (major) contained in peak 3 of Fig. 74.

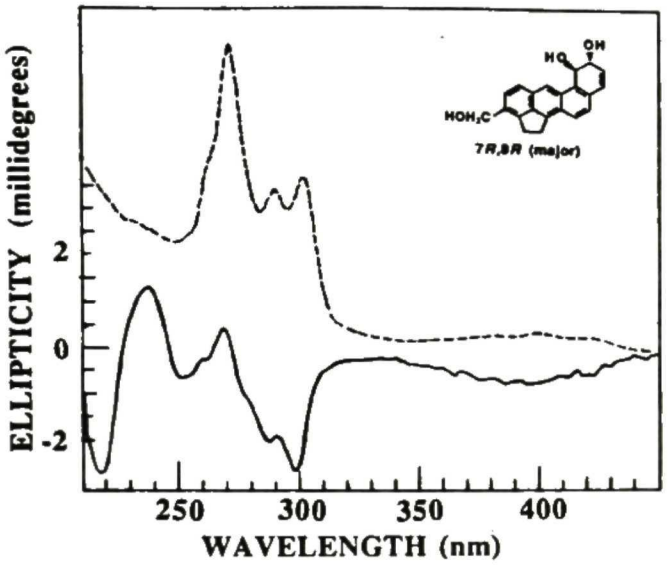
ELLIPTICITY (millidegrees)
2
0
-2
250
300
350
400
WAVELENGTH (nm)
HO
OH
HOH2C
7R,8R (major)

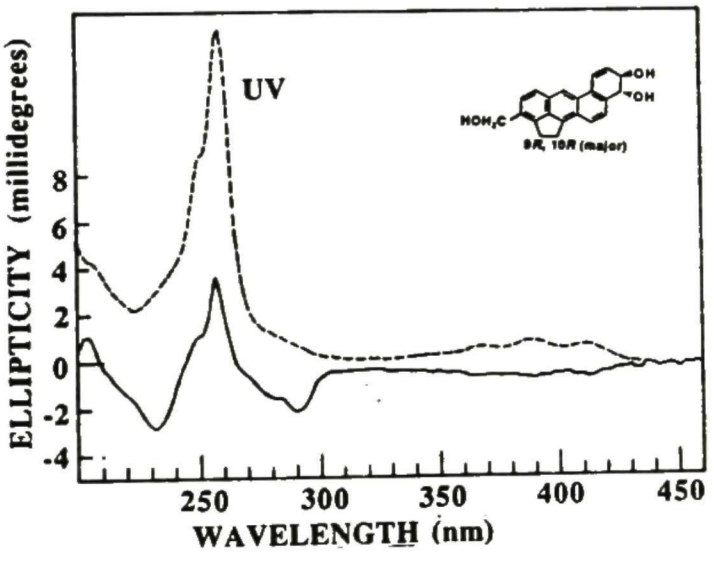
UV
ELLIPTICITY (millidegrees)
8
6
4
2
0
-2
-4
250
300
350
400
450
WAVELENGTH (nm)
OH
OH
HOH2C
9R, 10R (major)

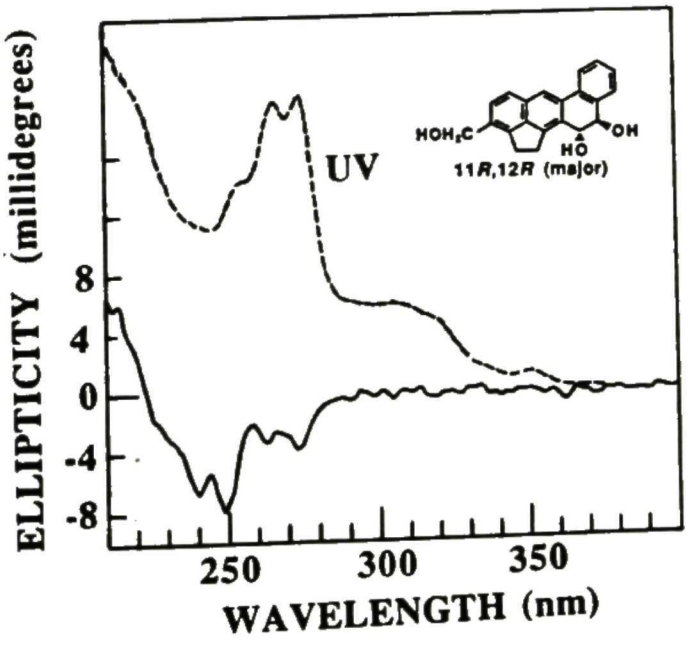
UV
ELLIPTICITY (millidegrees)
8
4
0
-4
-8
250
300
350
WAVELENGTH (nm)
HOH2C
OH
HO
11R,12R (major)

The minor metabolite in peak 8 was found to have a uv-vis spectrum and a retention time on reversed-phase HPLC similar to those of 3-OHMC-1-one detected in the metabolism of (±)1-OH-3MC (Fig. 47). 3-OHMC-1-one formed in the metabolism of 3-OHMC was probably derived from dehydrogenation at C_1 of the major metabolite 1-OH-3-OHMC.

8.3 *Absolute configuration and effect of enzyme inducers on enantiomeric composition of chiral metabolites*

Enantiomeric compositions of 3-OHMC 9,10-dihydrodiol, 2-OH-3-OHMC and 1-OH-3-OHMC formed in the metabolism of 3-OHMC by liver microsomes from control, PB-, 3MC- and PCB-treated rats were resolved on either *R*-DNBPG-C or *R*-DNBPG-I column as shown in Fig. 78 and Table 9. The major metabolite 3-OHMC 9,10-dihydrodiol (peak 4 in Fig. 74) had CD Cotton effects (Fig. 76) similar to those of 2*S*-OH-3MC 9*R*,10*R*-dihydrodiol (Fig. 29) indicating this metabolite contained a majority of the 9*R*,10*R* enantiomer. Enantiomeric ratios [(9*R*,10*R*):(9*S*,10*S*)] of 3-OHMC 9,10-dihydrodiol were 82:18 (control), 88:12 (PB), 93:7 (3MC) and 89:11 (PCB) (Table 9). The results indicated that all liver microsomal preparations catalyzed the formation of 3-OHMC 9,10-dihydrodiol enriched in the 9*R*,10*R*-enantiomer and liver microsomes from 3MC-treated rats were more stereoselective than other liver microsomal preparations.

Enantiomers of 2-OH-3-OHMC, a metabolite formed in the metabolism of 3-OHMC, were separated on *R*-DNBPG-I column (Fig. 36C) and had *R*/*S* ratios of 31:69 (control), 35:65 (PB), 4:96 (3MC) and 10:90 (PCB), respectively. The results indicated that P-450 isozymes in the liver of rats induced by 3MC and PCB had the highest stereoselectivity in catalyzing the formation of 2*S*-OH-3-OHMC. In comparison, 1-OH-3-OHMC formed in the metabolism of 3-OHMC had *R*/*S* enantiomeric ratios of 24:76 (control), 25:75 (PB), 44:56 (3MC) and 32:68 (PCB). The liver microsomes form untreated and PB-treated rats had the highest stereoselectivity toward the formation of 1*S*-OH-3-OHMC than those from 3MC and PCB-treated rats.

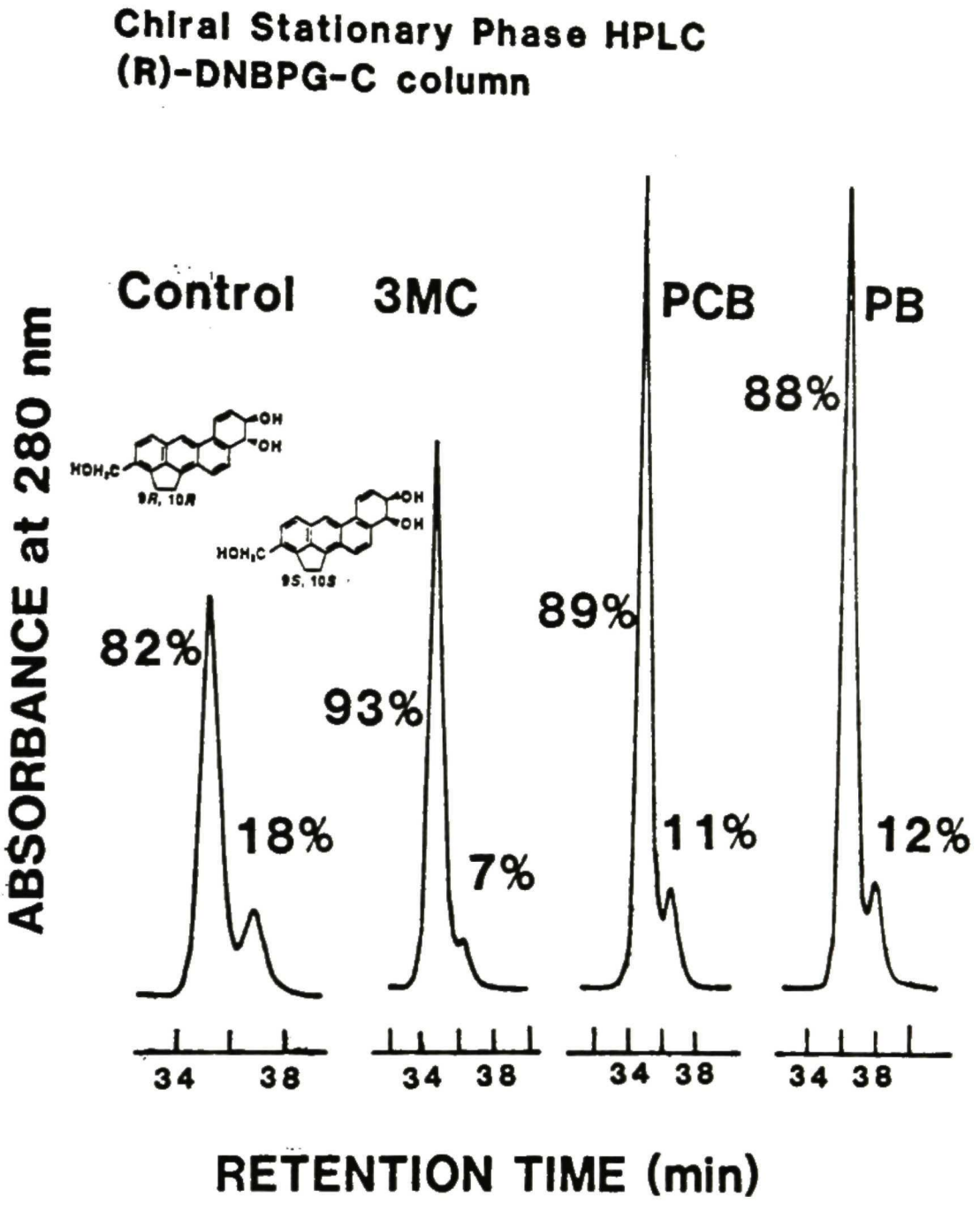

Figure 78. Chiral stationary phase HPLC separation and absolute configurations of metabolite 3-OHMC 9,10-dihydrodiol enantiomers contained in peak 4 of Fig. 74 are indicated in this figure.

8.4 *Effects of enzyme inducers on relative amount of metabolites*

The relative amounts of metabolites formed in the metabolism of 3-OHMC by liver microsomes from untreated (control), 3MC-, PB- and PCB-treated rats were determined with the aid of an internal standard (Table 8). The relative amounts of 3-OHMC 7,8-dihydrodiol formed were 3MC > PB ≈ PCB > control; 3-OHMC 11,12-dihydrodiol, PCB > PB > 3MC > control; 3-OHMC 9,10-dihydrodiol, PB > PCB > 3MC > control; 2-OH-3-OHMC, PB > control > PCB > 3MC.

9. *Metabolism of Racemic and Enantiomeric 3MC trans-1,2-diol*

9.1 *HPLC separation and identification of metabolites*

A mixture of metabolites, formed in a 30-min incubation of a racemic 3MC *trans*-1,2-diol with liver microsomes (0.25 mg protein per ml of incubation mixture) from PB-treated rats, was separated into more than 8 components by reversed-phase HPLC (Fig. 79). The various chromatographic peaks which have been identified were: 8-OH-3-OHMC *trans*-1,2-diol (peak 1), two diastereomeric 3MC *trans*-1,2-diol:9,10-dihydrodiols (peak 2) 8-OH-3MC *trans*-1,2-diol (peak 3), 7-OH-3MC *trans*-1,2-diol (peak 4), 9-OH-3MC *trans*-1,2-diol (peak 5), 10-OH-3MC *trans*-1,2-diol (peak 6), 3-OHMC *trans*-1,2-diol (peak 7), and the remaining 3MC *trans*-1,2-diol (peak 8). Peak 9 is 1-OH-3MC, an internal standard added for chromatography. Metabolites were characterized by uv-vis absorption, CD and mass spectral analyses and by comparison.

The major metabolite contained in peak 2 (Fig. 79) had uv-vis absorption and CD spectra (Fig. 80) similar to those of 2*S*-OH-3MC 9*R*,10*R*-dihydrodiol (Fig. 29). Mass spectral analysis indicated a molecular ion (M^+) at *m/z* 334 and two major fragment ions at *m/z* 316 (loss of H_2O) and 298 (loss of two H_2O). These data indicated that metabolite peak 2 was a 3MC *trans*-1,2-diol:9,10-dihydrodiol. 3MC *trans*-1,2-diol:9,10-dihydrodiol can be present as two diastereomers. However, the metabolite in peak 2 could not be separated into more than one component on silica gel and *R*-DNBPG-C columns. CD spectrum of the metabolite contained in peak 2 was similar to that of 2*S*-OH-3MC 9*R*,10*R*-dihydrodiol (Fig. 29). Hence the hydroxyl groups at 9,10 positions are predominantly in 9*R*,10*R* configuration. The absolute stereochemistry of the hydroxyl groups at C_1 and C_2 positions could not be deduced from the CD spectrum .

Two phenolic products (7-OH-3MC *trans*-1,2-diol and 8-OH-3MC *trans*-1,2-diol) contained in peaks 3 and 4 (Fig. 79) were found to have uv-vis absorption spectra (Figs. 82 and 83) similar to those of 1-OH-BA and 8-OH-2-OH-3MC (Fig. 21A) respectively.

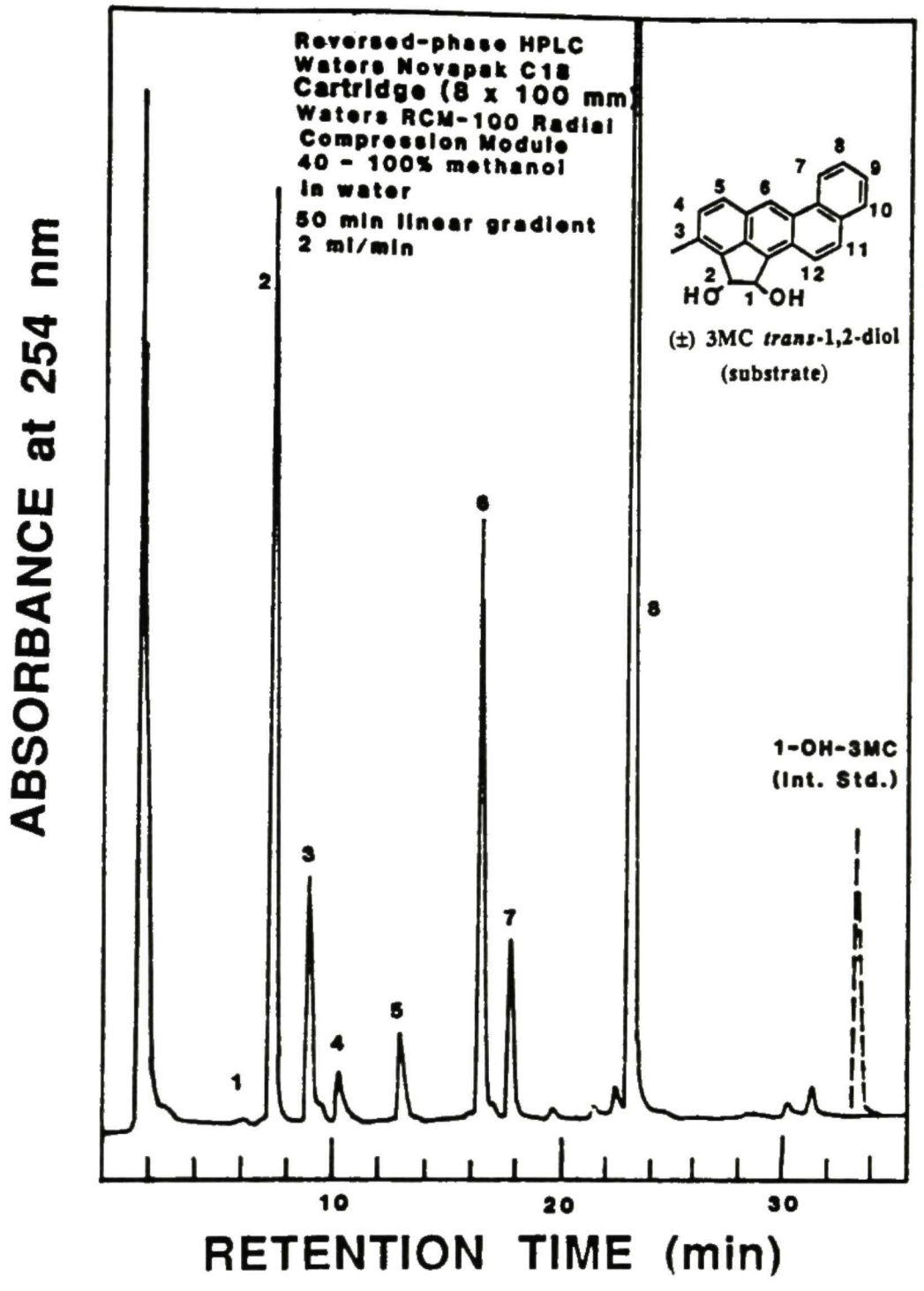

Figure 79. Reversed-phase HPLC separation of (±) 3MC *trans*-1,2-diol and its metabolites. This sample was prepared by incubation of (±) 3MC *trans*-1,2-diol for 30 min with liver microsomes (0.25 mg protein/ml incubation mixture) from PB treated rats. Identities of metabolites contained in various chromatographic peaks are described in the text and summarized in Table 10. 1-OH-3MC was used as a internal standard for quantitative study. The various chromatographic peaks are: peak 1, 8-OH-3-OHMC *trans*-1,2-diol; peak 2, a mixture of two diastereomers, 3MC *trans*-1,2-diol:9,10-dihydrodiols; peak 3, 8-OH-3MC *trans*-1,2-diol; peak 4, 7-OH-3MC *trans*-1,2-diol; peak 5, 9-OH-3MC *trans*-1,2-diol; peak 6, 10-OH-3MC *trans*-1,2-diol; peak 7, 3-OHMC *trans*-1,2-diol; peak 8, 3MC *trans*-1,2-diol (residual substrate); peak 9, 1-OH-3MC as an internal standard added.

Table 10. Relative amount of metabolites formed in the metabolism of (±) 3MC *trans*-1,2-diol, 3MC *trans*-1*S*,2*S*-diol, and 3MC *trans*-1*R*,2*R*-diol by rat liver microsomes

Metabolites[a] (peak No.)	Relative Amount (Metab./Int. Std.)[b]								
	PB			Control			3MC		
	Racemic	1*S*,2*S*	1*R*,2*R*	Racemic	1*S*,2*S*	1*R*,2*R*	Racemic	1*S*,2*S*	1*R*,2*R*
3MC *t*-1,2-diol: 9,10-dihydrodiol (2)	2.70±0.70	1.43±0.09	2.57±0.40	0.65±0.02	0.35±0.00	0.55±0.06	0.34±0.14	0.51±0.00	0.22±0.01
8-OH-3MC *t*-1,2-diol (3)	0.89±0.11	0.48±0.04	0.80±0.18	1.02±0.03	0.71±0.01	0.93±0.02	1.10±0.20	1.24±0.14	1.37±0.05
7-OH-3MC *t*-1,2-diol (4)	0.22±0.04	0.13±0.00	0.24±0.05	0.33±0.00	0.25±0.00	0.35±0.03	0.43±0.05	0.56±0.02	1.07±0.07
9-OH-3MC *t*-1,2-diol (5)	0.34±0.06	0.24±0.03	0.56±0.08	0.25±0.04	0.17±0.00	0.43±0.03	0.49±0.27	0.75±0.01	2.08±0.02
10-OH-3MC *t*-1,2-diol(6)	1.95±0.14	0.74±0.04	3.85±0.60	1.29±0.02	0.56±0.00	2.71±0.14	0.46±0.06	0.49±0.02	0.71±0.04
3-OHMC *t*-1,2-diol (7)	0.59±0.07	0.83±0.04	0.88±0.12	0.32±0.05	0.44±0.01	0.48±0.03	1.15±0.08	2.45±0.03	0.70±0.02
% substrate metabolized	28.71	23.50	33.49	14.60	17.84	16.92	47.74	33.12	31.60

a. 3MC *trans*-1,2-diol (40 nmol per ml of incubation mixture) was incubated with liver microsomes of rats untreated and treated with PB and 3MC (0.25 mg of protein per ml of incubation mixture) at 37°C for 30 min. The metabolite formed under chromatographic peak in Fig. 79 was numbered in parethesis

b. Relative amount was determined by the ratio under chromatographic area of each metabolite formed to internal standard (1-OH-3MC). HPLC separation of metabolites formed in metabolism of 3MC *trans*-1,2-diol was analyzed by using the column (Nova Pak C18, 4μ, 8mm id x 10 cm) eluted with a gradient from 40% methanol in water to methanol in 50 min at flow rate of 2 ml/min.

They both had M^+ at *m/z* 316 with a fragment ion at *m/z* 298 (loss of H_2O) by mass spectral analysis. The two phenols were probably derived by non-enzymatic rearrangement of 3MC *trans*-1,2-diol:7,8-epoxide precursor. However, since none of the two possible 3MC *trans*-1,2-diol:7,8-dihydrodiol diastereomers were detected as metabolites, it likely indicates that the 7,8-epoxides may be unstable and, if formed metabolically, it may be readily isomerized to form 7-OH-3MC *trans*-1,2-diol as well as the 8-OH-3MC *trans*-1,2-diol.

The metabolites contained in both peaks 5 and 6 had molecular ion (M^+) at *m/z* 316 with a fragment ion at *m/z* 298 (loss of H_2O) by mass spectral analysis. Their uv-vis absorption spectra (Figs. 84 and 85) were similar to those of 9-OH-2-OH-3MC (Fig. 32A) and 10-OH-2-OH-3MC (Fig. 32B), respectively. 7-OH-3MC *trans*-1,2-diol and 10-OH-3MC *trans*-1,2-diol had similar uv-vis absorption spectral properties. The location of phenolic group of metabolite peak 6 was confirmed by converting 3MC *trans*-1,2-diol:9,10-dihydrodiol (peak 2 in Fig. 79) to 9-OH-3MC *trans*-1,2-diol and 10-OH-3MC *trans*-1,2-diol derived by acid-catalyzed dehydration. The 10-OH-3MC *trans*-1,2-diol had an identical retention time on reversed-phase HPLC (Fig. 79) to that of peak 6.

The metabolite contained in peak 7 was identified as 3-OHMC *trans*-1,2-diol on the basis of its uv-vis absorption spectrum (Fig. 81) and mass spectral data [M^+ at *m/z* 316 and a fragment ion at *m/z* 298 (loss of H_2O)].

A minor metabolite contained in peak 1 was found to have a uv-vis absorption spectrum similar to that of 8-OH-2-OH-3MC (Fig. 21A). This metabolite was tentatively identified as 8-OH-3-OHMC *trans*-1,2-diol.

9.2 *Absolute configuration and effects of inducers on enantiomeric composition*

CD spectrum of the metabolite contained in peak 2 (Fig. 80) indicated the metabolite contained in peak 2 was enriched in 9*R*,10*R* enantiomer. Liver microsomes from 3MC-treated rats formed a 3MC *trans*-1,2-diol:9,10-dihydrodiol with the highest value of the CD

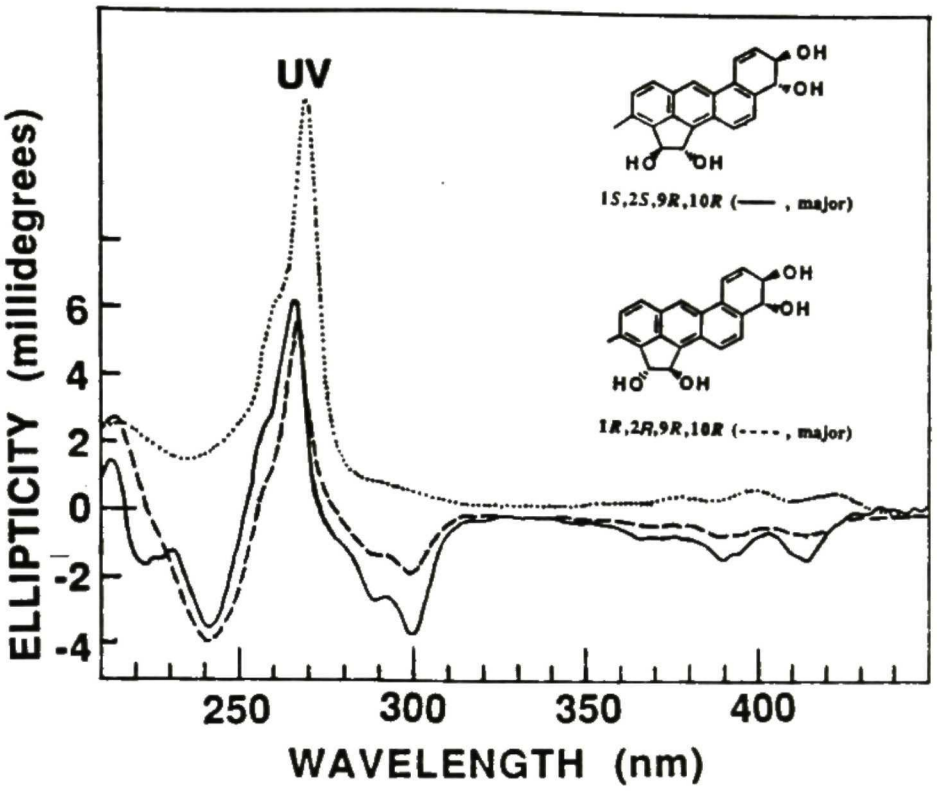

Figure 80. Uv-vis absorption (....., methanol) and CD spectra of 3MC *trans*-1*S*,2*S*-diol:9*R*,10*R*-dihydrodiol (major; ———, concn. 1.0 A_{268}/ml, methanol; Φ_{267}/A_{268} = 6.4 millidegrees) and 3MC *trans*-1*R*,2*R*-diol:9*R*,10*R*-dihydrodiol (major; ---------, concn. 1.0 A_{268}/ml, methanol; Φ_{267}/A_{268} = 5.7 millidegrees).

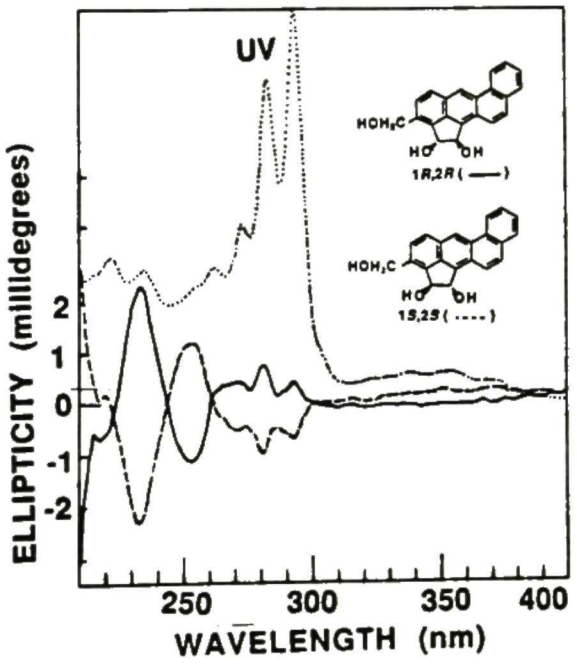

Figure 81. Uv-vis absorption (....., methanol) and CD spectra of the optically pure 3-OHMC *trans*-1*S*,2*S*-diol (-------, concn. 1.0 A_{302}/ml, methanol; Φ_{257}/A_{291} = 1.2 millidegrees) and 3-OHMC *trans*-1*R*,2*R*-diol (———, concn. 1.0 A_{291}/ml, methanol; Φ_{257}/A_{291} = - 1.2 millidegrees).

Cotton effect at 267 nm (Φ_{267}/A_{268} = 4.4 millidegrees by untreated rats, 3.2 by PB-treated rats, and 4.7 by 3MC-treated rats).

8-OH-3MC *trans*-1,2-diol (peak 3 of Fig. 79) had a CD Cotton band between 243 and 266 nm, indicating that the metabolite was mainly derived from 3MC *trans*-1*R*,2*R*-diol enantiomer (Fig. 83). The enantiomers of this metabolite, formed in the metabolism of (±)3MC *trans*-1,2-diol by three microsomal preparations, were resolved by *R*-DNBPG-C column (Fig. 86A) and were found to have (1*S*,2*S*:):(1*R*,2*R*) enantiomeric ratios of 22:78 (control), 25:75 (PB) and 28:71(3MC), respectively (Table 11). The results indicated all microsomal preparations preferentially catalyzed the formations of 3MC *trans*-1*R*,2*R*-diol:7,8-epoxides which were further isomerized to 8-OH-3MC *trans*-1*R*,2*R*-diol by non-enzymatic reaction.

The CD Cotton effects of the 7-OH-3MC *trans*-1,2-diol in peak 4, formed in the metabolism of racemic 3MC *trans*-1,2-diol by three microsomal preparations, also exhibited a negative CD Cotton band between 248 and 270 nm due to 1*R*,2*R* stereochemistry (Fig. 84). Metabolite peak 4 had enantiomeric compositions as shown in Table 11 and Fig. 86B.

An negative CD band of CD Cotton effects around 255 nm of both the 9-OH-3MC *trans*-1,2-diol (peak 5 in Fig. 84) and the 10-OH-3MC *trans*-1,2-diol (peak 6 in Fig. 85) indicated that both phenolic products were highly enriched in the 1*R*,2*R* enantiomers. The enantiomeric compositions were determined on *R*-DNBPG-C column (Figs. 86C and 86D) and had enantiomeric ratios [(1*S*,2*S*):(1*R*,2*R*)] of ~24:76 for 9-OH-3MC *trans*-1,2-diol by all three microsomal preparations and 11:89 (control), 13:87 (PB) and 42:57 (3MC) for 10-OH-3MC *trans*-1,2-diol, respectively. Enantiomeric compositions of 3-OHMC *trans*-1,2-diol (peak 7 in Fig. 79), formed in the metabolism of (±) 3MC *trans*-1,2-diol by all three microsomal preparations, were determined by CSP HPLC (Fig. 86E). The hydroxylation at C_3-methyl group of (±) 3MC *trans*-1,2-diol by liver microsomes from untreated and PB-treated rats was not enantioselective. However, the microsomes prepared from 3MC-

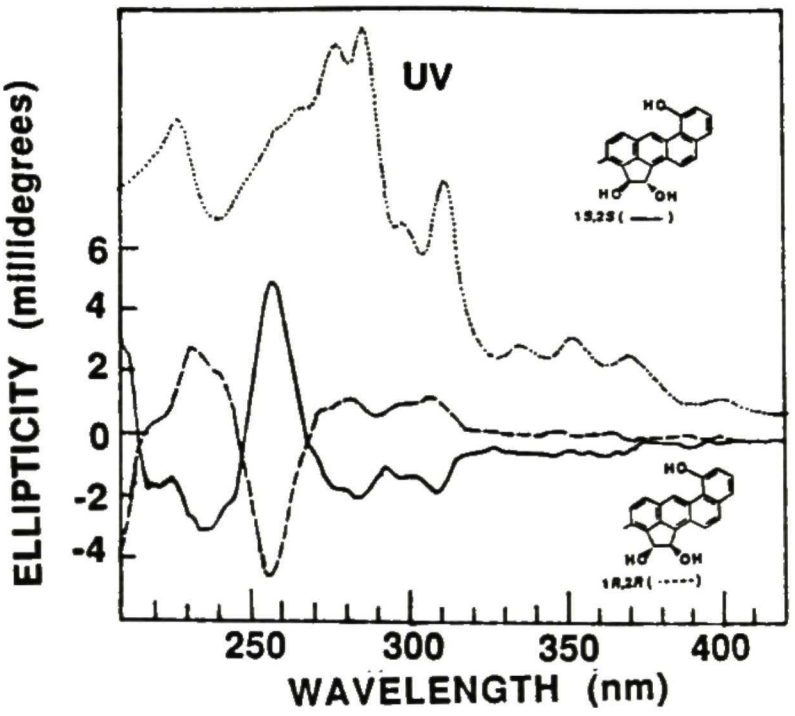

Figure 82. Uv-vis absorption (....., methanol) and CD spectra of the optically pure 7-OH-3MC *trans*-1*S*,2*S*-diol (—— , concn. 1.0 A_{287}/ml, methanol; Φ_{257}/A_{287} = 4.9 millidegrees) and 7-OH-3MC *trans*-1*R*,2*R*-diol (-------, concn. 1.0 A_{287}/ml, methanol; Φ_{257}/A_{287} = - 4.9 millidegrees).

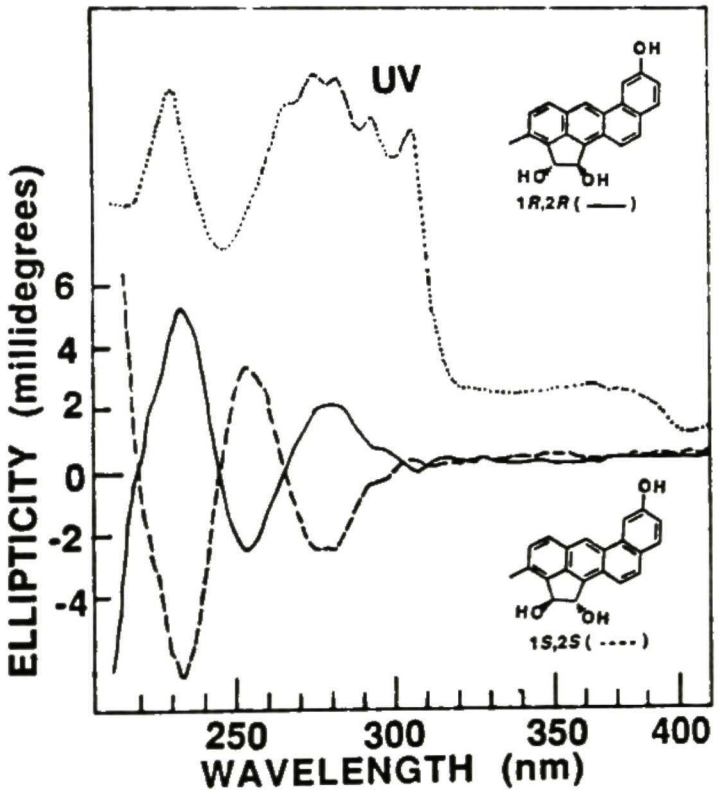

Figure 83. Uv-vis absorption (....., methanol) and CD spectra of the optically pure 8-OH-3MC *trans*-1*S*,2*S*-diol (--------, concn. 1.0 A_{287}/ml, methanol; Φ_{257}/A_{287} = 4.9 millidegrees) and 8-OH-3MC *trans*-1*R*,2*R*-diol (——, concn. 1.0 A_{287}/ml, methanol; Φ_{257}/A_{287} = - 4.9 millidegrees).

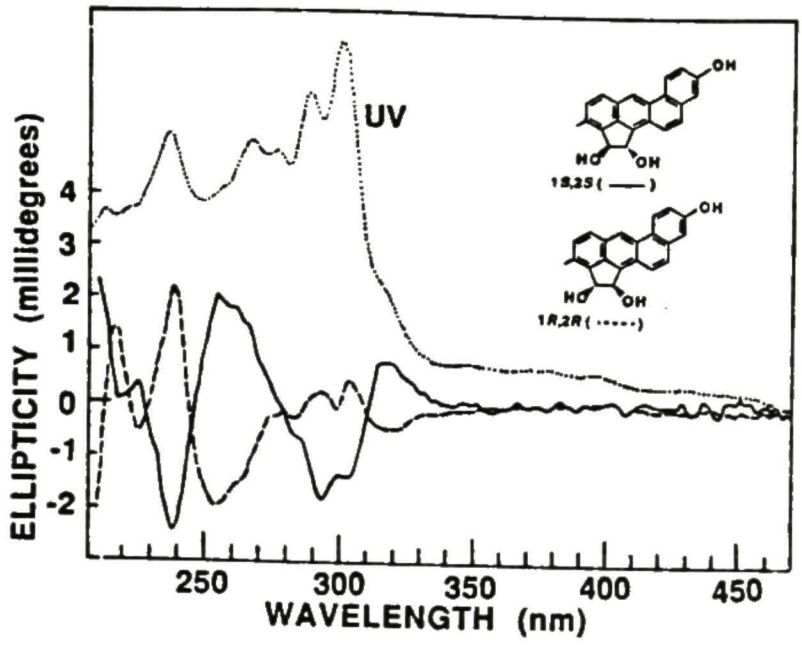

Figure 84. Uv-vis absorption (....., methanol) and CD spectra of the optically pure 9-OH-3MC *trans*-1*S*,2*S*-diol (———, concn. 1.0 A_{302}/ml, methanol; Φ_{255}/A_{302} = 2 millidegrees) and 9-OH-3MC *trans*-1*R*,2*R*-diol (---------, concn. 1.0 A_{302}/ml, methanol; Φ_{255}/A_{302} = - 2 millidegrees).

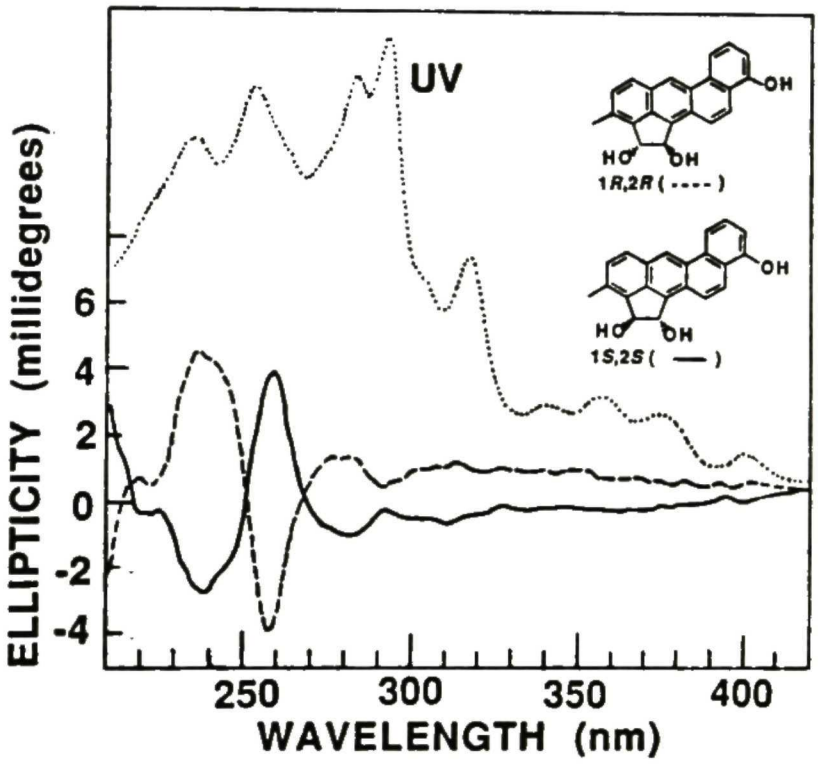

Figure 85. Uv-vis absorption (....., methanol) and CD spectra of the optically pure 10-OH-3MC *trans*-1*S*,2*S*-diol (——— , concn. 1.0 A_{291}/ml, methanol; Φ_{257}/A_{291} = 4.1 millidegrees) and 10-OH-3MC *trans*-1*R*,2*R*-diol (-------, concn. 1.0 A_{287}/ml, methanol; Φ_{257}/A_{291} = - 4.1 millidegrees).

treated rats catalyzed preferentially the formation of 3-OHMC *trans*-1*S*,2*S*-diol (56% enantiomeric excess). Since most phenolic metabolites were mainly derived from 3MC *trans*-1*R*,2*R*-diol, metabolism of (±)3MC *trans*-1,2-diol was enantioselective toward the 1*R*,2*R* enantiomer. Enantiomeric ratios [(1*S*,2*S*):(1*R*,2*R*)] of unreacted substrate (peak 8 in Fig. 79) were 59:41 (control), 75:25 (PB) and 66:34 (3MC).

9.3 Effects of enzyme inducers on the formations of metabolites

The products formed in the metabolism of (±) 3MC *trans*-1,2-diol, 3MC *trans*-1*S*,2*S*-diol and 3MC *trans*-1*R*,2*R*-diol were determined (Table 10). The relative amount of each metabolite formed from both the racemic and enantiomeric forms of 3MC *trans*-1,2-diol, by liver microsomes prepared from rats treated with different enzyme inducers were normalized against the internal standard. Effects of inducers on the relative amounts of 3MC *trans*-1,2-diol:9,10-dihydrodiol formed in the metabolism of (±) 3MC *trans*-1,2-diol were PB (2.7) > control (~0.7) > 3MC (~0.3); in the metabolism of 3MC *trans*-1*S*,2*S*-diol, PB (1.4) > 3MC (0.5) > control (~0.4); in the metabolism of 3MC *trans*-1*R*,2*R*-diol, PB (2.6) > control (~0.5) > 3MC (0.2). Thus liver microsomes from PB-treated rats had the highest activity in catalyzing the formation of 3MC *trans*-1,2-diol:9,10-dihydrodiol. The relative amount of 3MC *trans*-1,2-diol:9,10-dihydrodiol formed in rat liver microsomal metabolism also depended on the racemic and enantiomeric substrates used. 3MC *trans*-1*R*,2*R*-diol and (±)3MC *trans*-1,2-diol seem to be better substrates than 3MC *trans*-1*S*,2*S*-diol in the formation of 3MC *trans*-1,2-diol:9,10-dihydrodiol.

Various enzyme inducers altered relative amounts of metabolically formed phenolic products. Effects of inducers on the relative amounts of phenolic metabolites at C_7 and C_8 formed in the metabolism of both the racemic and the enantiomeric 3MC *trans*-1,2-diol were 3MC > control > PB. The relative amount of 8-OH-3MC *trans*-1,2-diol formed was greater than that of 7-OH-3MC *trans*-1,2-diol.

The formations of these phenols were found to be dependent on the racemic and enantiomeric substrates, as well as the enzyme inducers utilized. In the metabolism of

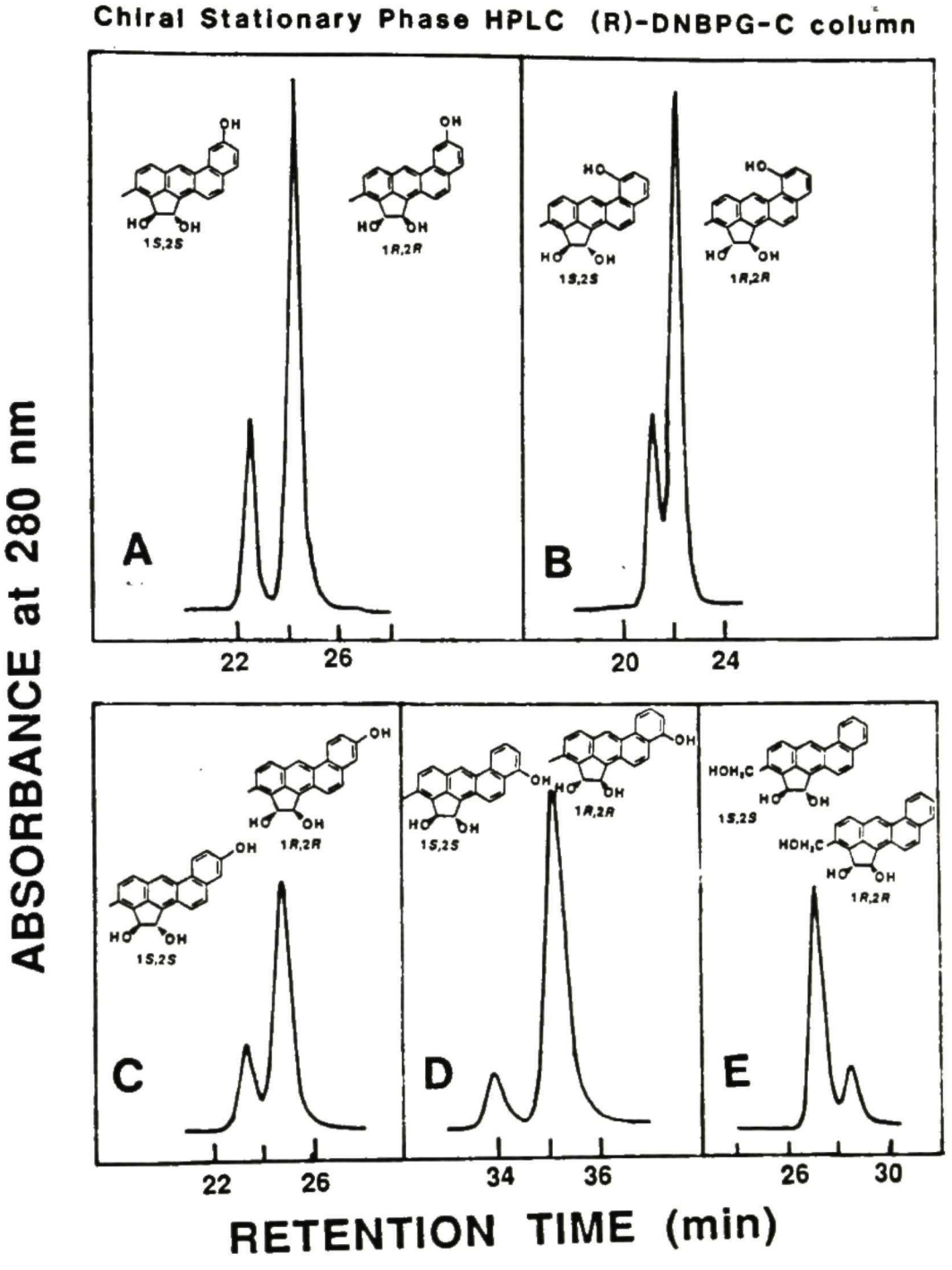

Figure 86. Chiral stationary phase HPLC separation and absolute configurations of metabolites 8-OH-3MC *trans*-1,2-diol (A), 7-OH-3MC *trans*-1,2-diol (B), 9-OH-3MC *trans*-1,2-diol (C), 10-OH-3MC *trans*-1,2-diol (D) and 3-OHMC *trans*-1,2-diol (E) enantiomers are indicated in this figure.

Table 11. Enantiomeric composition of metabolites formed in the metabolism of racemic 3MC *trans*-1,2-diol by rat liver microsomes.

Metabolites[a]	Enantiomeric Composition (%)[b] (1*S*,2*S* : 1*R*,2*R*)		
	Control (0.25 mg)	PB (0.25 mg)	3-MC (0.25 mg)
8-OH-3MC *trans*-1,2-diol	22.4:77.6	24.9:75.1	28.4:71.6
7-OH-3MC *trans*-1,2-diol	24.9:75.1	30.0:70.0	43.4:56.6
9-OH-3MC *trans*-1,2-diol	23.8:76.2	24.0:76.0	24.1:75.9
10-OH-3MC *trans*-1,2-diol	11.0:89.0	12.7:87.3	42.8:57.2
3-OHMC *trans*-1,2-diol	45.6:54.4	49.1:50.9	78.3:21.7
3-MC *trans*-1,2-diol (remaining substrate)	59.1:40.9	75.0:25.0	66.2:33.8

a. Racemic 3-MC *trans*-1,2-diol was incubated with liver microsomes (0.25 or 1.0 mg protein/ml of incubation mixture from untreated(control), PB-treated and 3MC treated rats. Each milliliter of reaction mixture contains 40 nmol of 3MC *trans*-1,2-diol and was incubated at 37°C for 30 min.

b. Enantiomeric ratio of metabolites was determined by CSP HPLC on a covalently bonded *R*-DNBPG column.

either racemic or an enantiomeric 3MC *trans*-1,2-diol, effects of inducers on the relative amount of phenolic metabolites at C_9 and C_{10} were PB > control > 3MC. Based on AUC's at 254 nm, ratio of 9-OH-3MC *trans*-1,2-diol to 10-OH-3MC *trans*-1,2-diol (Table 10) formed in the metabolism of 3MC *trans*-1*R*,2*R*-diol were 0.6:3.9 (PB), 0.4:2.7 (control) and 2.1:0.7 (3MC); in the metabolism of (±) 3MC *trans*-1,2-diol, 0.3:1.9 (PB), 0.2:1.3 (control) and 0.5:0.5 (3MC), respectively. Metabolism by liver microsomes from untreated and PB-treated rats on the relative ratios of 9-phenol to 10-phenol differed from that of 3MC-treated rats.

Effects of different inducers on the hydroxylation at C_3-methyl group in the metabolisms of the racemic and enantiomeric 3MC *trans*-1,2-diol were found to be 3MC > PB > control (Table 10). The relative amount of 3-OHMC *trans*-1,2-diol formed in the metabolisms of (±) 3MC *trans*-1,2-diol and 3MC *trans*-1*S*,2*S*-diol by liver microsomes from 3MC-treated rats were 3.0 and 5.6 fold greater than those by PB or control. This indicates that 3MC induced microsomal enzymes were more capable of driving hydroxylation reactions at the C_3-methyl group of (±) 3MC *trans*-1,2-diol or 3MC *trans*-1*S*,2*S*-diol than microsome enzymes from control or PB-induced.

10. *Metabolism of Racemic and Enantiomeric 3MC cis-1,2-diol*

10.1 *HPLC separation and identification of metabolites*

Four major and some other minor metabolites were formed in the metabolism of (±)3MC *cis*-1,2-diol by liver microsomes from PB-treated rats. The sample was obtained by using 0.25 mg protein of liver microsomes/ml of incubation mixture and an incubation time of 30 min. Metabolites were separated by reversed-phase HPLC. Chromatographic peaks are numbered as indicated in Fig. 87. The identities, spectral properties and relative amount of the formations of these metabolites from each chromatographic peak are indicated in Table 12 using 1-OH-3MC as an internal standard. The percentage of substrate metabolized in the metabolism of (±)3MC *cis*-1,2-diol by liver microsomes prepared from untreated (control), 3MC- and PB-treated rats was ~30%, ~41% and ~45%, respectively (Table 12).

The two major metabolites contained in peaks 2 and 4 of Fig. 87 were identified as diastereomeric 3MC *cis*-1,2-diol:9,10-dihydrodiols. These two metabolites had uv-vis absorption spectra (Figs. 88 and 89) similar to that of 2-OH-3MC 9,10-dihydrodiol (see Fig. 29). The mass spectra of peaks 2 and 4 of Fig. 87 were identical, M^+ at *m/z* 334 with two characteristic fragment ions at *m/z* 316 (loss of H_2O) and 298 (loss of two H_2O). CD spectra of the two products indicated Cotton effects (Figs. 88 and 89) similar to those of 2-OH-3MC 9*R*,10*R*-dihydrodiol (Fig. 29). The relative amounts of the diastereomeric 3MC 9,10-dihydrodiols under chromatographic peaks 2 and 4 was 59:41.

Peaks 7 and 9 were established to be 9-OH-3MC *cis*-1,2-diol and 10-OH-3MC *cis*-1,2-diol, respectively, by uv-vis absorption spectra (Figs. 90 and 91), which were similar to those of 9-OH-2-OH-3MC and 10-OH-2-OH-3MC, respectively (Fig. 32). Mass spectral analysis indicated that they both had M^+ at *m/z* 316 with a fragment ion at *m/z* 298 (loss of H_2O). 9-OH-3MC *cis*-1,2-diol and 10-OH-3MC *cis*-1,2-diol were formed with an AUC ratio of ~18:82 at 254 nm.

A minor metabolite contained in peak 3 had a uv-vis absorption spectrum (Fig. 92)

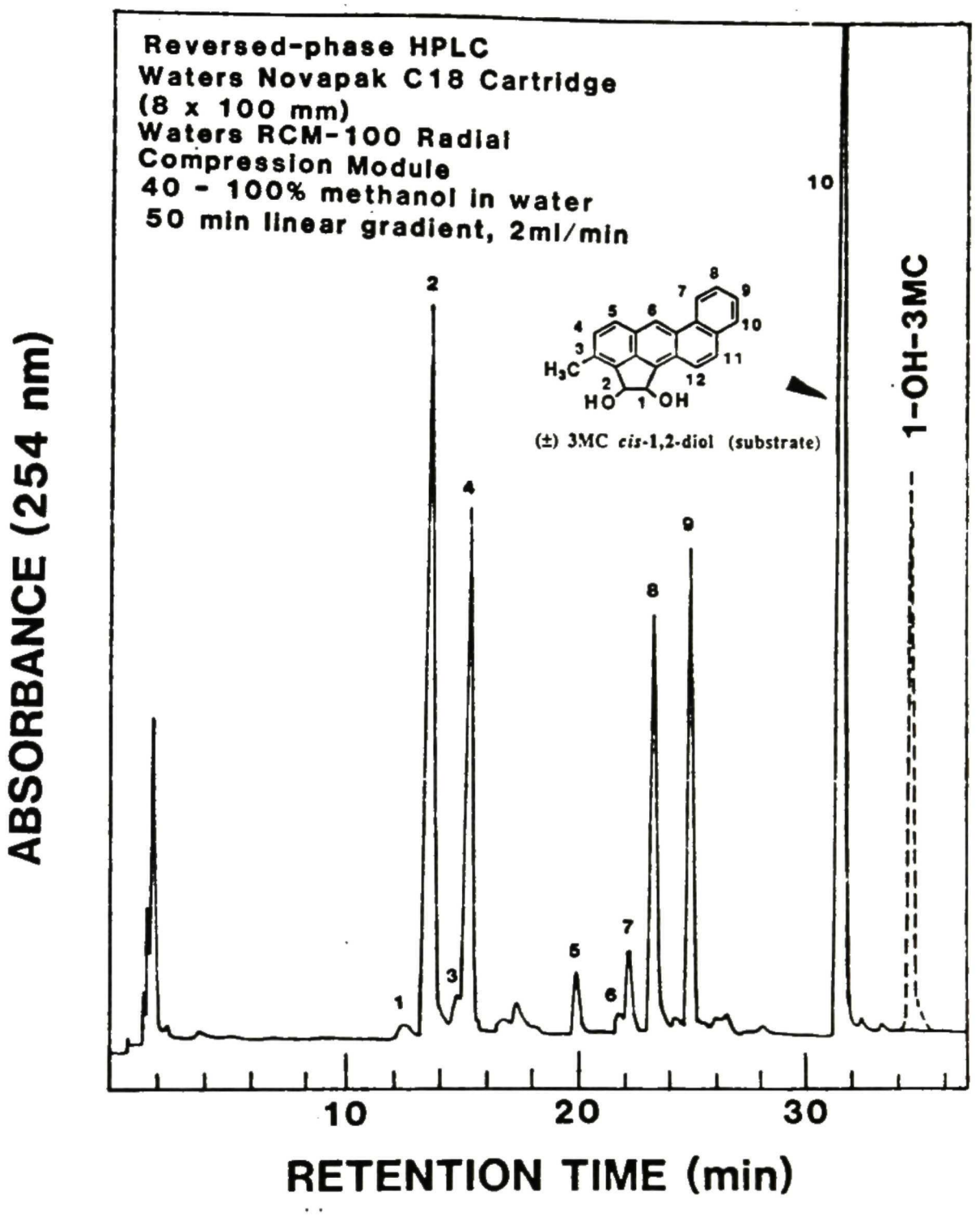

Figure 87. Reversed-phase HPLC separation of (±) 3MC *cis*-1,2-diol and its metabolites. This sample was prepared by incubation of (±) 3MC *cis*-1,2-diol for 30 min with liver microsomes (0.25 mg protein/ml incubation mixture) from PB treated rats. Identities of metabolites contained in various chromatographic peaks are described in the text and summarized in Table 12. 1-OH-3MC was used as a internal standard for quantitative study. peak 1, 8-OH-3-OHMC *cis*-1.2-diol; peak 2, 3MC *cis*-1.2-diol:9,10-dihydrodiol-a; peak 3, 10-OH-3-OHMC *cis*-1.2-diol; peak 4,3MC *cis*-1.2-diol:9,10-dihydrodiol-b; peak 5, 8-OH-3MC *cis*-1.2-diol; peak 6, 7-OH-3MC *cis*-1.2-diol; peak 7, 9-OH-3MC *cis*-1.2-diol; peak 8, 3-OHMC *cis*-1.2-diol; peak 9, 10-OH-3MC *cis*-1.2-diol; peak 10, remaining substrate 3MC *cis*-1.2-diol. 1-OH-3MC was added as internal standard.

Table 12. Relative amount of metabolites formed in the metabolism of (±) 3MC *cis*-1,2-diol, 3MC *cis*-1*S*,2*R*-diol and 3MC *cis*-1*R*,2*S*-diol by rat Liver microsomes

Identity[a]	(±) 3MC *cis*-1,2-diol			3MC *cis*-1S,2R-diol			3MC *cis*-1R,2S-diol		
	PB	3MC	Control	PB	3MC	Control	PB	3MC	Control
8-OH-3-OHMC *cis*-1,2-diol	0.08±0.01	0.14±0.01	0.02±0.01	0.01±0.00	0.19±0.00	ND[b]	0.04±0.00	0.09±0.01	0.01±0.00
3MC *cis*-1,2-diol:9,10-diol-a	1.72±0.12	0.36±0.01	0.54±0.00	0.27±0.02	0.07±0.0	0.07±0.00	0.92±0.05	0.47±0.01	0.30±0.00
10-OH-3-OHMC *cis*-1,2-diol	0.09±0.01	0.17±0.01	0.03±0.00	0.01±0.00	0.04±0.00	0.01±0.00	0.04±0.01	0.18±0.01	0.01±0.00
3MC *cis*-1,2-diol:9,10-diol-b	1.19±0.04	0.13±0.00	0.30±0.02	0.75±0.03	0.11±0.00	0.19±0.00	0.02±0.00	ND	0.01±0.00
8-OH-3MC *cis*-1,2-diol	0.15±0.01	0.39±0.01	0.15±0.00	0.09±0.01	0.06±0.00	0.06±0.00	0.29±0.01	0.85±0.01	0.25±0.00
7-OH-3MC *cis*-1,2-diol	0.05±0.00	0.57±0.03	0.09±0.00	0.07±0.01	0.15±0.01	0.06±0.00	0.05±0.00	0.72±0.01	0.05±0.00
9-OH-3MC *cis*-1,2-diol	0.19±0.00	0.66±0.00	0.17±0.00	0.13±0.01	0.96±0.06	0.06±0.00	0.06±0.01	0.16±0.01	0.05±0.00
3-OHMC *cis*-1,2-diol	0.89±0.01	0.68±0.02	0.40±0.00	0.43±0.03	0.31±0.02	0.15±0.01	0.98±0.04	0.79±0.02	0.29±0.01
10-OH-3MC *cis*-1,2-diol	0.87±0.01	0.59±0.01	0.73±0.00	0.47±0.02	0.15±0.01	0.21±0.01	0.20±0.01	0.79±0.01	0.14±0.01
% substrate metabolized	41.00	45.30	29.99	29.07	33.38	10.67	30.65	53.50	16.40

a. 3MC *cis*-1,2-diol (40 nmol per ml of incubation mixture) was incubated with liver microsomes of rats untreated and treated with PB and 3MC (0.25 mg of protein per ml of incubation mixture) at 37°C for 30 min. Relative amount was determined by the ratio under chromatographic area of each metabolite formed to internal standard (1-OH-3MC). HPLC separation of metabolites formed in metabolism of 3MC *cis*-1,2-diol was analyzed by using the column (Nova Pak C18, 4μ, 8mm id x 10 cm) eluted with a gradient from 40% methanol in water to methanol in 50 min at flow rate of 2 ml/min.

b. ND means metabolite shown was not detectable.

similar to that of 10-OH-2-OH-3MC (Fig. 32B) and a M^+ at *m/z* 332 with a fragment at *m/z* 318 (loss of H_2O). This metabolite was identified to be 10-OH-3-OHMC *cis*-1,2-diol.

The major metabolite contained in peak 8 had a uv-vis absorption spectrum (Fig. 93) identical to that of the 3MC *cis*-1,2-diol and a M^+ at *m/z* 316 with a fragment ion at *m/z* 298 (loss of H_2O) by mass spectral analysis. These results indicated that the metabolite had an additional hydroxyl group and was not phenolic in nature. Hence the metabolite contained in peak 8 was deduced to be 3-OHMC *cis*-1,2-diol.

The minor metabolites contained in peaks 6 and 5 in Fig. 87 had uv-vis absorption spectra (Figs. 94 and 95) similar to those of 1-OH-BA and 8-OH-2-OH-3MC (Fig. 21A), respectively. Mass spectra analysis indicated that they both had M^+ at *m/z* 316 and a fragment ion at *m/z* 298 (loss of H_2O). These two metabolites were identified as 7-OH-3MC *cis*-1,2-diol (peak 6) and 8-OH-3MC *cis*-1,2-diol (peak 5), respectively.

The minor and more polar metabolite contained in peak 1 had a uv-vis absorption spectrum (not shown) similar to that of 8-OH-3MC *cis*-1,2-diol (Fig. 95). Mass spectral analysis (M^+ at *m/z* 332) indicated that it contained an additional oxygen than 8-OH-3MC *cis*-1,2-diol. These data indicated that the metabolite contained in peak 1 was 8-OH-3-OHMC *cis*-1,2-diol.

10.2 *Absolute configuration and enantiomeric composition*

Optically pure 3MC *cis*-1*S*,2*R*-diol:9*S*,10*S*-dihydrodiol (peak 2 in Fig. 87) and 3MC *cis*-1*S*,2*R*-diol:9*R*,10*R*-dihydrodiol (peak 4 in Fig. 87) were prepared by incubation of an optically pure 3MC *cis*-1*S*,2*R*-diol by rat liver microsomes and subsequent purification by reversed-phase HPLC. Their CD spectral data (Φ_{266}/A_{267}) were shown to be 4.5 and -7.6 millidegrees (Figs. 88 and 89), respectively. The optically pure 3MC *cis*-1*R*,2*S*-diol:9*R*,10*R*-dihydrodiol (isolated as peak 2 in Fig. 87) and 3MC *cis*-1*R*,2*S*-diol:9*S*,10*S*-dihydrodiol (isolated as peak 4 in Fig. 87) were similarly prepared by incubation of 3MC *cis*-1*R*,2*S*-diol. 3MC *cis*-1*R*,2*S*-diol:9*R*,10*R*-dihydrodiol had a

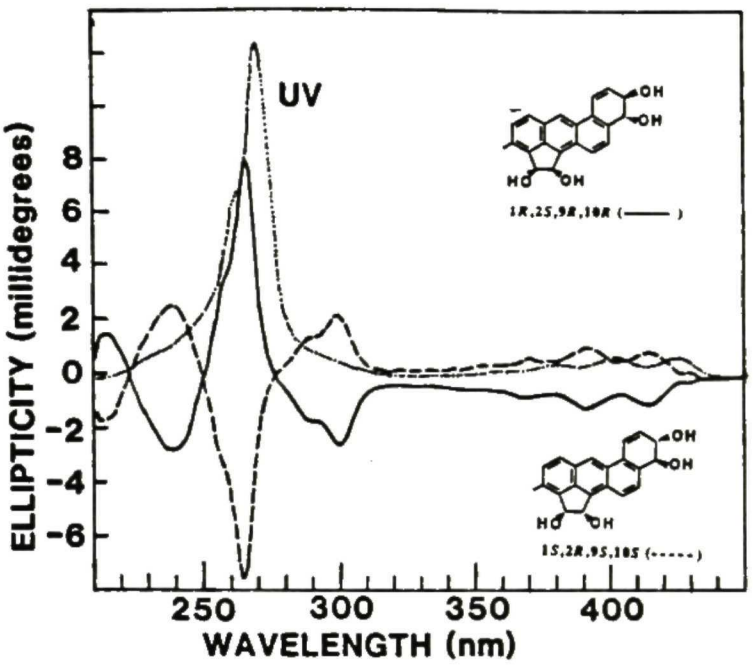

Figure 88. Uv-vis absorption (....., methanol) and CD spectra of 3MC *cis*-1*R*,2*S*-diol:9*R*,10*R*-dihydrodiol (———— , concn. 1.0 A_{267}/ml, methanol; Φ_{266}/A_{267} = 8.2 millidegrees) and 3MC *cis*-1*S*,2*R*-diol:9*S*,10*S*-dihydrodiol (-------- , concn. 1.0 A_{267}/ml, methanol; Φ_{266}/A_{267} = -7.6 millidegrees).

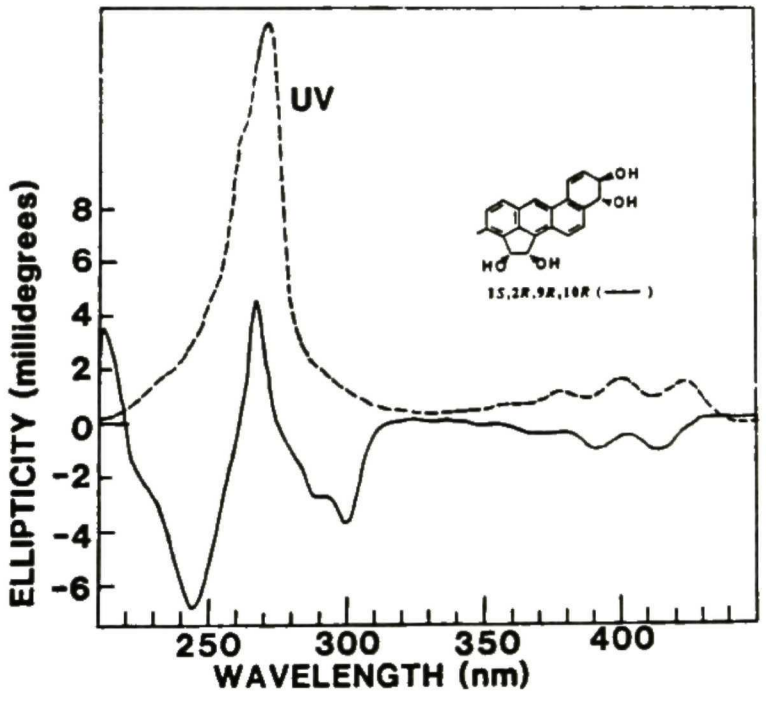

Figure 89. Uv-vis absorption (......, methanol) and CD spectra of 3MC *cis*-1*S*,2*R*-diol:9*R*,10*R*-dihydrodiol (———, concn. 1.0 A_{267}/ml, methanol; Φ_{266}/A_{267} = 4.5 millidegrees).

Φ_{266}/A_{267} value of 8.2 millidegrees (Fig. 88). Based on the CD data of optically pure enantiomers, the 3MC *cis*-1,2-diol:9,10-dihydrodiol contained in peak 2 of Fig. 87 was calculated to have a (1*R*,2*S*,9*R*,10*R*):32(1*S*,2*R*,9*S*,10*S*) enantiomer ratio of 64:32. Similarly, the diastereomeric 3MC *cis*-1,2-diol:9,10-dihydrodiol contained in peak 4 was found to have a (1*S*,2*R*,9*R*,10*R*):(1*R*,2*S*,9*S*,10*S*) enantiomer ratio of 91:9. Since the AUC ratio of peak 2 and peak 4 was 59:41, the relative amount of enantiomers contained in peaks 2 and 4 was 38 (1*R*,2*S*,9*R*,10*R*) ≈ 37 (1*S*,2*R*,9*R*,10*R*) > 21(1*S*,2*R*,9*S*,10*S*) > 4 (1*R*,2*S*,9*S*,10*S*). The liver microsomal enzymes of PB-treated rats were highly stereoselective in the formation of 9*R*,10*R*-enantiomer over that of 9*S*,10*S*-enantiomer. The results also indicated that the 1*S*,2*R*-enantiomer of 3MC *cis*-1,2-diol was enantioselectively metabolized in the formation of 9,10-dihydrodiol.

The enantiomeric ratios of phenolic products formed in metabolism of (±)3MC *cis*-1,2-diol from untreated, 3MC- and PB-treated rats are listed in Table 13. The positive CD Cotton effects between 220 and 300 nm of the 8-OH-3MC *cis*-1,2-diol (Fig. 95), 7-OH-3MC *cis*-1,2-diol (Fig. 94), 9-OH-3MC *cis*-1,2-diol (Fig. 90), 3-OH-3MC *cis*-1,2-diol (Fig. 93) and 10-OH-3MC *cis*-1,2-diol (Fig. 91) formed in the metabolism of 3MC *cis*-1*R*,2*S*-diol were found to be similar to that of 3MC *cis*-1*R*,2*S*-diol (Fig. 13) except for the magnitudes of $\Phi_{\sim 256}/A_{\lambda max}$ values in millidegrees due to additional substituent. The CD Cotton effects of the corresponding phenolic and C_3-hydroxylation products (Figs. 90-95) derived from the metabolism of 3MC *cis*-1*S*,2*R*-diol, were opposite forming mirror image to those spectra derived from the metabolism of 3MC *cis*-1*R*,2*S*-diol.

10.3 *Effects of enzyme inducers on the enantioselective metabolism of (±)3MC cis-1,2-diol*

The enantiomeric compositions of 3MC *cis*-1,2-diol:9,10-dihydrodiol formed in the metabolism of 3MC *trans*-1,2-diol could not be directly determined by CSP HPLC. Enantiomeric compositions of 3MC *cis*-1,2-diol:9,10-dihydrodiols contained in peaks 2 and 4 of Fig. 87 were determined respectively based on the CD spectral data of optically

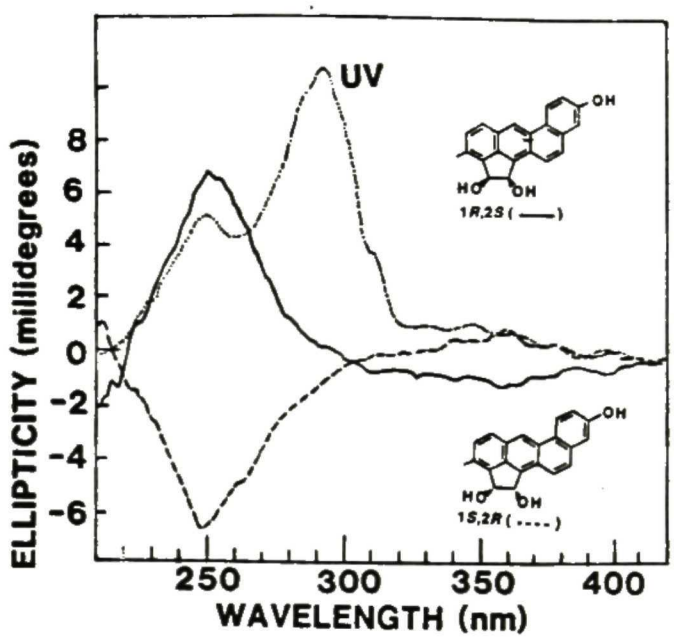

Figure 90. Uv-vis absorption (....., methanol) and CD spectra of 9-OH-3MC *cis*-1*R*,2*S*-diol (———, concn. 1.0 A_{292}/ml, methanol; Φ_{250}/A_{292} = 6.5 millidegrees) and 9-OH-3MC *cis*-1*S*,2*R*-diol (--------, concn. 1.0 A_{292}/ml, methanol; Φ_{250}/A_{292} = - 6.7 millidegrees).

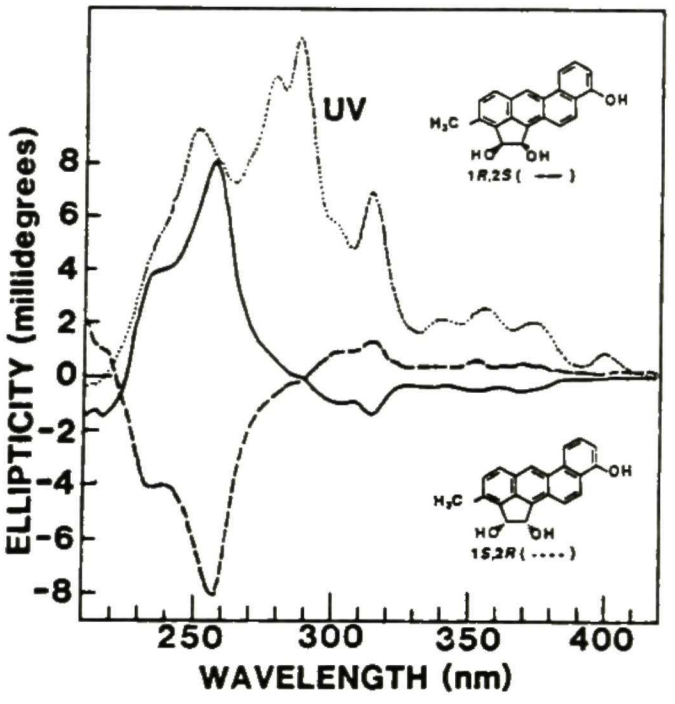

Figure 91. Uv-vis absorption (....., methanol) and CD spectra of 10-OH-3MC *cis*-1*R*,2*S*-diol (———, concn. 1.0 A_{292}/ml, methanol; Φ_{256}/A_{292} = 8.1 millidegrees) and 10-OH-3MC *cis*-1*S*,2*R*-diol (--------, concn. 1.0 A_{292}/ml, methanol; Φ_{256}/A_{292} = - 8.1 millidegrees).

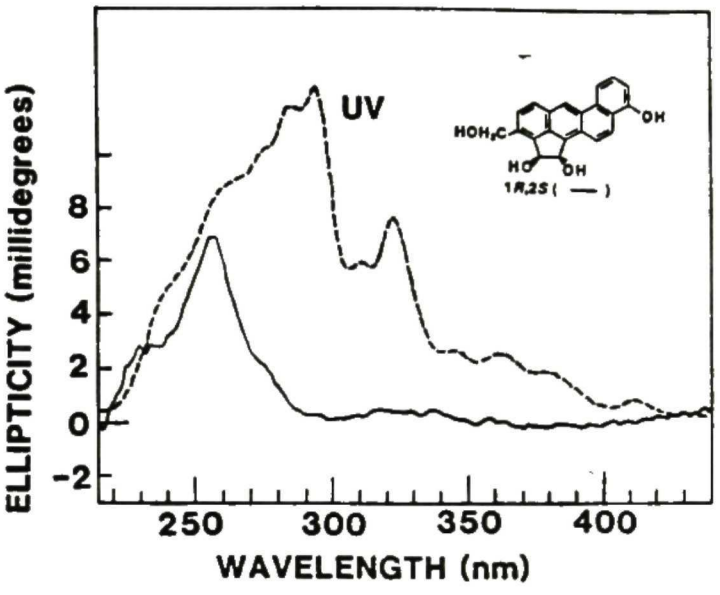

Figure 92. Uv-vis absorption (......, methanol) and CD spectra of 10-OH-3-OHMC *cis*-1*R*,2*S*-diol (———, concn. 1.0 A_{286}/ml, methanol; Φ_{256}/A_{286} = 6.9 millidegrees).

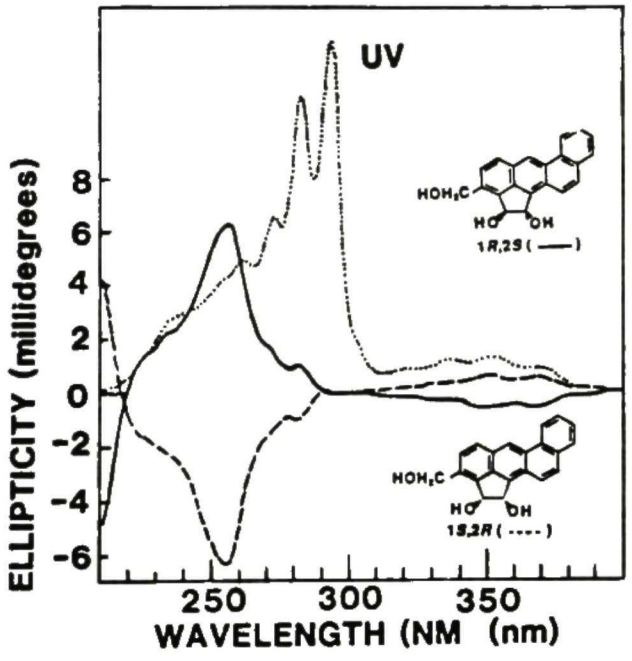

Figure 93. Uv-vis absorption (....., methanol) and CD spectra of 3-OHMC *cis*-1*R*,2*S*-diol (———, concn. 1.0 A_{294}/ml, methanol; Φ_{256}/A_{294} = 6.2 millidegrees) and 3-OHMC *cis*-1*S*,2*R*-diol (--------, concn. 1.0 A_{294}/ml, methanol; Φ_{256}/A_{294} = - 6.3 millidegrees).

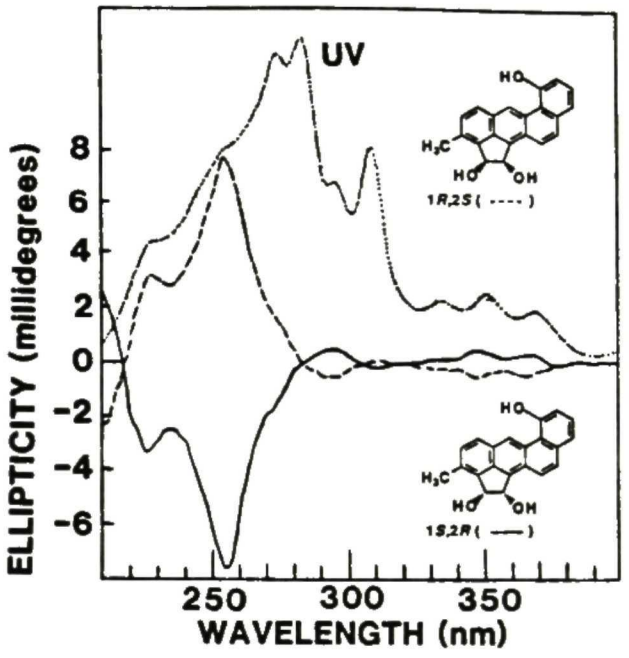

Figure 94. Uv-vis absorption (....., methanol) and CD spectra of 7-OH-3MC *cis*-1*R*,2*S*-diol (-------, concn. 1.0 A_{287}/ml, methanol; Φ_{255}/A_{287} = 7.7 millidegrees) and 7-OH-3MC *cis*-1*S*,2*R*-diol (———, concn. 1.0 A_{287}/ml, methanol; Φ_{255}/A_{287} = - 7.8 millidegrees).

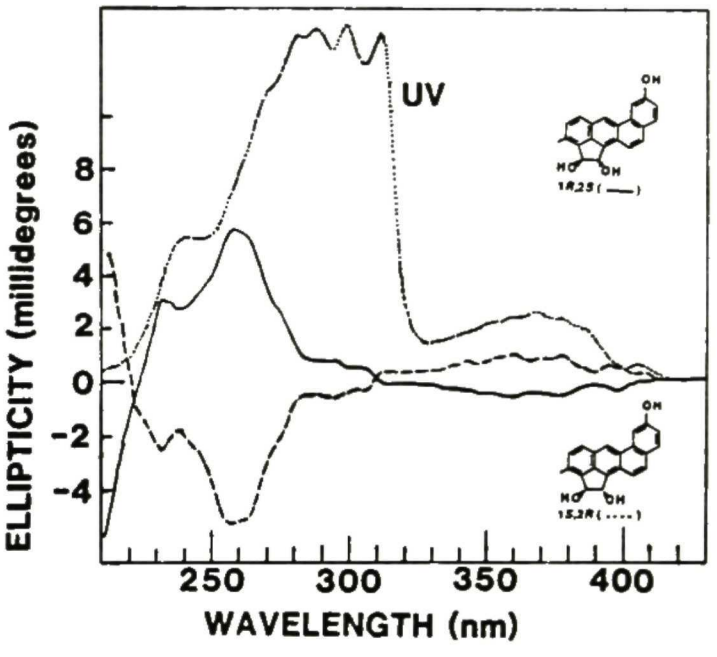

Figure 95. Uv-vis absorption (....., methanol) and CD spectra of 8-OH-3MC *cis*-1*R*,2*S*-diol (———, concn. 1.0 A_{293}/ml, methanol; Φ_{255}/A_{293} = 5.5 millidegrees) and 8-OH-3MC *cis*-1*S*,2*R*-diol (--------, concn. 1.0 A_{294}/ml, methanol; Φ_{255}/A_{293} = - 5.5 millidegrees).

pure 3MC *cis*-1,2-diol:9,10-dihydrodiol enantiomers. In the metabolism of (±) 3MC *cis*-1,2-diol, liver microsomes prepared from untreated and PB-treated rats produced 9,10-dihydrodiols enriched in the 9*R*,10*R*-enantiomer (64-91%). Since area ratios of the sum of chromatographic peak 2 and peak 4 of Fig. 87 was 1.81 in PB induction and 0.84 in control; relative amounts of 3MC *cis*-1,2-diol:9,10-dihydrodiol enantiomers formed in the metabolism of (±) 3MC *cis*-1,2-diol were 66 (1*R*,2*S*,9*R*,10*R*) > 21 (1*S*,2*R*,9*R*,10*R*) > 7 (1*S*,2*R*,9*S*,10*S*) ≈ 6 (1*R*,2*S*,9*S*,10*S*) in control and 38 (1*R*,2*S*,9*R*,10*R*) ≈ 37 (1*S*,2*R*,9*R*,10*R*) > 21(1*S*,2*R*,9*S*,10*S*) > 4 (1*R*,2*S*,9*S*,10*S*) in PB induction, respectively.

The enantiomeric compositions of phenolic and C_3-hydroxylation products formed in the metabolism of (±) 3MC *cis*-1,2-diol were directly resolved by CSP HPLC (Fig. 96). Effects of enzyme inductions on the stereoselective formations of phenolic and C_3-hydroxylation products formed lead to great differences as shown in Table 13. Enzyme induction with 3MC produced phenolic and C_3-hydroxylation enantiomers highly enriched in 1*R*,2*S* stereochemistry, indicating that 3MC-treated rat liver microsomal catalysis was highly enantioselective toward 3MC *cis*-1*R*,2*S*-diol substrate over liver microsomes from control and PB-treated rats. Enantiomeric compositions of the phenolic and C_3-hydroxylation products formed in the metabolism of (±)3MC *cis*-1,2-diol from 3MC induced microsomes were 7 phenol (~ 100% enriched in 1*R*,2*S*) > 8 phenol (95%) > 10 phenol (86%) > 3-OHMC *cis*-1*R*,2*S*-diol (68%) (Table 13). Untreated control and PB induced microsomes had different stereochemical effects than 3MC on the enantiomeric compositions of 7-OH-3MC *cis*-1,2-diol and 10-OH-3MC *cis*-1,2-diol (Table 13). Major phenolic enantiomers were enriched in the 1*S*,2*R* stereochemistry from both control and PB induced microsomal metabolism of (±) 3MC *cis*-1,2-diol as compared to the 1*R*,2*S* enriched from 3MC induced microsomes.

Enantiomeric disposition of substrate (±) 3MC *cis*-1,2-diol resulting from untreated control, 3MC- and PB-induced microsomal metabolism was also elicited as shown in Table

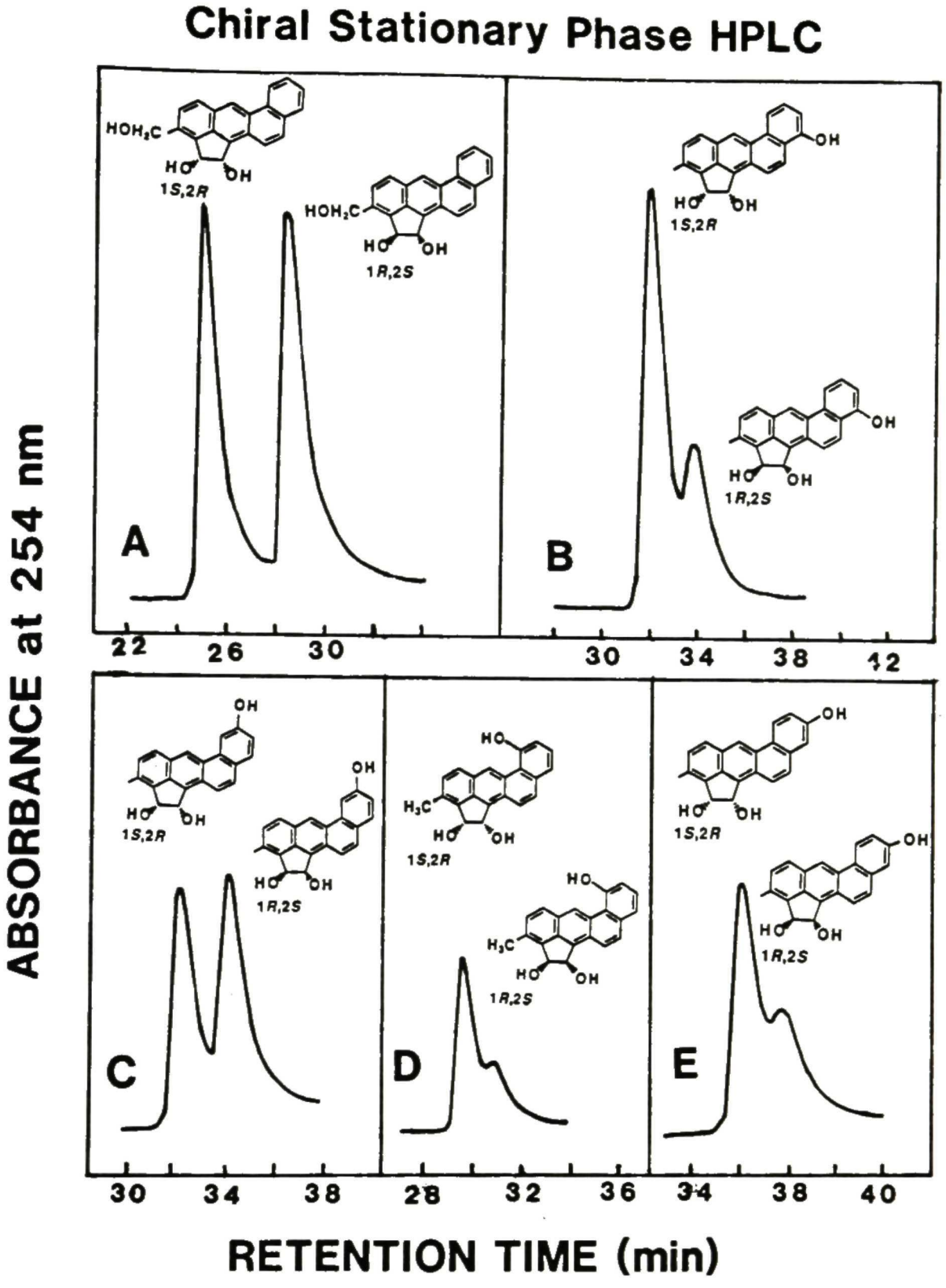

Figure 96. Chiral stationary phase HPLC separation and absolute configurations of metabolites 3-OHMC *cis*-1,2-diol (A), 10-OH-3MC *cis*-1,2-diol (B), 8-OH-3MC *cis*-1,2-diol (C), 7-OH-3MC *cis*-1,2-diol (D) and 9-OH-3MC *cis*-1,2-diol (E) enantiomers are indicated in this figure.

Table 13. Enantiomeric composition of metabolites formed in the metabolism of racemic 3MC *cis*-1,2-diol by rat liver microsomes

Metabolites[a]	Enantiomeric Composition (%)[b] [1*S* 2*R*: : 1*R*,2*S*]		
	Control	PB	3MC
8-OH-3MC *cis*-1,2-diol	43.2:56.8	33.4:66.6	4.7:95.3
7-OH-3MC *cis*-1,2-diol	65.3:34.7	63.0:37.0	0:100
9-OH-3MC *cis*-1,2-diol	55.5:44.5	52.5:47.5	ND
3-OHMC *cis*-1,2-diol	47.2:52.8	32.4:67.6	32.3:67.7
10-OH-3MC *cis*-1,2-diol	67.8:32.2	62.5:37.5	13.5:86.5
3MC *cis*-1,2-diol (remaining substrate)	45.2:54.8	25.6:74.4	57.6:42.4

a. Racemic 3MC *cis*-1,2-diol was incubated with liver microsomes (0.25 mg protein/ml of incubation mixture from untreated(control), PB-treated and 3MC treated rats. Each milliliter of reaction mixture contains 40 nmol of 3MC *cis*-1,2-diol and was incubated at 37°C for 30 min.

b. Enantiomeric ratio of metabolites was determined by CSP HPLC on a ionically bonded *R*-DNBPG column.

c. ND means enantiomer ratio was not detected.

12. Relative amounts of unmetabolized 3MC *cis*-1,2-diol enantiomers (1*S*,2*R*:1*R*,2*S*) were 45:55 (control), 26:74 (PB) and 58:42 (3MC) (Table 13), respectively. The enantioselectivity of untreated and PB induced microsomal enzymes favored the 1*S*,2*R*-enantiomer while that of 3MC favored the 1*R*,2*S*-enantiomer.

10.4 *Effects of enzyme induction on formation of metabolites formed in the (±) 3MC cis-1,2-diol and enantiomeric 3MC cis-1,2-diol*

The relative amounts of various metabolites formed in the metabolism of racemic and enantiomeric 3MC *cis*-1,2-diol by three rat liver microsomal preparations were determined with the aid of an internal standard (Table. 12). Liver microsomes and the substrate were used at 0.25 mg of protein and 40 nmol per ml of incubation mixture, respectively, and the reaction mixture was incubated for 30 min. Areas under the chromatographic peaks were normalized against that of an internal standard. For the purpose of comparing the relative amounts of metabolites formed, extinction coefficients of phenolic products at 254 nm were assumed to be identical.

The effects of inducers on the relative amount of 9,10-dihydrodiols (sum of peaks 2 and 4 of Fig. 87) formed in the metabolism of (±) 3MC *cis*-1,2-diol and 3MC *cis*-1*S*,2*R*-diol by rat liver microsomes were PB > Control > 3MC (Table 12) and in the metabolism of 3MC *cis*-1*R*,2*S*-diol, PB > 3MC > control. The relative amount of 9,10-dihydrodiols formed in the metabolism of (±) 3MC *cis*-1,2-diol by liver microsomes from PB-treated rats was greater than that formed in the metabolism of 3MC *cis*-1*S*,2*R*-diol or 3MC *cis*-1*R*,2*S*-diol.

The ratio of total phenolic products formed at C_7 and C_8 positions (sum of peak 5 and 6 of Fig. 87) to that of the internal standard formed in the metabolisms of racemic 3MC *cis*-1,2-diol and 3MC *cis*-1*R*,2*S*-diol by rat liver microsomes showed the effects of inducers to be 3MC » PB ≈ control. The relative amount of phenolic products at C_7 and C_8 formed in the metabolisms of 3MC *cis*-1*R*,2*S*-diol, (±) 3MC *cis*-1,2-diol and 3MC *cis*-1*S*,2*R*-diol from 3MC induced rat liver microsomes were 1.6 > 1.0 » 0.2, respectively.

the effects of inducers on the formations of phenolic products at C_9 and C_{10} in the metabolisms of the racemic and enantiomeric 3MC *cis*-1,2-diol were 3MC > PB > control.

Relative amounts of C_3-hydroxylation product 3-OHMC *cis*-1,2-diol were compared and the effects of enzyme inducers were PB > 3MC > control for both the racemic and enantiomeric 3MC *cis*-1,2-diol. The relative ratios of 3-OHMC *cis*-1,2-diol formed in the metabolism of (±) 3MC *cis*-1,2-diol, 3MC *cis*-1*S*,2*R*-diol and 3MC *cis*-1*R*,2*S*-diol were 0.9:0.4:1.0 in PB treatment , 0.7:0.3:0.8 in 3MC treatment and 0.4:0.1:0.3 in control, respectively. 3MC *cis*-1*R*,2*S*-diol and (±) 3MC *cis*-1,2-diol seem to be better substrates to be hydroxylated at the C_3-methyl sidechain than 3MC *cis*-1*S*,2*R*-diol. In the metabolism of the racemic and enantiomeric 3MC *cis*-1,2-diol, the effects of enzyme inducers on the percentage of substrate metabolized were 3MC (33-54%) > PB (29-41%) > control (11-30%). The differing ratios of metabolic products and disposition of these 3MC *cis*-1,2-diols were due to racemic and enantiomeric substrates used as well as various pretreatments of microsomal enzyme inducers.

DISCUSSION

Stereoselective formation and disposition of 1-OH-3MC and 2-OH-3MC in the metabolism of 3MC

In several studies reported earlier (Sims *et al.*, 1966, 1967; Cavalieri *et al.*, 1978; Eastman *et al.*, 1979; Thakker *et al.*, 1978; Stoming *et al.*, 1977; Tierney *et al.*, 1979), 1-OH-3MC and 2-OH-3MC have been consistently reported (Table 14) to be the most abundant metabolites of 3MC. However, conflicting results were reported on the relative amounts of 1-OH-3MC and 2-OH-3MC formed in the metabolism of 3MC by rat liver microsomes (Eastman *et al.*, 1979; Thakker *et al.*, 1978; Stoming *et al.*, 1977; Tierney *et al.* 1979). A [1-OH-3MC]:[2-OH-3MC] ratio of 32:68 (Stoming *et al.*, 1977) and of 43:57 (Tierney *et al.*, 1979) was reported in the metabolism of 3MC by liver microsomes from 3MC-treated rats. Another study reported that 2-OH-3MC was formed predominantly in the metabolism of 3MC by liver microsomes from Aroclor 1254-treated rats (Eastman *et al.*, 1979). In contrast, Thakker *et al.* (Thakker *et al.*, 1978) reported the ratios of [1-OH-3MC]:[2-OH-3MC], formed in the metabolism of 3MC by four rat liver microsomal preparations, were 78:22 (untreated control), 93:7 (PB-treated), 66:34 (3MC-treated), and 97:3 (prenenolone-16a-carbonitrile-treated), respectively. In this study, the amount of 2-OH-3MC formed in the metabolism of 3MC was consistently found to be higher than that of 1-OH-3MC by liver microsomes from untreated, PB-treated, and 3MC-treated rats (Table 1). The discrepancy of results in this and earlier studies (Eastman *et al.*, 1979; Thakker *et al.*, 1978; Stoming *et al.*, 1977; Tierney *et al.*, 1979) was apparently due to differences in analytical methods employed. By using 45% acetonitrile in water as the mobile phase in reversed-phase HPLC, Eastman and Bresnick (Eastman *et al.*, 1979) separated 2-OH-3MC (retention time 42 min) and 1-OH-3MC (retention time 47 min) and found that approximately 85% of the monohydroxylated ^{3}H-labeled metabolites cochromatographed with the authentic 2-OH-3MC. In other studies (Eastman *et al.*, 1979;

Table 14. Relative amounts of 1-OH-3MC and 2-OH-3MC formed in the metabolism of 3MC by various rat liver preparations.

Rat Liver Preparation	Pretreatment	1-OH-3MC (%)	2-OH-3MC (%)	Reference[a]
Microsomes	none	30 (34)[b]	70 (66)[b]	this report
Microsomes	none	78	22	Thakker *et al.*, 1978
Microsomes	PB	21 (15)[b]	79 (85)[b]	this report
Microsomes	PB	93	7	Thakker *et al.*, 1978
Microsomes	3MC	10 (2)[b]	90 (98)[b]	this report
Microsomes	3MC	43	57	Tierney *et al.*, 1979
Microsomes	3MC	32	68	Stoming *et al.*, 1977
Microsomes	3MC	66	34	Thakker *et al.*, 1978

a See original reference for experimental conditions.

b Two sets of numbers resulting from different incubation times are taken from Table 1 for ready comparison.

c PCN = prenenolone-16-a-carbonitrile, PCB = Aroclor 1254.

Thakker *et al.*, 1978; Stoming *et al.*, 1977; Tierney *et al.*, 1979), 1-OH-3MC and 2-OH-3MC were closely eluted under the reversed-phase HPLC conditions described and hence their relative amounts could not be reliably determined. In this study, 1-OH-3MC and 2-OH-3MC were first isolated by reversed-phase HPLC as a mixture, and their relative amounts were determined by normal-phase HPLC, which allowed baseline separation of 1-OH-3MC and 2-OH-3MC (Fig. 10).

In the previous studies of 3MC metabolism, Thakker *et al.* (1978) reported that pretreatment of rats with control, PB, PCN, and 3MC results in 4%, 10%, 16%, and 25% of the total metabolism of 3MC, respectively when the data are expressed as percent conversion. Later results indicated that PB-, PCB- (Aroclor 1254), and 3MC-pretreatment cause 1.8-, 4.2-, and 4.6-fold increase in the specific activities of the microsomal preparations, respectively, relative to those of the microsomes from control (Gangarosa and Stoming, 1983). However, in our reports, when 3MC was used to induce rats, total metabolism (15% or 35%) was less efficient than that of PB (17% or 39%, table 1). The discrepancy in inductive properties between our and early reports is probably due to different animal induction (dosage and number of injection of P-450 enzyme inducer to rats), substrate concentration, microsomal incubation (incubation time and volume) and analytical condition used, or remains unknown.

In view of our results (Table 1), the hydroxylation reaction is more regioselective at C_2 position than that at C_1 position of 3MC by all three rat liver microsomal preparations. The effect of enzyme inducers on the regioselectivity toward the C_2 position of 3MC by three rat liver microsomal preparations is: 3MC > PB > control. It is worthy to note that 2-OH-3MC is a considerably more potent carcinogen than 1-OH-3MC (Cavalieri *et al.*, 1978; Levin *et al.*, 1979). Since it is the most abundant metabolite, 2-OH-3MC may play an important role in the carcinogenic activity of 3MC. The metabolite(s) responsible for the carcinogenic activity of 2-OH-3MC has not been examined.

Rat liver microsomal metabolism at C_1 and C_2 positions of 3MC are 54-65% and 86-94% pro-*S* stereoselective, respectively (Table 1). However, as illustrated in Fig. 11, the pro-*S* hydroxylation reactions occur at opposite stereoheterotopic faces of the C_1-C_2 bond. The results indicate the preferred orientation of substrate (3MC)-enzyme (cytochrome P-450) interaction which result in the stereoselective hydroxylation at C_1 and C_2 positions. The reason(s) for the higher degree of pro-*S* stereoselectivity at C_2 than at C_1 remains unknown.

Rat liver microsomal metabolism of racemic 1-OH-3MC is selective toward the *S*-enantiomer (Table 1). In contrast, rat liver microsomal metabolism of racemic 2-OH-3MC is selective toward the *R*-enantiomer. It is interesting to note that the hydroxyl groups of 1*S*-OH-3MC and 2*R*-OH-3MC are on the same stereoheterotopic face of the C_1-C_2 bond (Fig. 11). It appears that the 1*S* and 2*R* hydroxyl groups are responsible for their higher affinities with the enzyme active site than the respective antipodes. The finding that the *S*-enantiomer is metabolized at a faster rate than the *R*-enantiomer by rat liver microsomal metabolism of racemic 1-OH-3MC indicates that the major and the minor 9,10-dihydrodiols (1-OH-3MC 9,10-dihydrodiol-*a* and 1-OH-3MC 9,10-dihydrodiol-*b*, respectively, Thakker *et al.*, 1978), formed in the metabolism of racemic 1-OH-3MC, are derived from the 1*S* and 1*R* enantiomer, respectively. 1-OH-3MC 9,10-dihydrodiol-*a* was reported to be more mutagenic and tumorigenic than 1-OH-3MC 9,10-dihydrodiol-*b* (Wood *et al.*, 1978; Levin *et al.*, 1979). Since the absolute configuration of enantiomeric 1-OH-3MC and 2-OH-3MC have been established, it is now possible to study the stereochemical metabolic activation and detoxification pathways of 3MC, 1-OH-3MC, and 2-OH-3MC in a more detailed manner.

Enantioselective aliphatic hydroxylations of racemic 1-OH-3MC

In the metabolism of 3MC, 1-OH-3MC and 2-OH-3MC by rat liver microsomes, both 3MC *trans*-1,2-diol and 3MC *cis*-1,2-diol were determined as metabolites (Stoming *et*

al., 1977; Tierney *et al.*, 1979; Thakker *et al.*, 1978 and Gardiner *et al.*, 1984). In the metabolism of 3MC by rat liver microsomes, 1-OH-3MC is enriched in the 1*S*-enantiomer (53-73%), whereas 2-OH-3MC is more enriched in the 2*S*-enantiomer (86-98%). In this study, the CSP HPLC resolution of enantiomeric 1-OH-3MC, 1-OH-3-OHMC, 3MC *trans*- and *cis*-1,2-diols; the elucidation of the absolute configuration of the resolved enantiomers and enantioselective hydroxylations at the C_2-carbon and the C_3-methyl group of racemic 1-OH-3MC were described.

Enantiomeric pairs of 1-OH-3MC, 1-OH-3-OHMC, 3MC *trans*-1,2-diol, and 3MC *cis*-1,2-diol were resolved by CSP HPLC on a covalently bonded *R*-DNBPG (Pirkle type 1A) column and their absolute configurations were established by CD chirality method and CSP HPLC (Figs. 8, 16, 14 and 22). Hydroxylation at the C_3-methyl group of racemic 1-OH-3MC was enantioselective toward the 1*R*-enantiomer over the 1*S*-enantiomer in a ratio of ~58/42, by cytochrome P-450 in liver microsomes from PB-treated rats. Hydroxylation at C_2-carbon of racemic 1-OH-3MC resulted in the formation of 3MC *trans*- and *cis*-1,2-diols in a ratio of ~1/3 (Fig. 18). The C_2-hydroxylation was enantioselective toward the 1*S*-enantiomer over the 1*R*-enantiomer in a ratio of ~3/1(Fig. 19), forming mostly the *cis*-1*R*,2*S* enantiomer (66.9%). In the C_2-hydroxylation of 1*S*-OH-3MC, *cis*-1,2-diol and *trans*-1,2-diol were formed in a ratio of ~67/9 (Fig. 19). In comparison, *cis*-1,2-diol and *trans*-1,2-diol were formed with a ratio of ~9/15 in the C_2-hydroxylation of 1*R*-OH-3MC. 3MC *trans*-1,2-diol formed in the metabolism of racemic 1-OH-3MC by liver microsomes from PB-treated rats was found to have a (1*S*,2*S*)/(1*R*,2*R*) enantiomer ratio of ~63/37 (Fig. 18) whereas the 3MC *cis*-1,2-diol formed had a (1*S*,2*R*)/(1*R*,2*S*) enantiomer ratio of ~12/88. These results indicate that PB-treated liver microsomes preferentially catalyze the stereoselective C_2-hydroxylation at a *cis* position relative to the C_1 of 1*S*-OH-3MC, which was the major enantiomer formed in the metabolism of 3MC (Table 1).

Stereoselective metabolism of 2S-OH-3MC

2-OH-3MC comprises the majority (70-90%, depending on the enzyme inducer used to treat the rats) of the hydroxylation products formed at C_1 and C_2 positions of 3MC by rat liver microsomes. Furthermore, 2-OH-3MC formed in the metabolism of 3MC by liver microsomes from untreated, PB-treated, and 3MC-treated rats is highly enriched in the 2*S*-enantiomer (enantiomeric excess 72-96%) as reported earlier (Shou and Yang, 1990a).

The substrate (2*S*-OH-3MC) used in this study was isolated from a mixture of metabolites formed by incubation of 3MC with liver microsomes from 3MC-treated rats. Consistent with the results of an earlier report, the 2-OH-3MC formed in the metabolism of 3MC by liver microsomes from 3MC-treated rats was highly enriched in the 2*S*-enantiomer (enantiomeric excess ~98%). The absolute configuration of the major 2-OH-3MC enantiomer formed in the metabolism of 3MC has been established in this study.

Because 2-OH-3MC is itself a potent carcinogen and 2*S*-OH-3MC is the most abundant metabolite of 3MC, the metabolic activation pathway(s) of 2*S*-OH-3MC may play an important role in the metabolic activation of 3MC. In this study, 16 metabolites have been detected as products formed by incubation of 2*S*-OH-3MC with rat liver microsomes. Among these metabolites, six are 9,10-dihydrodiols which may be further metabolized to form the biologically reactive bay region 9,10-diol-7,8-epoxides. Two diastereomeric 9,10-dihydrodiols were derived from 2*S*-OH-3MC; 2*S*-OH-3MC 9*R*,10*R*-dihydrodiol and 2*S*-OH-3MC 9*S*,10*S*-dihydrodiol in a ratio of ~9/1. Since microsomal epoxide hydrolase-catalyzed reactions occur predominantly at the nonbenzylic positions (Yang *et al.*, 1977; Lu *et al*, 1980), these results suggest that the metabolic precursor 9,10-epoxide has a (9*S*,10*R*)/(9*R*,10*S*) enantiomer ratio of ~9/1. Two more 9,10-dihydrodiols were probably derived from 2*S*-OH-3-OHMC since the latter was the most abundant metabolite of 2*S*-OH-3MC. 2*S*-OH-3-OHMC is a newly recognized metabolite of 2*S*-OH-3MC and its carcinogenic activity is yet unknown. The fifth 9,10-dihydrodiol is derived from 3MC-2-one which is a potent carcinogen (Sims *et al.*, 1967; Cavalieri *et al.*, 1978; Levin *et al.*, 1979) and one of the major metabolites of 2*S*-OH-3MC. The sixth 9,10-dihydrodiol may

be derived either from further metabolism of 3MC *cis*-1*S*,2*R*-diol or by (*cis*)-C_1-hydroxylation of 2*S*-OH-3MC 9*R*,10*R*-dihydrodiol or 2*S*-OH-3MC 9*S*,10*S*-dihydrodiol.

Three K-region 11,12-dihydrodiols were found as metabolites of 2*S*-OH-3MC; two diastereomeric 2*S*-OH-3MC 11,12-dihydrodiols and one 2*S*-OH-3-OHMC 11,12-dihydrodiol. In principle, two diastereomeric *trans*-11,12-dihydrodiols can be formed from 2*S*-OH-3-OHMC. However, the amount of the second 2*S*-OH-3-OHMC 11,12-dihydrodiol may be too small to be detected. The amounts of these K-region dihydrodiols formed are considerably lower than those of 2*S*-OH-3-OHMC or the 9,10-dihydrodiols derived from 2*S*-OH-3MC. 2*S*-OH-3MC 11*R*,12*R*-dihydrodiol and 2*S*-OH-3MC 11*S*,12*S*-dihydrodiol are formed in a ratio of ~77/23. The 11*S*,12*R*-epoxide may be the major enantiomer formed by epoxidation at the K-region of 2*S*-OH-3MC by liver microsomes from 3MC-treated rats. In the metabolism of 3MC by liver microsomes from 3MC-treated rats, ~91% of the 11,12-epoxide formed is the 11*S*,12*R*-enantiomer (Yang *et al.*, 1990). Both the 11*S*,12*R*-epoxide and the 11*R*,12*S*-epoxide of 3MC are regioselectively hydrated by microsomal epoxide hydrolase to form a 3MC 11,12-dihydrodiol with a (11*R*,12*R*)/(11*S*,12*S*) enantiomer ratio of 85/15 (Yang *et al.*, 1990).

The *trans*-1*R*,2*R*-diol and *cis*-1*S*,2*R*-diol are formed in a ratio of ~11:89 in the metabolism of 2*S*-OH-3MC by liver microsomes from 3MC-treated rats. Thus the stereoselective (*cis*)-C_1-hydroxylation is more prevalent than the (*trans*)-C_1-hydroxylation (see illustration at the top of Fig. 22). In the absence of the C_2-hydroxyl group, rat liver microsomal metabolism of 3MC resulted in the preferential formation of 1*S*-OH-3MC with an enantiomeric excess of 8-30%, depending on the enzyme inducer used to treat the rats (Osborne *et al.*, 1986). It should be pointed that, due to the addition of a chiral center at C_1, the hydroxyl group with 2*S* designation in an enantiomeric 2-OH-3MC is changed to 2*R* (and *vice versa*) in the enantiomeric 3MC *trans*- and *cis*-1,2-diols (see illustration at the top of Fig. 22). Thus the stereoselective hydroxylation at C_1 position of 3MC is highly dependent on whether there is a hydroxyl group at C_2.

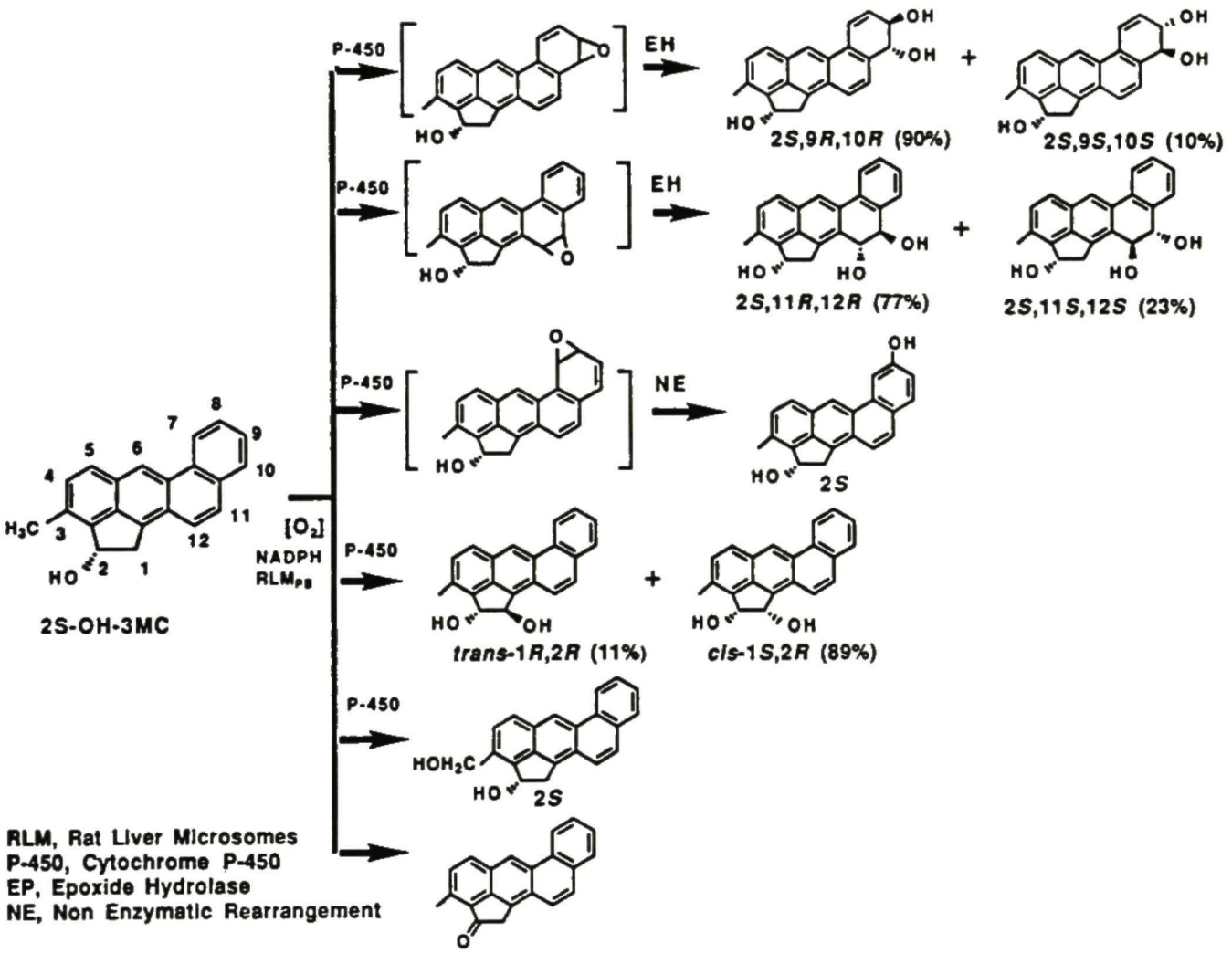

Figure 97. The major metabolic pathway of 2*S*-OH-3MC.

The carcinogenic activity of racemic 3MC *cis*-1,2-diol is weaker than that of racemic 1-OH-3MC (Sims, 1967). However, the carcinogenic activity of 3MC *trans*-1,2-diol has not been tested. A preliminary study in our laboratory indicated that a pair of diastereomeric 9,10-dihydrodiols are the predominant rat liver microsomal metabolites of 3MC *trans*-1,2-diol, indicating that 3MC *trans*-1,2-diol may also be activated at the 7,8,9,10 benzo-ring.

Our earlier finding that 2*S*-OH-3MC is the most abundant metabolite of 3MC and the present finding that 2*S*-OH-3-OHMC and two diastereomeric 2*S*-OH-3MC 9,10-dihydrodiols are major metabolites of 2*S*-OH-3MC are in contrast to the conclusions reported by Osborne *et al.* Identification of metabolic pathways of 2*S*-OH-3MC in this report should substantially enhance our understanding of the mechanism of metabolic activation of 3MC which is summarized in Fig. 97. The results reported to-date on the metabolism of 3MC and its C_1 and C_2 derivatives indicate that the procarcinogenic 9,10-dihydrodiols can be formed in the metabolism of 2*S*-OH-3MC. Tumorigenicity tests of these 9,10-dihydrodiols and their parent compounds should provide considerable insight into the roles of 7,8,9,10-benzo ring metabolism in the metabolic activation of the potent carcinogen 3MC.

Stereoselective metabolism of racemic 2-OH-3MC

Due to stereoheterotopic interaction between microsomal enzymes (cytochrome P-450 and epoxide hydrolase) and PAH substrate, racemic substrate 2-OH-3MC, was taken into more consideration in the stereoselective formations of enantiomeric metabolites by liver microsomes of rats treated with PB.

In this study, 19 metabolites have been detected as products formed by incubation of (±) 2-OH-3MC. Six of these metabolites are 9,10-dihydrodiols which may be further metabolized to form the bay region 9,10-diol-7,8-epoxides. Two major diastereomeric 2-OH-3MC 9,10-dihydrodiols contained in peaks 5 and 7 of Fig. 35 with a ratio of 54:46 had

their own enantiomeric compositions of 27 (2*S*,9*R*,10*R*) : 73 (2*R*,9*S*,10*S*) and 81 (2*R*,9*R*,10*R*) : 19 (2*S*,9*S*,10*S*), respectively. Relative amounts of the two pairs of enantiomers were 39.4 (2*R*,9*S*,10*S*) > 37.3 (2*R*,9*R*,10*R*) >14.6 (2*S*,9*R*,10*R*) > 8.7 (2*S*,9*S*,10*S*). The stereoselective formations of 2-OH-3MC 9,10-dihydrodiols in the metabolism of (±) 2-OH-3MC by liver microsomes of PB-pretreated rats were mainly derived from 2*R*-OH-3MC. This indicates that microsomal enzymes, which catalyze the epoxidations by cytochrome P-450b at the M region of 2-OH-3MC to 9,10-epoxides, and hydrations of 9,10-epoxides by epoxide hydrolase to 9,10-dihydrodiols enantioselectively fit the 2*R*-OH-3MC substrate better than 2*S*-OH-3MC, forming a majority of 2R-OH-3MC 9,10-dihydrodiols. Therefore, the enantioselective disposition of (±) 2-OH-3MC is toward 2*R*-OH-3MC over 2*S*-OH-3MC.

Since 2-OH-3MC 9,10-dihydrodiols and 2-OH-3-OHMC formed in the metabolism of (±) 2-OH-3MC were the most abundant metabolites, the two diastereomeric 2-OH-3-OHMC 9,10-dihydrodiols, contained in peak 1 and 2 of Fig. 35 were probably derived from both the C_3-hydroxylation of 2-OH-3MC 9,10-dihydrodiols and the hydration of 2-OH-3-OHMC 9,10-epoxides formed through the epoxidation reaction at the double bond between C_9 and C_{10} of 2-OH-3-OHMC. Only one pair of 2-OH-3-OHMC 9,10-dihydrodiol enantiomers in peak 1 can be separated by the *R*-DNBPG-C column which produced a ratio of 62 (9*R*, 10*R*):38 (9*S*, 10*S*) with unknown stereochemistry of the hydroxyl group at C_2.

Three K-region 11,12-dihydrodiols were found as metabolites of 2-OH-3MC: two diastereomeric 2-OH-3MC 11,12-dihydrodiols and one 2-OH-3-OHMC-11,12-dihydrodiol. It is interesting to note that major enantiomers of the 2-OH-3MC 11,12-dihydrodiols were enriched in 2*S*,11*R*,12*R* and 2*S*,11*S*,12*S* absolute configurations which were derived from 2*S*-OH-3MC. The formations of dihydrodiols of 2-OH-3MC at either the M or K region in the metabolism of (±) 2-OH-3MC were dependent on the stereochemistry of hydroxyl group at C_2. In other words, the 2*R*-OH-3MC was readily

metabolized to form the major 2*R*-OH-3MC 9,10-dihydrodiols while the 2*S*-OH-3MC was metabolized to form the major 2*S*-OH-3MC 11,12-dihydrodiols.

The 3MC *trans*-1,2-diol and 3MC *cis*-1,2-diol are formed in a ratio of 2:8 in the metabolism of (±)2-OH-3MC by liver microsomes from PB treated rats. In Table 4, the 1*S*,2*S*-diol (68%) in a pair of 3MC *trans*-1,2-diol enantiomers and 1*R*,2*S*-diol (82%) in a pair of 3MC *cis*-1,2-diol enantiomers were major components and were all derived from 2*R*-OH-3MC. These results suggest that liver microsomal enzymes from PB-treated rats in catalyzing the C_1-hydroxylation reaction at the *cis* or *trans* position of 2-OH-3MC preferentially metabolize 2*R*-OH-3MC. C_1-hydroxylation of 2*R*-OH-3MC driven by cytochrome P-450b prefers the *cis*-position of 2*R*-OH-3MC over *trans*-position, forming a majority of *cis*-1*R*,2*S*-diol.

In above results, the M region between C_9 and C_{10} of the 2-OH-3-OHMC, 3MC-2-one, 3MC *cis*-1,2-diol and (±) 2-OH-3MC in microsomal incubation with NADPH-generating system can be oxidized to produce their corresponding 9,10-epoxides which are further hydrated to 9,10-dihydrodiols. Further epoxidations of these 9,10-dihydrodiols between C_7 and C_8 may form the bay region 9,10-diol-7,8-epoxides. Many DNA-binding studies of the 9,10-diol-7,8-epoxides possibly derived from 3MC, 3MC 9,10-dihydrodiol, 3-OHMC and 1-OH-3-OHMC, 1-OH-3MC and 1-OH-3MC 9,10-dihydrodiol have been reported (Cooper *et al.*, 1980; King *et al.*, 1977; King *et al.*, 1978; Eastman *et al.*, 1979; Osborne *et al.*, 1983; 1986 and Phillips *et al.*, 1978). Since 2-OH-3MC has been shown to have higher carcinogenic activity and to be the most abundant metabolite in the metabolism of 3MC, the bay region 7,8,9,10-benzo ring stereoselective metabolism of 2-OH-3MC in the metabolic activation of the potent carcinogen 3MC should be taken into consideration.

Stereoselective metabolism of 3MC-2-one

In this study, we have demonstrated that 3MC-2-one *trans*-9,10-dihydrodiol is the most abundant metabolite in 3MC-2-one metabolism by liver microsomes from untreated,

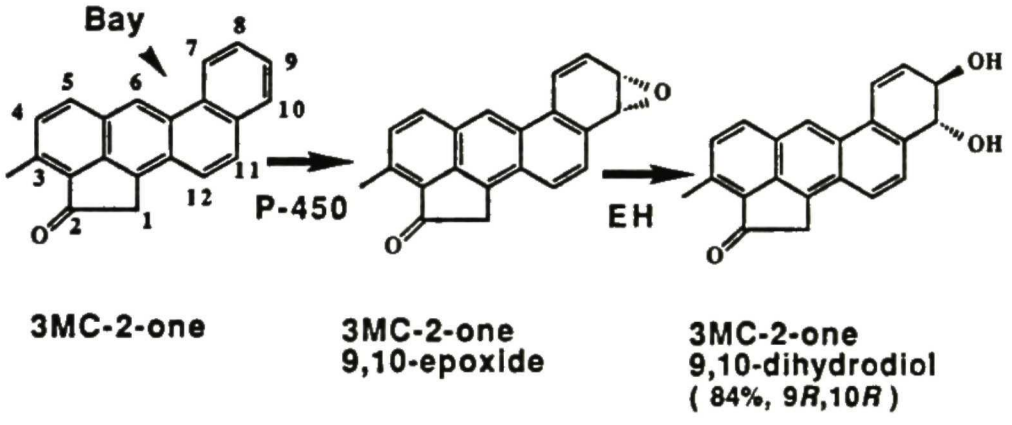

Figure 98. The major oxidative pathway of 3MC-2-one.

PB-treated, and 3MC-treated rats. Thus it was surprising that in earlier studies (Cavalieri *et al.*, 1978; Sims *et al.*, 1966) the *trans*-9,10-dihydrodiol was not found as a rat liver microsomal metabolite of 3MC-2-one. It was reported that the majority (70-90%, depending on the enzyme inducer used to treat the rats) of the hydroxylation products formed at C_1 and C_2 positions of 3MC by rat liver microsomes is 2-OH-3MC. Since 3MC-2-one is one of the oxidative metabolites of 2-OH-3MC (Cavalieri *et al.*, 1978; Sims *et al.*, 1966) and is known to be a potent carcinogen (Sims *et al.*, 1967; Cavalieri *et al.*, 1978 Wood *et al.*, 1978; Levin *et al.*, 1979), 3MC-2-one and its *trans*-9,10-dihydrodiol may also play important roles in the metabolic activation of 3MC.

The metabolically formed 3MC-2-one *trans*-9,10-dihydrodiol is highly enriched in the 9*R*,10*R*-enantiomer. Determination of enantiomeric compositions of the metabolically formed 3MC-2-one *trans*-9,10-dihydrodiol in several experiments suggested that the 9*R*,10*R*-enantiomer is further metabolized at a faster rate than the 9*S*,10*S*-enantiomer. The importance of absolute stereochemistry and relative rate of further metabolism of such potentially procarcinogenic 9,10-dihydrodiol metabolite has been well documented in the metabolic activation of the most extensively studied aromatic carcinogen benzo[*a*]pyrene (Conney *et al.*, 1982). Presumably 3MC-2-one *trans*-9*R*,10*R*-dihydrodiol (Fig. 98) is the metabolic precursor of the potentially reactive ultimate carcinogenic bay-region 3MC-2-one 9,10-diol-7,8-epoxides (*anti* and *syn* isomers), a pathway similar to the metabolic epoxidation at the 9,10-double bond of benzo[*a*]pyrene 7*R*,8*R*-dihydrodiol (Conney *et al.*, 1982). The metabolic fate, mutagenic and tumorigenic activities of 3MC-2-one *trans*-9,10-dihydrodiol should be evaluated in a later study.

Stereoselective metabolism of racemic 1-OH-3MC

Many biological tests have exhibited that major C_1 and C_2 hydroxylation products 1-OH-3MC and 2-OH-3MC had carcinogenic and mutagenic activities. When strain TA98 of *salmonella typhimurium* with hepatic microsomal source of metabolizing enzyme was

used to detect mutagens, 1-OH-3MC was metabolically activated to a 10-fold greater extent than was 3MC and was the most active compound tested (Wood *et al.*, 1978). 1-OH-3MC 9,10-dihydrodiol and 3MC-2-one as the most active compounds, were also activated to a greater extent than was 3MC. When strain TA100 and Chinese hamster V79 cells with hepatic microsomal system were used to detect mutations, 1-OH-3MC 9,10-dihydrodiol had a greater effect than 3MC, 4,5-, 7,8-, 11,12- or 2a,3-dihydrodiol(Wood *et al.*, 1978). Diastereomeric 3MC 9,10-dihydrodiol-*a* was more active both in *S. Typhimurium* strain TA100 and V79 cells than that designated 1-OH-3MC 9,10-dihydrodiol-*b*. In topical application of tumorigenicity on mouse skin, the average numbers of tumors per mouse showed that 1-OH-3MC 9,10-dihydrodiol diastereomers, 3MC, 2-OH-3MC and 3MC-2-one were about equipotent as tumor initiators and that 1-OH-3MC had approximately one-fourth the activity of the most active compounds (Sims, 1967).

The fluorescence spectra of DNA adducts isolated from the skin of mice treated with 3MC were examined by Vigny *et al.* (1977) and by Cooper *et al.* (1980) and showed the anthrancene-like emission, indicating that metabolic activation of 3MC involved the saturation on the 7,8,9,10-ring. King *et al.* (1977; 1978) detected five products of DNA adducts in mouse embryo cells in culture and demonstrated that adducts formed in these cells arise from the 9,10-diol 7,8-epoxides derived from both 1-OH-3MC and 3MC. All the tests were carried out in the presence of metabolizing systems and provided the evidence for bay-region activation of 3MC and 1-OH-3MC to form ultimate carcinogen 9,10-diol-7,8-epoxides.

In metabolic studies, few reports of the metabolism of 1-OH-3MC have been completed (Thakker *et al.*, 1978; Gardiner *et al.*, 1984). Most metabolites formed in the metabolism of 1-OH-3MC were not characterized. Only structures of two isomeric *trans*- and *cis*-1,2-diol of 3MC, and two predominantly diastereomeric 1-OH-3MC 9,10-dihydrodiols assigned as *a* and *b* with unknown stereochemistry were found. Due to the high mutagenic and carcinogenic activities of 1-OH-3MC 9,10-dihydrodiol, we were

interested in studying of the activation pathways of stereoselective metabolism of 1-OH-3MC leading to the formation of ultimate carcinogenic metabolites.

A major metabolic pathway of (±)1-OH-3MC by liver microsomes from PB treated rats is characterized in Fig. 99. There are five 9,10-dihydrodiols formed in the metabolism of (±) 1-OH-3MC. Two diastereomeric 1-OH-3MC 9,10-dihydrodiols contained in peaks 6 and 7 of Fig. 44 which were established as 9,10-dihydrodiol-*a* and *b* of 1-OH-3MC by Thakker *et al.* (1978) were major metabolites in a ratio of 63:37. The absolute configurations of enantiomers in these two diastereomers were first determined in this study. The diastereomer in peak 6 of Fig. 44 contained a pair of enantiomers (1*S*-OH-3MC 9*R*,10*R*-dihydrodiol and 1*R*-OH-3MC 9*S*,10*S*-dihydrodiol) which were separated on *R*-DNBPG-I column with enantiomeric composition of 79:21. The diastereomer in peak 7 of Fig. 44 contained a pair of enantiomers (major component 1*R*-OH-3MC 9*R*,10*R*-dihydrodiol and minor 1*S*-OH-3MC 9*S*,10*S*-dihydrodiol). 1-OH-3MC 9,10-dihydrodiol enantiomers contained in peak 7 of Fig. 44 were separated by CSP HPLC. The mutagenic and carcinogenic studies showed that diastereomer formed in peak 6 had more activity than the diastereomer in peak 7 (Wood *et al.*, 1978; Levin *at al.*, 1979). Hence 1*S*-OH-3MC 9*R*,10*R*-dihydrodiol as a major enantiomer (79%) and potential procarcinogen contained in peak 6 plays a possible important role in the stereochemical metabolic activation pathway and carcinogenicity of both 1-OH-3MC and 3MC.

The tertiary metabolites 1-OH-3-OHMC 9,10-dihydrodiol in peak 1, 3MC *cis*-1,2-diol:9,10-dihydrodiol in peak 3 and 3MC-1-one 9,10-dihydrodiol in peak 8 of Fig. 44 are also precursors of their corresponding 9,10-diol-7,8-epoxides. These are possibly derived from major metabolites 1-OH-3-OHMC, 3MC *cis*-1,2-diol and 3MC-1-one respectively and from 1-OH-3MC 9,10-dihydrodiols. CD spectra indicated that these 9,10-dihydrodiol metabolites contain a majority of 9*R*,10*R*-enantiomers. Even though carcinogenic activities have not been tested, these 9*R*,10*R*-dihydrodiols as precursors of bay region 9,10-diol-

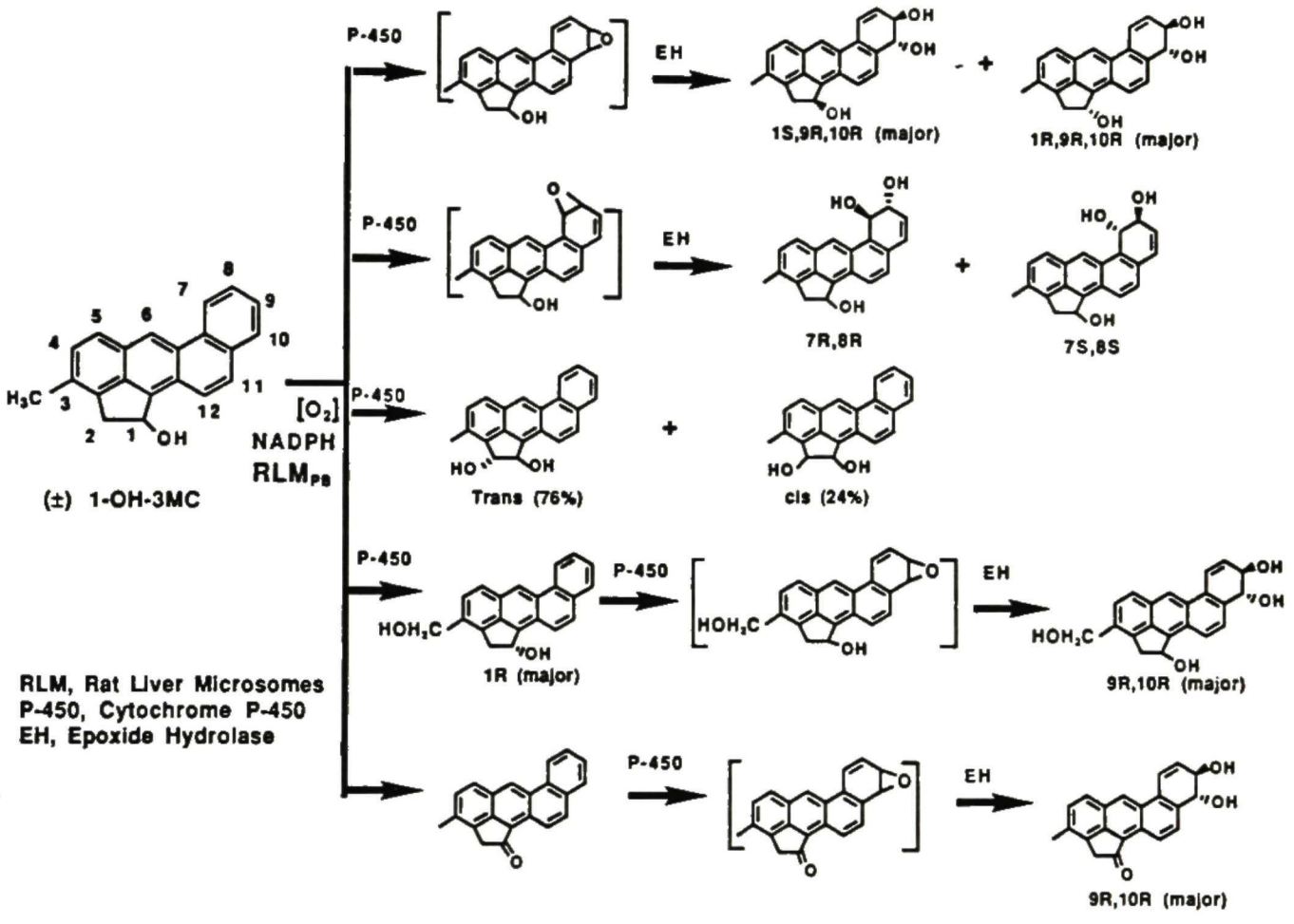

Figure 99. The major metabolic pathway of (±)1-OH-3MC.

7,8-epoxides should be taken into account when considering the carcinogenicity of 1-OH-3MC and 3MC .

Some phenolic products at C_9 and C_{10} of 1-OH-3MC contained in peaks 4, 5, 14 and 16 of Fig. 44 were also formed in the metabolism of (±)1-OH-3MC by rat liver microsomes. The metabolites were mainly derived from non-enzymatic rearrangement of 9,10-epoxides. Metabolic formations of more stable phenolic products at C_9 and C_{10} of 1-OH-3MC were implicated to be metabolic inactivation pathways due to blockage of bay region diol-epoxide formation.

The bay region 1-OH-3MC 7,8-epoxides are precursors of the 1-OH-3MC 7,8-dihydrodiols formed in peak 1a of Fig. 45 by hydration with microsomal epoxide hydrolases. Meanwhile, the 7,8-epoxides also can be rearranged by a non-enzymatic reactions to result in two phenolic products, 7-OH-1-OH-3MC and 8-OH-1-OH-3MC contained in peaks 11 and 13 of Fig. 44 . The metabolic formations of the 7,8-dihydrodiols and phenolic products at C_7 and C_8 are mainly dependent on the stability of 7,8-epoxide itself and the interaction of 7,8-epoxide substrates with epoxide hydrolase. Our findings suggest that 1-OH-3MC 7,8-epoxides were not good substrates for the microsomal epoxide hydrolase and most were readily isomerized to form their phenolic products. In considering that the portion between C_7 and C_8 which is located in the bay region and is similar to that of B[a]P *trans*-9,10-dihydrodiol, the hydroxyl groups of the bay region 1-OH-3MC *trans*-7,8-dihydrodiol are forced to adopt a quasidiaxial conformation (Yang *et al.*, 1980, 1981). Due to this conformation, the relatively more polar 7,8-dihydrodiol had a early retention time which eluted in peak 1 of Fig. 44 and was much shorter than other dihydrodiols with the quasidiequatorial conformations. The phenolic products formed at C_7 and C_8 seem to be greater than 1-OH-3MC 7,8-dihydrodiols based on HPLC chromatographic profile of Fig. 44.

Comparative metabolism of [^{3}H] 1-OH-3MC by rat and human liver microsomes

The metabolic profiles of [^{3}H] 1-OH-3MC by rat and human liver microsomal systems appeared to be similar patterns as seen in Fig. 71. Cytochrome P-450 systems exist in both rat liver microsomes and can be induced by prior administration of 3MC and PB, as shown by the higher level of metabolites formed with induction as compared to untreated rat (control) and human liver microsomes. The radioactive metabolites can be characterized by co-migration with unlabeled known metabolites as UV markers on reversed phase HPLC. Formations of radioactive metabolites formed from various microsomal incubations were quantitated by liquid scintillation counting.

The metabolic activation of 1-OH-3MC into bay region 9,10-diol-7,8-epoxides is thought to be an important step in carcinogenesis of this substrate. Enzyme-mediated sources prepared from the animals and cells have been shown to catalyze the formation of adducts to DNA *in vitro* as a result of the metabolic formation of 1-OH-3MC 9,10-diol-7,8-epoxides (Cooper *et al.*, 1980; King *et al.*, 1977, 1978 and Eastman *et al.*, 1979). Although lower metabolism of 1-OH-3MC from human liver microsomes occurred, the metabolic pattern was substantially similar to that of rat liver microsomal metabolism and the formation of all 9,10-dihydrodiols accounted for ~10% of total metabolism. Treatment of the rats with PB and 3MC stimulated 2.5 and 9.7 fold increase in the formation of 9,10-dihydrodiols when using 0.5 mg microsomal protein per ml incubation mixture, as that observed with control. Liver microsomes from untreated rats caused 2.8 fold increase of 9,10-dihydrodiols formed in the metabolism of 1-OH-3MC as that from human when using the same microsomal concentration. It is interesting to note that metabolic formations were found to vary depending on microsomes used from different species, type of enzyme induction and microsomal protein concentration. The HPLC profile of formation (15 - 58 % of total products) of 3MC *cis*-1,2-diol from [^{3}H] 1-OH-3MC metabolism was different than from that from unlabeled 1-OH-3MC metabolism. This difference may be due to the various incubation and analytical conditions employed as well as metabolic rate and extinction coefficient of molecules.

Our findings suggest that human liver microsomes are capable of metabolizing 1-OH-3MC. This data leads to an understanding that human liver microsomal metabolism of 1-OH-3MC involves an activation process similar to rats. Even though the quantity of 9,10-dihydrodiol metabolites was less than that observed from liver microsomes of untreated rats (control), 9,10-dihydrodiols, as precursors of known ultimate tumorigenic moieties of 1-OH-3MC, formed from either rat or human liver microsomes is an important factor to consider.

Stereoselective metabolism of 3-OHMC

3-OHMC, one of three alcoholic products, has recently been implicated to be an important metabolic intermediate in forming reactive product(s) that bind covalently to DNA in 3MC-treated cultured mouse embryo cells (Osborne *et al.*, 1986) and in various tissues of mice treated with 3MC (Lu *et al.*, 1990). Furthermore, 1-OH-3MC and 2-OH-3MC are believed to contribute little to the formation of DNA binding adducts in 3MC-treated mouse embryo cells in culture (Osborne *et al.*, 1986).

Several metabolism studies have claimed tentative identification of 3-OHMC as a metabolite of 3MC (Sims, 1966; Eastman *et al.*, 1979; Thakker *et al.*, 1978; Osborne *et al.*, 1086; Lu *et al.*, 1990). 3-OHMC, 1-OH-3MC, and 2-OH-3MC have an identical molecular weight and uv-vis absorption spectrum. The lack of an authentic compound and an analytical system which allows the separation of the structurally similar 3-OHMC, 1-OH-3MC, and 2-OH-3MC has precluded the definitive identification of 3-OHMC as a metabolite of 3MC. In the study by Osborne *et al.* (Osborne *et al.*, 1986), a 3-methoxymethylcholanthrene (3-MeOMC) was used as an authentic compound for the purpose of identifying 3-OHMC as a metabolite. However, since 2-methoxy-3MC was not shown to be chromatographically separable from 3-MeOMC, Osborne *et al.* (Osborne *et al.*, 1986) may have mistaken 2-OH-3MC for 3-OHMC. In our study, it was found that

the amount of 2-OH-3MC formed in the metabolism of 3MC is substantially higher than that of 1-OH-3MC.

Comparing the regioselectivity of various cytochrome P-450 isozymes on C_1, C_2 and 3-methyl side-chain hydroxylation of 3MC molecule, the relative ratios of [1-OH3MC]:[2-OH3MC]:[3-OHMC] were 31:42:27 (control), 19:43:38 (PB-treated), 7:79:14 (3MC-treated) and 12:65:23 (PCB-treated) respectively for 10-min incubation and 24:46:30 (control), 19:43:38 (PB-treated), 4:83:13 (3MC-treated) and 29:55:16 (PCB) respectively for 30-min incubation (Table 7). The relative amount of monohydroxylated 3MC formations in 3MC metabolism by all four microsomal preparations were 2-OH-3MC > 3-OHMC > 1-OH3MC. These results indicate that cytochrome P-450 isozymes in liver microsomes from 3MC-treated rats had the highest regioselectivity toward the C_2 position. Meanwhile, induction effects of cytochrome P-450 isozymes on activation and inactivation of 3MC metabolism become important factors to evaluate. It is obvious that 3MC-induced cytochrome P-450 forms hydroxylate more regioselectively the C_2 position and play important roles in the activation of 3MC metabolism since 2-OH-3MC exhibits nearly the highest biological activities of all oxidized compounds with an aliphatic five membered ring.

DNA binding studies *in vivo* and *in vitro* by Osborne *et al.* (Osborne *et al.*, 1986) and Eastman *et al.*(Eastman *et al.*, 1979) showed that 3-OH-3MC bound to DNA more effectively in this regard than either 1-OH-3MC or 2-OH-3MC when using mouse embryo cells and a microsome-catalyzed-DNA system, and contributed the most activity to the formation of these adducts indicating that 3-OHMC was a major precursor. These results suggested that major binding to DNA is possibly mediated via *trans*-9,10-dihydrodiol, presumably through the subsequent hydroxylation at 3-methyl sidechain to a vicinal diol-epoxide as prescribed by the bay region hypothesis.

In some studies, 3MC 9,10-dihydrodiol was not found as a metabolite of 3MC (Osborne *et al.*, 1986). By analyzing metabolite-DNA binding adducts derived from 3MC-

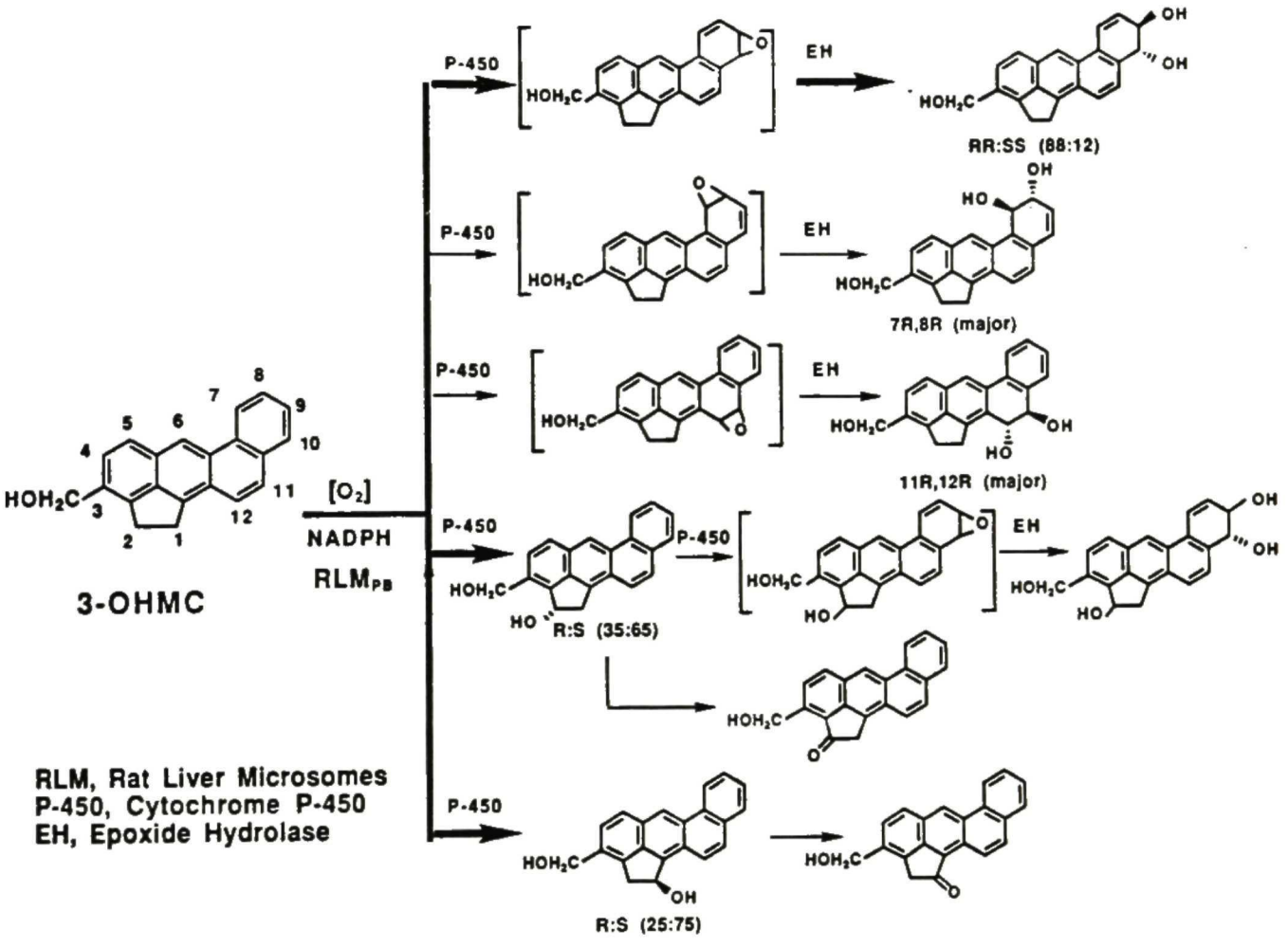

Figure 100. The major metabolic pathway of 3-OHMC.

treated mouse embryo cells, Osborne *et al.* reported that only a minor proportion (3-8%) was derived from *anti*-9,10-diol-7,8-epoxide of 3MC. Some (11-28%) were derived from *syn*-9,10-diol-7,8-epoxide of 3MC, and most of the adducts were derived from 9,10-diol-7,8-epoxides (*anti* and *syn* isomers) of 3-OHMC (37-51%) and 1-OH-3-OHMC (29-35%). In that study, Osborne *et al.* prepared ^{3}H-labeled 3-OHMC by incubation of ^{3}H-labeled 3MC with liver microsomes from Aroclor 1254-treated rats. It was reported (Osborne *et al.*, 1986) that 3-OHMC accounted for ~20% of all the metabolites formed (based on the description that 3-OHMC accounted for 2% of all the radioactivity on the TLC plate, using a sample containing 90% of unmetabolized 3MC).

Although the metabolism of 3MC has been extensively investigated in rat liver microsomes, very little is known about the metabolites derived from 3-OHMC. In this study, eight metabolites formed in the metabolism of 3-OHMC by liver microsomes from control, PB-treated, 3MC-treated and PCB-treated rats were characterized and relative amounts were determined by adding an internal standard. The 3-OHMC 9,10-dihydrodiol contained in peak 4 was found to be a major metabolite. Effects of enzyme inducers on the formation of 3-OHMC 9,10-dihydrodiol were PB > PCB > 3MC > control. Enantiomers of 3-OHMC 9,10-dihydrodiol formed by the four microsomal preparations were separated on a chiral column. Similar enantiomeric compositions resolved by CSP HPLC as seen in Fig. 78 indicate that all the induced microsomal enzymes preferentially catalyze the formation of 3-OHMC 9*R*,10*R*-dihydrodiol. 3-OHMC 7,8-dihydrodiol and 3-OHMC 11,12-dihydrodiol as minor dihydrodiols in the metabolism of 3-OHMC were purified and were shown to contain a majority of *R*,*R*-enantiomers. Meanwhile, C_1 and C_2 hydroxylation of 3-OHMC also occurred, forming 1-OH-3-OHMC and 2-OH-3-OHMC which could be partly converted to their corresponding ketone products. These observations suggest that epoxidation at the double bond between C_9 and C_{10} and hydroxylations at C_1 and C_2 are major bio-oxidative steps in metabolic pathway of 3-OHMC characterized in Fig. 100. Not many phenolic products in the metabolism of 3-

OHMC were formed except 8-OH-3-OHMC which co-eluted on reversed phase HPLC with 1-OH-3-OHMC in peak 5 of Fig. 74. In previous studies, using HPLC, Eastman *et al.* (Eastman *et al.*, 1979) examined the mixture of nucleoside adducts obtained from DNA that was incubated with 3MC in the presence of a rat liver microsomal system. They showed that one of several diastereomeric 9,10-dihydrodiols with higher level of reaction with DNA was derived by monohydroxylation at C_3-methyl sidechain of 3MC. The available evidence on the metabolic activation of 3-OHMC in our study indicates that 3-OHMC 9,10-dihydrodiol formed in 3MC metabolism arises from initial hydroxylation at C_3-methyl group and further oxidation at the M region of 3MC.

Metabolism of 3MC trans-1,2-diol

Very few studies on the mutagenicity and carcinogenicity of 3MC *trans*-1,2-diol have been reported to date. The relationship between the metabolic product 3MC *trans*-1,2-diol formed in the metabolism of 3MC and its carcinogenic activity has not been clear. However, in considering the bay region theory of PAHs, it is questionable as to whether all the biological activity is mediated through 3MC *trans*-1,2-diol via the intermediate formations of 9,10-dihydrodiols since some 3MC aliphatic derivatives such as 1-OH-3MC have been exhibited to be active by the formation of 9,10-dihydrodiols.

The most abundant product formed in the metabolism of (±) 3MC *trans*-1,2-diol by liver microsomes of PB-treated rats was 9,10-dihydrodiol, a possible mixture of diastereomers contained in peak 2 of Fig. 79. The relative amount of 9,10-dihydrodiol from (±) 3MC *trans*-1,2-diol metabolism had varying degrees depending on enzyme inducers utilized and was 2.70 (PB) > 0.65 (control) > 0.34 (3MC). Since the relative amount of 9,10-dihydrodiol derived from 3MC *trans*-1*R*,2*R*-diol in liver microsomal metabolism by untreated and PB-treated rats was more substantial than that from 3MC *trans*-1*S*,2*S*-diol as shown in Table 10, 3MC *trans*-1*R*,2*R*:9*R*,10*R*-dihydrodiol should be the greatest stereoisomer in the mixture of 9,10-dihydrodiol diastereomers contained in

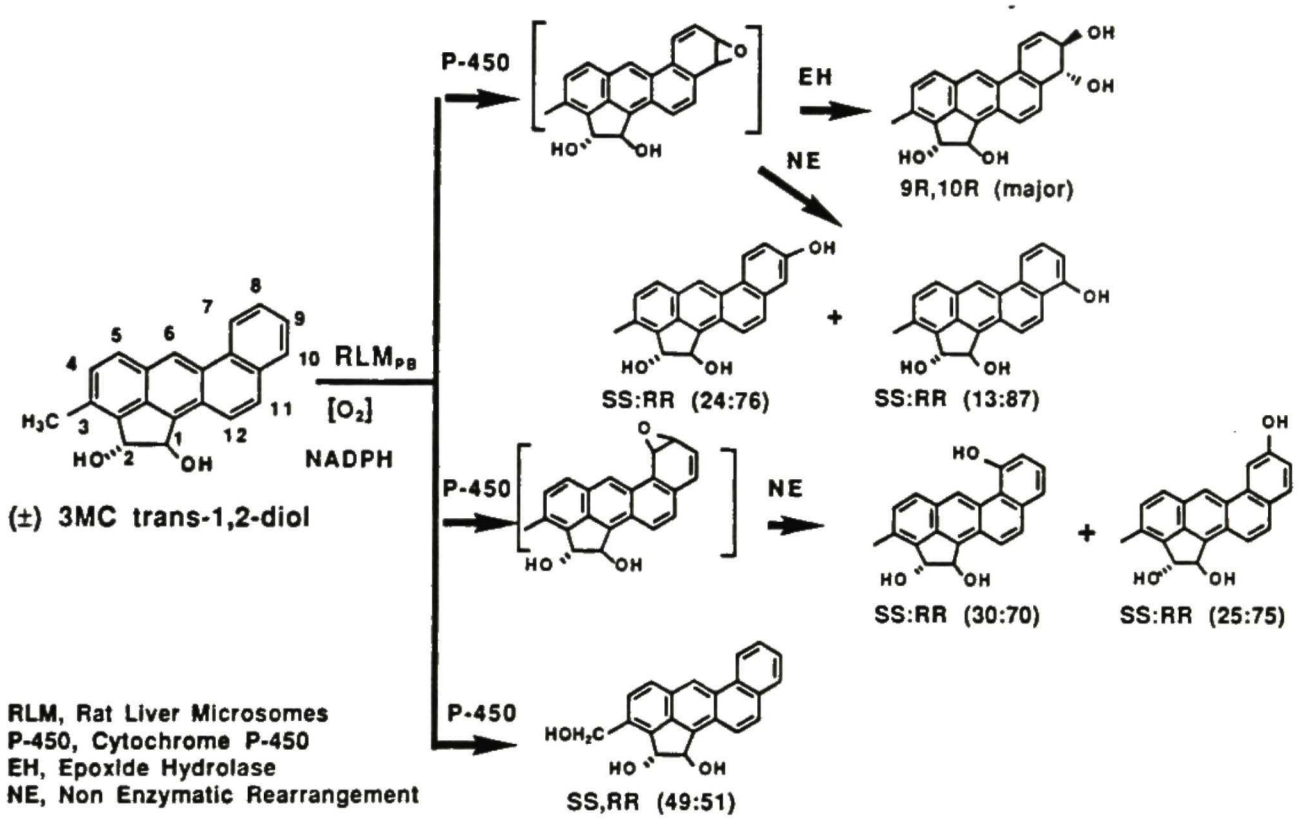

Figure 101. The major metabolic pathway of (±)3MC *trans*-1,2-diol.

peak 2 of Fig. 79. The available evidence of stereochemical products formed in microsomal metabolism reflects the possible stereoselective activation pathway of 3MC *trans*-1,2-diol. However, how the metabolically formed polar bay region 3MC *trans*-1,2-diol:9,10-diol-7,8-epoxides penetrate membranes and bind DNA in the cell nucleus to exhibit their biological activity remains unknown.

Four isomeric phenols at 7,8,9,10 benzo-ring formed in the metabolism of 3MC *trans*-1,2-diol were found and were believed to be derived from non enzymatic isomerization of the 7,8-epoxides and 9,10-epoxides. CD spectra of their optically pure phenolic and C_3-hydroxylation enantiomers, induced by the C_1 and C_2 chiral centers, from the metabolism of enantiomeric 3MC *trans*-1,2-diol were determined which presented characteristics of major Cotton effects similar to those of either parent 3MC *trans*-1*R*,2*R*-diol or 3MC *trans*-1*S*,2*S*-diol. The ellipticity (millidegrees) of optically pure phenolic enantiomers is known to vary slightly with location of a hydroxyl group due to stereo-interaction between the hydroxyl group and the benz[a]anthrancene nucleus. However, CD spectra of 3-OHMC *trans*-1,2-diol exhibited Cotton effects identical to those of each 3MC *trans*-1,2-diol enantiomer, because hydroxylation at the 3-methyl sidechain does not directly affect the aromatic system of benz[*a*]anthracene nucleus. If their extinction coefficients were assumed to be similar, 10-OH-3MC *trans*-1*R*,2*R*-diol (relative amount = 3.85) formed in the metabolism of 3MC *trans*-1*R*,2*R*-diol by liver microsomes of PB-treated rats and 9-OH-3MC *trans*-1*R*,2*R*-diol (2.08) from 3MC-treated ones respectively, were the most abundant metabolites in all microsomal incubations of both the racemic and enantiomeric 3MC *trans*-1,2-diols (Table 10). Enantiomers of all phenolic products formed at C_7, C_8, C_9 and C_{10} were enriched in 1*R*,2*R* stereochemistry which range 57 - 89% as seen in Table 11, indicating that these metabolites were likely rearranged from 7,8-epoxides and 9,10-epoxides of 3MC *trans*-1*R*,2*R*-diol rather than those from 3MC *trans*-1*S*,2*S*-diol. Effects of enzyme inducers on formations of phenolic products of 3MC *trans*-1*R*,2*R*-diol in metabolism of (±) 3MC *trans*-1,2-diol were PB ≈ control (70-89% in 1*R*,2*R*) > 3MC (57-76%).

Taken together, the major metabolic pathway of 3MC *trans*-1,2-diol by rat liver microsomal incubation is characterized in Fig. 101. These results indicate that dihydrodiols formed at bay and M region in the metabolism of (±)3MC *trans*-1,2-diol from all microsomal preparations are mainly derived from 3MC *trans*-1*R*,2*R*-diol. The role of 3MC *trans*-1*R*,2*R*-diol:9*R*,10*R*-dihydrodiol in the metabolic pathway of 3MC *trans*-1,2-diol and 3MC has yet to be determined. It is significant to note the large quantity of phenolic products formed as a possible inactivation pathway in the metabolism of 3MC *trans*-1,2-diol. The possible role of the metabolites in the activation of 3MC *trans*-1,2-diol remains speculative since the biological activities of metabolites have not been tested.

Metabolism of 3MC cis-1,2-diol

The metabolic products of 3MC in rat liver homogenate include both 3MC *cis*-1,2-diol and 3MC *trans*-1,2-diol, with the *cis*-isomer predominating (Sims, 1966). Sims has tested the carcinogenicity of many of the metabolites of 3MC by injecting these compounds subcutaneously into C_{57} black mice (Sims, 1967). Under the conditions used in this work, the *cis*-isomer induced a few tumours with comparatively long latent periods. Microsome-mediated alkylation of DNA by [^{3}H]-3MC routinely exhibited that 3MC *cis*-1,2-diol was one of 14 radioactive peaks when the deoxyribonucleoside-bound adducts were chromatographed on HPLC (Eastman *et al.*, 1979) .

In our study, *in vitro* microsomal incubation of 3MC *cis*-1,2-diol produced nine 3MC *cis*-1,2-diol metabolites. Two diastereomeric 3MC *cis*-1,2-diol:9,10-dihydrodiols, contained in peaks 2 and 4 of Fig. 87 formed from PB-treated rat liver microsomes were the most abundant metabolites. Peaks 2 and 4 of Fig. 87 were mainly enriched in 1*R*,2*S*,9*R*,10*R* and 1*S*,2*R*,9*R*,10*R* absolute configurations, respectively. This indicated that the formations of 3MC *cis*-1,2-diol:9,10-dihydrodiols, in the metabolism of 3MC *cis*-1,2-diol, by rat liver microsomes highly selected 9*R*,10*R* stereochemistry and did not significantly exhibit substrate enantioselectivity at region between C_1 and C_2. A resulting

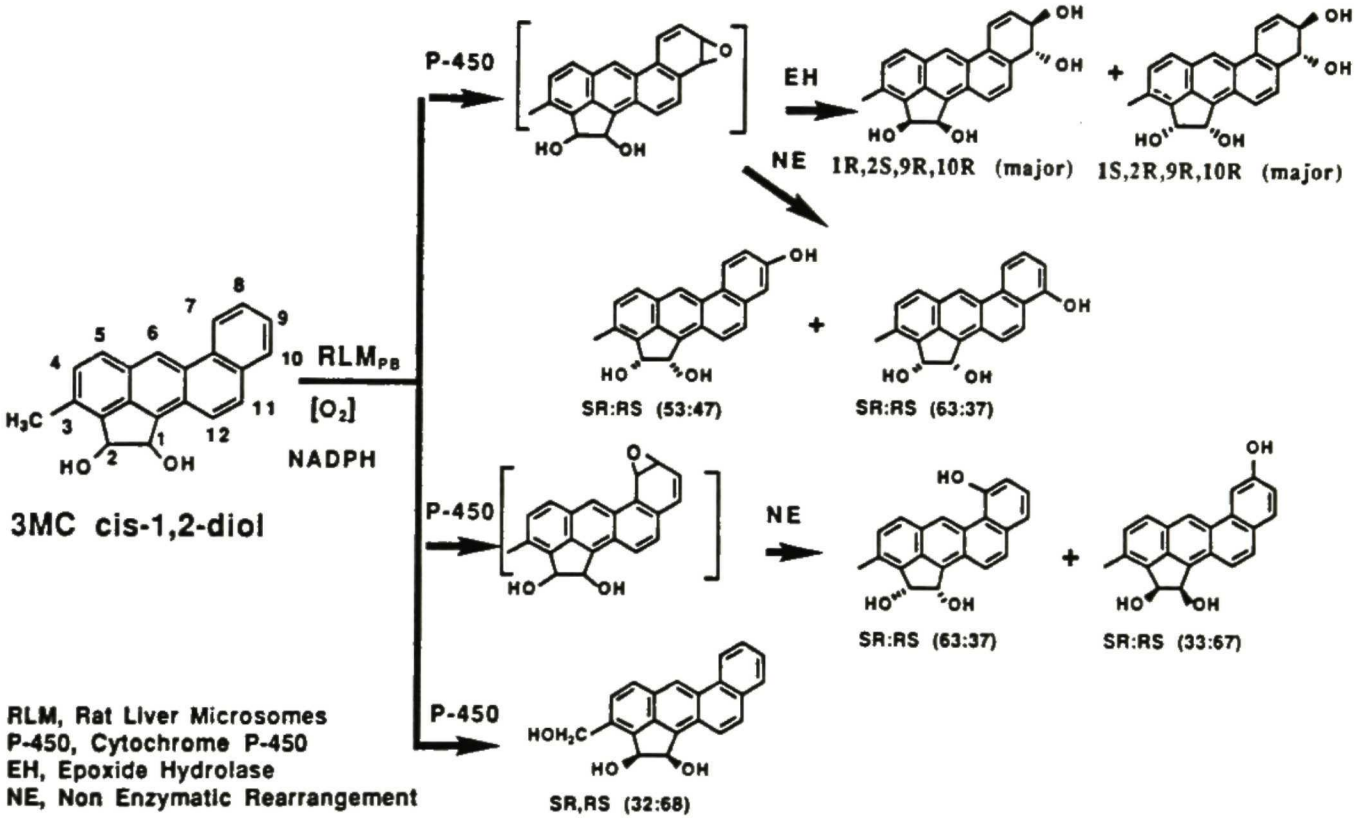

Figure 102. The major metabolic pathway of (±)3MC *cis*-1,2-diol.

stereoselective pathway of (±)3MC *cis*-1,2-diol metabolism from rat liver microsomes is clearly characterized as shown in Fig. 102.

The 3-OHMC *cis*-1,2-diol in peak 8 and 10-OH-3MC *cis*-1,2-diol in peak 9 of Fig. 87 were major metabolites, formed in the metabolism of (±)3MC *cis*-1,2-diol from all pretreatment rat liver microsomes, and were products of C_3-hydroxylation and of non-enzymatic rearrangement of the 9,10-epoxides respectively. The relatively higher amounts (Table 12) of phenolic products at C_9 and C_{10} formed in the metabolism of (±) 3MC *cis*-1,2-diol by liver microsomes of 3MC-treated rats indicated that the 3MC induced cytochrome P-450c isozymes catalyze the formations of 9,10-epoxides. However, these formed epoxides may not be good substrates to be hydrated to corresponding dihydrodiols by microsomal epoxide hydrolase. Alternatively, the concentration of epoxide hydrolase contained in 3MC induced rat liver microsomes may not be sufficient to convert these epoxides to dihydrodiols. Hence the epoxides formed at the region between C_9 and C_{10} were non-enzymatically isomerized to be their corresponding phenolic products. The formations of the 9,10-dihydrodiol metabolites demonstrated that epoxide hydrolase contained in liver microsomes from PB-induced rats is significant in the conversion of 9,10-epoxides to 9,10-dihydrodiols which may be oxidized to ultimate carcinogen bay region 9,10-diol-7,8-epoxides.

CD spectra of optically pure phenolic and C_3-hydroxylated enantiomers were obtained by metabolism of 3MC *cis*-1*S*,2*R*-diol and 3MC *cis*-1*R*,2*S*-diol. The Cotton effects of each pair of enantiomers displayed opposite and mirror image characteristics. Enantiomers of these compounds formed in the metabolism of (±) 3MC *cis*-1,2-diol were separated by CSP HPLC and enantiomeric compositions differed with enzyme inducer used and with the location of aromatic ring hydroxyl groups. 3MC induction caused stereoselective effects on the formations of all phenolic and C_3-hydoxylation products enriched in 3MC *cis*-1*R*,2*S*-diol (68-100%, Table 13). Control and PB inducer had similar effects on the formation of phenols and 3-OHMC *cis*-1,2-diol, showing that

phenolic products at C_7, C_9 and C_{10} were enriched in 1*S*,2*R* stereochemistry, and that products at C_8 and C_3-methyl group were enriched in 1*R*,2*S* stereochemistry. The results of the formation of phenolic enantiomers, produced in the metabolism of (±) 3MC *cis*-1,2-diol, reflect the stereoselectivity of microsomal enzymes by various inducers and the ease of isomerization arising from the corresponding metabolically formed epoxides. Hence the stereoselective pathway of (±) 3MC *cis*-1,2-diol metabolism from PB-treated rat liver microsomes is shown in Fig. 102.

In conclusion, 3MC is a potent carcinogen and requires metabolism by mammalian drug-metabolizing enzyme systems to exert its biological activity. 3MC 9,10-dihydrodiol, a precursor of the bay region 9,10-diol-7,8-epoxides, was reported in one study to be a major rat liver microsomal metabolite of 3MC (Tierney *et al.*, 1990). In other studies, 3MC 9,10-dihydrodiol was either not found as a metabolite (Sims *et al.*, 1966; Tierney *et al.*, 1979; Thakker *et al.*, 1978; Bürki *et al.*, 1972; Stoming *et al.*, 1977) or a minor metabolite (Eastman *et al.*, 1979; Stoming *et al.*, 1977; MacNicoll *et al.*, 1980) of 3MC. As a minor metabolite, 3MC 9,10-dihydrodiol, a proximate carcinogen formed in 3MC metabolism, is not taken into account in the activation pathway of 3MC. The carcinogenicity of the more active 1-OH-3MC 9,10-dihydrodiols derived from the metabolism of both 1-OH-3MC and 3MC takes its place. Further metabolism of major secondary and tertiary metabolites of 3MC become important steps in producing more 9,10-dihydrodiols through hydroxylation at C_1, C_2 and C_3-methyl sidechains. These may play an important role in contributing biological activities exhibited by 3MC rather than 3MC 9,10-dihydrodiol itself. C_1, C_2 and C_3-methyl positions of 3MC are major sites of oxidative metabolism by microsomal isozymes, forming 1-OH-3MC, 2-OH-3MC, 3-OHMC, 3MC *trans*-1,2-diol and 3MC *cis*-1,2-diol. 1-OH-3MC and 2-OH-3MC can be further oxidized to corresponding ketones 3MC-1-one and 3MC-2-one, respectively. Many studies reported that these major metabolites formed in the metabolism of 3MC

showed varying degrees of biological activities including alkylation of DNA, mutagenesis and carcinogenesis, except for 3MC *trans*-1,2-diol.

Absolute configurations of 1-OH-3MC, 2-OH-3MC, 3MC *trans*- and *cis*-1,2-diol were determined by CD chirality method and CSP HPLC. In this report, stereoselective metabolisms of 3MC oxidative derivatives at C_1, C_2 and C_3-methyl positions were carried out by rat liver microsomes. The major metabolically formed 9,10-dihydrodiols were derived from 3MC derivatives and were mainly enriched in the 9*R*,10*R* stereochemistry. Relative amounts of 9,10-dihydrodiols formed depended on substrates employed including racemic and enantiomeric compounds, rate of metabolism and enzyme inducers utilized. Phenolic products at C_7, C_8, C_9, C_{10} benzo-ring were also obtained and represent a likely detoxification process and inactivation pathway of 3MC. Effects of the enzyme inducer 3MC enhanced the formation of the phenolic metabolites. C_3-hydroxylation products formed in metabolisms of 3MC and its C_1 and C_2 derivatives were found to be major metabolites in most cases and some were further converted to corresponding 9,10-dihydrodiols, such as 1-OH-3-OHMC 9,10-dihydrodiols and 2-OH-3-OHMC 9,10-dihydrodiols. Some minor 7,8-dihydrodiols (bay region) and 11,12-dihydrodiols (K region) were formed in the metabolism of 1-OH-3MC and 2-OH-3MC. Results of our studies elucidate that ring positions of 3MC at C_7, C_8, C_9 and C_{10} are active sites of oxidative metabolism of 3MC derivatives by rat liver microsomes in both activation and detoxification pathways. CD spectra and stereochemistries of most dihydrodiols and phenolic products formed in the metabolisms of 3MC derivatives were determined. Enantiomeric compositions of some metabolites formed were resolved by using CSP HPLC and used to characterize the stereoselective metabolic pathways. Microsomal metabolisms of [^{3}H] 1-OH-3MC from rat and human liver appear to have similar patterns. This predicts that a possible similar metabolic pathway of 1-OH-3MC by human liver microsomes may exist as that observed by rat liver microsomes. Effects of 3MC inducer

on formations of metabolites resulted in more enhanced metabolism of [^{3}H] 1-OH-3MC in all microsomal preparations from rats.

These studies characterize the overall metabolic pathway (activation and detoxification) of major secondary and tertiary metabolites at C_1, C_2 and C_3-methyl positions formed in 3MC metabolism by rat liver microsomes. The results provide a clearer understanding of 3MC carcinogenicity exhibited by metabolic factors; underlying reason(s) for the intrinsic activities of the C_1, C_2 and C_3-methyl derivatives of 3MC; and availability of a chemical source of 9,10-dihydrodiols as proximate carcinogens for further biological tests.

REFERENCES

Alvares, A.P., Schilling, G., Garbut, A. and Kuntzman, R. Studies on the hydroxylation of 3,4-benzo[*a*]pyrene by hepatic microsomes. Effect of albumin on the rate of hydroxylation of 3,4-benzo[a]pyrene. *Biochem. Pharmacol.* 19,1449-1455 (1970)

Ames, B.N., McCann, J., and Yamasaki, E. Methods for detecting carcinogens and mutagens with the Salmonella/Mammalian-microsome mutagenicity test. *Mutation Res.* 31:347-364 (1975)

Cavalieri, E. L. and Rogan, E. G. One-electron oxidation in aromatic hydrocarbon carcinogenesis, in Polycyclic Hydrocarbons and Carcinogenesis edited by Ronald G. Harvey. p289-306; Am. Chem. Soc. Washington D.C. (1985)

Cavalieri, E., Rogan, E and Sinha, D. Carcinogenicity of aromatic hydrocarbons directly applied to rat mammary gland. *J. Cancer Res. Clin. Oncology* 114:3-9 (1988)

Cavalieri, E., Rogan, E., Higginbotham, S., Cremonesi, P. and Salmasi, S. Tumor-initiating activity in mouse skin and carcinogenicity in rat mammary bland of fluorinated derivatives of benzo[a]pyrene and 3-methylcholanthrene. *J. Cancer Res. Clin. Oncology* 114:16-22 (1988)

Cavalieri, E., Roth, R., Althoff, J., Grandjean, C., Patil, K., Marsh, S., and McLaughlin, D. Carcinogenicity and metabolic profiles of 3-methylcholanthrene oxygenated derivatives at the 1 and 2 position. *Chem.-Biol. Interac.* 22:69-81 (1978)

Cavalieri, E., Roth, R., and Rogan, E. Hydroxylation and conjugation at the benzylic carbon atom: a possible mechanism of carcinogenic activation for some methyl-substituted aromatic hydrocarbons, in Polynuclear Aromatic Hydrocarbons: 3rd Int Symp on Chemistry and Biology - Carcinogenesis and Mutagenesis, Jones, P.W. and Leber, P., Eds., Ann Arbor Science Publisher, Ann Arbor, Mich., (1979)

Cavalieri, E., Roth,R. and Rogan, E.G. Metabolic activation of aromatic hydrocarbons by one-electron oxidation in relation to the mechanisms of tumor initiation, in Polynuclear

Aromatic Hydrocarbons: Chemistry, Metabolism and carcinogenesis edited by Freudenthal, R. and Jones, P. Vol. Raven Press, New York, p181; (1976).

Chiu, P.-L. and Yang, S.K. Metabolism of 7,8-Dihydrobenzo[*a*]pyrene by rat liver microsomal enzymes and mutagenicity of metabolites. *Cancer Res.* 46:5084-5094 (1986)

Chiu, P.-L., Weems, H.B., Fu, P.P., and Yang, S.K. Absolute configuration and the unusual quasidiequatorial conformation of *trans*-7,8-dihydroxy-7,8-dihydro-7-methylbenzo[*a*]pyrene enantiomer and its diacetate and dimenthoxyacetate derivatives. *Chem.-Biol. Interac.* 52:265-277 (1985)

Chou, M. W., Chiu, P.-L., Fu, P. P. and Yang, S. K. Effect of enzyme induction on the stereoselective metabolism of optically pure (-) 1*R*,2*R*- and (+)1*S*,2*S*-dihydroxy-1,2-dihydrobenz[*a*]anthrancenes to vicinal 1,2-dihydrodiol 3,4-epoxides by rat liver microsomes. *Carcinogenesis* 4:629-638 (1983)

Chouroulinkov, I., Gentil, A., Tierney, B., Grover P. L. and Sims, P. The initiation of tumors on mouse skin by dihydrodiols derived from 7,12-dimethylbez[*a*]anthracene and 3-methylcholanthrene. *Int. J. Cancer* 24:455-460 (1979)

Conney, A. H.: Induction of microsomal enzymes by foreign chemicals and carcinogenesis by polycyclic aromatic hydrocarbons: G.H.A. Clowes memorial lecture. *Cancer Res.* 42:4875-4917 (1982)

Conney, A.H., Gillette, J.R., Inscoe, J.K., Trams, E.R. and Posner, H.S. Induced synthesis of liver microsomal enzymes whtich metabolized foreign compounds. *Science* 130:1478-1479 (1959)

Cook, J.W., Loudon, J.D. and Williams, W.F. *J. Chem. Soc.* 45:911 (1950)

Cooper, C.S., Vigny, P., Kindts, M., Grover, P.L., and Sims, P. Metabolic activation of 3-methylcholanthrene in mouse skin: fluorescence spectral evidence indicates the involvement of diol-epoxides formed in the 7,8,9,10-ring. *Carcinogenesis* 1:855 (1980)

Eastman, A. and Bresnick, E. Metabolism and DNA binding of 3-methylcholanthrene *Cancer Res.* 39:4316-4321 (1979)

Estabrook, R. W., Werringloer, J., Capdevila, J. and Prough, R.A. In "Polycyclic Hydrocarbons and Cancer" (H.V. Gelboin and P.O.P.Ts'o, eds.) P.285. Academic Press, New York, (1978)

Fieser, L.F. and Hershberg, E.B. The oxidation of methylcholanthrene and 3,4-benzpyrene with lead tetraacetate, further derivatives of 3,4-benzpyrene. *J. Am. Chem. Soc.* 60:2542-2548 (1938)

Flesher, J.W. and Sydnor, K.L. Possible role of 6-hydroxymethylbezo[a]pyrene as a proximate carcinogen of benzo[a]pyrene and 6-methylbenzo[a]pyrene. *Int. J. cancer* 11:443 (1973)

Fu, P.P., Harvey, R.G., and Beland, F.A. Molecular orbital theoretical prediction of the isomeric products formed from reactions of arene oxides and related metabolites of polycyclic aromatic hydrocarbons. *Tetrahedron* 34:857-866 (1978)

Gangarosa, M.A. and Storming,T.A. The metabolism of 3-methylcholanthrene by liver lung microsomes: Effect of enzyme inducing agents. *Cancer Letters* 20,323-331 (1983)

Gardiner, E.M. and Stoming, T.A. The metabolism of 1-hydroxy- and 2-hydroxy-3-methylcholanthrene by liver microsomes: Effect of enzyme inducing agents. *Letters* 24:103-110 (1984)

Harada, N. and Nakanishi, K. *Circular Dichroic Spectroscopy. Exciton Coupling in organic Stereochemistry*. University Science Books, Mill Valley, CA (1983).

Harada, N.and Nakanishi, K. The exciton chirality method and its application to configurational and conformational studies of natural products. *Acc. Chem. Res.* 5:257 (1972)

Harvey, R.G., Goh, S.H. and Cortez, C. "K-region" oxides and related oxidized metabolites of carcinogenic aromatic hydrocarbons. *J. Am. Chem. Soc.* 97:3468-3478 (1975)

Hueper, W.C. and Conway,W.D. "Chemical Carcinogenesis and Cancers." C.C. Thomas, Springfield, Illinois (1972)

Jacobs, S. A., Cortez, C. and Harvey, R. G. Synthesis of potential proximate and ultimate carcinogenic metabolites of 3-methylcholanthrene. *Carcinogenesis* 4:519-522 (1983)

Jacobs, S.A., Cortez C. and Harvey, R.G. Synthesis of potential proximate and ultimate carcinogenic metabolites of 3-methylcholanthrene. *Carcinogenesis* 4,519-522 (1983)

Jerina, D. M., Lehr, R.E., Yagi, H., Hernandez, O., Dansette, P.M., Wislocki, P. G., Wood, A.W., Chang, R.L., Levin, W., and Conney, A.H. Mutagenicity of benzo[*a*]pyrene derivatives and the description of a quantum mechanical model which predicts the ease of carbonium ion formation from diol epoxides, in In Vitro Metabolic Activation and Mutagenesis Testing, Deserres, F.J., Fouts, J.R., Bend, J.R. and Philpot, R.M., Eds., Elsevier/North-Holland Biomedical, Amsterdam, pp159-177, (1976).

Jerina, D.M., and Daly, J.W. Oxidation at carbon, in Drug Metabolism, Parke, D.V. and Smith, R., Eds., Taylor and Frances Ltd., London, 15, (1976).

Jerina, D.M., Yagi, H., Lehr, R.E.,Thakker, D.R., Schaefer-Ridder, M., Karle, J.M., Levin, W.,Wood, R.L.Chang, and A.H. Conney, in "Polycyclic Hydrocarbons and Cancer", H.V.Gelboin and P.O.P.Ts'o, eds. P.173. Academic Press, New York (1978)

Kim, Y.H., Tishbee, A. and Gil-Av, E. Optical resolution of mutagenic and carcinogenic derivatives of polyaromatic hydrocarbons by high pressure liquid chromatography on a chiral support. *J.C.S. Chem. Commun.* 75:568 (1981)

King, H.W., Osborne, M.R. and Brookes, P. The metabolism and DNA binding of 3-methylcholanthrene. *Int . J. Cancer* 20:564 (1977)

King, H.W., Osborne, M.R., and Brookes, P. The identification of 3-methylcholanthrene-9,10-dihydrodiol as an intermediate in the binding of 3-methylcholanthrene to DNA in cells in culture. *Chem. Biol. Interact.* 20:367-371 (1978)

Koreeda, M., Moore, P.D., Wislocki, P.G., Levin, W., Conney, A.H., Yagi, H. and Jerina, D.M. Binding of benzo[*a*]pyrene 7,8-diol-9,10-epoxides to DNA, RNA and protein of mouse skin occurs with high stereoselectivity. *Science*. 199:778-781 (1977)

Lee, H. and Harvey, R.G. Synthesis of oxygenated derivatives of 3-methylcholanthrene. Org. *Prep. Proc. Internat.* 20:123-128 (1988)

Levin, W., Buening, M.K. Wood, A.W., Chang, R.L., Thakker, D.R., Jerina, D.M. and Conney, A.H.: Tumorigenic activity of 3-methylcholanthrene metabolites on mouse skin and in newborn mice. *Cancer Res.* 39:3549-3553 (1979)

Levin, W., Chang, R.L., Wood, A.W., Thakker, D.R., Yagi,H., Jerina, D.M. and Conney, A.H.: Tumorigenicity of optical isomers of the diastereomeric bay-region 3,4-diol-1,2-epoxides of benzo(c)phenanthrene in murine tumor models. *Cancer Res.* 46:2257-2261 (1986)

Lowry, O.H., Rosebrough, N.J., Farr, A.L. and Randall, R.J. Protein measurement with the folin phenol reagent. *J. Biol.Chem.* 193:265-275 (1951)

Lu, A.Y.H., Kuntzman, R., West, S. and Conney, A.H. Reconstituted liver microsomal enzyme system that hydroxylates drugs, other foreign compounds and endogenous substrates I. Determination of substrate specificity by the cytochrome P-450 and P-448 fractions. *Biochem. Biophys. Res. Commun.* 42:1200-1206 (1971)

Lu, A.Y.H., Kuntzman, R., West, S., Jacobson, M. and Conney, A.H. Reconstituted liver microsomal enzyme system that hydroxylates drugs, other foreign compounds, and endogenous substrates II. Role of the cytochrome P-450 and P-448 fractions in drug and steroid hydroxylations. *J. Biol. Chem.* 247:1727-1743 (1972)

Lu, A.Y.H. and West, S.B. Multiplicity of mammalian microsomal cytochrome P-450. *Pharmacological Reviews* 31:277-295 (1980)

Lu, A.Y.H., Levin, W., Vore, M., Conney, A.H., Thakker, D.R., Holder., G., and Jerina, D.M. Metabolism of benzo[a]pyrene by purified liver microsomal cytochrome P-448 and epoxide hydrase. In Carcinogenesis, vol. 1, *Polynuclear Aromatic Hydrocarbons:*

Chemistry, Metabolism and Carcinogenesis, ed. by R.I.Freudenthal and P.W. Jones, pp. 115-126. Raven Press, New York, (1976)

Lu, L.J.W., Harvey, R.G., Lee, H., Baxter, J., and Anderson, L.M. Age, Tissue, Ah genotype-dependent differences in the binding of 3-methylcholanthrene and its metabolite(s) to mouse DNA. *Cancer Res.* 50:4239-4247 (1990)

Malaveille, C., Bartsch, H., Baker, S., Tierney, B., Hewer, A., Grover, P.L., and Sims, P. Metabolic activation of 3-methylcholanthrene: Mutagenic and transforming activities of the 9,10-dihydrodiol. *Biochem. Biophys. Res. Commun.* 85:1568-1574 (1978)

Newman, M.S. In "Polynuclear Aromatic Hydrocarbons: Chemistry, Metabolism, and Carcinogenesis" (R.I.Freudenthal and P.W.Jones, eds.), Vol. 1, p.203. Raven Press, New York, (1976)

Osborne, M. R. The reaction of 3-methylcholanthrene-diolepoxide with DNA, in *Polynuclear Aromatic Hydrocarbons*: Mechanisms, Method and Metabolism, Cooke, M. and Dennis, A.J., eds., Battelle Press, Columbus, Ohio, 987, (1983)

Osborne, M.R., Brookes, P., Lee, H. and Harvey, R.G. The reaction of a 3-methylcholanthrene diol epoxide with DNA in relation to the binding of 3-methylcholanthrene to the DNA of mammalian cells. *Carcinogenesis* 7:1345-1350 (1986)

Pal, K., Grover, P.L. and Sims, P. The induction of sister chromatid exchanges by dihydrodiols derived from 7,12-dimethylben[a]anthracene and 3-methylcholanthrene *Cancer Letters* 7:45-49 (1979)

Phillips, D.H., Grover, P.L., and Sims, P. The covalent binding of polycyclic hydrocarbons to DNA in the skin of mice of different strains. *Int. J. Cancer* 22:478-494 (1978)

Pirkle, W.H., Finn, J.M., Hamper, B.C., Schreiner, J. and Pribish, J.R. A useful and conveniently accessible chiral stationary phase for the liquid chromatographic separation of enantiomers. in:" Asymmetric Reactions and Processes in Chemistry.", Eliel, E.l., Otsuba, S. (eds.): ACS symposium Series No. 185. American Chemical Society, Washington, DC, pp. 245-260 (1982)

Pirkle, W.H., Finn, J.M., Schreiner, J. L. and Hamper, B.C. A widely useful chiral stationary phase for the high-performance liquid chromatography separation of enantiomers. *J. Am. Chem. Soc.* 103:3964-3966 (1981)

Pirkle, W.H., House, D.W. and Finn, J.M. Broad spectrum resolution of optical isomers using chiral high-performance liquid chromatographic bonded phases. *J. Chromatogr.* 192:143-158 (1980)

Rogan, E.G., Cavalieri, E.L., Walker, B.A., Balasubramanian, R., Wislocki, P.G., Roth, R.W., and Saugier, R.K. Mutagenicity of benzylic acetates, sulfates and bromides of polycyclic aromatic hydrocarbons. *Chem. Biol. Interact.* 58:253 (1986)

Schoental, R. In"Polycyclic Hydrocarbons" (E.Clar, ed.), p.133. Academic Press, New York, (1964)

Shou, M. and Yang, S.K. Regioselective and stereoselective metabolisms of pyrene and 1-bromopyrene by rat liver microsomes and effects of enzyme inducers. *Drug. Metab. Disp.* 16:173-183 (1988)

Shou, M. and Yang, S.K. 1- and 2-Hydroxy-3-methylcholanthrene: Regioselective and stereoselective formations in the metabolism of 3-methylcholanthrene and enantioselective disposition in rat liver microsomes. *Carcinogenesis* 11:933-940 (1990a)

Shou, M. and Yang, S.K. 9,10-Dihydroxy-9,10-dihydro-3-methylcholanthrene-2-one: A principal metabolite of the potent carcinogen 3-methylcholanthrene-2-one by rat liver microsomes. *Carcinogenesis* 11:689-695 (1990b)

Shou, M. and Yang, S.K. Enantioselective aliphatic hydrxylations of racemic 1-hydroxy-3-methylcholanthrene by rat liver microsomes. *Chirality* 2:141-149 (1990c)

Shou, M and Yang, S.K. Metabolism of 2*S*-hydroxy-3methylcholanthrene by rat liver microsomes. *Carcinogenesis* 11:2037-2045 (1990d)

Shubik, P. Current staus of chemical carcinogenesis. *Proc. Natl. Acad. Sci.* USA 69:1052 (1972)

Sims, P. and Grover, P. L. Involvement of dihydrodiols and diol-epoxides in the metabolic activation of polycyclic hydrocarbons other than benzo[*a*]pyrene. In: *Polycyclic Hydrocarbons and Cancer*. Vol. 3, Gelboin, H. V. and Ts'o, P. O. P., eds., New York: Academic Press. pp. 117-181 (1981).

Sims, P. Qualitative and quantitative studies on the metabolism of a series of aromatic hydrocarbons by rat-liver preparations. *Biochem. Pharmacol.* 19:795:818 (1970)

Sims, P. The carcinogenic activities in mice compounds related to 3-methylcholanthrene. *Int. J. Cancer* 2:505-508 (1967)

Sims, P.l. and Grover, P.L. *Adv. Cancer Res.* 20:165 (1974)

Sims, P. The metabolism of 3-methylcholanthrene and some related compounds by rat liver homogenates. *Biochem. J.* 98:215-228 (1966)

Stoming, T.A., and Gerardot, R.J. High pressure liquid chromatographic separation of the metabolites of 3-methylcholanthrene. *Life Sci.* 20:113-116 (1977)

Stoming,T.A., Bormstein, W. and Bresnick, E. The metabolism of 3-methylcholanthrene by rat liver microsomes. *Biochem. Biophys. Res. Commun.* 79:461-469 (1977)

Sydnor, K.L., Bergo, C.H. and Flesher, J.W. Effects of various substitutents in the 6-position on the relative carcinogenic activity of a series of benzo[a]pyrene derivatives. *Chem. Biol. Interact.* 29:159 (1980)

Thakker, D.R., Levin, W., Stoming, T.A., Conney, A.H. and Jerina, D.M. In "Carcinogenesis: A comprehensive survey. Vol. 3: Polynuclear aromatic hydrocarbons" edited by Jones, P.W. and Freudenthal, R.I. eds. pp253-264; (1978) Raven Press, New York

Thakker, D.R., Levin, W., Wood, A.W., Conney, A.H., Stoming, T.A., and Jerina, D.M. Metabolic formation of 1,9,10-trihydroxy-9,10-dihydro-3-methylcholanthrene: a potential proximate carcinogen from 3-methylcholanthrene. *J. Am. Chem. Soc.* 100:645-647(1978)

Thakker, D.R., Yagi,H., Akagi, H., Koreeda, M., Lu, A.Y.H. Levin, W., Wood, A.W., Conney, A.H., and Jerina, D.M. Metabolism of benzo[a]pyrene. Stereoselective metabolism of benzo[a]pyrene and benzp[a]pyrene 7,8-dihydrodiol to diol epoxides. *Chem.-Biol. Interact.* 16:281-300 (1977)

Thomas, P.E., Reik, L.M., Ryan, D.E., and Levin, W. Regulation of three forms of cytochrome P-450 and epoxide hydrolase in rat liver microsomes. Effects of age, sex, and induction. *J. Biol. Chem.* 256:1044-1052 (1981)

Tierney, B. and Bresnick, E. Sims, P., Grover, P. Microsomal and nuclear metabolism of 3-methylcholanthrene. *Biochem. Pharmacol.* 28:2607-2610 (1979)

Tierney, B. Hewer, A., Rattle, H., Grover, P. L. and Sims, P. The formation of dihydrodiols by chemical or enzymic oxidation of 3-methylcholanthrene. *Chem-Biol. Interact.* 23:121-135 (1978)

Tierney, B., Abercrombie, B., Walsh, C., Hewer, A., Grover, P.L., and Sims, P. The preparation of dihydrodiols from 7-methylbenz[*a*]anthracene. *Chem-Biol. Interact.* 21: 289-298 (1978).

Tierney, B., Burden, P., Hewer, A., Ribeiro, O., Walsh, C., Rattle, H., Grover, P.L. and Sims, P. High-performance liquid chromatography of isomeric dihydrodiol of polycyclic hydrocarbons. The effect of conformation on elution order. *J. Chromatogr.* 176:329 (1979)

Vigny, P., Duquesme, M., Coulomb, C., Tierney, B., Grover, P.L. and Sims, P. Fluorescence spectral studies on the metabolic activation of 3-methylcholanthrene and 7,12-dimethylbez[a]anthrancene in mouse skin. *FEBS Leett.*.82:278 (1977)

Watabe, T., Hakamata, Y., Hiratsuka, A., and Ogura, K. A 7-hydroxymethyl sulphate ester as an active metabolite of the carcinogen, 7-hydroxymethylbenz[a]anthracene. *Carcinogenesis* 7:207 (1986)

Watabe, T., Hiratsuka, A., Ogura, K., and Edoh, K. A reactive hydroxymethyl sulfate ester formed regioselectively from the carcinogen, 7,12-

dihydroxymethylbenz[a]anthracene, by rat liver sulfotransferase. *Biochem. Biophys. Res. Commun.* 131:694 (1985)

Watabe, T., Ishixuka, T., Fujieda, T., Hiratsuka, A. and Ogura, K. Sulfate esters of hydroxymethylbenz[*a*]anthracenes as active metabolites of 7,12-dimethylbenz[a]anthracene *Jpn. J. Cancer Res.* 76:684 (1985)

Weems, H.B., Mushtag, M. and Yang, S.K. Absolute configurations of K-region epoxide enantiomers of 3-methylcholanthrene, Benz[a]anthracene, and Benzo[*a*]pyrene. *Anal. Chem.* 59:2679-2688 (1987)

Weems, H.B., Mushtaq, M., and Yang, S.K. Resolution of enantiomeric epoxides of polycyclic aromatic hydrocarbons by chiral stationary phase high-performance liquid chromatography. *Anal. Biochem.* 148:328-338 (1985)

Wood, A. W., Chang, R. L., Levin, W., Thomas, P. E., Tyan,D., Stoming,T. A., Thakker, D. R., Jerina, D. M. and Conney, A. H. Metabolic activation of 3-methylcholanthrene and its metabolites to products mutagenic to bacterial and mammalian cells. *Cancer Res.* 38:3398-3404 (1978)

Wood, A.W., Chang, R.L., Levin, W., Yagi, H., Thakker, D.R., Jerina, D.M. and Conney, A.H. Differences in mutagenicity of the optical enantiomers of the diastereomeric benzo[*a*]pyrene 7,8-diol-9,10-epoxides. *Biochem. Biophys. Res. Commun.* 77:1389-1396 (1977)

Wynder, E.L. and Mauchi, K. Etiological and preventive aspects of human cancer. *Prev. Med.* 1,300-334 (1972)

Yang, S.K. and Fu, P.P. Stereoselective metabolism of 7-methylbenz[*a*]anthracene: Absolute configuration of five dihydrodiol metabolites and the effect of dihydrodiol conformation on circular dichroism spectra. *Chem.-Biol. Interac.* 49:71-88 (1984)

Yang, S.K. and Li, X.C. Direct enantiomeric resolution of cyclic alcohol derivatives of polycyclic aromatic hydrocarbons by chiral stationary phase high-performance liquid chromatography. *J. Chromatogr.* 291:265-273 (1984)

Yang, S.K. Mushtaq, M., Weems, H.B. and Fu, P.P. Chiral recognition mechanisms in the direct resolution of diol enantiomers of some polycyclic aromatic hydrocarbons by high performance liquid chromatography with chiral stationary phases. *J. Liq. Chromatogr.* 9:473-492 (1986)

Yang, S.K., Mushtaq, M., Bao, Ziping, Weems, H.B., Shou, M. and Lu, X.L. Improved enantiomeric separation of dihydrodiols of polycyclic aromatic hydrocarbons on chiral stationary phases by derivatization to O-methyl ethers. *J. Chromatogr.* 461:377-395 (1989)

Yang, S.K. Stereoselectivity of cytochrome P-450 isozymes and epoxide hydrolase in the metabolism of polycyclic aromatic hydrocarbons. *Biochem. Pharmacol.* 37:61-70 (1988)

Yang, S.K., Chou, M.W. and Fu, P.P. Metabolic and structural requirements for the carcinogenic potencies of unsubstituted and methyl-substituted polycyclic aromatic hydrocarbons. In: *Carcinogenesis: Fundamental Mechanisms and Environmental Effects*, B. Pullman, P.O.P. Ts'o and H. Gelboin (eds.), D. Reidel Publishing Co., Dordrecht-Holland, pp. 143-156 (1980)

Yang, S.K., Roller, P.P. and Gelboin, H.V. Enyzmatic mechanism of benzo[*a*]pyrene conversion to phenols and diols and an improved high-pressure liquid chromatographic separation of benzo[*a*]pyrene derivatives. *Biochemistry* 16:3680 (1977)

Yang, S.K., McCourt, D.W., Leutz, J. C. and Gelboin, H.V. Benzo[a]pyrene diol epoxides: mechanism of enzymatic formation and optically active intermediates. *Science* 196:1199-1201 (1977)

Yang, S.K., Mushtaq, M., Weems, H.B., Miller, D.W. and Fu, P.P. Stereoselective formation and hydration of 12-methylben[a]anthracene 5,6-epoxide enantiomers by rat liver microsomal enzymes. *Biochem. J.* 245:191-204 (1987)

Yang, S.K., Prasanna, P., Weems, H.B., Jacobs, M.M., and Fu, P.P. Metabolism of the potent carcinogen 3-methylcholanthrylene by rat liver microsomes. *Carcinogenesis* 11:1195-1201 (1990)

Yang, S.K., Weems, H.B. and Mushtaq, M. Chiral stationary phase HPLC separation of enantiomeric oxygenated derivatives of polycyclic aromatic hydrocarbons and application to metabolism studies. in: Chirality and Biological Activity published by Alan R. Liss , Inc. pp81-109 (1990)